Univerzita Karlova v Praze
Přírodovědecká fakulta

Vývojová a buněčná biologie



Mgr. Rita Hrabáková

PROTEOMOVÁ ANALÝZA ÚČINKU PROTINÁDOROVÝCH LÉČIV A CHARAKTERIZACE MECHANISMŮ NÁDOROVÉ REZISTENCE

PROTEOME ANALYSIS OF ANTI-CANCER DRUG EFFECTS AND CHARACTERISATION OF DRUG RESISTANCE

Disertační práce

Školitel: RNDr. Hana Kovářová, CSc.

Praha

Prohlášení:

Prohlašuji, že jsem závěrečnou práci zpracovala samostatně a že jsem uvedla všechny použité informační zdroje a literaturu. Tato práce ani její podstatná část nebyla předložena k získání jiného nebo stejného akademického titulu.

V Praze, dne..... Rita Hrabáková

.....

Mé poděkování patří zejména školitelce RNDr. Haně Kovářové, CSc. za podporu a lidský přístup během studia.

Za cenné rady a příjemnou pracovní atmosféru děkuji všem kolegům z ÚŽFG AV ČR, v.v.i., MBÚ AV ČR, v.v.i. a Laboratoře experimentální medicíny LF UP a FN v Olomouci, zvláště pak Mgr. Jiřině Tylečkové, Ing. Petru Haladovi, PhD. a Mgr. Madhu Kollareddymu. Děkuji také své rodině a přátelům za jejich podporu a trpělivost.

Práce vznikla za finanční podpory výzkumných záměrů ÚŽFG AV ČR, v.v.i. (RVO67985904) a MBÚ AV ČR, v.v.i. (RVO61388971), Centra nádorové proteomiky (LC07017) a interních grantů (ÚŽFG /09/03, ÚŽFG /10/01).

Abstract

Despite significant progress in the development of anti-cancer drugs, there is still a need for novel therapeutic strategies that would improve the outcome of cancer patients. Using proteomic technologies and cell lines with different phenotype of p53 tumour suppressor, we monitored cancer cell response to anti-cancer treatment with focus on the development of drug resistance. The different levels of metabolic proteins were identified in our study which may help to explain different anti-cancer activity of drugs with only a subtle difference in structure. More importantly, proteins associated with the development of drug resistance were identified and such expression changes have become a focus of interest. Our findings demonstrate a higher protein level of serine hydroxymethyltransferase, serpin B5 and calretinin in cancer cells resistant to Aurora kinase inhibitors. Such proteins promote the tumour growth with no apparent impact of p53 phenotype whilst voltage-dependent anion-selective channel protein 2 contributes to the development of resistance only in cells with functional p53 which is accompanied by the decreased level of elongation factor 2. On the other hand, cancer cells with loss of p53 appear to amplify alternative mechanisms such as protection against oxidative stress. The results indicate that not only quantitative protein changes but also other parameters such as post-translational modification(s) and subcellular localisation have a critical role to play in drug resistance. Only specific forms of Y-box binding protein 1 and HSP70/90-organizing protein contribute to the development of drug resistance to cyclin-dependent kinases inhibitors. We believe that this work will stimulate further research, ultimately leading to the clarification of protein functionalities as novel targets for cancer therapy. This study highlights several proteins which might allow stratification of cancer patients in clinics and opens up an interesting avenue in translational research.

Abstrakt

Cílená onkologická léčba je namířena proti specifickým molekulám zodpovědným za karcinogenezi a růst nádorů. Účinek této efektivní terapie je však stejně jako u konvenční chemoterapie závislý na výbavě nádorových buněk, které mohou rozvíjet rezistenci. Pro studium mechanismů působení protinádorových léčiv a charakterizaci nádorové rezistence jsme využili modely lidských buněčných linií s různým fenotypem nádorového supresoru p53 a podrobily je kvantitativní proteomické analýze. Podařilo se nám identifikovat proteiny významně ovlivněné působením léčiv podobné struktury a také proteiny účastnící se rozvoje nádorové rezistence. Po ošetření buněk protinádorovými léčivy docházelo k bezprostřednímu ovlivnění buněčného metabolismu, který byl u rezistentních buněk modulován trvale. Zjistili jsme, že k rozvoji nádorové rezistence k působení inhibitorů Aurora kináz významně přispívá vysoká hladina proteinů serinhydroxymethyltransferázy, serpinu B5 a calretininu, které podporují progresi nádoru nezávisle na expresi proteinu p53. Voltage-dependent anion-selective channel protein 2 se účastní rozvoje rezistence pouze u nádorových buněk s funkčním p53 a tyto buňky vykazují také nízkou expresi elongačního faktoru 2. Buňky s mutovaným p53 pak během rozvoje rezistence posilují antioxidační mechanismy. Klíčovou úlohu v odpovědi na protinádorovou léčbu mají specifické varianty proteinů. S rozvojem rezistence k působení inhibitorů cyklin-dependentních kináz dochází v nádorových buňkách k významnému posunu v poměru kyselých a bazických forem Y-box vázajícího proteinu 1 a proteinu organizujícího Hsc70/Hsp90, které jsou doprovázené také změnou buněčné lokalizace. Pouze určité formy těchto proteinů jsou zodpovědné za progresi nádorového onemocnění a rozvoj nádorové rezistence. Další charakterizace proteinů může vést k nalezení biomarkerů pro stratifikaci onkologických pacientů a rozvoji efektivních léčebných postupů.

Obsah

1. Úvod 3
1.1. Proteomika 3
1.1.1. Separační metody 4
1.1.2. Hmotnostní spektrometrie 5
1.1.3. Protilátkové přístupy 9
1.2. Kvantitativní proteomika 13
1.3. Izoformy a modifikace proteinů 15
1.4. Hledání biomarkerů 15
1.5. Modely 18
1.5.1. Léčba nádorových onemocnění 19
1.5.2. Inhibitory Aurora kináz 21
1.5.3. Inhibitory cyklin–dependentních kináz 22
1.5.4. Antracyklinová antibiotika 24
1.5.5. Nádorová rezistence 24
2. Cíle Práce 26
3. Metody 27
3.1. Ustavení rezistentních nádorových linií 27
3.2. 2DE 28
3.3. 2D-LC 29
3.4. MALDI MS 30
3.5. Verifikace proteomických dat 30
3.6. Funčkní interpretace dat 31
3.7. Deplece majoritních proteinů 32
4. Výsledky 33
4.1. Charakterizace mechanismů nádorové rezistence k působení inhibitorů Aurora kináz 33
4.2. Charakterizace mechanismů nádorové rezistence k působení inhibitorů cyklin-dependentních kináz 50
4.3. Charakterizace mechanismů působení antracyklinů na nádorové buňky 63
4.4. Analýza reálných biologických vzorků v rámci hledání kandidátních proteinů pro včasnou diagnostiku ovariálního hyperstimulačního syndromu. 91

5. Diskuze 106
5.1. Charakterizace mechanismů nádorové rezistence k působení inhibitorů Aurora kináz 106
5.2. Charakterizace mechanismů nádorové rezistence k působení inhibitorů cyklin-dependentních kináz 111
5.3. Charakterizace mechanismů působení antracyklinů na nádorové buňky 114
5.4. Analýza reálných biologických vzorků v rámci hledání kandidátních proteinů pro včasnou diagnostiku ovariálního hyperstimulačního syndromu 117
6. Závěr 120
7. Citovaná literatura 122
8. Použité zkratky 138
9. Přehled publikací 140
9.1. Publikace v časopise s IF 140
9.2. Publikace přijaté k uveřejnění v časopise s IF 140
9.3. Patentové žádosti 140
9.4. Publikace v časopise bez IF 141
9.5. Publikace v knižních sbornících 141
9.6. Prezentace výsledků 141
9.6.1. Přednášky 141
9.6.2. Plakátová sdělení 142
9.6.3. Spoluautorství 142
10. Curriculum Vitae 144

1. Úvod

Proteomické technologie zaznamenávají velký zájem vědecké společnosti díky svému potenciálu odhalit řadu dosud nepopsaných dějů, které probíhají v organismech za fyziologických i patologických stavů. Poprvé použil označení "proteom" Marc Wilkins v roce 1994 pro soubor proteinů, které se nachází za daných podmínek na určitém místě. Takové proteiny mají charakteristickou strukturu a vykonávají specifickou funkci, která se může lišit podle aktuálních požadavků organismu, např. pod vlivem nepříznivých podmínek (N. L. Anderson and Anderson 1998). Uceleným pohledem proteomika přispívá např. k rozvoji diagnostických metod, zdokonalení léčebných postupů a vývoji velmi účinných léků.

Z důvodu velké variability proteinů, včetně jejich post-translačních modifikací a celé řady proteinových interakcí představuje proteom mnohem složitější systém než genom a transkriptom, jejichž charakterizace vede rovněž k lepšímu pochopení biologických procesů. Zatímco genom je za fyziologických podmínek ve všech buňkách organismu stálý, proteom a jeho změny určuje funkce a lokalizace jednotlivých buněk. Ke studiu genové exprese značně přispěla transkriptomika. Ukázalo se ale, že hladina mRNA v řadě případů neodpovídá hladině proteinu a přepsaná genetická informace neznamená vždy proteinovou translaci (Rogers et al. 2008). Studium proteinů je tedy nenahraditelný způsob, jak pochopit mechanismy, kterými buňky disponují za určitých stavů.

Neodlučitelným nástrojem proteomiky je **hmotnostní spektrometrie** (z angl. *Mass Spectrometry*, MS). Tato citlivá a specifická analytická technika dokáže rychle a s vysokou přesností určit hmotnost částic a odliší tak molekuly s různým složením jako jsou proteiny/peptidy a další sloučeniny. Pokud je spektrometr napojený na účinnou separaci, můžeme na základě chování v elektrickém nebo magnetickém poli identifikovat jednotlivé proteiny a mapováním proteomů získáme odpověď na řadu biologických otázek. Toho lze vedle studia patologických stavů využít také při sledování účinku nových, ale i zavedených léčiv, jejichž mechanismus účinku není přesně znám. Identifikace proteinů, které se účastní rozvoje onemocnění, může také vést k nalézení markerů tolik potřebných v klinickém prostředí pro včasný a účinný terapeutický zásah.

1.1. Proteomika

Proteom představuje soubor proteinů, které se nachází v určitou dobu na určitém místě zahrnující veškeré jejich formy a modifikace (N. L. Anderson and Anderson 1998).

Zatímco v genomu je zapsána informace pro přibližně 20–25 tisíc nezastupitelných proteinů, po sestřihu RNA a post-translačních modifikacích (PTM) je počet unikátních proteinů odhadován na milióny (Jensen 2004; Matlin et al. 2005). Globální studium proteinů a charakterizace dynamiky jejich složení proto představuje velmi složitý úkol. Pro studium molekulárních mechanismů je třeba určit lokalizaci procesů v organismu i samotných buňkách. Teprve poté je možné zabývat se hojností určitých forem proteinů, jejich modifikacemi a biologickou funkcí. Současné proteomické přístupy jsou založené na separačních metodách a MS nebo na interakci s protilátkami. Techniky můžeme rozdělit na objevné (z angl. *Discovery*), které pro analýzu nepotřebují předchozí znalost složení proteinů, a cílené (z angl. *Targeted*), které ze znalosti složení vychází.

1.1.1. Separační metody

S využitím účinných separačních technik se významně snižuje komplexita vzorku. Proteiny/peptidy je možné analyzovat pomocí MS až po frakcionaci na základě fyzikálních a chemických vlastností jako je izoelektrický bod (pI), náboj, velikost/molekulová hmotnost (z angl. *Molecular Weight*, MW) a hydrofobicita. Separační metody dělíme na elektromigrační a chromatografické.

Mezi **elektromigrační metody** řadíme izoelektrickou fokusaci (z angl. *IsoElectric Focusing*, IEF), SDS polyakrylamidovou gelovou elektroforézu (z angl. *Sodium Dodecyl Sulfate PolyAcrylamide Gel Electrophoresis*, SDS-PAGE), nativní elektroforézu (z angl. *Blue Native PolyAcrylamide Gel Electrophoresis*, BN-PAGE) a další jejich modifikace. Amfoterní molekuly proteinů migrují při IEF v gradientu pH v elektrickém poli až do místa, kde se jejich celkový náboj rovná nule, a dělí se tedy podle pI (Righetti and Drysdale 1973). Při SDS-PAGE obklopuje denaturační detergent SDS proteiny v roztoku a uděluje všem stejný záporný náboj. Proteiny pak migrují k anodě v polyakrylamidovém gelu, který tvoří molekulové síto a rozděluje proteiny podle velikosti (Shapiro et al. 1967). Proteiny lze také rozdělit nejprve pomocí IEF podle pI a následně pomocí SDS-PAGE podle velikosti v separaci označované jako 2D elektroforéza (z angl. *2D electrophoresis*, 2DE). Zatímco SDS vytváří podmínky denaturační, pro analýzu komplexů nebo pro sledování aktivní konformace proteinů je třeba zachovat nativní podmínky a BN-PAGE v takovém případě rozděluje proteiny podle velikosti, tvaru, struktury a náboj uděluje modrá barva Coomassie (Wittig et al. 2006).

Kapalinová chromatografie (z angl. *Liquid Chromatography*, LC) slouží k separaci látek na základě různé afinity k stacionární a mobilní fázi. Mobilní fáze unáší vzorek

chromatografickým systémem a přivádí ho ke koloně, která specificky interaguje s proteiny/peptidy ve vzorku a podle složení aminokyselin je různou silou váže. Použitím chromatografické kolony s reverzní fází (z angl. *Reversed Phase*, RP) dochází k separaci na základě různé hydrofobicity. Na matrici kolony jsou navázané vysoce hydrofobní alifatické řetězce různé délky (C2–C18), mobilní fázi tvoří gradient organického rozpouštědla, který z kolony postupně uvolňuje proteiny/peptidy vzorku. Jedná se o nejčastější způsob přímého (on-line) spojení LC s MS (Henry and Meleady 2011). V případě iontoměničové chromatografie (z angl. *Ion Exchange Chromatography*, IEC) se proteiny/peptidy vážou na kolonu na základě specifických interakcí s nabitým nosičem (katex, anex) a mobilní fází je gradient iontové síly. Obdobou IEF v chromatografickém provedení je tzv. chromatofokusace (z angl. *ChromatoFocusing*, CF), kde se proteiny vážou na IEC kolonu a mobilní fází je gradient pH (Gunther et al. 2012). IEC se s oblibou používá pro analýzu PTM (Edelmann 2011).

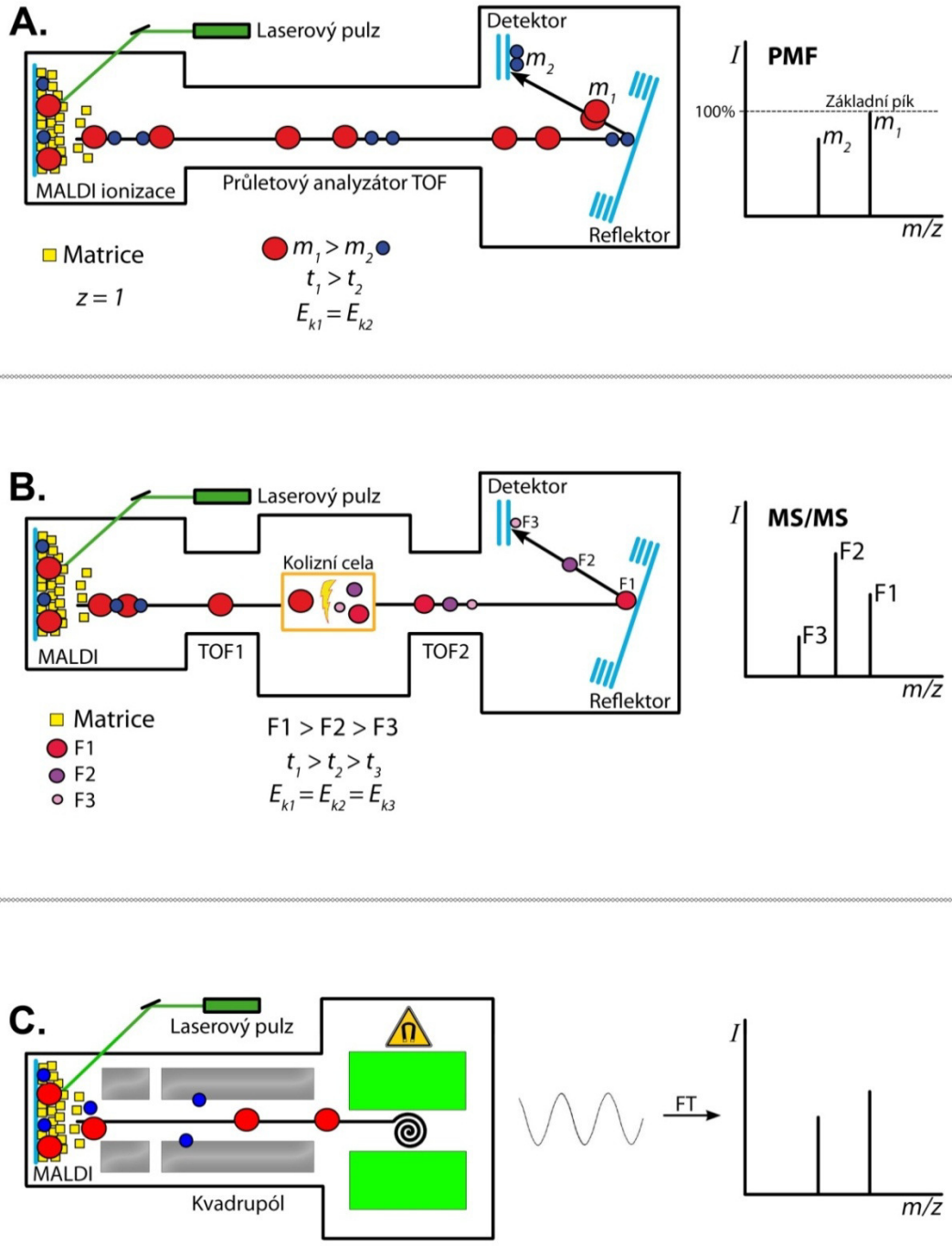
Gelová chromatografie (z angl. *Size Exclusion Chromatography*, SEC) se používá pro hrubou frakcionaci zejména proteinů a velkou výhodou této techniky je možnost izolace proteinových komplexů za nativních podmínek a následné funkční studium proteinů (Gao et al. 2010). Při SEC se velké proteiny pohybují rychleji, zatímco malé jsou brzděny interakcí s póry gelu. Pro purifikaci proteinových komplexů se používá také afinitní chromatografie (z angl. *Affinity Chromatography*, AC) (Zoumaro-Djayoon et al. 2012). Na kolonu se zakotví ligand (protein, protilátka, DNA apod.) a specifickou interakcí s ligandem jsou vychytávány proteiny/peptidy vzorku, které společně tvoří funkční celky. Afinitní chromatografie se využívá také k odstranění proteinů o vysoké koncentraci, tzv. depleci. Příkladem může být deplece majoritních proteinů plazmy jako je albumin a imunoglobuliny pomocí protilátek (Faulkner et al. 2011; Q. Zhang et al. 2011). Stejně jako elektromigrační metody je možné s výhodou kombinovat také chromatografické separace, např. IEC-RPLC a IEF-RPLC (Antberg et al. 2012), RP-RPLC (McQueen and Krokhin 2012), CF-RPLC (Sheng et al. 2011), AC-2DE (Santamaria et al. 2012), AC-RPLC (Zoumaro-Djayoon et al. 2012), SEC-IEC-RPLC (Jacobs et al. 2004).

1.1.2. Hmotnostní spektrometrie

S využitím moderních MS technologií dnes můžeme detekovat hladinu tisíců proteinů a mapovat tak proteomy určitých tkání, buněk nebo jejich organel (Domon and Aebersold 2010). Specifickým štěpením proteinů pomocí proteáz vznikají peptidy s určitým počtem aminokyselin, tj. fragmenty definované hmotnosti. Po udělení náboje *z* v ionizačním zdroji

prochází peptidové ionty určité hmotnosti *m* hmotnostním analyzátorem ve vakuu a detektor pak zaznamenává jejich intenzitu *I* (obr. 1A). Následným porovnáním naměřených spekter (poměr *m/z* vynesený proti relativní *I* jednotlivých iontů) s teoretickými údaji v databázi je možné zjistit identitu proteinů. Tato metoda peptidového mapování (z angl. *Peptide Mass Fingerprinting*, **PMF**) označuje identifikaci proteinů na základě unikátních profilů peptidů definované hmotnosti (Pappin et al. 1993).

Připojením dalšího analyzátoru přes kolizní celu (**MS/MS**) je možné použít první MS pro rozlišení peptidových iontů a výběr jednoho peptidu, v kolizní cele tento peptid podrobit fragmentaci aplikací vyšší energie a v druhém MS detekovat produkty této fragmentace (obr. 1B). Tandemovou hmotnostní spektrometrií je možné zjistit primární strukturu (složení jednotlivých aminokyselin včetně PTM) a proteiny tak sekvenovat *de novo* (Shevchenko et al. 1996). Instrumentaci a parametry vyhledávání v příslušné databázi volíme vždy podle druhu vzorku, množství proteinu a přesnosti měření. Úspěšná identifikace vyžaduje dostatek proteinu s unikátní sekvencí a MS s dostatečnou citlivostí, přesností a rozlišením.



Obrázek 1. Schéma hmotnostních spektrometrů používaných v disertační práci. A. MALDI-TOF (z angl. *Matrix-Assisted Laser Desorption/Ionization Time-Of-Flight*). B. MALDI-TOF/TOF. C. FT-ICR (z angl. *Fourier Transform Ion Cyclotron Resonance*). Převzato a upraveno podle souhrnného článku Aebersold and Mann 2003. Vysvětlivky: *z*, náboj ; *t*, doba letu; E_k, kinetická energie; *m*, hmotnost mateřského peptidu; *F*, hmotnost peptidového fragmentu; *I*, relativní intenzita; PMF, peptidové mapování (z angl. *Peptide Mass Fingerprinting*); FT, Fourierova transformace.

V přímém napojení na LC se pro ionizaci peptidů používá elektrosprej (z angl. *Electrospray Ionization*, **ESI**). Aplikací vysokého napětí dochází v ESI-MS k nabití kapek analytu, které jsou přiváděny vyhřívanou kapilárou do vakua analyzátoru. V důsledku odpaření organického rozpouštědla se postupně zmenšuje objem kapek a zvyšuje se hustota náboje, což vede k opakovanému rozpadu (Coulombické štěpení) a převedení jednotlivých iontů z kapalné do plynné fáze (Fenn et al. 1989). Další šetrnou technikou v proteomických aplikacích je ionizace laserem za účasti matrice (z angl. *Matrix-Assisted Laser Desorption/Ionization,* **MALDI**). Analyt není přiváděn z LC do analyzátoru přímo, ale nanáší se společně s matricí (nízkomolekulární aromatická kyselina) v organickém rozpouštědle na kovovou destičku, kde společně krystalizují. Po vypaření rozpuštědla dopadá na krystaly laserový paprsek, jeho energii nejprve absorbuje matrice, která následně uděluje náboj molekule analytu a ionty jsou převedeny z pevné do plynné fáze (obr. 1) (Karas and Hillenkamp 1988). Výběr vhodné matrice a intenzity laseru omezuje nežádoucí fragmentaci a umožňuje tak jednoduchou interpretaci spektra. Zatímco při ESI vznikají vícenásobně nabité ionty, MALDI primárně generuje jedenkrát nabité ionty a lépe toleruje soli ve vzorku.

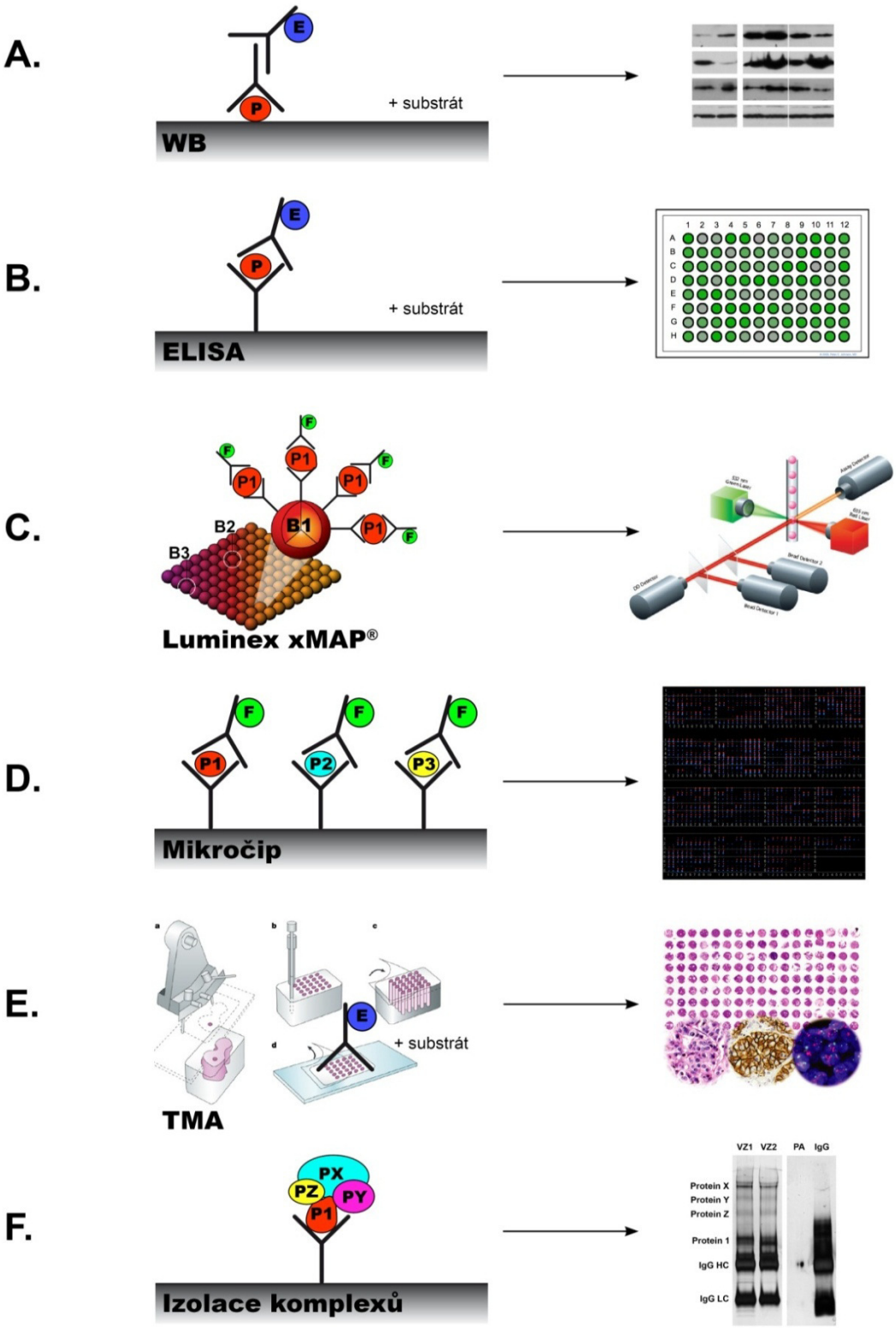
Nejčastěji se MALDI používá ve spojení s průletovým analyzátorem (z angl. *Time-Of-Flight,* **TOF**) nebo iontově cyklotronovou rezonancí s Fourierovou transformací (z angl. *Fourier Transform Ion Cyclotron Resonance,* **FT-ICR**) (obr. 1). TOF je trubicový analyzátor, který uděluje stejně nabitým iontům stejnou kinetickou energii a přivádí je k detektoru. Nejrychleji přitom trubicí putují nejlehčí ionty a nejtěžší dopadají na detektor jako poslední (Yip and Hutchens 1992). Doba letu *t* pak určuje *m/z* iontů. Ve spojení s pulzní ionizací zaznamenává TOF celé hmotnostní spektrum. Letová trubice může být doplněna o reflektor, který koriguje pohyb iontů o stejné *m/z* ale rozdílné kinetické energii, prodlužuje dráhu letu a zvyšuje tak rozlišení a přesnost měření. FT-ICR analyzátor určuje *m/z* podle frekvence pohybu iontů po cyklotronové orbitě v homogenním magnetickém poli a disponuje mnohem vyšší rozlišovací schopností a přesností (Marshall et al. 1998). Cyklotronový pohyb indukuje proudový obraz, ten je amplifikován a ionty jsou pak detekovány jako superpozice sinusoidálních vln, které se převádí do hmotnostního spektra Fourierovou transformací.

Na podobném principu pracuje hmotnostní analyzátor typu Orbitrap. Ionty v Orbitrapu obíhají centrální elektrodu, působením elektrostatické síly podélně oscilují a generují tak v detektoru proudový obraz (Hu et al. 2005). Frekvenci oscilace určuje *m/z* iontů a hmotnostní spektra jsou podobně jako u ICR vytvořena Fourierovou transformací. Jedná se o velmi citlivý analyzátor s vysokou přesností a dynamickým rozsahem. Oscilující elektrické pole určuje pohyb iontů také v iontové pasti (z angl. *Ion Trap,* IT) a kvadrupólovém analyzátoru

(z angl. *Quadrupole*, Q), které se používají jako jednodušší hmotnostní filtry. V tandemovém spojení je možné kombinovat analyzátory stejného typu (např. TOF/TOF), jako hybridní označujeme spojení různých analyzátorů (např. Q-TOF).

1.1.3. Protilátkové přístupy

Pomocí afinitních technik založených na protilátkách je možné odhalit kvalitativní i kvantitivní rozdíly proteinů včetně jejich modifikací v komplexních vzorcích bez předchozí separace (Wingren and Borrebaeck 2004). Specifické protilátky se používají v řadě aplikací jako je např. imunoblot (z angl. *Western Blot*, WB), enzymová imunoanalýza (z angl. *Enzyme-Linked ImmunoSorbent Assay*, ELISA), Luminex xMAP®, proteinové mikročipy, tkáňové profilování (z angl. *Tissue MicroArrays*, TMA) a také při izolaci/purifikaci proteinů a jejich komplexů. Vychytávání protilátkami probíhá na podobném principu (obr. 2), liší se však množství analyzovaných proteinů, množství potřebného vzorku, způsob detekce signálu (kolorimetrie, chemiluminiscence, fluorescence), kvantifikace (absolutní, relativní, semikvantifikace), uspořádání (plošné, v roztoku) a v neposlední řadě zpracování dat.



Obrázek 2. Schéma metod založených na protilátkách. A. WB (z angl. *Western Blot*). B. ELISA (z angl. *Enzyme-Linked ImmunoSorbent Assay*). C. Luminex xMAP® (převzato a upraveno podle http://www.panomics.com). D. Proteinový mikročip. E. TMA (z angl. *Tissue MicroArrays*), převzato a upraveno podle souhrnného článku Sauter et al. 2003. F. Izolace proteinových komlexů. Vysvětlivky: P, protein; E, konjugovaný enzym; F, fluorescenční značka; B, fluorescenční kulička (z angl. *Bead*).

WB, též označovaný jako imunoblot, se používá k detekci proteinů po rozdělení podle velikosti nebo struktury pomocí gelové elektroforézy. Rozdělené proteiny se přenesou z gelu na povrch membrány, která je inkubována se specifickou protilátkou namířenou proti konkrétnímu proteinu. Tato primární protilátka může být přímo značená pro detekci nebo se na ní váže sekundární druhově-specifická protilátka s konjugovaným enzymem. Po aplikaci vhodného substrátu je detekován signál, jehož kvantitu je možné denzitometricky vyhodnotit a relativně pak porovnat hladinu jednotlivých proteinů mezi vzorky. Nevýhodou této analytické techniky je její semikvantitativní charakter. Jedná se ale o rychlou a jednoduchou metodu vhodnou zejména pro verifikaci proteomických dat (Acosta-Martin et al. 2011; Dai et al. 2011).

Přesnější a rychlejší kvantifikace je možná pomocí **ELISA** testu, kde jsou v případě sendvičového uspořádání protilátky zakotvené na povrchu mikrotitrační destičky. Po aplikaci vzorku a vychytání proteinu je přidána další protilátka s konjugovaným enzymem. Ten opět umožňuje po přidání substrátu detekci signálu a porovnáním se standardem také absolutní kvantifikaci proteinů (Makawita et al. 2011; Tiberti et al. 2010). Místo enzymu může být na protilátce konjugovaná i fluorescenční značka, jejíž signál lze měřit přímo, bez přidání substrátu. Tento typ imunoanalýzy našel pro svou rychlost a možnost automatizace široké uplatnění v klinických laboratořích. Nevýhodou ELISA metod je možnost měření hladiny pouze jednoho proteinu a vysoká spotřeba vzorku v případě analýzy více proteinů.

V klinických laboratořích proto našla uplatnění multiplexní technologie **Luminex xMAP®**, která dokáže s využitím mikrosfér kvantifikovat desítky unikátních proteinů v roztoku minimálního objemu během jedné analýzy (Craig-Schapiro et al. 2011; Daemen et al. 2008; B. K. Kim et al. 2009). Na povrchu mikrosfér s různým fluorescenčním značením jsou zakotvené různé protilátky, které specificky vážou vybrané proteiny ze vzorku. Druhá protilátka s fluorescenčním značením se pak váže na vychytané proteiny a určuje při porovnání se standardem jejich absolutní množství. Na rozdíl od metod ELISA může být u této multiplexní techniky v jedné jamce mikrotitrační destičky až několik desítek mikrosfér, což vede k významné úspoře vzorku i času analýzy. Alternativou v plošném uspořádání jsou **proteinové mikročipy** detekující velká množství proteinů v nejrůznějších vzorcích (Barderas et al. 2012; Loch and Strickler 2012; Sandstrom et al. 2012).

Další technikou je **TMA** profilování používané pro studium velkého množství řezů tkání. Navázáním protilátky s konjugovaným enzymem a přidáním substrátu je možné detekovat stovky proteinů na jednom druhu tkáně (Hodgkinson et al. 2012; C. Li et al. 2012; Pawar et al. 2011). Nevýhodou však může být značná heterogenita odebrané tkáně. Důležitým

krokem multiplexních metod i TMA je důkladné a správné vyhodnocení dat, které je s přibývajícím počtem analyzovaných proteinů náročnější, zejména ze statistického pohledu. S využitím protilátkových technik je ale možné jak identifikovat molekulární mechanismy, tak najít markery pro stratifikaci řady onemocnění, které by přispěly ke zdokonalení diagnostických a léčebných postupů.

Izolace proteinů a jejich komplexů pomocí protilátek umožňuje studium proteinových interakcí a signálních drah (Beaufour et al. 2012; Fang et al. 2012; Ruperez et al. 2012). Pro izolaci komplexů za nativních podmínek se s oblibou používají protilátky zakotvené na pevném povrchu jako jsou agarózové kuličky nebo chromatografické kolony. Změnou podmínek na denaturační pak lze oddělit a identifikovat jednotlivé proteiny komplexu. Důležitým aspektem při analýze interakcí jsou nespecifické vazby proteinů na protilátku nebo samotný povrch, kde jsou protilátky ukotveny. Proto je vždy nezbytné vzít tyto aspekty do úvahy a zařadit do plánovaného pokusu dostatek negativních kontrolních vzorků. Pro interpretaci dat se využívaji softwary, které na základě známých, experimentálních a predikovaných interakcí vytváří **interakční mapy** (Brown and Jurisica 2007; Smoot et al. 2011; Snel et al. 2000; Thomas et al. 2003). Otázkou ale zůstává spolehlivost vyhodnocení, protože překryv mezi databázemi interakcí je minimální a různé softwary tak generují různé výsledky. Řešením by mohla být databáze sestavená integrací primárních dat, odstraněním falešně pozitivních interakcí a přiřazením 3-D struktury interakčních proteinů (De Las Rivas and Fontanillo 2010). Do té doby však budou interakční mapy představovat pouze pomocný nástroj pro studium interaktomu a důvěryhodnost bude vždy určovat biologický kontext (Kohli et al. 2012; Saha et al. 2012; Van Leene et al. 2010).

Protilátkové metody pomohly rozšířit naše povědomí o celé řadě procesů. Tyto přístupy jsou ale závislé na dostupnosti jednotlivých protilátek, a proto byl v roce 2005 vytvořen **Atlas lidských proteinů** (z angl. *Human Protein Atlas*) (Uhlen et al. 2005). Jeho cílem bylo vyrobit specifické protilátky proti celému proteomu a charakterizovat expresi a lokalizaci proteinů v lidských tkáních za fyziologických podmínek a během nádorového bujení. Byl tak vytvořen důležitý nástroj pro biologický a lékařský výzkum. Na modelových oganismech a v případě studia určitých modifikací proteinů ale není použitelnost protilátek zaručena a pro získaní detailních a reprodukovatelných výsledků je pak nezbytná validace protilátkových testů (např. ELISA). Test musí splňovat základní analytické charakteristiky, což může v klinickém výzkumu vyžadovat několikaměsíční měření celé řady parametrů (Uhlen and Hober 2009).

1.2. Kvantitativní proteomika

V rámci sledování buněčné dynamiky je třeba posuzovat míru exprese proteinů a také míru jejich modifikace. Složení aminokyselin určuje ionizační vlastnosti proteinů/peptidů a velikost MS signálu proto neodpovídá jeho celkovému množství ve vzorku. I přes minimální množství ve vzorku často detekujeme peptidy s vyšším zastoupením např. bazických aminokyselin a naopak přicházíme o hojně zastoupené peptidy s neutrálními alifatickými aminokyselinami. Kvantifikace probíhá podle zvoleného způsobu separace na úrovni proteinů nebo peptidů a může být **relativní** nebo **absolutní**. I přes intenzivní snahy o zlepšení zůstává slabinou proteomických experimentů obtížná reprodukovatelnost a robustnost měření mezi jednotlivými laboratořemi (Hause et al. 2011). Z důvodu obrovské komplexity proteinů/peptidů v biologických vzorcích je proto u relativních porovnání nezbytná **verifikace** proteomických dat nezávislou technikou.

Rozdělené intaktní **proteiny** se mohou relativně porovnávat např. pomocí 2D gelové elektroforézy nebo 2D kapalinové chromatografie (Balonova et al. 2010; Deford et al. 2009; McDonald et al. 2006; Wen et al. 2012). S rychlým vývojem metod LC-MS/MS poklesl v poslední době zájem o tyto techniky. Jejich velkou výhodou však zůstává poměrně vysoká robustnost analýz a možnost detekce PTM, které mění na úrovni intaktních proteinů izoelektrický bod, hmotnost nebo hydrofobicitu (např. fosforylace, glykosylace, zkrácení řetězce) (Deford et al. 2009; Di Michele et al. 2010; Layton et al. 2012; Samyn et al. 2009).

Prvním krokem **2DE** je IEF, která rozděluje proteiny podle pI. V druhém směru jsou proteiny děleny podle MW pomocí SDS-PAGE a výsledná 2D mapa proteinových skvrn (spot) je podrobena obrazové analýze. Výběr druhu barvení pro detekci a kvantifikaci proteinů určuje především citlivost, linearitu signálu a dynamický rozsah. Fluoresenční barvení splňuje uvedená kritéria nejlépe, k získání obrazu je však zapotřebí skener s příslušnými lasery a detektory. Software při vyhodnocení měří fluorescenční signál jednotlivých spot, ten pak integruje a signál jednotlivých spot k této integrované hodnotě vztahuje. Následuje porovnání relativních hodnot mezi vzorky a hledání rozdílné hladiny proteinů. Nalezené diferecní spoty se po obarvení gelu vyříznou a podrobí MS analýze. Výběr barvy pro vizualizaci spot je pro úspěšnou identifikaci proteinů kritický. Dobrou kompatibilitu s MS zajišťují modré barvy Coomassie (např. koloidní G-250) a reverzní barvení zinkem. **2D-LC** rozděluje proteiny například podle pI pomocí chromatofokusace a následně podle hydrofobicity pomocí reverzní fáze. Software po normalizaci porovnává

relativní kvantitu rozdělených chromatografických píků. Nalezené píky (frakce proteinů) rozdílné mezi studovanými vzorky jsou identifikovány opět pomocí MS.

Kvantitativní "**shotgun**" proteomika štěpí proteiny ještě před separací a je založena na měření fragmentačních spekter s využitím tandemového spektrometru. **Peptidy** je možné po separaci kvantifikovat pomocí tzv. **label-free** přístupu a MS s vysokým rozlišením a přesností. Signál peptidů je integrován podobně jako u 2DE. Po normalizaci se k celkové hodnotě vztahuje signál jednotlivých peptidů a relativně tak můžeme porovnat jejich hladinu mezi vzorky (Bauer et al. 2012; Mosley et al. 2011). Další možností je porovnat hladinu peptidů metabolickým nebo chemickým **značením pomocí stabilních izotopů** (Boersema et al. 2010; Geiger et al. 2012; Giron et al. 2011; Petrak et al. 2011). Tímto způsobem se vyhneme možné záměně peptidů, které se uvolňují v podobném čase (label-free), nevýhodou značení však zůstávají vyšší náklady a časová náročnost.

Pro absolutní kvantitativní stanovení proteinů se používají výše uvedené **protilátkové metody** (ELISA, Luminex xMAP®), které jsou alternovány MS metodami jako je **SRM** (z angl. *Selected Reaction Monitoring*, SRM). Předpokladem pro úspěšné provedení SRM analýzy je přítomnost proteotypického peptidu, tzn. peptidu unikátního pro daný protein, který je dobře ionizovatelný a po definované fragmentaci se nachází ve spektru reprodukovatelně. Na základě dat naměřených pro přirozené a syntetické peptidy byla vytvořena databáze proteotypických peptidů, tzv. SRMAtlas, který představuje důležitý nástroj pro plánování SRM analýz (Deutsch et al. 2008). Analyzátory typu kvadrupól slouží při SRM jako filtry pro izolaci vybraných prekurzorů a jejich fragmentů. Místo klasického zaznamenávání spekter se při SRM monitorují specifické páry prekurzorových a fragmentových iontů, tzv. "přechody" (z angl. *Transition*), jejichž celková intenzita odpovídá množství konkrétního proteinu.

V jediném experimentu je pak možné monitorovat několik přechodů typických pro daný protein/proteiny a proto má tato technika multiplexní character a je označována také jako MRM (z angl. *Multiple Reaction Monitoring*). SRM/MRM nachází uplatnění a) při souběžné analýze až 40 proteinů (L. Anderson and Hunter 2006), b) při kvantifikaci izoforem a PTM proteinů (Held et al. 2010; Narumi et al. 2012; J. Wu et al. 2012), c) v případě nedostupnosti protilátek (Makawita and Diamandis 2010). Velkou předností, která přibližuje SRM/MRM do klinického prostředí, je reprodukovatelné měření v nezávislých laboratořích (Kuhn et al. 2012). Limitací SRM/MRM však může být nízká hladina proteinu a značná komplexita biologických vzorků. Omezení lze překonat nabohacením určitých proteinů/peptidů (N. L. Anderson et al. 2004; Stahl-Zeng et al. 2007;

Unwin et al. 2009) a deplecí majoritních proteinů (Sheng et al. 2011). Frakcionace vzorku významně snižuje komplexitu a detekční limit pro kvantifikaci proteinů je pak srovnatelný např. s ELISA testem (Fortin et al. 2009; Qian et al. 2008).

1.3. Izoformy a modifikace proteinů

Pomocí MS s vysokou rozlišovací schopností a přesností lze odlišit a také kvantifikovat jednotlivé izoformy a PTM proteinů včetně jejich pozice v řetězci aminokyselin (Contrepois et al. 2010; Held et al. 2010; Mounicou et al. 2010; Olsen et al. 2006). Právě tyto izoformy a PTM významně ovlivňují funkci a aktivitu proteinů. Řada PTM (např. fosforylace) je však přechodná, málo stabilní, nebo v nízkém zastoupení v porovnání k celkové hladině proteinu ve vzorku. Poslední z uvedených limitací lze obejít nabohacením modifikovaných proteinů/peptidů pomocí IEC (Edelmann 2011; Narumi et al. 2012) nebo použitím AC s navázanými protilátkami (J. Wu et al. 2012; Zoumaro-Djayoon et al. 2012). Pro studium PTM na úrovni intaktních proteinů se používá 2DE a 2D-LC (Deford et al. 2009; Di Michele et al. 2010; Layton et al. 2012; Samyn et al. 2009).

Reverzibilní **fosforylace** patří mezi nejčastější a nejlépe charakterizovanou modifikaci proteinů (Ytterberg and Jensen 2010). Způsobuje konformační změny proteinů a reguluje tak důležité procesy, které v organismu paralelně probíhají, zejména buněčnou signalizaci (E. Li and Hristova 2006). Nezastupitelnou úlohu v mezibuněčné komunikaci mají **glykoproteiny**, které se nacházejí na povrchu buněk a v krevní plazmě, kam jsou po buněčné sekreci dopraveny krevním oběhem (Gahmberg and Tolvanen 1996; Polanski and Anderson 2007). Izolací fosforylovaných a glykosylovaných forem proteinů se proto v posledních letech zabývaly proteomické týmy po celém světě a pomohly tak odkrýt nové skutečnosti v oblasti buněčné signalizace a komunikace (Bock et al. 2012; Gundry et al. 2009; Munoz and Heck 2011; Rigbolt et al. 2011). Je však známo více než 200 typů PTM a úkolem nových technologií bude zaměřit se i na další modifikace proteinů, např. ubikvitinace (Jensen 2004).

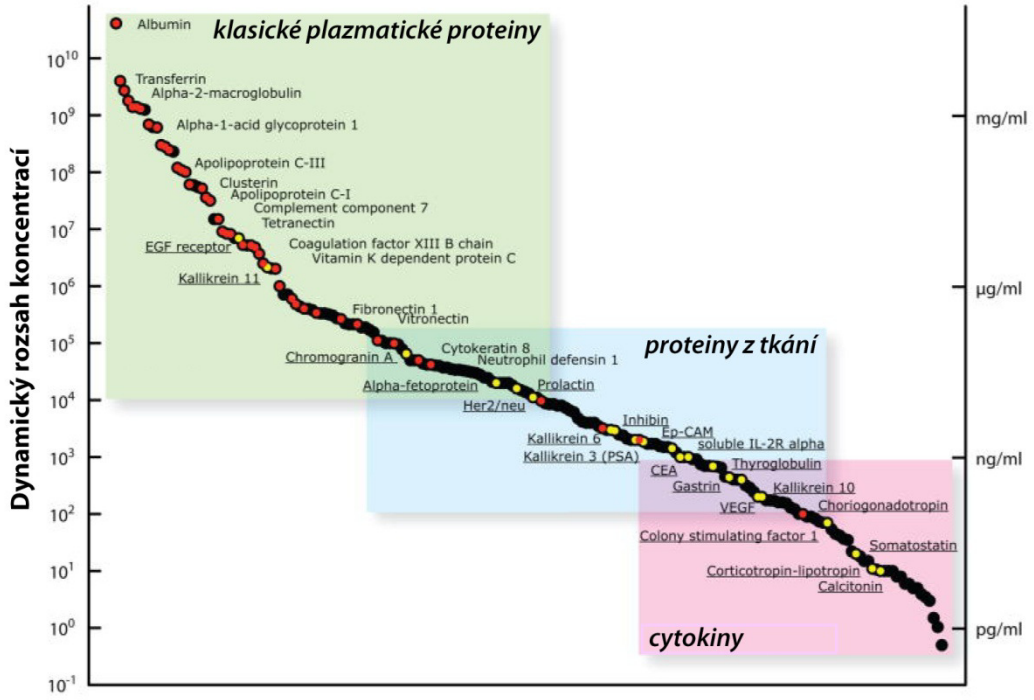
1.4. Hledání biomarkerů

Podle Úřadu pro kontrolu potravin a léčiv (z angl. *Food and Drug Administration*, FDA), vládní agentury Spojených států amerických, je biomarker definován jako ukazatel normálního biologického procesu, patogenního procesu nebo farmakologické odpovědi na terapeutický zásah, který je možné objektivně měřit a hodnotit. S využitím proteomických technologií lze odhalit strukturu a funkci proteinů včetně jejich interakcí a tyto poznatky

mohou přispět k nalezení biomarkerů a k rozvoji efektivních diagnostických a léčebných postupů. Cílem je vyvinout pro konkrétní onemocnění prediktivní, diagnostický a/nebo prognostický test, který by pomohl při volbě vhodné terapie a také při jejím monitorování (Farlow et al. 2010; Pan et al. 2012).

Potenciálním zdrojem biomarkerů jsou sekretované proteiny, které odráží stav buněk/organismu za určitých podmínek. Tento subproteom, označovaný také jako sekretom, obsahuje kromě proteinů extracelulárního prostoru a proteinů uvolněných z buněk také růstové faktory, imunoregulační cytokiny a další bioaktivní molekuly důležité pro mezibuněčnou komunikaci, růst, diferenciaci, apoptózu a další buněčné procesy. Sekretované proteiny mohou pronikat do tělních tekutin a krevním oběhem se mohou dostat až do plazmy.

Plazma představuje nejkomplexnější lidský sekretom, který vedle klasických plazmatických proteinů syntetizovaných v játrech (albumin, fibrinogen, atd.) a buňkami imunitního systému (imunoglobuliny) obsahuje také hormony, cytokiny a proteiny uvolněné z tkání následkem akutního poškození nebo rozvoje onemocnění (N. L. Anderson and Anderson 2002). Odběry krve/plazmy je možné u pacientů provádět opakovaně nez nutnosti invazivního zákroku, avšak z důvodu velkého rozsahu koncentrací jednotlivých proteinů a mimořádné dynamiky složení během fyziologických i patologických procesů (obr. 3) je velmi obtížné hledat biomarkery přímo v plazmě. Jak už bylo zmíněno, majoritní proteiny plazmy je možné odstranit pomocí protilátek (Faulkner et al. 2011; Q. Zhang et al. 2011) a sekretované proteiny nabohatit selektivní izolací N-glykopeptidů (Stahl-Zeng et al. 2007; Surinova et al. 2011). Deplecí však přicházíme o proteiny, které se na majoritní složky plazmy vážou. Náročnější zpracování vzorku navíc vždy vnáší do analýzy určitou chybu a není ideálním řešení pro klinické laboratoře, jejichž preferencí je co nejjednodušší získání reprodukovatelného výsledku. Lepší cestou by tedy bylo zdokonalení MS instrumentace.

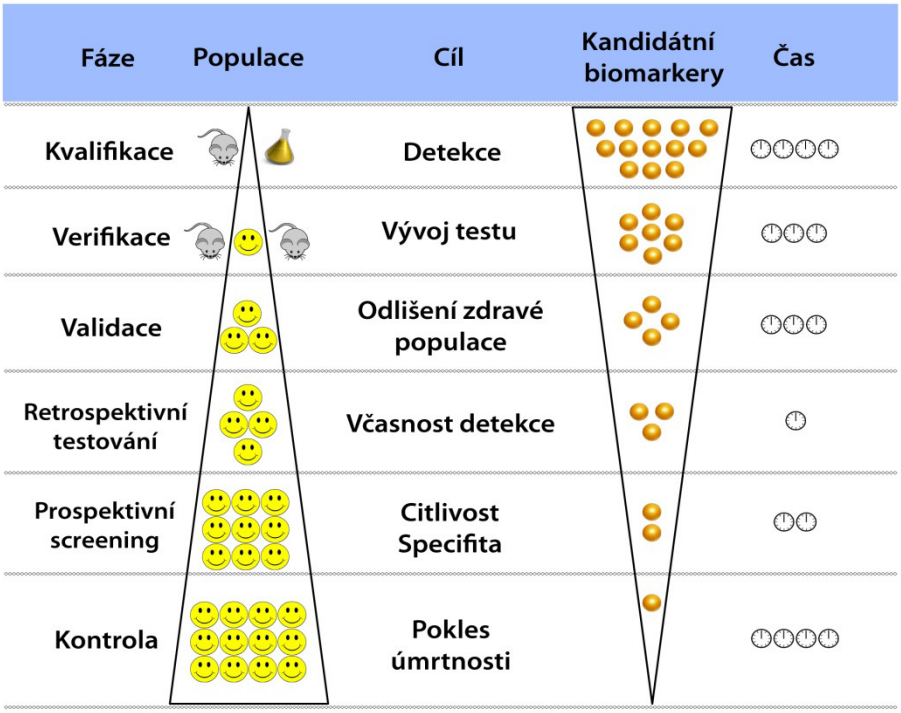


Obrázek 3. Proteom lidské plazmy. Zastoupení proteinů plazmy v dynamickém rozsahu 12 řádů je znázorněné na logaritmickém měřítku. V levé části obrázku jsou klasické plazmatické proteiny o vysoké koncentraci, uprostřed jsou proteiny uvolněné z tkání a napravo cytokiny s velmi nízkou hladinou. Převzato a upraveno podle N. L. Anderson and Anderson 2002.

Velmi slibným materiálem pro hledání biomarkerů je **moč**, konečná destinace většiny plazmatických proteinů (M. J. Kim et al. 2011). Odběr je velmi snadný a v případě funkční glomerulární filtrace je moč zbavena proteinů molekulární hmotnosti nad 45 kDa, tzn. majoritní části plazmy. Ledviny tak tvoří fyziologický systém pro depleci proteinů. Komplikací může být asymptomatické onemocnění ledvin a různé množství vody v organismu. Zpracování moči je navíc z důvodu rychlé degradace a časté mikrobiální kontaminace poněkud obtížné. Alternativou k přímé analýze plazmy a moči by mohla být preselekce biomarkerů *in vitro* v kondiciovaném médiu buněk (H. Y. Wu et al. 2009; C. C. Wu et al. 2010) nebo *in vivo* v proximálních tělních tekutinách jako je mozkomíšní mok, intersticiální tekutina nádoru nebo synoviální tekutina (Gibson et al. 2009; Gromov et al. 2010; Suk 2010) a následná validace v plazmě.

Identifikace kandidátních biomarkerů je ale jen začátek cesty, která vyžaduje dlouholetou spolupráci výzkumné a klinické laboratoře ale také komerční sféry. Nejprve musí být důkladně posouzena potřeba nového testu, klinická využitelnost a účinnost vynaložených prostředků. Teprve pak je možné hledat vhodné vzorky a spolehlivou metodu pro testování. V pre-analytické fázi se hodnotí zejména biologická variabilita, vliv zpracování vzorku,

stabilita během přepravy, dlouhodobé skladování, efekt opakovaného přemražování, apod. Se zvyšujícím se počtem testovaných vzorků, ubývá také kandidátních proteinů a pouze zlomek uspěje v klinickém testování, které je velmi nákladné a časově náročné (obr. 4). Proteomika nachází uplatnění jak při hledání kandidátních biomarkerů, tak při testování velkého počtu vzorků. V případech, kdy ELISA naráží na překážky jako je zkřížená reaktivita, přítomnost autoprotilátek apod., je možné využít pro přesné, reprodukovatelné a robustní měření metodu SRM, která má také výhodu kvantifikace více analytů v jednom měření.



Obrázek 4. Vývoj nového klinického testu. Převzato a upraveno podle Simpson et al. 2008.

1.5. Modely

Disertační práce pojednává o využití proteomických technologií při studiu nádorové léčby se zaměřením na analýzu účinku protinádorových léčiv a charakterizaci mechanismů nádorové rezistence. Pro studium těchto mechanismů byly využity **modely lidských buněčných linií** odvozených z kolorektálního karcinomu (HCT116), T-lymfoblastické leukémie (CCRF-CEM) a adenokarcinomu plic (A549). Buněčné linie se získávají z nádorů přímo nebo cílenou selekcí pomocí mutagenů z primárních kultur a jejich výhodou je neomezené dělení, tedy relativně nekonečný zdroj materiálu. Takové buňky představují jednoduchý model pro složité biologické systémy, který můžeme po ošetření léčivem podrobit

analýze. Selekce nesmrtelných buněk je ale doprovázena také chromozomálními změnami a je třeba mít vždy na paměti, že buňky jsou mutované.

Biologické systémy jsou charakteristické svou variabilitou a poznatky z analýzy buněčných linií je proto nezbytné ověřovat v reálných vzorcích primárních buněk či tkání. Zatímco buňky v kultuře odpovídají na různé stimuly pouze na základě vlastní výbavy, v organismu reagují na změnu podmínek také okolní tkáně a dochází k velmi komplexním procesům. Tkáně zároveň odpovídají na celou řadu dalších stimulů a odlišit reakci na jednotlivé procesy je prakticky nemožné. V proteomických aplikacích, které se zabývají globálním studiem proteinů, hraje **biologická variabilita** významnou roli. Klíčové je proto pečlivé plánování experimentů a zařazení dostatečného počtu kvalifikovaně získaných vzorků, které umožní překonat inter-individuální variabilitu a nalézt proteiny skutečně zodpovědné za pozorovaný znak. Na základě vlastní zkušenosti s reálnými biologickými vzorky zastávám názor, že takový materiál by měl být podroben analýze pouze kvalifikovaným proteomikem s využitím vhodně vybraných postupů.

1.5.1. Léčba nádorových onemocnění

Nádorová onemocnění představují v současné době jednu z nejčastějších příčin úmrtí (Jemal et al. 2011). Za normálních okolností je organismus schopen rozpoznat mutace DNA a takové populace buněk podle míry poškození opraví nebo zneškodní a zamezí tak jejich množení. Pokud se mutované buňky vymknou kontrole, začnou v organismu autonomně růst na úkor zdravých tkání, jejichž funkce jsou vlivem nádorového bujení narušeny. Nezhoubné benigní nádory jsou obvykle dobře ohraničené od svého okolí a lze je chirurgicky odstranit bez větších následků. V případě maligního růstu pronikají nádorové buňky do okolní tkáně, tvoří metastázy a jejich léčba vyžaduje vedle chirurgického zákroku také léčbu ozářením (radioterapie) a/nebo cytostatiky (chemoterapie) pro likvidaci mikroskopických ložisek, které by mohly způsobit relaps onemocnění.

Podle míry a lokalizace zasažení tkáně/tkání se volí druh i dávka **chemoterapie**. Mezi nejčastěji používaná cytostatika, která potlačují buněčné dělení a růst nádorů, patří antimetabolity, alkylační a interkalační léčiva, inhibitory topoizomeráz, mitotické jedy, taxany a cytostatická antibiotika. Princip léčby vychází z předpokladu, že rychle se dělící buňky nádoru jsou citlivější k působení toxických léčiv než buňky zdravé. Většina dospělých diferencovaných buněk se již nerozmnožuje a chemoterapie na ně nepůsobí. Výjimkou jsou buňky tkání, které podléhají časté obnově, tj. buňky trávicího traktu, jater, krve apod.

Poškození těchto buněk během chemoterapie způsobuje vážné vedlejší účinky, jejichž následky mohou být i trvalé.

I přes zmírnění obtíží řadou podpůrných léků a optimalizací dávek cytostatik vychází konvenční chemoterapie pouze ze statistického hodnocení různých léčebných režimů a přesný mechanismus působení některých léčiv nebyl doposud ani popsán. Místo omezování růstu nádorových buněk systémovou léčbou s toxickými účinky je mnohem perspektivnější hledání příčin rozvoje onemocnění a vývoj nových cílených léků. **Cílená onkologická léčba** je namířená proti specifickým molekulám zodpovědným za karcinogenezi a růst nádorů. Aplikací biologických léků dochází nejen k omezení nežádoucích efektů ale také ke zvýšení účinnosti léčby.

V klinické praxi se používají nízkomolekulární organické látky, které vážou s vysokou afinitou biomolekuly a inhibují tak jejich funkci v učitých tkáních. Příkladem může být gefitinib, inhibitor receptoru pro růstový faktor EGF (z angl. *Epidermal Growth Factor*), používaný v terapii karcinomu plic (Ciardiello 2000); antagonista estrogenového receptoru tamoxifen používaný u karcinomu prsu (Ward 1973); inhibitor tyrosin kináz imatinib používaný v terapii chronické myeloidní leukémie a dalších malignit (Buchdunger et al. 1996); nebo také proteasomální inhibitor bortezomid používaný v terapii mnohočetného myelomu (Teicher et al. 1999). Jejich velikost a chemické vlastnosti umožňují průchod buněčnou membránou a vazbu na cílové molekuly. Ve snaze zabránit abnormálnímu růstu pak ovlivňují buněčnou signalizaci. FDA schválila také cílenou léčbu pomocí monoklonálních protilátek, které váží např. HER2 (z angl. *Human Epidermal Growth Factor Receptor 2*) u karcinomu prsu (trastuzumab, (Baselga et al. 1998)), receptor pro EGF u kolorektálního karcinomu (cetuximab, (Waxman and Herbst 2002)), nebo receptor pro VEGF-A (z angl. *Vascular Endothelial Growth Factor A*), jehož inhibice brání angiogenezi u celé řady pokročilých karcinomů (bevacizumab, (2002)).

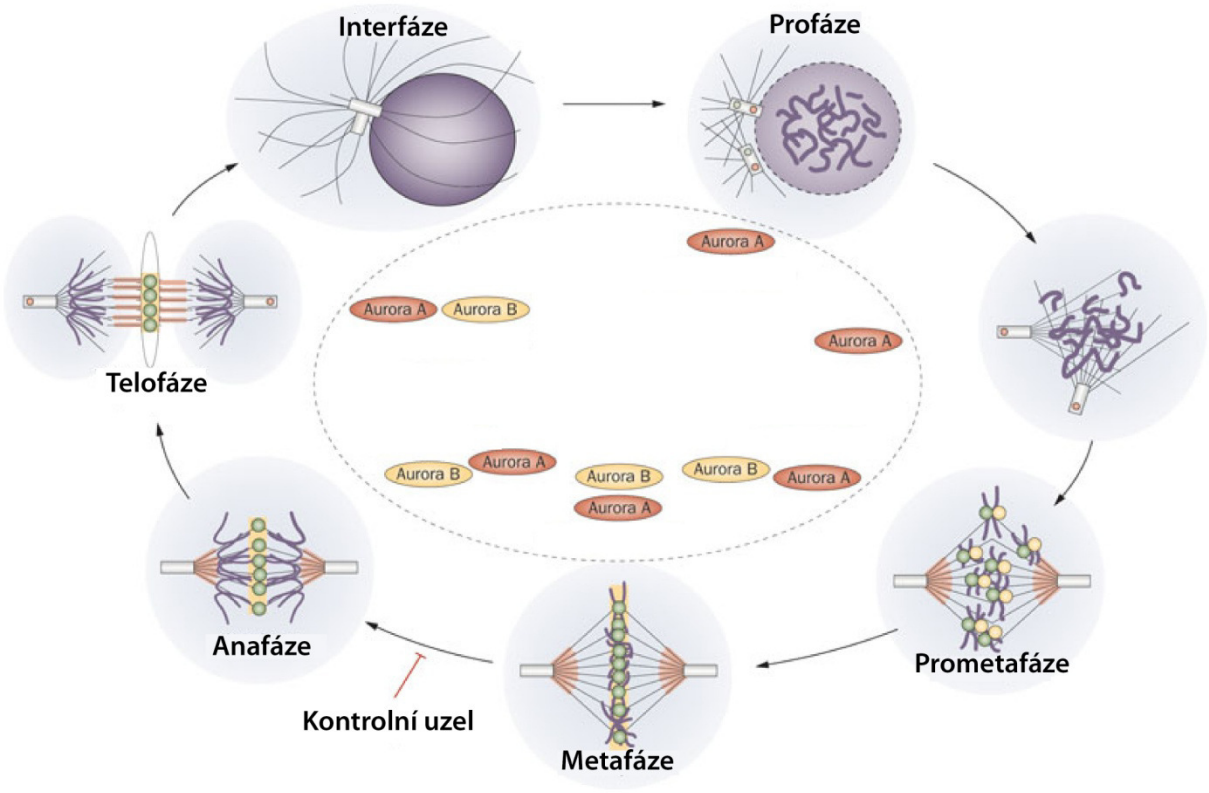
Proliferace buněk způsobující růst nádorů je podmíněna chybnou regulací buněčného cyklu. Během tohoto cyklu dochází k replikaci DNA v S-fázi (syntéza) a rozdělení buňky v M-fázi (mitóza). Intervaly mezi těmito fázemi se označují jako G-fáze (z angl. *Gap*) a buňky během nich prochází řadou kontrolních mechanismů, které vyhodnocují podmínky pro buněčné dělení. V G_1-fázi dochází k růstu buněčné hmoty, syntéze nukleotidů a tvorbě potřebných enzymů. Nachází se zde hlavní kontrolní uzel pro přechod G_1/S (restrikční), který pouští proliferující buňky do S-fáze a terminálně diferencované buňky posílá do klidové G_0-fáze, ve které plní svou funkci, stárnou a umírají. Po replikaci DNA v S-fázi dochází v G_2-fázi k dalšímu posouzení stavu pro přechod G_2/M (z angl. *Mitosis Promoting Factor*),

následuje zdvojení organel a zahájení tvorby dělícího vřeténka. Během vlastní mitózy se oddělí jádra (karyokineze) a nakonec celé buňky (cytokineze). V profázi vzniká dělící vřeténko, chromozómy kondenzují a jaderná membrána se rozpadá. Během metafáze se chromozómy vážou na mikrotubuly vřeténka a seskupují se v ekvatoriální rovině. V anafázi chromatidy putují podél vřeténka k opačných pólům, po oddělení se v telofázi začne znovu tvořit jaderná membrána a buňky se zaškrcením úplně oddělí. I během mitózy je nezbytná kontrola a to chromozómů, které musí být na konci metafáze správně navázány na mikrotubuly dělícího vřeténka (z angl. *Spindle Assembly Checkpoint*). Teprve pak může buňka vstoupit do anafáze.

Buněčné děje jsou striktně regulované a přesně vyvážené tak, aby odpovídaly aktuálním požadavkům organismu. **Proteinkinázy** jsou regulační molekuly přenášející fosfátové skupiny na zbytky aminokyselin, nejčastěji serinu, threoninu a tyrosinu. Tato kovalentní modifikace, označovaná také jako fosforylace, patří mezi post-translační modifikace s nejvyšší frekvencí výskytu a její hlavní funkce spočívá v regulaci klíčových procesů jako je **buněčná signalizace**. Signál je od receptoru přenášen kaskádou reakcí a jeho šíření je umožněno postupnou změnou aktivity jednotlivých proteinů. Fosforylace mění konformaci proteinů (např. enzymů) a způsobuje tak jejich aktivaci nebo inhibici. Důsledkem modifikace signálních proteinů dochází k ovlivnění funkce dalších intracelulárních proteinů, což vede k regulaci prakticky jakéhokoliv aspektu buněčného chování, např. metabolismu, proliferace a diferenciace. V této práci se zaměřuji na nová perspektivní léčiva, která inhibují serin/threonin proteinkinázy účastnící se abnormální proliferace nádorových buněk.

1.5.2. Inhibitory Aurora kináz

Geny kódující proteiny, které se účastní kontrolních mechanismů buněčné proliferace, nazýváme onkogeny a jejich mutace a/nebo zvýšená exprese vede k rozvoji nádorových onemocnění. Aurora kinázy (AURK) jsou důležité onkoproteiny klíčové pro regulaci buněčného dělení (obr. 5) (Kollareddy et al. 2008). Aurora A kontroluje vstup buněk do mitózy, zrání centrozomů, bipolární uspořádání dělícího vřeténka, vyrovnání chromozómů v metafázi a dokončení cytokineze. Aurora B je zodpovědná za kondenzaci chromozómů, připojení dělícího vřeténka a centromer, chromozomální bi-orientaci a cytokinezi. Velmi důležitá je součinnost AURK-A a AURK-B. AURK-C zastává podobné funkce jako AURK-B, doplňuje její funkce a je potřebná pro cytokinezi.



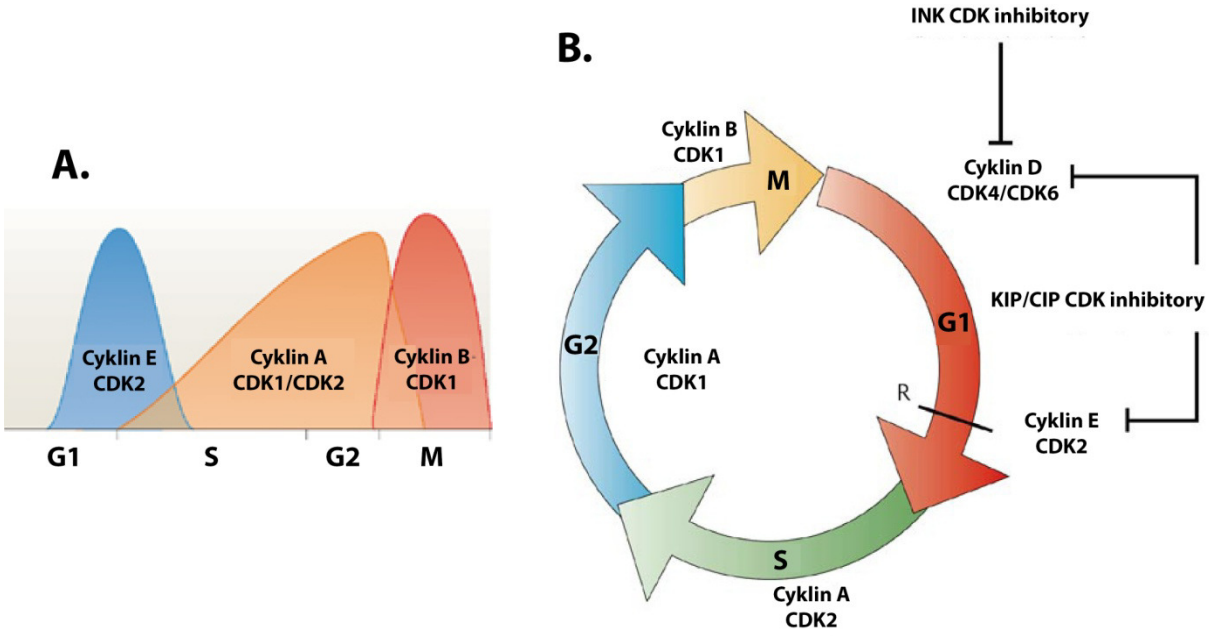
Obrázek 5. Aurora kinázy a regulace bunečného dělení. Převzato a upraveno podle souhrnného článku Komlodi-Pasztor et al. 2011.

Odchylky v expresi AURK vážně narušují kontrolní mechanismy buněčného dělení, zejména mitózy, způsobují tak genetickou nestabilitu a mohou vést k rozvoji nádoru. Tyto odchylky se nachází u různých typů nádorů a léčiva inhibující funkci AURK by mohla najít uplatnění v léčbě onkologických onemocnění. Do klinických zkoušek proto byly zařazeny inhibitory specifické pro AURK-A (např. MLN8237), AURK-B (např. AZD1152) a také pan-specifické AURK inhibitory (např. PHA-739358, AT9283, CYC116) (Kollareddy et al. 2012). V této práci byl testován biologicky dostupný inhibitor **CYC116**, jehož protinádorový účinek vychází z inhibice AURK-A, B, C a také receptoru pro VEGF-2 (Kollareddy et al. 2012; Wang et al. 2010).

1.5.3. Inhibitory cyklin–dependentních kináz

Cyklin–dependentní kinázy (CDK) mají klíčovou úlohu v regulaci buněčného cyklu. Přechod mezi jednotlivými fázemi reguluje hladina cyklinů, které jsou v průběhu buněčného cyklu postupně syntetizovány (obr. 6A). Po navázání cyklinu aktivuje CDK cílové proteiny, které v buňce spouští procesy nezbytné pro přechod do další fáze, např. syntézu potřebných enzymů a dalších cyklinů. Pro různé fáze buněčného cyklu jsou potřeba různé komplexy

cyklin-CDK (obr. 6). V časné fázi G_1 reguluje buněčné procesy cyklin D společně s CDK4 a CDK6. S-fázi spouští cyklin E prostřednictvím CDK2, za dokončení S-fáze a přechod do G_2 je pak zodpovědný komplex cyklin A-CDK2. Pro fázi G_2 zůstává cyklin A, ale aktivační funkci přebírá CDK1, která po syntéze a navázání cyklinu B spouští M-fázi, tedy mitotické dělení buněk. Vedle hladiny cyklinů regulují CDK také inhibitory z rodiny INK (z angl. *Inhibitor of Kinase*), CIP (z angl. *CDK Interacting Protein*) a KIP (z angl. *Kinase Inhibitory Protein*), které inaktivují komplexy cyklin–CDK (obr. 6B).



Obrázek 6. Cyklin-dependentní kinázy a kontrola buněčného cyklu. Převzato a upraveno podle souhrnných článků Dehay and Kennedy 2007 a Hochegger et al. 2008.

CDK přímo interagují s onkogeny i nádorovými supresory a jejich abnormální aktivace nebo porucha inhibice CDK vede ke vzniku nádorů (Pucci and Giordano 1999). Snížení aktivity CDK pomocí syntetických inhibitorů tedy představuje slibnou strategii v léčbě nádorových onemocnění (Rizzolio et al. 2010). Objev olomoucinu stál na počátku vývoje nové generace protinádorových léčiv blokujících CDK1 a homologní kinázy (Vesely et al. 1994). Následně byly vyvinuty velmi specifické a mnohem účinnější inhibitory jako je roskovitin a bohemin (De Azevedo et al. 1997; Chmela et al. 2001). Klinické testování prokázalo terapeutickou účinnost *in vitro* a biologickou dostupnost *in vivo* (Raynaud et al. 2005). Nyní se roskovitin podrobuje klinickému testování s perspektivou použití pro léčbu pokročilých solidních nádorů. V klinických zkouškách se testuje pro léčbu různých solidních tumorů také SCH727965 a PD0332991, pro léčbu hematologických malignit pak flavopiridol, AT7519M a LEE011. V této práci byl testován syntetický inhibitor odvozený ze struktury

olomoucinu, **bohemin**, jehož protinádorový účinek vychází z inhibice CDK a má za následek narušení metabolismu buněk (Kovarova et al. 2000; Skalnikova et al. 2005).

1.5.4. Antracyklinová antibiotika

Antracykliny, produkty bakterií *Streptomyces peucetius*, poškozují buňky vazbou na DNA a používají se k velmi účinné léčbě celé řady onkologických onemocnění. Mechanismus účinku antracyklinů vychází z interkalace DNA, která brání její replikaci v rychle rostoucích buňkách. Následkem interkalace dochází ke stabilizaci topoisomerázy II, která za normálních okolností rozvolňuje řetězce DNA a je potřebná jak pro replikaci tak transkripci. Poškození buněk způsobuje během léčby antracykliny také tvorba volných kyslíkových radikálů. Působení volných radikálů však poškozuje také zdravé tkáně a mezi nejčastější důvody ukončení léčby patří kardiotoxicita. V této práci se zabýváme účinkem antracyklinů, daunorubicinu a doxorubicinu, a také antracyklinového analogu, mitoxantronu.

Daunorubicin se používá nejčastěji v kombinaci s dalšími cytostatiky k léčbě akutní formy leukémie (Cortes-Funes and Coronado 2007). **Doxorubicin** je strukturou velmi podobný daunorubicinu, má však mnohem širší spektrum účinku a nachází uplatnění jak při léčbě hematologických malignit tak solidních nádorů (Cortes-Funes and Coronado 2007). **Mitoxantron** je antrachinonové cytostatikum používané k léčbě solidních nádorů i leukémií a je charakteristické menší toxicitou ale také nižší aktivitou (Hande 1998). I přes značnou strukturální podobnost působí tato léčiva na onkologická onemocnění s různou účinností a otázkou tedy zůstává mechanismus účinku, kterým pravděpodobně nebude pouhá interkalace DNA, inhibice topoisomerázy II a tvorba kyslíkových radikálů.

1.5.5. Nádorová rezistence

Účinnost protinádorové léčby závisí nejen na druhu léčiva, ale také na molekulární výbavě nádorových buněk. Ve snaze nezatěžovat organismus toxickými dávkami léčiv jsou často onkologickým pacientům podávány sub-terapeutické dávky, které mohou způsobit rozvoj nádorové rezistence. Ta představuje vedle vážných vedlejších účinků hlavní problém protinádorové léčby a může značně komplikovat jak probíhající léčbu, tak aplikaci dalších účinných léků.

Nádorové buňky odolávají účinku léčiv všemi dostupnými prostředky. V první řadě se snaží zabránit samotnému vstupu léčiva do buňky např. sníženou expresí membránových

přenašečů (Guo et al. 1999). Pokud buňka nezabrání vstupu léčiva, snaží se ho rychle vyloučit prostřednictvím ABC (z angl. *ATP-Binding Casette*) transportních pump (Gottesman et al. 2002). Tyto transmembránové proteiny využívají energii ATP k přenosu různých látek a zvýšenou expresí způsobují rezistenci nejen k podanému léčivu ale také k řadě dalších léčiv. Tento jev, označovaný také jako **mnohočetná rezistence** (z angl. *Multi-Drug Resistance*, MDR), je nejčatěji způsobený trvale zvýšenou expresí P-gp (glykoprotein P), MRP2 (z angl. *Multidrug Resistance-Associated Protein 2*), LRP (z angl. *Lung Resistance–Associated Protein*) nebo BCRP (z angl. *Breast Cancer Resistance Protein*). Dalším mechanismem rozvoje rezistence může být inaktivace a/nebo detoxifikace léčiva např. pomocí glutathion S–transferázy (Cullen et al. 2003), cytochromu P450 (Seredina et al. 2012) nebo glukuronidací (Cummings et al. 2002).

Pokud selhávají "fyziologické" mechanismy nádorových buněk, jsou na řadě reparační procesy. Bylo prokázáno, že zvýšená kapacita buněk opravovat DNA doprovází nejen karcinogenezi, ale způsobuje také nádorovou rezistenci (Chaney and Sancar 1996; Sarkaria et al. 2008). Při narušení integrity genomu spouští buňky signální kaskády, zastavují buněčný cyklus a opravují poškozenou DNA. Jedná se o sérii komplexních dějů, jejichž rovnováha je klíčová pro osud buněk. Pokud je poškození příliš rozsáhlé, je buňka odsouzena k apoptóze. Hlavní úlohu v regulaci těchto procesů má **protein p53**. Tento transkripční faktor reguluje za běžných podmínek expresi proteinů, které kontrolují buněčné dělení a apotózu (Levine 1997). V případě nevratného poškození indukuje apoptózu také na úrovni mitochondrií (Moll et al. 2005). Protein p53 je mutovaný u více než poloviny nádorových onemocnění (Hollstein et al. 1991) a některé jeho mutace zvyšují také rezistenci na protinádorovou léčbu (Gasco and Crook 2003). Existuje však mnoho dalších způsobů, jak nádorové buňky brání apoptóze po podání protinádorového léčiva (Longley and Johnston 2005; Wilson et al. 2009).

Další charakterizace molekulárních mechanismů nádorové rezistence je nezbytná pro hlubší pochopení těchto procesů, určení molekulárního fenotypu nádorů a vývoj nových účinných léků. Cílem je také nalezení prediktivních markerů odpovědi na protinádorovou léčbu, stratifikace onkologických pacientů a tolik potřebná personalizace léčby. Sledováním vhodné kombinace markerů je třeba monitorovat léčbu a dosáhnout tak mnohem vyšší úspěšnosti.

2. Cíle Práce

S využitím současných proteomických technik na bázi 2D elektroforézy a 2D kapalinové chromatografie jsme sledovali kvantitativní změny proteinů. Proteiny jsme identifikovali pomocí hmotnostní spektrometrie a na základě funkční interpretace nalezených změn jsme se snažili popsat biochemické mechanismy doprovázející sledované podmínky.

Hlavním cílem práce byla identifikace proteinů, které doprovází **rozvoj nádorové rezistence** se zaměřením na charakterizaci mechanismů nádorové rezistence, identifikaci cílů pro nová léčiva a také hledání kandidátních markerů pro stratifikaci onkologických pacientů a monitorování protinádorové léčby. Studovali jsme mechanismy:

- **Rezistence k působení inhibitorů Aurora kináz.**
- **Rezistence k působení inhibitorů cyklin-dependentních kináz.**

Dalším specifickým cílem byl podrobný popis mechanismů **působení protinádorových léčiv**. Charakterizovali jsme:

- **Působení antracyklinů na nádorové buňky.**

Poslední částí práce byla **analýza reálných biologických vzorků** v rámci:

- **Hledání kandidátních proteinů pro včasnou diagnostiku ovariálního hyperstimulačního syndromu.**

3. Metody

Prvním a nejdůležitějším krokem experimentů byla pečlivá příprava proteomických analýz, zejména výběr vhodného modelu. Pro studium rozvoje nádorové rezistence a charakterizaci mechanismů účinku protinádorových léčiv jsme zvolili lidské buněčné linie (nádorové buňky) ošetřené protinádorovým léčivem. Pro optimalizaci dávky léčiva a potvrzení rezistence na protinádorové léčivo bylo třeba posuzovat jeho účinnost a cytotoxicitu. Měřili jsme proto pomocí testu MTT (3-[4,5-dimethylthiazol-2-yl]-2,5-difenyl tetrazolium bromid) koncentraci léčiva, při které dochází k inhibici 50 % buněk (**IC_{50}**) (Dzubak et al. 2006). V rámci hodnocení vlivu léčiv na expresi proteinů jsme také zjišťovali **čas do spuštění apoptózy** (aktivace kaspáz), podle kterého jsme optimalizovali dobu působení léčiv. Ošetření buněk, ustavení rezistentních linií, meření cytotoxicity a času do apoptózy probíhalo ve spolupráci s Laboratoří experimentální medicíny LF UP a FN v Olomouci.

3.1. Ustavení rezistentních nádorových linií

Nádorové buňky HCT116 odvozené z kolorektálního karcinomu byly vystaveny krátkodobému působení inhibitorů AURK (CYC116 nebo ZM447439) ve vysoké dávce. Po několika týdnech byly izolovány přežívající kolonie, MTT test potvrdil vysoký stupeň rezistence k inhibitorům a několik klonů rezistentních buněk bylo nadále udržováno v dávce inhibitoru několikanásobně převyšující IC_{50} pro vytvoření selekčního tlaku (udržení rezistence).

T-lymfoblastické leukemické buňky CCRF–CEM byly použity k odvození rezistence na bohemin, inhibitor CDK. Ošetření začalo dávkou, která umožnila přežití 10 % nádorových buněk (TCS_{10}, z angl. *Tumor Cells Survival*) a postupně byla dávka zvyšována až na 10 × TCS_{50}. Buňky byly ustaveny dlouhodobou kultivací v subletální dávce, která byla součástí kultivačních podmínek i po ustavení rezistence pro vytvoření selekčního tlaku (Noskova et al. 2002). Na rozdíl od buněk HCT116 rezistentních na inhibitory AURK byly jednotlivé rezistentní klony po ustavení spojeny do směsné, tzv. bulk kultury.

Stejným způsobem byly ustaveny buňky plicního adenokarcinomu A549 rezistentní na bohemin. Pro validace jsme dále použili buňky CCRF-CEM rezistentní na vinkristin, danurorubicin a cytarabin a buňky A549 rezistentní na vinkristin a paklitaxel. Tyto buňky byly ustaveny podle stejného protokolu s tím rozdílem, že bulk kultury nebyly vystaveny selekčnímu tlaku a kultivační podmínky byly stejné jako pro původní (senzitivní) linie

(Noskova et al. 2002). Ošetření buněk vyvolávalo zkříženou rezistenci a některé buňky dokonce vykazovaly zvýšenou expresi ABC transportních pump s fenotypem MDR.

3.2. 2DE

Pro separaci intaktních proteinů buněk HCT116 rezistentních k působení inhibitorů AURK a buněk CCRF-CEM ošetřených antracykliny jsme použili 2DE. Z buněk jsme pomocí vhodného pufru extrahovali proteiny, určili jsme jejich celkové množství ve vzorku a podrobili je analýze. Abychom zachytili co nejvíce kvantitativních změn, proteiny jsme dělili v první dimenzi podle pI v nelineárním gradientu pH 4–7 a 6–11. Optimalizace protokolu představovala časově nejnáročnější krok. Z důvodu zcela odlišných vlastností neutrálních a bazický proteinů vyžadoval každý gradient specifické podmínky pro reprodukovatelnou separaci. Zatímco proteiny v **pH 4–7** bylo možné nanášet v množství až 2 mg přímo pomocí rehydratace se vzorkem (z angl. *In-Gel Rehydratation*), bazické proteiny v **pH 6–11** jsme museli nanášet až po rehydrataci se samotným pufrem pomocí pohárků umístěných v kyselejší anodické části gradientu (z angl. *Cup-Loading*) v množství maximálně 100 μg, aby nedocházelo ke ztrátě nebo vysrážení bazických proteinů. Na každý strip jsme aplikovali 50 μA a pozvolný vzestup napětí. Gradienty pH vyžadovaly také různé parametry **IEF**: pro pH 4–7 jsme zvolili maximální napětí 5000 V a celkovou fokusaci 50–55 kVh, pro pH 6–11 pak maximální napětí 8000 V a celkovou fokusaci 15–20 kVh.

Pro zisk kvalitní sady proteinů je nutné rozrušit terciární a kvartérní struktury redukcí disulfidových vazeb a zabránit jejich reoxidaci procesem alkylace. Zatímco bazický gradient vykazoval lepší výsledky s využitím redukčního činidla dithiothreitol (DTT) s následnou alkylací prostřednictvím jodacetamidu (z angl. *Iodoacetamide,* IAA), pro neutrální gradient byl vhodnější dithiodiethanol (DeStreak), který po rozrušení zůstává navázaný a kombinuje tak oba procesy (Olsson et al. 2002). Vazba DeStreaku však není tak stabilní jako kombinace DTT/IAA a pro udržení rozvolněné konformace bylo nezbytné přidat DeStreak také do ekvilibračního pufru. Dále je třeba brát v úvahu následné identifikace pomocí MS a v takovém případě jsme vždy volili variantu 2-krokové ekvilibrace s DTT a IAA.

Po IEF separaci v gradientu pH a ekvilibraci v pufru s SDS jsme proteiny přenesli na **10%** nebo **12%** polyakrylamidový gel a rozdělili je v druhé dimenzi podle MW pomocí **SDS-PAGE**. Pro porovnání kvantity jsme připravili analytické gely s nižší nanáškou (50–100 μg) obarvené fluorescenční barvou **Sypro RUBY**, která patří mezi nejcitlivější druhy barvení s velmi dobrým dynamickým rozsahem a linearitou signálu. Kvantitativní porovnání

jsme provedli s využitím softwaru **REDFIN Solo** (Ludesi). Při vyhodnocení se nejprve vytváří 2D fúzní obraz (pI vs. MW), který je aplikován na všechny gely. Intenzita signálu je na každém gelu integrována, signál jednotlivých spot se po normalizaci vztahuje k celkové hodnotě a hledají se kvantitativní rozdíly. Proteiny jsme pro MS analýzu rozdělili na preparativním gelu (nanáška 100–1000 μg) a zviditelnili **reverzním barvením** za použití imidazolu a zinku (Hardy and Castellanos-Serra 2004). Jedná se o velmi citlivé barvení, které na rozdíl od srovnatelně citlivých protokolů (např. barvení stříbrem) nemodifikuje proteiny a je tak zcela kompatibilní s MS. 2DE experimenty jsme prováděli vlastními silami v Ústavu živočišné fyziologie a genetiky AV ČR.

3.3. 2D-LC

Chromatografickou 2D frakcionaci (PF 2D, Beckman Coulter) jsme použili pro analýzu buněk CCRF-CEM rezistentních k působení inhibitoru CDK. Z buněk jsme pomocí vhodného pufru extrahovali proteiny, zbavili jsme vzorek solí pomocí kolony **PD10** a určili jsme celkové množství proteinu ve vzorku. V první dimenzi jsme intaktní proteiny (3,6 mg) separovali podle pI pomocí **chromatofokusace** v lineárním gradientu **pH 8,5–4,0**. U výstupu z kolony zaznamenával UV detektor signál směsí proteinů a monitoroval tak jejich kvantitu. Proteiny jsme sbírali v intervalech pH 0,3 a získali jsme celkem 15 frakcí, které byly následně rozděleny v druhé dimenzi podle hydrofobicity na koloně s reverzní fází **C-18** v gradientu voda/acetonitril s přídavkem kyseliny trifluoroctové. Na výstupu z kolony jsme opět měřili signál UV a frakce jednotlivých intaktních proteinů nebo jejich jednoduchých směsí jsme sbírali do 96-jamkové destičky v intervalu 0,13 min.

Software **ProteVue** (PF 2D, Beckman Coulter) pak z UV chromatogramů vytvořil 2D mapu senzitivních a rezistentních buněk (pI vs. hydrofobicita). Stejný software převedl kvantitativní informace (intenzitu píků) z jednotlivých frakcí první dimenze (CF) do chromatogramu druhé dimenze (RP). Relativní porovnání jsme provedli pomocí softwaru **Viper** (Ludesi). Zatímco při 2DE se vytváří fúzní obraz, při 2D-LC se vybírá reprezentativní chromatogram, podle kterého se ostatní chromatogramy vyrovnávají. Po normalizaci a spárování píků stejného retenčního času jsme porovnávali jejich kvantitu (plochu jednotlivých píku vztaženou na celkovou plochu všech píků určité frakce). Diferenční proteiny jsme identifikovali ve frakcích z druhé dimenze. 2D-LC experimenty jsme prováděli vlastními silami v Ústavu živočišné fyziologie a genetiky AV ČR.

3.4. MALDI MS

Diferenční proteiny jsme identifikovali pomocí **MALDI-TOF/TOF** nebo **MALDI-FT-ICR**. Proteiny z gelu jsme po odbarvení (chelatace pomocí glycinu v 30 % acetonitrilu) a důkladném promytí štěpili pomocí proteázy **trypsin** (37 °C, inkubace přes noc). Frakce z 2D-LC jsme vysušili a proteiny rozpustili v pufru s trypsinem (37 °C, inkubace přes noc). V případě potřeby jsme extrahované peptidy zbavili solí použitím nanokolon plněných reverzní fází (Gobom et al. 1999). Přečištěné a zakoncentrované peptidy jsme pak nanesli společně s matricí (**kyselina α-kyano-4-hydroxyskořicová**) na MALDI destičku. U vzorků s dostatkem proteinu jsme nanesli směs peptidů rovnou na destičku a po vypaření jsme je převrstvili tenkou vrstvou matrice.

Spektra jsme měřili na hmotnostním spektrometru Ultraflex III MALDI-TOF/TOF s technologií LIFT pro MS/MS analýzu (Bruker Daltonics) nebo APEX-Qe FTMS instrument se supravodivým magnetem (9.4 T) a kombinovaným iontovým zdrojem ESI/MALDI (Bruker Daltonics). **Interní kalibrace** na monoizotopické $[M+H]^+$ produkty autoproteolýzy trypsinu (842,5 a 2211,1 Da) umožnila databázové vyhledávání s chybou 20–30 ppm (Ultraflex III MALDI-TOF/TOF) nebo 3 ppm (APEX-Qe FTMS). Po vyloučení známých kontaminací (autoštěpy trypsinu, keratiny, aktin, apod.) včetně modifikovaných forem (např. oxidace) a aduktů s alkalickými kovy ($[M+Na]^+$, $[M+K]^+$) jsme vyhledávali proteiny pomocí **MASCOT** v databázi pro lidské proteiny **Swiss-Prot** (Ultraflex III MALDI-TOF/TOF) nebo pomocí **ProFound** v databázi pro lidské proteiny **IPI** (APEX-Qe FTMS). Proteiny, které byly na hranici úspěšné identifikace jsme podrobili **MS/MS** analýze pro potvrzení identity. MS experimenty jsme prováděli ve spolupráci s Laboratoří charakterizace molekulární struktury v Mikrobiologickém ústavu AV ČR.

3.5. Verifikace proteomických dat

Z důvodu obrovské komplexity proteinů v buňkách je u relativních kvantitativních porovnání nezbytná verifikace proteomických dat nezávislou technikou. Zvolili jsme metodu **Western blot**, která detekuje proteiny pomocí specifické protilátky po rozdělení pomocí SDS-PAGE a přenesení na PVDF (polyvinylidendifluoridovou) membránu. Na specifickou primární protilátku jsme navázali sekundární, druhově-specifickou, protilátku s konjugovanou křenovou peroxidázou. Tento enzym po přidání substrátu generoval chemiluminiscenční signál, který jsme zachytili na fotografický film. Semikvantitativní charakter této metody spočívá v mnohonásobném zesílení signálu vazbou protilátek, a proto není vhodná pro ověřování sotva patrných rozdílů v expresi proteinů. V naší práci jsme se proto zaměřili

na markantní kvantitativní rozdíly. WB jsme prováděli vlastními silami v Ústavu živočišné fyziologie a genetiky AV ČR.

Buňky CCRF-CEM rezistentní k působení boheminu byly analyzované také pomocí **imunohistochemie**. Buňky jsme zalili parafinem a z malých bločků pak byly připraveny tenké řezy. Ty jsme zamontovali na mikroskopická sklíčka, buňky jsme zbavili parafinu a zafixovali. Po navázání primární protilátky jsme aplikovali sekundární biotinylovanou protilátku, která váže prostřednictvím streptavidinu alkalickou fosfatázou. Po přidání substrátu jsme pozorovali ve světelném mikroskopu chromogenní reakci. Ani tato technika není kvantitativní, ale umožňuje určení buněčné lokalizace proteinů. Imunohistochemické experimenty jsme prováděli ve spolupráci s Laboratoří experimentální medicíny LF UP a FN v Olomouci.

3.6. Funčkní interpretace dat

Pro pochopení mechanismů nádorové rezistence a odpovědi buněk na protinádorovou léčbu bylo třeba přeložit znalost kvantitativních proteinových změn do jazyka buněčných procesů. Základním prostředkem bylo důkladné **prohledávání odborné literatury** s důrazem na kvalitní recentní práce a propojení stávajících informací s našimi poznatky. Skládáním jednotlivých částí mozaiky tak vznikal jasnější obraz ukazující snahu nádorových buněk překonat účinky léčby a dále se nekontrolovaně dělit. Druhým přístupem byl globální pohled prostřednitvím klasifikačních softwarů (PANTHER), které využívají informace z **Gene Ontology** (GO). GO shromažďuje data z různých databází a pomáhá tak popisovat molekulární funkce proteinů a biologické procesy včetně jejich lokalizace. Vychází však pouze z dostupných a již popsaných dějů, zatímco proteiny mohou za různých podmínek vykonávat specifické a dosud nepoznané funkce. Abychom takové funkce odhalili, je zapotřebí odprostit se od základních znalostí proteinů a podívat se na jejich fungování nezaujatě, např. prostřednictvím jejich interakcí s dalšími proteiny. Pro navržení mechanismů nádorové rezistence jsme využili software **NAVIGaTOR** a jednu z nejobsáhlejších databází známých a predikovaných interakcí proteinů, Interologous Interaction Database (I2D). K nalezení odpovědí pomáhají také statistické prostředky. V případě dobře plánovaného experimentu je možné zařadit do analýzy léčiva s podobnou strukturou a předpokládaným mechanismem působení a s využitím **multivariační analýzy** (např. *Principal Component Analysis*, PCA) pak lze objektivně klasifikovat skutečné podobnosti či rozdílnosti působení těchto léčiv a hledat proteiny zodpovědné za různé účinky při léčbě onkologických onemocnění. Tento přístup jsme zvolili pro analýzu buněk CCRF-CEM ošetřených různými

antracykliny. Funkční interpretace jsme prováděli vlastními silami v Ústavu živočišné fyziologie a genetiky AV ČR, multivariační statistické analýzy jsme prováděli ve spolupráci s Laboratoří experimentální medicíny LF UP a FN v Olomouci.

3.7. Deplece majoritních proteinů

V rámci hledání kandidátních proteinů pro včasnou diagnostiku ovariálního hyperstimulačního syndromu (OHSS) jsme analyzovali reálné biologické vzorky folikulární tekutiny, které se svým složením do značné míry podobají krevní plazmě (Jarkovska et al. 2010). Abychom snížili dynamický rozsah koncentrací proteinů a mohli tak detekovat i proteiny s nízkou hladinou, bylo potřeba odstranit ze vzorku majoritní proteiny. Zvolili jsme imunoafinitní purifikaci 12 proteinů nejvíce zastoupených v plazmě (ProteomeLab IgY-12 LC10, Beckman Coulter: **albumin, IgG, transferin, fibrinogen, IgA, α2-makroglobulin, IgM, α1-antitrypsin, haptoglobin, α1-kyselý glykoprotein, apolipoproteiny A-I** a **A-II**). Na kolonu se zakotvenými protilátkami jsme nanesli 20 mg proteinů v nativním pufru. Vzorky zbavené majoritních proteinů (97 %) bylo potřeba zakoncentrovat pomocí odstředivé filtrace (Amicon Ultra 15 kDa). Tyto vzorky jsme rozpustili ve vhodném pufru pro 2DE a 2D-LC. Deplece majoritních proteinů jsme prováděli vlastními silami v Ústavu živočišné fyziologie a genetiky AV ČR.

4. Výsledky

4.1. Charakterizace mechanismů nádorové rezistence k působení inhibitorů Aurora kináz

v publikaci

Cancer Cell Resistance to Aurora Kinase Inhibitors:
Identification of Novel Targets for Cancer Therapy

Hrabáková R, Kollareddy M, Tylečková J, Halada P, Hajdúch M, Gadher SJ, Kovářová H.

výsledky přijaté k uveřejnění v časopise J Proteome Res. (DOI: 10.1021/pr300819m)
IF (2012): 5.11; 5-year IF (2012): 5.41

European Patent Office Application No. 11192330.6 – 2402
Method of Determination of Cancer Cell Drug Sensitivity towards Aurora Kinase Inhibitors and Overcoming their Resistance
Kollareddy M, Hajdúch M, Džubák P, Srovnal J, **Hrabáková R**, Kovářová H

Prohlášení spoluautorů

„Prohlašuji, že Rita Hrabáková se patřičně podílela (70%) na plánování proteomických experimentů, jejich provedení, interpretaci výsledků a sepisování této práce."

V Liběchově, dne..... RNDr. Hana Kovářová, CSc.

.....……...

Europäisches Patentamt
European Patent Office
Office européen des brevets

European Patent Office
80298 MUNICH
GERMANY
Tel. +49 (0)89 2399 - 0
Fax +49 (0)89 2399 - 4465

Hrabakova, Rita
Teplicka 548
41801 Bilina
REPUBLIQUE TCHEQUE

For any questions about this communication:
Tel.:+31 (0)70 340 45 00

Date: 06.02.12

Reference	Application No./Patent No.
	11192330.6 - 2402

Applicant/Proprietor: Palacky University, Olomouc, et al

Designation as inventor - communication under Rule 19(3) EPC

You have been designated as inventor in the above-mentioned European patent application. Below you will find the data contained in the designation of inventor and further data mentioned in Rule 143(1) EPC:

DATE OF FILING : 07.12.11

PRIORITY : / /

TITLE : Method of determination of cancer cell drug sensitivity towards Aurora kinase inhibitors and overcoming their resistance

DESIGNATED STATES : AL AT BE BG CH CY CZ DE DK EE ES FI FR GB GR HR HU IE IS IT LI LT LU LV MC MK MT NL NO PL PT RO RS SE SI SK SM TR

INVENTOR (PUBLISHED = 1, NOT PUBLISHED = 0):

1/Kollareddy, Madhusudhan Reddy/D.No. 11-1-204 Santhinagar-2nd Lane Kovur, Nellore/524137 Andhra Pradesh/IN
1/Hajduch, Marian/Norbercany- Trhavice 5/79305 Moravsky Beroun/CZ
1/Dzubak, Petr/Horni Hejcinska 124/2/77900 Olomouc - Hejcin/CZ
1/Srovnal, Josef/Mosnerova 1308/16B/77900 Olomouc - Nova Ulice/CZ
1/Hrabakova, Rita/Teplicka 548/41801 Bilina/CZ
1/Kovarova, Hana/Pernerova 2082/53002 Pardubice/CZ

DECLARATION UNDER ARTICLE 81 EPC:
The applicant(s) has (have) acquired the right to the European patent.

Receiving Section

Europäisches Patentamt • European Patent Office • Office européen des brevets

EPO Form 1048 10.09

Journal of proteome research

Article

pubs.acs.org/jpr

Cancer Cell Resistance to Aurora Kinase Inhibitors: Identification of Novel Targets for Cancer Therapy

Rita Hrabakova,[†] Madhu Kollareddy,[‡] Jirina Tyleckova,[†] Petr Halada,[§] Marian Hajduch,[‡] Suresh Jivan Gadher,[∥] and Hana Kovarova*[,†]

[†]Institute of Animal Physiology and Genetics, AS CR, v.v.i., Laboratory of Biochemistry and Molecular Biology of Germ Cells, Rumburska 89, 277 21 Libechov, Czech Republic

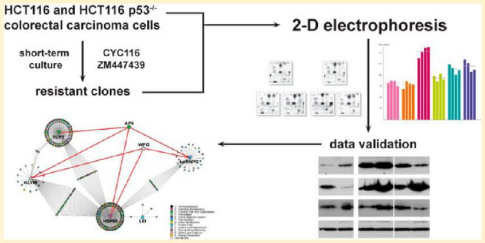
[‡]Institute of Molecular and Translational Medicine, Laboratory of Experimental Medicine, Palacky University and University Hospital in Olomouc, Faculty of Medicine and Dentistry, Hnevotinska 5, 775 15 Olomouc, Czech Republic

[§]Institute of Microbiology, AS CR, v.v.i., Laboratory of Molecular Structure Characterisation, Videnska 1083, 142 20 Prague, Czech Republic

[∥]Life Technologies, Frederick, Maryland 21704, United States

S *Supporting Information*

ABSTRACT: Drug resistance is the major obstacle to successful cancer therapy. Our study focuses on resistance to Aurora kinase inhibitors tested as anticancer drugs in clinical trials. We have used 2D electrophoresis in the pH ranges of 4−7 and 6−11 followed by protein identification using MALDI-TOF/TOF to compare the protein composition of HCT116 colon cancer cells either sensitive to CYC116 and ZM447439 inhibitors or resistant toward these drugs. The analysis also included $p53^{+/+}$ and $p53^{-/-}$ phenotypes of HCT116 cells. Our findings demonstrate that platelet-activating factor acetylhydrolase and GTP-binding nuclear protein Ran contribute to the development of resistance to ZM447439 only where resistance is related to p53. On the other hand, serine hydroxymethyltransferase was found to promote the tumor growth in cells resistant to CYC116 without the influence of p53. Computer modeling of interaction networks highlighted a direct link of the p53-independent mechanism of resistance to CYC116 with autophagy. Importantly, serine hydroxymethyltransferase, serpin B5, and calretinin represent the target proteins that may help overcome resistance in combination therapies. In addition, serpin B5 and calretinin appear to be candidate biomarkers that may be accessible in patients for monitoring of cancer therapy with ease.



KEYWORDS: *Aurora kinase inhibitors, resistance, p53, apoptosis, autophagy, platelet-activating factor acetylhydrolase, Ran, serine hydroxymethyltransferase, serpin B5, calretinin*

INTRODUCTION

Despite significant progress in the development of anticancer drugs, there is still a need for novel therapeutic strategies that would overcome development of drug resistance and improve the outcome of cancer patient therapy. Extensive efforts have been made to develop the therapy directed toward specific genetic alterations present predominantly or exclusively in tumors but not in normal cells. Aurora kinases (AURKs), which are comprised of three family members, Aurora-A, Aurora-B, and Aurora-C, are essential regulators of mitotic events including G2/M transition, spindle organization, chromosome segregation, and cytokinesis. Because AURKs are frequently overexpressed in human cancers, they have emerged as attractive therapeutic targets.[1] Accordingly, inhibitors of AURKs with potent antiproliferative and antiapoptotic effects have evolved, too.[2]

In the present study, we have taken into account an experimental and well-characterized AURK inhibitor ZM447439, 4-(4-(*N*-benzoylamino)anilino)-6-methoxy-7-(3-(1-morpholino)propoxy)quinazoline, which has been found to inhibit AURK-A and AURK-B,[3] and a novel AURK inhibitor CYC116, ([4-(2-amino-4-methyl-thiazol-5-yl)pyrimidin-2-yl]-(4-morpholin-4-ylphenyl)-amine]), which inhibits not only AURK-A, AURK-B and AURK-C, but also angiogenesis promoter VEGFR2 (vascular endothelial growth factor receptor 2).[2,4]

A major obstacle to successful cancer therapy is the presence of dormant and/or drug resistant cells, which may later evoke disease relapse. In response to anticancer treatment, changes in different cellular processes are triggered as tumors struggle to survive where mechanisms of extreme importance including pharmacological, physiological, and altered survival pathway parameters come into play. For instance, the overexpression of

Received: August 30, 2012

ACS Publications © XXXX American Chemical Society

dx.doi.org/10.1021/pr300819m | *J. Proteome Res.* XXXX, XXX, XXX−XXX

drug transport pumps can lead to the increased drug efflux, which usually manifests as multidrug resistance.[5] Additionally, activated DNA repair and impaired apoptosis have been implicated in the development of drug resistance.[6,7] Cancer stem cell phenomenon and epigenetic regulation that simultaneously influence expression of multiple genes might also contribute to the acquisition of drug resistance.[8,9] Nevertheless, molecular mechanisms of drug resistance have not yet been fully elucidated in spite of numerous studies carried out to date.

Previous studies have described mutations in p53 tumor suppressor gene in over 50% of human malignancies including colorectal cancer.[10] Some forms and/or combinations of p53 mutants may also enhance resistance of tumor cells to anticancer drugs.[11] In response to genotoxic stress and hypoxia, p53 transcriptionally activates upstream genes important for cell cycle arrest, DNA repair, or apoptosis[12] and can also induce apoptosis by nontranscriptional inhibition of bcl-2 and bcl-xl proteins at the mitochondrial membrane level.[13] Additionally, there is an important interaction between p53 and AURK, and deregulation of functional balance might trigger chromosome instability and carcinogenesis.[14]

Interaction of p53 with AURK-A suppresses its oncogenic activity.[15] On the other hand, AURK-A phosphorylates p53, resulting in p53 protein turnover and its transcriptional activity.[16] It has been shown that pharmacological inhibition of AURK-A provides a growth advantage to cells that have suffered from p53 loss or alternatively may lead to complete loss of wild-type p53 activity.[14] It remains obscure how p53 affects the development of resistance to AURK inhibitors in cancer cells.

Currently, proteomic approaches represent promising tools in our understanding of the molecular mechanisms of various diseases and a quest for disease biomarkers as well as specific targets for novel drugs. We have used 2D electrophoresis in pH ranges of 4−7 and 6−11 to compare sensitive and resistant HCT116 human colon cancer cells with $p53^{+/+}$ (wild-type) and $p53^{-/-}$ phenotypes. Using MALDI-TOF/TOF, we have identified proteins that may contribute to the acquisition of resistance toward CYC116 and ZM447439 AURK inhibitors. Such protein alterations have also been examined in CCRF-CEM human T-lymphoblastic leukemia cells carrying p53 mutations[17] and A549 human lung adenocarcinoma cells with p53 wild-type phenotype[18] resistant to diverse anticancer drugs. On the basis of our findings, we propose novel targets for drugs, which may prevent or overcome the drug resistance and highlight candidate markers that could be used to monitor anticancer therapy in patients.

■ EXPERIMENTAL SECTION

Chemicals

Unless otherwise stated, all chemicals were obtained from Sigma-Aldrich (St. Louis, MO).

Cell Culture and Sample Preparation

HCT116 $p53^{+/+}$ (wild-type) and HCT116 $p53^{-/-}$ cell lines derived from a human colon carcinoma were purchased from Horizon Discovery Ltd. (Cambridge, United Kingdom) and cultured in DMEM supplemented with 10% FCS (PAN-Biotech GmbH, Aidenbach, Germany), penicillin (Biotika, Prague, Czech Republic), and streptomycin at 37 °C and 5% CO_2. Cells resistant to AURK inhibitors were derived by short-term exposure of parental sensitive cells directly to 1 μM (cytotoxic dose above IC_{50} for both inhibitors) CYC116 (Cyclacel Ltd., Dundee Technopole, Dundee, Scotland, United Kingdom) or ZM447439 (AstraZeneca Pharmaceuticals Ltd., London, United Kingdom). After 5 weeks, several colonies were isolated, and a MTT-based proliferation assay was performed as described previously[19] to confirm resistance to AURK inhibitors. The resistance was evaluated as a fold increase calculated by dividing mean IC_{50} values of respective resistant clones and parental $p53^{+/+}$ and $p53^{-/-}$ sensitive cells.

In the present study, two clones resistant to CYC116 with wild-type $p53^{+/+}$ alleles (R1.2 and R1.3), two clones resistant to CYC116 with mutated $p53^{-/-}$ alleles (R2.1 and R2.2), two clones resistant to ZM447439 with wild-type $p53^{+/+}$ alleles (R3.1 and R3.2), and two clones resistant to ZM447439 with mutated $p53^{-/-}$ alleles (R4.2 and R4.3) were analyzed. Clones exhibited high resistance with a fold increase of IC_{50} as follows: 82 and 63 for R1.2 and R1.3, 64 and 41 for R2.1 and R2.2, 83 for both R3.1 and R3.2, and 38 and 39 for R4.2 and R4.3, respectively. All clones were maintained at 1 μM concentration of AURK inhibitors.

The CCRF-CEM (human T-lymphoblastic leukemia cells) and A549 (human lung adenocarcinoma) cell lines were obtained from American Tissue Culture Collection (ATCC, Manassas, VA). The CCRF-CEM and A549 cells were cultured at 37 °C and 5% CO_2 in RPMI 1640 and DMEM, respectively, with 5 g/L glucose, 2 mM glutamine, 10% FCS (PAN-Biotech GmbH), penicillin (Biotika), and streptomycin. The CCRF-CEM cells resistant to daunorubicin, vincristine, or cytarabine as well as A549 cells resistant to vincristine or paclitaxel were established as described previously[20] and grown in the media mentioned above.

Cells were grown to 80% confluency in Petri dish, rinsed with cold PBS, and solubilized in 500 μL of extraction buffer consisting of 7 M urea, 2 M thiourea, 3% w/v CHAPS (Carl Roth GmbH, Karlsruhe, Germany), 2% v/v Nonidet 40, 5 mM TCEP, protease inhibitor cocktail (complete Mini, Roche, Mannheim, Germany), and phosphatase inhibitor cocktail (PhosSTOP, Roche, Mannheim, Germany). Cell lysates were left for 30 min at room temperature to optimize protein extraction and centrifuged at 20000g at 4 °C for 1 h, and the clarified protein extracts were kept at −80 °C until used. The protein concentration of each sample was estimated using the Pierce 660 nm protein assay kit (Thermo Scientific, Rockford, IL) according to the manufacturer's protocol.

2-DE and Evaluation of Protein Spot Differences

2-DE was carried out using Protean IEF Cell (Bio-Rad, Hercules, CA) for the first dimension and Protean II xi Cell (Bio-Rad) for the second dimension. Polyacrylamide gel strips with an IPG of 4−7 and 6−11 (180 mm × 3 mm × 0.5 mm, GE Healthcare, Uppsala, Sweden) were loaded with 100 and 70 μg of proteins, respectively. For the pH range 4−7, protein extracts were diluted to 130 μL with extraction buffer and dissolved in 230 μL of rehydration buffer: 7 M urea, 2 M thiourea, 4% CHAPS, 200 mM DeStreak reagent (GE Healthcare, Uppsala, Sweden), 2% IPG buffer pH 4−7 (GE Healthcare), protease inhibitor cocktail, phosphatase inhibitor cocktail, and a trace of bromophenol blue. Proteins were loaded into IPG strips using overnight in gel rehydration at 50 V, and IEF was performed at the following voltages: 200 V for 10 h, 600 V for 30 min, 1000 V for 30 min, and 5000 V for the time period necessary to reach 50000 Vh in total. After IEF separation, IPG strips were equilibrated in 50 mM Tris-HCl, pH 6.8 (Carl Roth GmbH), 6 M urea, 30% glycerol (Penta, Prague, Czech Republic), 4% SDS, and 100 mM DeStreak reagent for 25 min.

dx.doi.org/10.1021/pr300819m | J. Proteome Res. XXXX, XXX, XXX−XXX

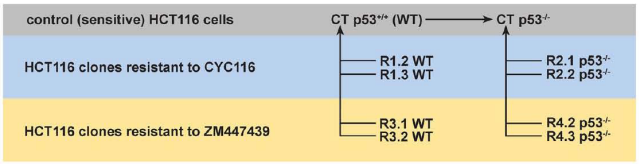


Figure 1. Clones resistant to CYC116 or ZM447439 AURK inhibitors analyzed using 2-DE. Wild-type (WT) $p53^{+/+}$ resistant cells were compared to sensitive HCT116 $p53^{+/+}$ cells, and resistant cells carrying $p53^{-/-}$ alleles were compared to sensitive HCT116 $p53^{-/-}$ cells.

For the pH range 6−11, IPG strips were passively rehydrated overnight without sample in 340 μL of rehydration buffer with 0.5% IPG buffer, pH 6−11 (GE Healthcare), and 30 mM DTT instead of DeStreak reducing agent. Protein extracts were diluted to 150 μL with extraction buffer supplemented by 65 mM DTT and 0.5% IPG buffer, pH 6−11. After 15 min, free thiol groups were alkylated by 30 mM iodoacetamide, a trace of bromophenol blue was added, and cup-loading was applied. IEF was performed at the following voltages: 150 V for 12 h, 1000 V for 1 h, 8000 V for 3 h, and 8000 V for the time period necessary to reach 20000 Vh in total. After IEF separation, IPG strips were equilibrated for 20 min as described above but with 8% SDS and without reducing agent (DeStreak).

For preparative gels, IPG strips were loaded with 500 and 130 μg of total protein for pH 4−7 and pH 6−11, respectively. Prior to the second dimension, the focused proteins were reduced (1% DTT) and alkylated (4% iodoacetamide) in two 15 min steps via equilibration.

The equilibrated proteins were transferred from the IPG strips onto a 10% SDS-PAGE gels (180 mm × 180 mm × 1 mm). SDS-PAGE was carried out at a constant current of 40 mA per gel until the bromophenol blue line reached the bottom of the gel. Analytical gels were stained with SYPRO Ruby protein gel stain (Bio-Rad) and digitized at 500 DPI resolution using a Pharos FX scanner (Bio-Rad). Protein spots on preparative gels were visualized by reverse staining using a zinc salt.[21]

For further evaluation, 2-DE gel images were subjected to REDFIN Solo analysis (http://www.ludesi.com/, Ludesi, Malmo, Sweden).[22] All resistant clones were compared in pairs with relevant (sensitive) control either HCT116 $p53^{+/+}$ (wild-type) or HCT116 $p53^{-/-}$ cell line (Figure 1), and differential expression of proteins was determined by applying the criteria of significance with $p < 0.05$ and fold-change values > ±1.20. The calculations (Student's t test) were performed by REDFIN software from the mean normalized volumes of four biological replicates, which were grown and processed independently.

Enzymatic In-Gel Digestion

Spots showing a significant expression change ($p < 0.05$) were excised from zinc-stained preparative gels and cut into small pieces. To complex zinc ions, gel pieces were incubated for 5 min in 50 mM Tris-HCl pH 8.3 (Carl Roth GmbH), 200 mM glycine, and 30% acetonitrile (Merck Millipore, Bilerica, MA). The gel pieces became transparent, and after complete destaining, the chelating solution was removed, and gels were rinsed twice with 50 mM Tris-HCl, pH 8.3 (Carl Roth GmbH). Then, gels were washed with water, shrunk by dehydration in acetonitrile, and reswollen in water. The washing step was repeated three times, and gels were partly dried in a SpeedVac concentrator. Gels were rehydrated in a cleavage buffer containing 25 mM 4-ethyl-morpholine, 5% acetonitrile, and trypsin (3.3 ng/μL; Promega, Madison, WI) and incubated overnight at 37 °C. The digestion was stopped by the addition of 5% trifluoroacetic acid in acetonitrile, and the aliquot of the resulting peptide mixture was desalted using a GELoader microcolumn (Eppendorf, Prague, Czech Republic) packed with a Poros Oligo R3 material.[23] The purified and concentrated peptides were eluted from the microcolumn in several droplets directly onto MALDI plate using 1 μL of α-cyano-4-hydroxycinnamic acid matrix solution (5 mg/mL in 50% acetonitrile and 0.1% trifluoroacetic acid).

Protein Identification by MALDI-TOF/TOF Mass Spectrometry

MALDI mass spectra were measured on an Ultraflex III MALDI-TOF/TOF instrument (Bruker Daltonics, Bremen, Germany) equipped with a smartbeam solid state laser and LIFT technology for MS/MS analysis. PMF spectra were acquired in the mass range of 700−4000 Da and calibrated internally using the monoisotopic $[M + H]^+$ ions of trypsin autoproteolytic fragments (842.5 and 2211.1 Da). For PMF database searching, peak lists in XML data format were created using the flexAnalysis 3.0 program with SNAP peak detection algorithm. No smoothing was applied, and a maximal number of assigned peaks was set to 50. After peak labeling, all known contaminant signals were removed.

The peak lists were searched using in-house MASCOT search engine against the Swiss-Prot 2011_09 database subset of human proteins with the following search settings: peptide tolerance of 30 ppm, missed cleavage site value set to one, variable carbamidomethylation of cysteine, oxidation of methionine, and protein N-terminal acetylation. No restrictions on protein molecular weight and pI value were applied. Proteins with a Mascot score over the threshold 56 calculated for the used settings were considered as identified. If the score was lower or only slightly higher than the threshold value, the identity of protein candidate was confirmed by MS/MS analysis. In addition to the above-mentioned MASCOT settings, a fragment mass tolerance of 0.6 Da and instrument type MALDI-TOF/TOF were applied for MS/MS spectra searching.

Classification of Protein Changes in HCT116 Resistant Cells and Computer Modeling of Interaction Networks

To assign the roles in biological processes, differentially expressed proteins were searched against the PANTHER 7.0 (http://www.pantherdb.org/).[24] Stringent criteria were further applied to select protein changes overlapping among resistant clones and alterations present exclusively in all four clones resistant to CYC116 or in all four clones resistant to ZM447439, irrespective of p53, as well as those present in all four $p53^{+/+}$ clones or in all four $p53^{-/-}$ clones resistant to both AURK inhibitors were searched. In addition, protein changes present in two clones either $p53^{+/+}$ or $p53^{-/-}$ and typical for CYC116 or ZM447439 were also evaluated. Furthermore, selection of candidate biomarkers of resistance to AURK inhibitors was performed according to the presence of significant protein

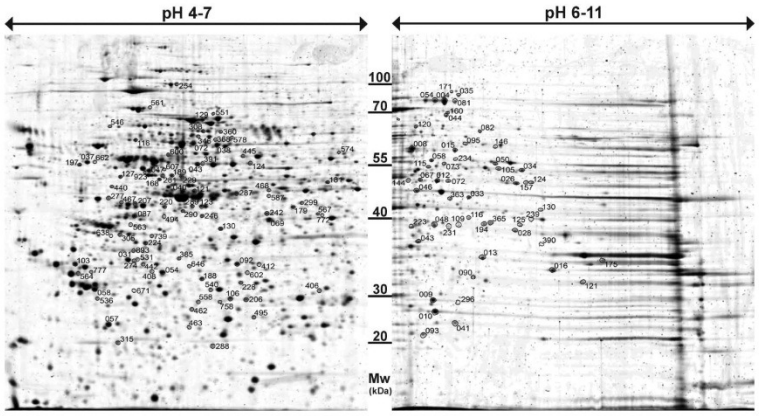


Figure 2. Significantly regulated protein spots in HCT116 cells resistant to AURK inhibitors. Representative maps of 2-DE gels in pH 4–7 and 6–11 show the protein spots significantly regulated in resistant cells ($p < 0.05$) with numbers generated by REDFIN software. Spot numbers of pH 4–7 and 6–11 are in tables marked with N (neutral) and B (basic), respectively.

changes in at least five out of eight HCT116 resistant clones irrespective of inhibitor used and p53 phenotype.

To enhance observed proteomic data, selected identified proteins were introduced into the Interologous Interaction Database 1.95 of known and predicted mammalian and eukaryotic protein–protein interactions (http://ophid.utoronto.ca/ophidv2.201/index.jsp).[25] Protein–protein interaction networks were visualized using NAVIGaTOR 2.2.1 (http://ophid.utoronto.ca/navigator/).

Western Blot Analysis

Cell lysates were dissolved in SDS sample buffer, and 5 μg of the protein extracts was separated in 12% SDS-PAGE gels using Mini Protean II Cell (Bio-Rad). Proteins were then transferred to Immobilon-P membranes (Merck Millipore) using a semidry blotting system (Biometra, Gottingen, Germany) and transfer buffer containing 48 mM Tris, pH 9.2, 39 mM glycine (Carl Roth GmbH), and 20% methanol (Lach-Ner, Neratovice, Czech Republic). The membranes were blocked for 1 h with 5% nonfat dry milk in TBS, pH 7.4, with 0.05% Tween 20 and incubated overnight with primary antibodies directed against β-tubulin (anti-β-tubulin, 1:20000, Sigma, St. Louis, MO); platelet-activating factor acetylhydrolase IB subunit β (anti-PAFAH1B2, 1:1000, Abcam, Cambridge, United Kingdom); GTP-binding nuclear protein Ran (anti-Ran, 1:4000, Abcam); serine hydroxymethyltransferase (anti-SHMT2, 1:6000, Sigma Prestige Antibodies, St. Louis, MO); serpin B5 (anti-SERPINB5, 1:1000, Aviva Systems Biology, San Diego, CA); calretinin (anti-CALB2, 1:6000, Sigma Prestige Antibodies); and voltage-dependent anion-selective channel protein 2 (anti-VDAC2, 1:3000, Aviva Systems Biology). Peroxidase-conjugated secondary antibodies were diluted in 5% nonfat dry milk/TBS, pH 7.4, with 0.05% Tween 20 and applied as appropriate. Antimouse IgG antibody (Jackson Immunoresearch, Suffolk, UK) and antirabbit IgG antibody (Jackson Immunoresearch, Suffolk, UK) were diluted 1:10000, and antichicken IgY (Abcam) was diluted 1:100000. The ECL+ chemiluminiscence detection system (GE Healthcare) was used to detect specific protein bands on Western blot, and membranes were then exposed to CL-XPosure films (Thermo Scientific, Rockford, IL) in three independent experiments.

RESULTS

Overview of Proteome Changes in $p53^{+/+}$ and $p53^{-/-}$ HCT116 Cells Resistant to AURK Inhibitors

To characterize changes in protein expression involved in the development of drug resistance to AURK inhibitors, sensitive and resistant HCT116 cells with or without p53 were lysed, extracted proteins were separated by 2-DE in pH gradients 4–7 and 6–11, and protein spots were visualized by fluorescent SYPRO Ruby protein gel stain. Using REDFIN software, 984 and 390 protein spots in pH 4–7 and pH 6–11, respectively, were detected and matched in all gels of all analyzed samples (eight resistant clones, two sensitive parental cells, and four biological replicates of each sample). As shown in Figure 1, gels corresponding to the clones R1.2 and R1.3 resistant to CYC116 and carrying $p53^{+/+}$ were compared to sensitive HCT116 $p53^{+/+}$ counterparts, and CYC116 resistant clones R2.1 and R2.2 carrying $p53^{-/-}$ alleles were compared to sensitive HCT116 $p53^{-/-}$ cells. Similarly, the gels corresponding to cells resistant to ZM447439 (R3.1, R3.2, R4.2, and R4.3) were analyzed.

A statistical comparison revealed 144 significantly different protein spots with minimal fold-change $\pm$1.20 and present in at least one of all eight resistant clones (Figure 2 and Supplementary Table 1 in the Supporting Information). Among these proteins, 51 (35%) were up-regulated and 63 (44%) were down-regulated in cells resistant to AURK inhibitors. The remaining 30 proteins (21%) have shown distinct regulation among resistant clones. Identified proteins from 144 spots represented 127 unique proteins, and 82 and 45 proteins were found in pH ranges 4–7 and 6–11, respectively. Fifteen proteins were present in two spots (031N, 274N; 037N, 662N; 129N, 467N; 168N, 281N; 197N, 495N; 290N, 739N; 305N, 638N; 360N, 095B; 564N, 777N; 012B, 067B; 028B, 125B; 034B, 105B; 035B, 171B; 044B, 160B; and 124B, 157B), two proteins were present in three spots (043N, 124N, 391N; and 004B, 054B, 081B), and there were only two spots each

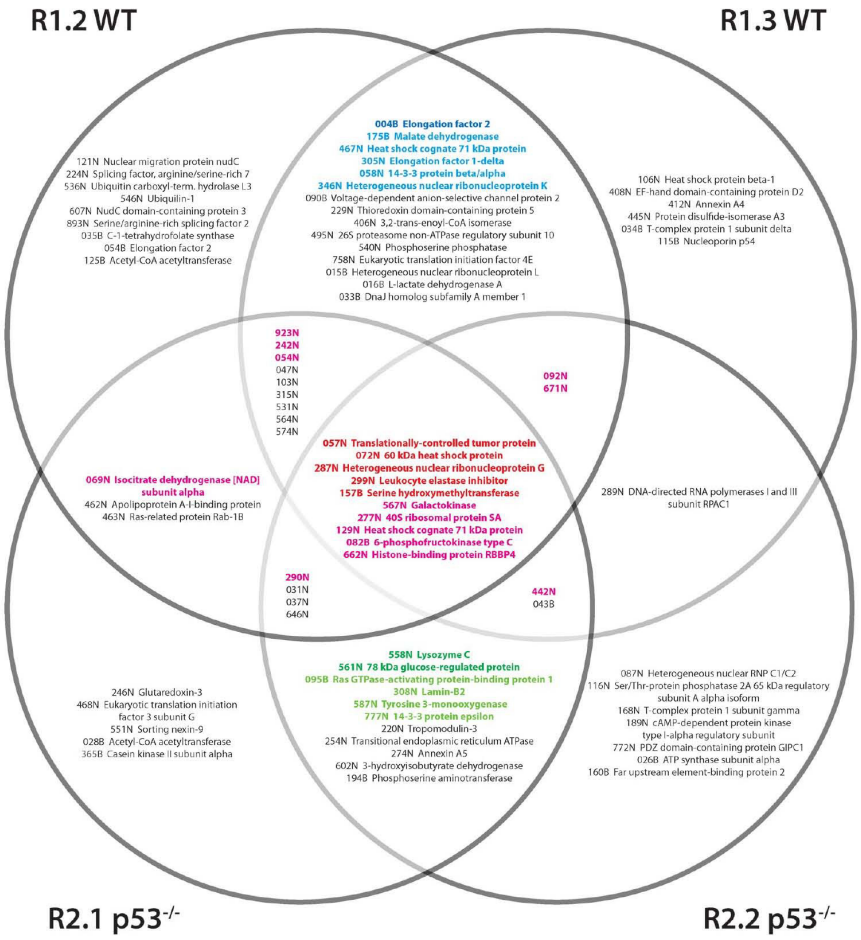


Figure 3. Venn diagram of proteins differentially expressed in HCT116 cells resistant to CYC116 and the overlap between cell types. In the diagram, the proteins in red color highlight p53-independent changes specific for CYC116 resistance (Table 1). The changes related to p53 phenotype are indicated in blue (WT) and green ($p53^{-/-}$) colors where the light shade represents CYC116 specific changes (Table 3), while the dark shade further indicates the protein(s) also overlapping with the ZM447439 (Table 2). The black color indicates the proteins regulated in at least one resistant clone (Supplementary Table 1 in the Supporting Information). The magenta color displays the proteins regulated in at least five out of total eight resistant clones without any selectivity to a specific kind of AURK inhibitor or p53 phenotype (Figure 6).

containing two proteins (197N, 146B), thus indicating high resolution of protein fractionation applied in this study. Mass spectrometric data of all identified proteins are presented in Supplementary Table 2 in the Supporting Information.

Involvement of identified proteins in biological processes classified by PANTHER database 7.0 according to Gene Ontology is provided in the Supplementary Table 3 in the Supporting Information. The majority of identified proteins are involved in metabolic processes of proteins, lipids, carbohydrates, and nucleic acids; however, this study also revealed proteins participating in signal transduction, cell cycle, developmental processes, transport, and the immune system.

Overlap of Protein Alterations among HCT116 Resistant Cells

Figures 3 and 4 show Venn diagrams of proteins differentially expressed in individual HCT116 resistant cells and the overlap between the cell types. It was evident that the number of significant protein changes shared among HCT116 resistant cells was not too high. The highest overlap was observed between cells resistant to CYC116 carrying $p53^{+/+}$ (clones R1.2 and R1.3) and $p53^{-/-}$ (clones R2.1 and R2.2). These p53-independent changes specific for CYC116 resistant cells (Figure 3 and Table 1) included a decrease in translationally controlled tumor protein (spot 057N), 60 kDa heat shock protein (spot 072N), and heterogeneous nuclear ribonucleoprotein G (spot 287N) and an

dx.doi.org/10.1021/pr300819m | J. Proteome Res. XXXX, XXX, XXX−XXX

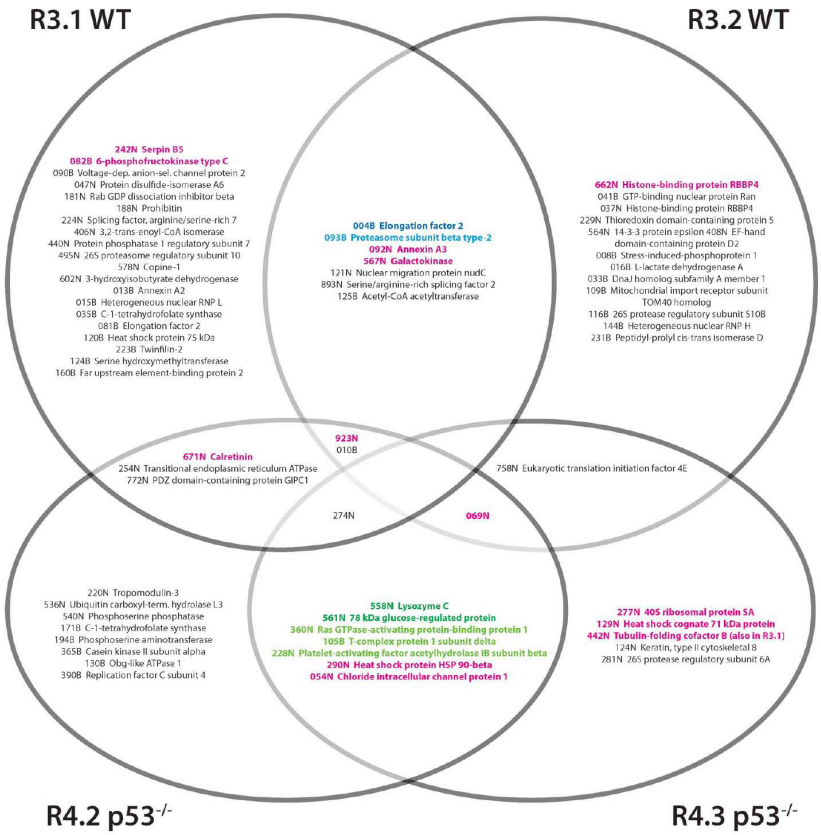


Figure 4. Venn diagram of proteins differentially expressed in HCT116 cells resistant to ZM447439 and the overlap between cell types. In this diagram, the changes related to p53 phenotype are indicated in blue (WT) and green ($p53^{-/-}$) where the lighter shade of color represents ZM447439 specific changes (Table 3) and the dark shade further indicates the protein(s) also overlapping with the CYC116 (Table 2). The black color indicates the proteins regulated in at least one resistant clone (Supplementary Table 1 in the Supporting Information). The magenta color displays the proteins regulated in at least five out of total eight resistant clones without any selectivity to a specific kind of AURK inhibitor or p53 phenotype (Figure 6).

Table 1. Protein Changes Typical for Individual AURK Inhibitors Irrespective of p53 Phenotype[a]

		CYC116				ZM447439[b]			
		$p53^{+/+}$		$p53^{-/-}$		$p53^{+/+}$		$p53^{-/-}$	
spot no.	protein name	R1.2	R1.3	R2.1	R2.2	R3.1	R3.2	R4.2	R4.3
057N	translationally controlled tumor protein	−1.86	−1.67	−2.82	−1.76				
072N	60 kDa heat shock protein	−1.63	−1.32	−1.57	−1.25				
287N	heterogeneous nuclear ribonucleoprotein G	−3.07	−2.23	−2.00	−1.90				
299N	leukocyte elastase inhibitor	1.89	1.91	2.98	2.50				
157B	serine hydroxymethyltransferase	1.46	1.82	1.43	1.31				

[a]Fold-change values for proteins significantly regulated in HCT116 resistant cells. [b]No p53-independent protein changes typical for ZM447439 resistant cells were found.

increase in leukocyte elastase inhibitor (spot 299N) and serine hydroxymethyltransferase (spot 157B). On the contrary, we did not find any overlap between cells resistant to ZM447439 carrying $p53^{+/+}$ (clones R3.1 and R3.2) and $p53^{-/-}$ (clones R4.2 and R4.3) (Figure 4 and Table 1).

We also observed that both CYC116 and ZM447439 resistant cells were characterized by differential expression of elongation factor 2 (spot 004B) exclusively in all four $p53^{+/+}$ clones (R1.2, R1.3, R3.1, and R3.2; Figures 3 and 4), while all four $p53^{-/-}$ clones (clones R2.1, R2.2, R4.2, and R4.3; Figures 3 and 4)

Table 2. Protein Changes Common to Both AURK Inhibitors Dependent on p53 Phenotype

		CYC116				ZM447439			
		$p53^{+/+}$		$p53^{-/-}$		$p53^{+/+}$		$p53^{-/-}$	
spot no.	protein name	R1.2	R1.3	R2.1	R2.2	R3.1	R3.2	R4.2	R4.3
004B	elongation factor 2	−1.72	−1.31			−1.93	−1.48		
558N	lysozyme C			1.33	1.43			1.63	1.33
561N	78 kDa glucose-regulated protein			−1.90	−1.80			−1.76	−2.10

Table 3. Protein Changes Typical for Individual AURK Inhibitors Related to p53 Phenotype[a]

		CYC116				ZM447439			
		$p53^{+/+}$		$p53^{-/-}$		$p53^{+/+}$		$p53^{-/-}$	
spot no.	protein name	R1.2	R1.3	R2.1	R2.2	R3.1	R3.2	R4.2	R4.3
175B	malate dehydrogenase	2.56	1.82						
467N	heat shock cognate 71 kDa protein	1.61	2.05						
305N	elongation factor 1-δ	1.43	1.50						
058N	14-3-3 protein β/α	−1.20	−1.67						
346N	heterogeneous nuclear ribonucleoprotein K	−1.33	−1.48						
095B	Ras GTPase-activating protein-binding protein 1			1.29	1.41				
308N	lamin-B2			−2.03	−4.60				
587N	tyrosine 3-monooxygenase			−1.38	−1.51				
777N	14-3-3 protein ε			−1.83	−1.71				
093B	proteasome subunit β type-2					1.84	2.08		
360N	Ras GTPase-activating protein-binding protein 1							1.93	1.82
105B	T-complex protein 1 subunit δ							1.23	1.27
228N	platelet-activating factor acetylhydrolase IB subunit β							−2.13	−2.19

[a]Fold-change values for proteins significantly regulated in HCT116 resistant cells.

exhibited variant levels of lysozyme C (spot 558N) and 78 kDa glucose-regulated protein (spot 561N) (Table 2).

Protein Changes in HCT116 Resistant Cells Typical for Individual AURK Inhibitors Related to p53 Phenotype

As mentioned above, we selected the group of proteins significantly changed in p53-independent manner in cells resistant to CYC116 only. In addition to these, there were other proteins typical for cells resistant to CYC116 with protein alterations related to p53 phenotype. Three proteins, namely, malate dehydrogenase (spot 175B), heat shock cognate 71 kDa protein (spot 467N), and elongation factor 1-δ (spot 305N) were significantly increased as well as two proteins, 14-3-3 protein β/α (spot 058N) and heterogeneous nuclear ribonucleoprotein K (spot 346N), were significantly decreased in two clones resistant to CYC116 carrying $p53^{+/+}$ (clones R1.2 and R1.3; Figure 3 and Table 3) but not in the clones carrying $p53^{-/-}$ (clones R2.1 and R2.2). Conversely, Ras GTPase-activating protein-binding protein 1 (spot 095N) was typically increased, while lamin-B2 (spot 308N), tyrosine 3-monooxygenase (spot 587N), and 14-3-3 protein epsilon (spot 777N) were decreased in HCT116 cells resistant to CYC116 carrying $p53^{-/-}$ (clones R2.1 and R2.2; Figure 3 and Table 3) but not in the clones $p53^{+/+}$ (clones R1.2 and R1.3).

As compared to what we could observe in cells resistant to CYC116, the number of protein alterations related to p53 phenotype typical for cells resistant to ZM447439 was limited to four proteins only. Proteasome subunit β type-2 (spot 93B) was significantly higher in $p53^{+/+}$ clones (clones R3.1 and R3.2; Figure 4 and Table 3) but not in the clones carrying $p53^{-/-}$ (clones R4.2 and R4.3), three proteins with an increased level of Ras GTPase-activating protein-binding protein 1 (spot 360N) and T-complex protein 1 subunit δ (spot 105B) and decreased level of platelet-activating factor (PAF) acetylhydrolase IB subunit β (spot 228N) were changed in $p53^{-/-}$ clones resistant to ZM447439 (clones R4.2 and R4.3; Figure 4 and Table 3) but not in the clones $p53^{+/+}$ (clones R3.1 and R3.2).

Computer Modeling of Possible Interaction Networks in HCT116 Resistant Cells

UniProtKB accessions of the proteins from Table 1 were introduced into Interologous Interaction Database to identify possible interaction partners, and Figure 5 depicts their interaction network generated by NAVIGaTOR software. In total, 435 interactions were recognized for translationally controlled tumor protein (TCPT), 60 kDa heat shock protein (HSP60), heterogeneous nuclear ribonucleoprotein G (hnRNPG), leukocyte elastase inhibitor (LEI), and serine hydroxymethyltransferase (GLYM) (Supplementary Table 4 in the Supporting Information). Computer modeling highlighted a high number of mediated interactions among these proteins and revealed interconnectivity via autophagy protein 5 (AP5, ATG5_HUMAN) and WD repeat domain phosphoinositide-interacting protein 2 (WPI2, WIPI2_HUMAN), indicating their possible role in resistance to CYC116.

Quest for Candidate Biomarkers of Resistance to AURK Inhibitors

In a quest for common candidate markers of resistance to AURK inhibitors, the proteins significantly changing their levels ($p < 0.05$) in at least five out of total eight resistant clones without any selectivity to a specific kind of inhibitor or p53 phenotype were searched. On the basis of these criteria, 13 selected proteins (Figure 6) including 26S protease regulatory subunit 6B (PRS6B, spot 923N), serpin B5 (SPB5, spot 242N), annexin A3 (ANXA3, spot 092N), calretinin (CALB2, spot 671N), heat shock protein HSP 90-β (HSP90B, spot 290N), and galactokinase (GALK1, spot 567N) were found to represent the proteins that were up-

dx.doi.org/10.1021/pr300819m | J. Proteome Res. XXXX, XXX, XXX−XXX

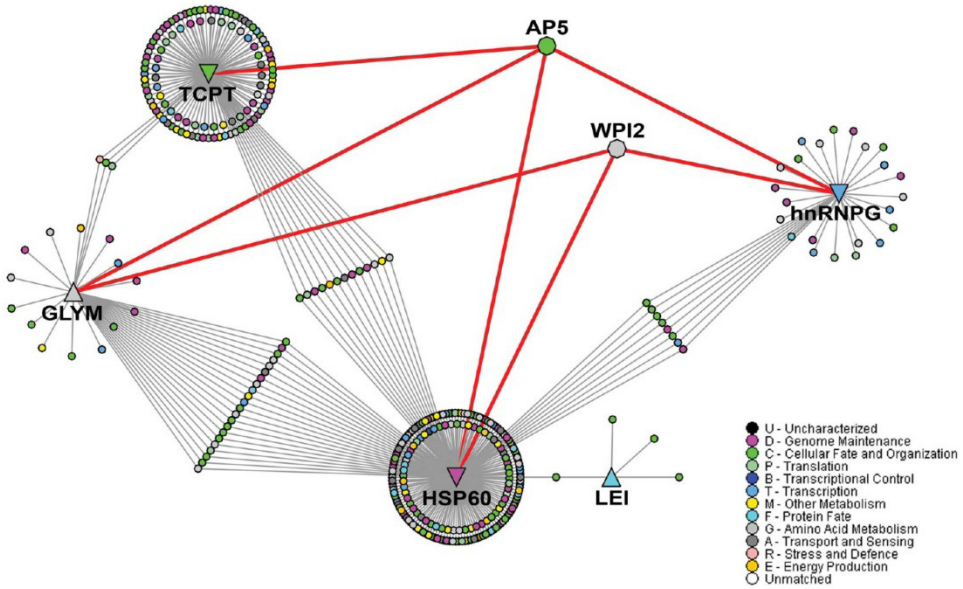


Figure 5. p53-independent interaction network in CYC116 resistant cells. Computer modeling of possible protein−protein interactions in HCT116 cells resistant to CYC116 depicts a high number of mediated interactions among proteins from Table 1 (translationally controlled tumor protein, TCPT; 60 kDa heat shock protein, HSP60; heterogeneous nuclear ribonucleoprotein G, hnRNPG; leukocyte elastase inhibitor, LEI; and serine hydroxymethyltransferase, GLYM) and highlighted by red link interconnections via autophagy protein 5 (AP5) and WD repeat domain phosphoinositide-interacting protein 2 (WPI2). The network generated by NAVIGaTOR software is best interpreted as follows: nodes represent proteins, and edges between nodes represent physical interactions between proteins. Proteins regulated specifically in all HCT116 clones resistant to CYC116 are indicated by a triangle (up- or down-regulated), and interacting proteins retrieved by Interologous Interaction Database and NAVIGaTOR software are indicated by an ellipse. The color of nodes represents Gene Ontology functionality.

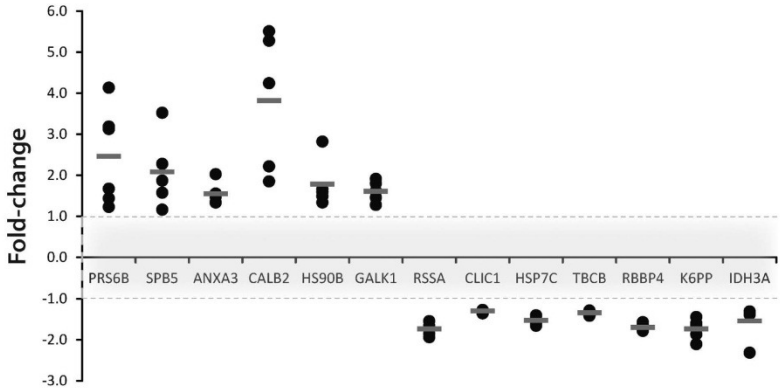


Figure 6. Biomarker candidates. Fold-change values for proteins significantly regulated in at least five out of eight resistant clones as compared to the corresponding control (fold-change > ±1.0, $p < 0.05$) are shown in the dot-plot graph. 26S protease regulatory subunit 6B (PRS6B, $n = 6$), serpin B5 (SPB5, $n = 5$), annexin A3 (ANXA3, $n = 5$), calretinin (CALB2, $n = 5$), heat shock protein HSP 90-β (HSP90B, $n = 5$), galactokinase (GALK1, $n = 6$), 40S ribosomal protein SA (RSSA, $n = 5$), chloride intracellular channel protein (CLIC1, $n = 5$), heat shock cognate 71 kDa protein (HSP7C, $n = 5$), tubulin-folding cofactor B (TBCB, $n = 5$), histone-binding protein RBBP4 (RBBP4, $n = 5$), 6-phosphofructokinase type C (K6PP, $n = 5$), and isocitrate dehydrogenase [NAD] subunit α (IDH3A, $n = 5$).

regulated in resistant clones; 40S ribosomal protein SA (RSSA, spot 277N), chloride intracellular channel protein (CLIC1, spot 054N), heat shock cognate 71 kDa protein (HSP7C, spot 129N), tubulin-folding cofactor B (TBCB, spot 442N), histone-binding

dx.doi.org/10.1021/pr300819m | J. Proteome Res. XXXX, XXX, XXX−XXX

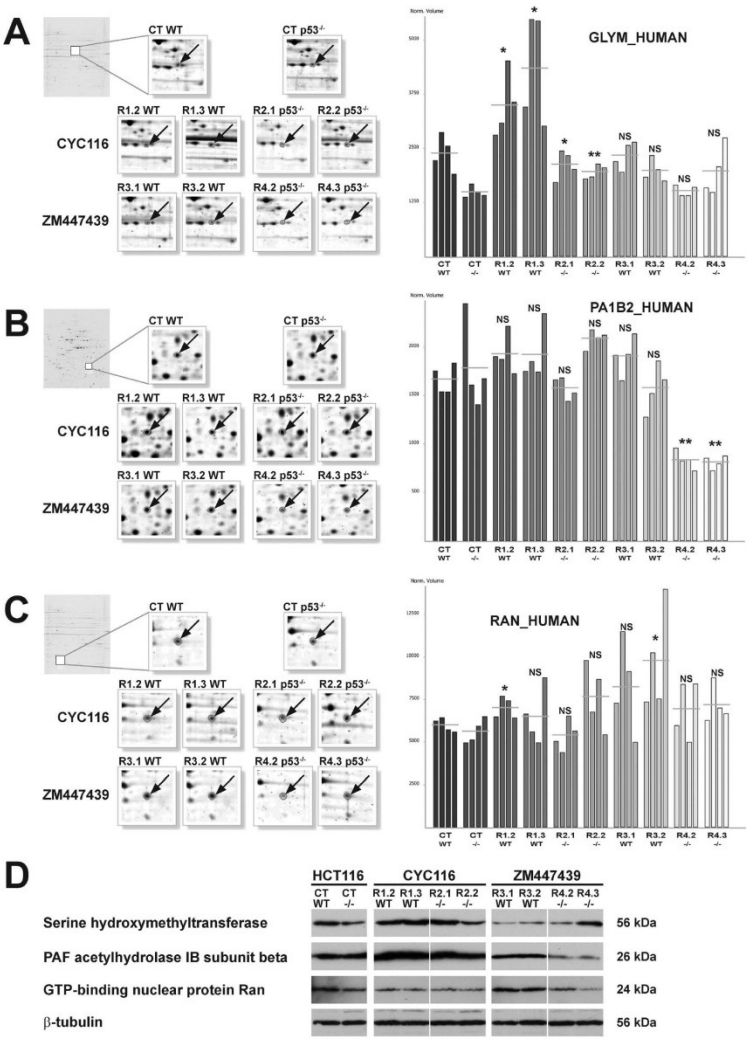


Figure 7. Protein changes in HCT116 resistant cells typical for individual AURK inhibitors. Significantly regulated protein spots between HCT116 sensitive (CT, control) cells and cells resistant to AURK inhibitors are indicated by arrows in the zoomed 2D gel images on the left with graphs on the right, generated by REDFIN software depicting normalized spot volumes in four individual gels. (A) Serine hydroxymethyltransferase, GLYM_HUMAN; (B) PAF acetylhydrolase IB subunit β, PA1B2_HUMAN; (C) GTP-binding nuclear protein Ran, RAN_HUMAN (NS, not significant; $*p < 0.05$, $**p < 0.01$, and $***p < 0.001$, as compared to corresponding sensitive cell line HCT116 with wild-type $p53^{+/+}$ (WT) or mutated $p53^{-/-}$). (D) Western blot analysis of serine hydroxymethyltransferase, PAF acetylhydrolase IB subunit β, and GTP-binding nuclear protein Ran. Sensitive and resistant cells were examined using specific antibodies, and β-tubulin was used as a loading control.

protein RBBP4 (RBBP4, spot 662N), 6-phosphofructokinase type C (K6PP, spot 082B), and isocitrate dehydrogenase [NAD] subunit α (IDH3A, spot 069N) were the proteins down-regulated in resistant clones.

Verification of Selected Proteomic Data

Among significantly reproducible protein changes in HCT116 cells resistant to CYC116 and ZM447439 AURK inhibitors, 2-fold and higher changes were reached by translationally controlled tumor protein, heterogeneous nuclear ribonucleo-protein G, leukocyte elastase inhibitor, and 78 kDa glucose-regulated protein (Tables 1 and 2); malate dehydrogenase, heat shock cognate 71 kDa protein, lamin-B2, proteasome subunit β type-2, and PAF acetylhydrolase IB subunit β (Table 3); 26S protease regulatory subunit 6B, serpin B5, annexin A3, calretinin,

dx.doi.org/10.1021/pr300819m | J. Proteome Res. XXXX, XXX, XXX−XXX

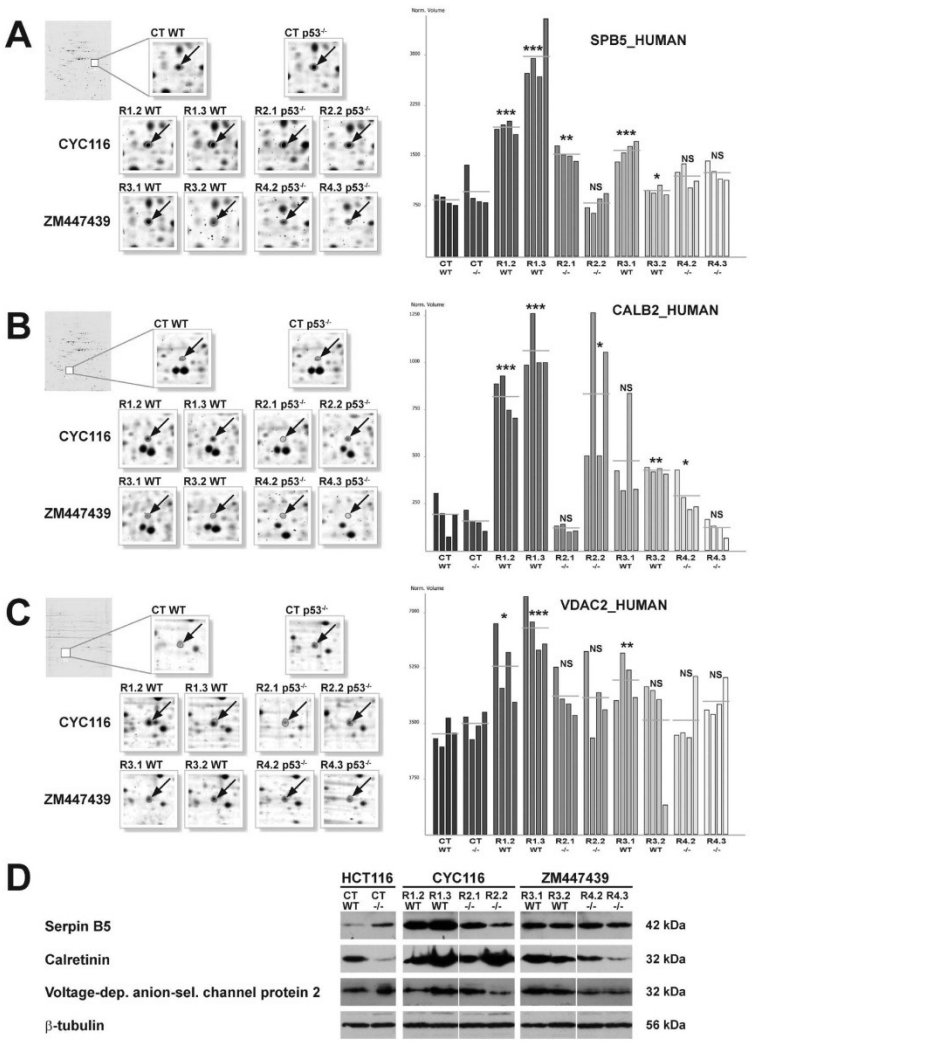


Figure 8. Apoptosis-related protein changes in HCT116 resistant cells. Significantly regulated protein spots between HCT116 sensitive (CT, control) cells and cells resistant to AURK inhibitors are indicated by arrows in the zoomed 2D gel images on the left with graphs on the right, generated by REDFIN software depicting normalized spot volumes in four individual gels. (A) Serpin B5, SPB5_HUMAN; (B) Calretinin, CALB2_HUMAN; (C) voltage-dependent anion-selective channel protein 2, VDAC2_HUMAN (NS, not significant; $*p < 0.05$, $**p < 0.01$, and $***p < 0.001$, as compared to corresponding sensitive cell line HCT116 with wild-type $p53^{+/+}$ (WT) or mutated $p53^{-/-}$). (D) Western blot analysis of serpin B5, calretinin, and voltage-dependent anion-selective channel protein 2. Sensitive and resistant cells were examined using specific antibodies, and β-tubulin was used as a loading control.

heat shock protein HSP 90-β, 6-phosphofructokinase type C, and isocitrate dehydrogenase [NAD] subunit α (Figure 6). While this may reflect the importance of these proteins in the regulation of resistance development, the role of many other less prominent protein alterations should not be ignored. To this end, we selected proteins representing some of the above-mentioned groups for verification by Western blot analysis.

Leukocyte elastase inhibitor and serine hydroxymethyltransferase are the proteins whose expression was typically increased in cells resistant to CYC116 inhibitor. The level of serine hydroxymethyltransferase (spot 157B, GLYM_HUMAN), a potential target enzyme for cancer therapy,[26] showed increase on 2-DE and Western blot in all clones resistant to CYC116 (Figure 7), confirming its independence on p53 phenotype. Interestingly,

dx.doi.org/10.1021/pr300819m | J. Proteome Res. XXXX, XXX, XXX−XXX

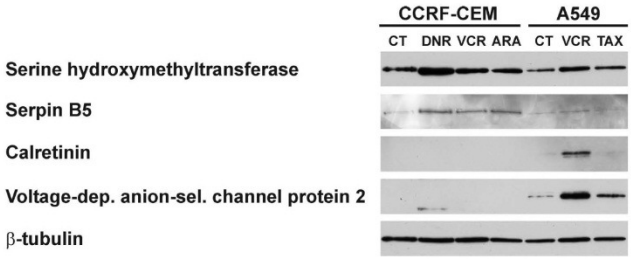


Figure 9. Protein changes in different cancer cells resistant to various anticancer drugs. The expression levels of serine hydroxymethyltransferase, serpin B5, calretinin, and voltage-dependent anion-selective channel protein 2 were measured by Western blotting in CCRF-CEM and A549 cells (CT, control) and cells resistant to daunorubicin (DNR), vincristine (VCR), cytarabine (ARA), and paclitaxel (TAX). β-tubulin was used as a loading control.

PAF acetylhydrolase IB subunit β (spot 228N, PA1B2_HUMAN) was the typical down-regulated protein in $p53^{-/-}$ HCT116 cells resistant to ZM447439 only, and Western blotting allowed verification of this protein (Figure 7). Additionally, GTP-binding nuclear protein Ran (spot 041B, RAN_HUMAN) typical for $p53^{+/+}$ HCT116 cells resistant to ZM447439 was included in the verification for its role in the translocation of p53 through the nuclear pore complex.[27] Despite the fact that significant up-regulation of this protein was observed in only one clone with 2-DE analysis, Western blotting confirmed up-regulation of the protein in both ZM447439 resistant HCT116 $p53^{+/+}$ clones (Figure 7).

Among significant protein changes in at least five out of total eight clones resistant to AURK inhibitors, serpin B5 and calretinin, previously described in regulating apoptosis,[28,29] showed visible overexpression in HCT116 cells. In seven out of eight resistant clones, considerable increase in serpin B5 (spot 242N, SPB5_HUMAN) and calretinin (spot 671N, CALB2_HUMAN) levels were observed, thus further detailing the information obtained using 2-DE (Figure 8). The changes in voltage-dependent anion-selective channel protein 2 (spot 090B, VDAC2_HUMAN), a crucial component in mitochondrial apoptosis,[30] were less pronounced in 2-DE with significantly increased level in majority of $p53^{+/+}$ HCT116 resistant clones detected by Western blot in clones R3.1, R3.2, and R1.3 but not in R1.2 (Figure 8).

Involvement of Selected Proteins in Cancer Cell Resistance to Individual Anticancer Agents

To assess the role of selected proteins from this study in the development of resistance to different chemotherapeutics in different cancer cells, T-lymphoblastic leukemia CCRF-CEM cells carrying p53 mutations and A549 lung adenocarcinoma cells with p53 wild-type phenotype resistant to anticancer drugs with diverse structures and mechanistic targets[20] were examined. Using these cells, no changes in PAF acetylhydrolase and GTP-binding nuclear protein Ran were found (data not shown). However, the different levels of serine hydroxymethyltransferase, serpin B5, calretinin, and voltage-dependent anion-selective channel protein 2 in resistant cells as compared to corresponding controls were examined (Figure 9). Serine hydroxymethyltransferase and serpin B5 were up-regulated in CCRF-CEM cells resistant to daunorubicin, vincristine and cytarabine and in A549 cells resistant to vincristine. Calretinin and voltage-dependent anion-selective channel protein 2 were detectable only in A549 cells showing a noticeable increase in cells resistant to vincristine.

DISCUSSION

The efficiency of specific regimens in cancer therapy can be improved by selective inhibition of AURKs.[2] Despite great expectations from such an approach, the development of resistance toward this type of cancer treatment has to be thoroughly investigated to avoid potential therapy failure. The published data demonstrate a variety of molecular mechanisms leading to the induction of resistance to anticancer drugs including the occurrence of drug-resistant Aurora B mutants after treatment by AURK inhibitors.[5−9,31] Nevertheless, there is a need to better describe such mechanisms and to translate these findings into clinical laboratory with predominant focus on expressed proteins that could be used as markers for therapy monitoring as well as targets for novel anticancer drugs.

In the present study, we considered CYC116 AURK inhibitor, which has been tested in phase I clinical evaluation,[2] and a model inhibitor ZM447439. By short-term culture in high doses of CYC116 and ZM447439, resistant cells were established, and 2D electrophoresis followed by MALDI-TOF/TOF was performed to comprehensively compare sensitive and resistant HCT116 colon cancer cells. The different levels of metabolic proteins such as isocitrate dehydrogenase, phosphoserine aminotransferase, and 40S ribosomal protein SA were identified, which have been already described in a number of proteomic studies of various drug-resistant cancer cell lines[32] and may reflect general response of cells to toxicity. The proteins directly involved in tumor progression and apoptosis were identified in our study, and important changes observed have become a focus of interest.

We identified several candidates; however, most protein changes were observed in individual resistant clones. Combining clones with the same p53 phenotype resistant to the single AURK inhibitor has led to the elimination of proteins expressed differently as a result of sporadic response to anticancer treatment. Because of the low overlap of expression changes between resistant cells, we hypothesize that colon cancer cells resort to different mechanisms to resist cell death induced by CYC116 and ZM447439. CYC116, which is highly effective at lower concentrations as compared to ZM447439,[2,3] was found to be a more specific and with amplified response in resistant cells.

Unlike ZM447439, CYC116 resistant cells expressed several proteins differently regardless of p53. Although these proteins are mainly involved in metabolism of proteins and nucleic acids, computer modeling revealed a high number of mediated interactions among these proteins, linking a variety of biological processes. Interestingly, direct interconnections with autophagy protein 5 and WD repeat domain phosphoinositide-interacting

dx.doi.org/10.1021/pr300819m | J. Proteome Res. XXXX, XXX, XXX−XXX

protein 2 were observed, highlighting a possible role of autophagy process in p53-independent mechanisms of resistance to CYC116 AURK inhibitor. Autophagy, a lysosome-dependent degradation of cytoplasmic organelles and long-lived proteins, is frequently activated in cancer cells.[33] Recently, autophagy has been linked to drug resistance in cancer therapy, and, together with apoptosis, it has a critical role to play in determining cellular fate of tumor cells.[34−37] In HCT116 cells, regulation of translationally controlled tumor protein, 60 kDa heat shock protein, heterogeneous nuclear ribonucleoprotein G, leukocyte elastase inhibitor, and serine hydroxymethyltransferase and their direct interactions with two autophagy participating proteins appear to control the development of resistance to CYC116 AURK inhibitor.

Serine hydroxymethyltransferase plays a pivotal role in channelling metabolites between amino acid and nucleotide metabolism, as it reversibly catalyzes the conversion of serine into glycine while hydroxymethyl group is transferred to 5,6,7,8-tetrahydrofolate. The resultant compound is the sole precursor of purine biosynthesis, which is required for cell division. Hence, serine hydroxymethyltransferase have been indicated as a potential target enzyme for cancer therapy.[26] With regards to the revealed up-regulation of this enzyme in all HCT116 clones resistant to CYC116 and also in CCRF-CEM and A549 resistant cells with no apparent impact of p53 phenotype, we propose serine hydroxymethyltransferase as a target molecule that may resolve the problem of drug resistance to cancer therapy.

Recently, it was shown that inhibition of AURK was needed for efficient cell cycle arrest, which was mediated by induced p53 up-regulation via ATM/ATR protein kinases.[38] Other studies have indicated that inhibition of AURKs may provide a growth advantage to cells that have suffered from p53 loss.[14] Our study, using HCT116 colon cancer cells with and without p53, allowed us to characterize the impact of p53 phenotype on protein differences associated with resistance to AURK inhibitors. Elongation factor 2 was down-regulated specifically in $p53^{+/+}$ cells resistant to both CYC116 and ZM447439 AURK inhibitors. Yin et al. demonstrated that via association with elongation factor 2, p53 is involved in protein translation.[39] Accordingly, p53 might regulate translation in HCT116 cells and contribute to the development of resistance to AURK inhibitors. HCT116 cells with loss of p53 resistant to both CYC116 and ZM447439 AURK inhibitors were characterized by differential expression of lysozyme C and 78 kDa glucose-regulated protein. Lysozyme C, a protein specifically up-regulated in all $p53^{-/-}$ resistant cells, is known to protect cells against oxidative stress.[40] Therefore, such a protective mechanism may contribute to the resistance to AURK inhibitors in these cells. The second protein specifically regulated in all $p53^{-/-}$ resistant cells, 78 kDa glucose-regulated protein, has been previously associated with cancer and resistance to therapy.[41−43] Contrary to what was expected, the level of this antiapoptotic protein was lower in HCT116 resistant cells.

Among the proteins specifically regulated in cells resistant to ZM447439, two proteins were associated with the development of drug resistance with respect to p53 background. While PAF acetylhydrolase was specifically down-regulated in $p53^{-/-}$ resistant cells, the increased level of GTP-binding nuclear protein Ran was observed only in $p53^{+/+}$ resistant cells. PAF (1-*O*-alkyl-2-acetyl-*sn*-glyceryl-3-phosphorylcholine) deacetylation catalyzed by PAF acetylhydrolase induces the loss of PAF lipid messenger activity.[44] Such an inactivation has been demonstrated to affect tumor growth, vascularization, and cell motility.[45] More interestingly, elevated PAF acetylhydrolase levels have been detected in the tumor tissues of patients with colorectal cancer as compared with healthy individuals.[46] These findings subsequently led us to hypothesize that in colon cancer cells, the decreased level of PAF acetylhydrolase may contribute to resistance development in cells that lack p53. Ran, a member of the ras oncogene family, is known to mediate nucleocytoplasmic transport of small RNAs and proteins, and its activity is essential for mitotic spindle assembly.[47] Previous studies suggested Ran as a promising molecular target for RNA interference-based therapeutics against a variety of tumors,[48,49] and these researchers proved that silencing of Ran induced colorectal cancer cells to undergo apoptosis. Our study extended the above-mentioned observation showing that Ran-mediated regulation of apoptosis depends on p53 expression.

Mutated p53 can enhance resistance to anticancer drugs also by up-regulation of multidrug resistance protein 1 (MDR1).[50] MDR1, also known as P-glycoprotein, is a member of ATP-binding cassette transporters located on cell membrane responsible for a tissue-specific excretion of cytotoxic agents out of tumor cells.[51] In the present study, resistant cell lines of different histogenetic origin and p53 phenotype were analyzed. Consistently with previous studies, CCRF-CEM resistant cells with p53 mutations show an increased expression and activity of MDR1 and p53 wild-type A549 cells highly express LRP (lung resistance-related protein), both manifesting a stable multidrug resistance.[20] Further studies on such multidrug resistance in HCT116 resistant cells would add to our findings.

Regulation of apoptosis plays a pivotal role in the development of drug resistance in cancer therapy.[52] In the present study, we found a higher level of proteins associated with apoptotic cell death, such as serpin B5, calretinin, and voltage-dependent anion-selective channel protein 2 in HCT116 cell resistant to AURK inhibitors. Serpin B5, the so-called maspin, has been proved to suppress the growth of various tumors including breast, prostatic, and cervical carcinomas,[53−55] while promoting the growth of tumors in the colon.[28] Previous studies also linked serpin B5 to resistance in cancer therapy, which suggested that the protein could be a target for novel anticancer drugs.[56−58] We found that serpin B5 up-regulated in HCT116 cells resistant to AURK inhibitors and also in CCRF-CEM cells and A549 resistant cells, indicating its role in the development of resistance in a p53-independent manner.

Because of the unequivocal role of calcium in apoptosis, a relationship between calretinin and resistance to drug-induced cell death has been hypothesized.[59] This protein, which is expressed in poorly differentiated colon carcinomas,[60] plays a key role in processes such as message targeting and intracellular calcium buffering. The expression of calretinin in our study was substantially increased in cells resistant to AURK inhibitors and also in A549 cells resistant to vincristine but not in CCRF-CEM cells. Similar to calretinin, voltage-dependent anion-selective channel protein 2 was not detectable in CCRF-CEM cells; however, a higher level was demonstrated in $p53^{+/+}$ cells resistant to AURK inhibitors and in A549 cells resistant to vincristine. Voltage-dependent anion-selective channel protein 2 forms a channel through the mitochondrial outer membrane and acts as a crucial component in mitochondrial apoptosis.[30]

Options in cancer therapy are often limited to regimes based on statistical evaluation. Hence, there is a particular need for biomarkers to aid early detection of drug resistance. Taking into consideration that serpin B5 and calretinin were up-regulated with the highest fold-changes in almost all resistant cells used in

our study, they ultimately represent the most promising molecules for cancer therapy monitoring. Moreover, serpin B5 with secreted annotation could be released by tumors into the bloodstream, where it can be noninvasively assessed during defined therapy, adding to signature of biomarkers useful in cancer treatment.

■ CONCLUSIONS

Characterization of mechanisms leading to the development of drug resistance in cancer therapy is crucial to identifying targets for novel anticancer drugs, which may selectively eliminate resistant cells in specific disease stage. We have shown that serine hydroxymethyltransferase, PAF acetylhydrolase, GTP-binding nuclear protein Ran, serpin B5, calretinin, and voltage-dependent anion-selective channel protein 2 contribute to the development of drug resistance to AURK inhibitors. Following verification of observed protein changes, the overexpression of serine hydroxymethyltransferase, serpin B5, calretinin, and voltage-dependent anion-selective channel protein 2 was evident also in leukemia CCRF-CEM and lung adenocarcinoma A549 cells resistant to distinct anticancer drugs, suggesting that targeting these proteins may overcome the problem of drug resistance in cancer therapy. The study outlined here has been the key "stepping-stone" to current ongoing studies on selected proteins and their levels in cancer patient samples with focus on their functionality as novel targets for cancer therapy. After further validation, monitoring of calretinin and serpin B5 levels may have a profound impact in cancer treatment in clinics. We believe that these in-depth studies will stimulate future research, ultimately leading to improved understanding of drug resistance in cancer therapy and, in particular, to the clarification of proteins functionality.

■ ASSOCIATED CONTENT

Supporting Information

Supplementary Table 1, regulated proteins in HCT116 cells resistant to AURK inhibitors; Supplementary Table 2, mass spectrometric data of identified proteins; Supplementary Table 3, involvement of regulated proteins in biological processes; and Supplementary Table 4, I2D protein−protein interaction search results. This material is available free of charge via the Internet at http://pubs.acs.org.

■ AUTHOR INFORMATION

Corresponding Author

*Tel: +420 315 639 582. Fax: +420 315 639 510. E-mail: kovarova@iapg.cas.cz.

Author Contributions

The manuscript was written with contributions from all authors. All authors have given approval to the final version of the manuscript.

Notes

The authors declare no competing financial interest.

■ ACKNOWLEDGMENTS

We greatly acknowledge Jaroslava Supolikova for skillful technical assistance. This work was supported in part by the Ministry of Education, Youth and Sports (Grant LC07017) and by Institutional Research Projects RVO67985904 (IAPG, AS CR, v.v.i.) and RVO61388971 (IMIC, AS CR, v.v.i.). An infrastructural part of this project was supported from the Operational Program Research and Development for Innovations (CZ.1.05/2.1.00/01.0030).

■ ABBREVIATIONS

AURK, Aurora kinase; PAF, platelet-activating factor; MDR1, multidrug resistance protein 1

■ REFERENCES

(1) Kollareddy, M.; Dzubak, P.; Zheleva, D.; Hajduch, M. Aurora kinases: Structure, functions and their association with cancer. *Biomed. Pap. Med. Fac. Univ. Palacky Olomouc Czech Repub.* **2008**, *152* (1), 27−33.

(2) Kollareddy, M.; Zheleva, D.; Dzubak, P.; Brahmkshatriya, P. S.; Lepsik, M.; Hajduch, M. Aurora kinase inhibitors: Progress towards the clinic. *Invest. New Drugs* **2012**, *30*, 2411−2432.

(3) Ditchfield, C.; Johnson, V. L.; Tighe, A.; Ellston, R.; Haworth, C.; Johnson, T.; Mortlock, A.; Keen, N.; Taylor, S. S. Aurora B couples chromosome alignment with anaphase by targeting BubR1, Mad2, and Cenp-E to kinetochores. *J. Cell Biol.* **2003**, *161* (2), 267−280.

(4) Wang, S.; Midgley, C. A.; Scaerou, F.; Grabarek, J. B.; Griffiths, G.; Jackson, W.; Kontopidis, G.; McClue, S. J.; McInnes, C.; Meades, C.; Mezna, M.; Plater, A.; Stuart, I.; Thomas, M. P.; Wood, G.; Clarke, R. G.; Blake, D. G.; Zheleva, D. I.; Lane, D. P.; Jackson, R. C.; Glover, D. M.; Fischer, P. M. Discovery of N-phenyl-4-(thiazol-5-yl)pyrimidin-2-amine aurora kinase inhibitors. *J. Med. Chem.* **2010**, *53* (11), 4367−4378.

(5) Gottesman, M. M.; Fojo, T.; Bates, S. E. Multidrug resistance in cancer: role of ATP-dependent transporters. *Nat. Rev. Cancer* **2002**, *2* (1), 48−58.

(6) Elsaleh, H.; Powell, B.; McCaul, K.; Grieu, F.; Grant, R.; Joseph, D.; Iacopetta, B. P53 alteration and microsatellite instability have predictive value for survival benefit from chemotherapy in stage III colorectal carcinoma. *Clin. Cancer Res.* **2001**, *7* (5), 1343−1349.

(7) Youn, C. K.; Kim, M. H.; Cho, H. J.; Kim, H. B.; Chang, I. Y.; Chung, M. H.; You, H. J. Oncogenic H-Ras up-regulates expression of ERCC1 to protect cells from platinum-based anticancer agents. *Cancer Res.* **2004**, *64* (14), 4849−4857.

(8) Dean, M. Cancer stem cells: Implications for cancer causation and therapy resistance. *Discovery Med* **2005**, *5* (27), 278−82.

(9) Glasspool, R. M.; Teodoridis, J. M.; Brown, R. Epigenetics as a mechanism driving polygenic clinical drug resistance. *Br. J. Cancer* **2006**, *94* (8), 1087−92.

(10) Hollstein, M.; Sidransky, D.; Vogelstein, B.; Harris, C. C. p53 mutations in human cancers. *Science* **1991**, *253* (5015), 49−53.

(11) Gasco, M.; Crook, T. p53 family members and chemoresistance in cancer: what we know and what we need to know. *Drug Resist. Updates* **2003**, *6* (6), 323−328.

(12) Vousden, K. H.; Lu, X. Live or let die: The cell's response to p53. *Nat. Rev. Cancer* **2002**, *2* (8), 594−604.

(13) Moll, U. M.; Wolff, S.; Speidel, D.; Deppert, W. Transcription-independent pro-apoptotic functions of p53. *Curr. Opin. Cell Biol.* **2005**, *17* (6), 631−636.

(14) Mao, J. H.; Wu, D.; Perez-Losada, J.; Jiang, T.; Li, Q.; Neve, R. M.; Gray, J. W.; Cai, W. W.; Balmain, A. Crosstalk between Aurora-A and p53: Frequent deletion or downregulation of Aurora-A in tumors from p53 null mice. *Cancer Cell* **2007**, *11* (2), 161−173.

(15) Chen, S. S.; Chang, P. C.; Cheng, Y. W.; Tang, F. M.; Lin, Y. S. Suppression of the STK15 oncogenic activity requires a transactivation-independent p53 function. *EMBO J.* **2002**, *21* (17), 4491−4499.

(16) Katayama, H.; Sasai, K.; Kawai, H.; Yuan, Z. M.; Bondaruk, J.; Suzuki, F.; Fujii, S.; Arlinghaus, R. B.; Czerniak, B. A.; Sen, S. Phosphorylation by aurora kinase A induces Mdm2-mediated destabilization and inhibition of p53. *Nat. Genet.* **2004**, *36* (1), 55−62.

(17) Cheng, J.; Haas, M. Frequent mutations in the p53 tumor suppressor gene in human leukemia T-cell lines. *Mol. Cell. Biol.* **1990**, *10* (10), 5502−5509.

(18) Zhang, L.; Zhang, J.; Hu, C.; Cao, J.; Zhou, X.; Hu, Y.; He, Q.; Yang, B. Efficient activation of p53 pathway in A549 cells exposed to L2,

a novel compound targeting p53-MDM2 interaction. *Anticancer Drugs* **2009**, *20* (6), 416−424.
(19) Dzubak, P.; Hajduch, M.; Gazak, R.; Svobodova, A.; Psotova, J.; Walterova, D.; Sedmera, P.; Kren, V. New derivatives of silybin and 2,3-dehydrosilybin and their cytotoxic and P-glycoprotein modulatory activity. *Bioorg. Med. Chem.* **2006**, *14* (11), 3793−3810.
(20) Noskova, V.; Dzubak, P.; Kuzmina, G.; Ludkova, A.; Stehlik, D.; Trojanec, R.; Janostakova, A.; Korinkova, G.; Mihal, V.; Hajduch, M. In vitro chemoresistance profile and expression/function of MDR associated proteins in resistant cell lines derived from CCRF-CEM, K562, A549 and MDA MB 231 parental cells. *Neoplasma* **2002**, *49* (6), 418−425.
(21) Hardy, E.; Castellanos-Serra, L. R. "Reverse-staining" of biomolecules in electrophoresis gels: analytical and micropreparative applications. *Anal. Biochem.* **2004**, *328* (1), 1−13.
(22) Stastna, M.; Behrens, A.; McDonnell, P. J.; Van Eyk, J. E. Analysis of protein composition of rabbit aqueous humor following two different cataract surgery incision procedures using 2-DE and LC-MS/MS. *Proteome Sci.* **2011**, *9* (1), 8.
(23) Gobom, J.; Nordhoff, E.; Mirgorodskaya, E.; Ekman, R.; Roepstorff, P. Sample purification and preparation technique based on nano-scale reversed-phase columns for the sensitive analysis of complex peptide mixtures by matrix-assisted laser desorption/ionization mass spectrometry. *J. Mass Spectrom.* **1999**, *34* (2), 105−116.
(24) Thomas, P. D.; Campbell, M. J.; Kejariwal, A.; Mi, H.; Karlak, B.; Daverman, R.; Diemer, K.; Muruganujan, A.; Narechania, A. PANTHER: A library of protein families and subfamilies indexed by function. *Genome Res.* **2003**, *13* (9), 2129−2141.
(25) Brown, K. R.; Jurisica, I. Online predicted human interaction database. *Bioinformatics* **2005**, *21* (9), 2076−2082.
(26) Agrawal, S.; Kumar, A.; Srivastava, V.; Mishra, B. N. Cloning, expression, activity and folding studies of serine hydroxymethyltransferase: A target enzyme for cancer chemotherapy. *J. Mol. Microbiol. Biotechnol.* **2003**, *6* (2), 67−75.
(27) Sorokin, A. V.; Kim, E. R.; Ovchinnikov, L. P. Nucleocytoplasmic transport of proteins. *Biochemistry (Moscow)* **2007**, *72* (13), 1439−1457.
(28) Payne, C. M.; Holubec, H.; Crowley-Skillicorn, C.; Nguyen, H.; Bernstein, H.; Wilcox, G.; Bernstein, C. Maspin is a deoxycholate-inducible, anti-apoptotic stress-response protein differentially expressed during colon carcinogenesis. *Clin. Exp. Gastroenterol.* **2011**, *4*, 239−253.
(29) Stevenson, L.; Allen, W. L.; Proutski, I.; Stewart, G.; Johnston, L.; McCloskey, K.; Wilson, P. M.; Longley, D. B.; Johnston, P. G. Calbindin 2 (CALB2) regulates 5-fluorouracil sensitivity in colorectal cancer by modulating the intrinsic apoptotic pathway. *PLoS One* **2011**, *6* (5), e20276.
(30) Roy, S. S.; Ehrlich, A. M.; Craigen, W. J.; Hajnoczky, G. VDAC2 is required for truncated BID-induced mitochondrial apoptosis by recruiting BAK to the mitochondria. *EMBO Rep.* **2009**, *10* (12), 1341−1347.
(31) Girdler, F.; Sessa, F.; Patercoli, S.; Villa, F.; Musacchio, A.; Taylor, S. Molecular basis of drug resistance in aurora kinases. *Chem. Biol.* **2008**, *15* (6), 552−562.
(32) Zhang, J. T.; Liu, Y. Use of comparative proteomics to identify potential resistance mechanisms in cancer treatment. *Cancer Treat. Rev.* **2007**, *33* (8), 741−756.
(33) Mizushima, N.; Klionsky, D. J. Protein turnover via autophagy: implications for metabolism. *Annu. Rev. Nutr.* **2007**, *27*, 19−40.
(34) Han, W.; Sun, J.; Feng, L.; Wang, K.; Li, D.; Pan, Q.; Chen, Y.; Jin, W.; Wang, X.; Pan, H.; Jin, H. Autophagy inhibition enhances daunorubicin-induced apoptosis in K562 cells. *PLoS One* **2011**, *6* (12), e28491.
(35) Ma, X. H.; Piao, S.; Wang, D.; McAfee, Q. W.; Nathanson, K. L.; Lum, J. J.; Li, L. Z.; Amaravadi, R. K. Measurements of tumor cell autophagy predict invasiveness, resistance to chemotherapy, and survival in melanoma. *Clin. Cancer Res.* **2011**, *17* (10), 3478−3489.
(36) Qadir, M. A.; Kwok, B.; Dragowska, W. H.; Le, K. H.; Bally, D.; Gorski, M. B.; Macroautophagy, S. M. inhibition sensitizes tamoxifen-resistant breast cancer cells and enhances mitochondrial depolarization. *Breast Cancer Res. Treat.* **2008**, *112* (3), 389−403.
(37) Yoon, J. H.; Ahn, S. G.; Lee, B. H.; Jung, S. H.; Oh, S. H. Role of autophagy in chemoresistance: regulation of the ATM-mediated DNA-damage signaling pathway through activation of DNA-PKcs and PARP-1. *Biochem. Pharmacol.* **2012**, *83* (6), 747−757.
(38) Dreier, M. R.; Grabovich, A. Z.; Katusin, J. D.; Taylor, W. R. Short and long-term tumor cell responses to Aurora kinase inhibitors. *Exp. Cell Res.* **2009**, *315* (7), 1085−1099.
(39) Yin, X.; Fontoura, B. M.; Morimoto, T.; Carroll, R. B. Cytoplasmic complex of p53 and eEF2. *J. Cell Physiol.* **2003**, *196* (3), 474−482.
(40) Liu, H.; Zheng, F.; Cao, Q.; Ren, B.; Zhu, L.; Striker, G.; Vlassara, H. Amelioration of oxidant stress by the defensin lysozyme. *Am. J. Physiol. Endocrinol. Metab.* **2006**, *290* (5), E824−E832.
(41) Chang, Y. J.; Huang, Y. P.; Li, Z. L.; Chen, C. H. GRP78 Knockdown Enhances Apoptosis via the Down-Regulation of Oxidative Stress and Akt Pathway after Epirubicin Treatment in Colon Cancer DLD-1 Cells. *PLoS One* **2012**, *7* (4), e35123.
(42) Zhang, L. H.; Zhang, X. Roles of GRP78 in physiology and cancer. *J. Cell Biochem.* **2010**, *110* (6), 1299−1305.
(43) Zhou, H.; Zhang, Y.; Fu, Y.; Chan, L.; Lee, A. S. Novel mechanism of anti-apoptotic function of 78-kDa glucose-regulated protein (GRP78): Endocrine resistance factor in breast cancer, through release of B-cell lymphoma 2 (BCL-2) from BCL-2-interacting killer (BIK). *J. Biol. Chem.* **2011**, *286* (29), 25687−25696.
(44) Tjoelker, L. W.; Stafforini, D. M. Platelet-activating factor acetylhydrolases in health and disease. *Biochim. Biophys. Acta* **2000**, *1488* (1−2), 102−123.
(45) Biancone, L.; Cantaluppi, V.; Del Sorbo, L.; Russo, S.; Tjoelker, L. W.; Camussi, G. Platelet-activating factor inactivation by local expression of platelet-activating factor acetyl-hydrolase modifies tumor vascularization and growth. *Clin. Cancer Res.* **2003**, *9* (11), 4214−4220.
(46) Denizot, Y.; Truffinet, V.; Bouvier, S.; Gainant, A.; Cubertafond, P.; Mathonnet, M. Elevated plasma phospholipase A2 and platelet-activating factor acetylhydrolase activity in colorectal cancer. *Mediators Inflammation* **2004**, *13* (1), 53−54.
(47) Clarke, P. R.; Zhang, C. Spatial and temporal coordination of mitosis by Ran GTPase. *Nat. Rev. Mol. Cell Biol.* **2008**, *9* (6), 464−477.
(48) Honma, K.; Takemasa, I.; Matoba, R.; Yamamoto, Y.; Takeshita, F.; Mori, M.; Monden, M.; Matsubara, K.; Ochiya, T. Screening of potential molecular targets for colorectal cancer therapy. *Int. J. Gen. Med.* **2009**, *2*, 243−257.
(49) Xia, F.; Lee, C. W.; Altieri, D. C. Tumor cell dependence on Ran-GTP-directed mitosis. *Cancer Res.* **2008**, *68* (6), 1826−1833.
(50) Thottassery, J. V.; Zambetti, G. P.; Arimori, K.; Schuetz, E. G.; Schuetz, J. D. p53-dependent regulation of MDR1 gene expression causes selective resistance to chemotherapeutic agents. *Proc. Natl. Acad. Sci. U.S.A.* **1997**, *94* (20), 11037−11042.
(51) Bush, J. A.; Li, G. Regulation of the Mdr1 isoforms in a p53-deficient mouse model. *Carcinogenesis* **2002**, *23* (10), 1603−1607.
(52) Pommier, Y.; Sordet, O.; Antony, S.; Hayward, R. L.; Kohn, K. W. Apoptosis defects and chemotherapy resistance: molecular interaction maps and networks. *Oncogene* **2004**, *23* (16), 2934−2949.
(53) Lovric, E.; Gatalica, Z.; Eyzaguirre, E.; Kruslin, B. Expression of maspin and glutathionine-S-transferase-pi in normal human prostate and prostatic carcinomas. *Appl. Immunohistochem. Mol. Morphol.* **2010**, *18* (5), 429−432.
(54) Yeom, S. Y.; Jang, H. L.; Lee, S. J.; Kim, E.; Son, H. J.; Kim, B. G.; Park, C. Interaction of testisin with maspin and its impact on invasion and cell death resistance of cervical cancer cells. *FEBS Lett.* **2010**, *584* (8), 1469−1475.
(55) Zou, Z.; Anisowicz, A.; Hendrix, M. J.; Thor, A.; Neveu, M.; Sheng, S.; Rafidi, K.; Seftor, E.; Sager, R. Maspin, a serpin with tumor-suppressing activity in human mammary epithelial cells. *Science* **1994**, *263* (5146), 526−529.
(56) Ben Shachar, B.; Feldstein, O.; Hacohen, D.; Ginsberg, D. The tumor suppressor maspin mediates E2F1-induced sensitivity of cancer cells to chemotherapy. *Mol. Cancer Res.* **2010**, *8* (3), 363−372.
(57) Feng, X. P.; Yi, H.; Li, M. Y.; Li, X. H.; Yi, B.; Zhang, P. F.; Li, C.; Peng, F.; Tang, C. E.; Li, J. L.; Chen, Z. C.; Xiao, Z. Q. Identification of

biomarkers for predicting nasopharyngeal carcinoma response to radiotherapy by proteomics. *Cancer Res.* **2010**, *70* (9), 3450−3462.
(58) Nam, E.; Park, C. Maspin suppresses survival of lung cancer cells through modulation of Akt pathway. *Cancer Res. Treat.* **2010**, *42* (1), 42−47.
(59) Boyer, J.; Allen, W. L.; McLean, E. G.; Wilson, P. M.; McCulla, A.; Moore, S.; Longley, D. B.; Caldas, C.; Johnston, P. G. Pharmacogenomic identification of novel determinants of response to chemotherapy in colon cancer. *Cancer Res.* **2006**, *66* (5), 2765−2777.
(60) Haner, K.; Henzi, T.; Pfefferli, M.; Haner, K.; Salicio, V.; Schwaller, B. A bipartite butyrate-responsive element in the human calretinin (CALB2) promoter acts as a repressor in colon carcinoma cells but not in mesothelioma cells. *J. Cell Biochem.* **2010**, *109* (3), 519−531.

4.2. Charakterizace mechanismů nádorové rezistence k působení inhibitorů cyklin-dependentních kináz

v publikaci

Cancer Drug-Resistance and a Look at Specific Proteins: Rho GDP-Dissociation Inhibitor 2, Y-Box Binding Protein 1 and HSP70/90 Organizing Protein in Proteomics Clinical Application

Skalníková H, Martinková J, **Hrabáková R**, Halada P, Dziechciarková M, Hajdúch M, Gadher SJ, Hammar A, Enetoft D, Fotsstrom-Olsson O, Kovářová H.

J Proteome Res. 2011 Feb 4; 10(2): 404-15. Epub 2010 Dec 3
IF (2011): 5.46; 5-year IF (2011): 5.62

Prohlášení spoluautorů

„Prohlašuji, že Rita Hrabáková se patřičně podílela (30 %) na plánování proteomických experimentů, jejich provedení, interpretaci výsledků a sepisování této práce."

V Liběchově, dne..... RNDr. Hana Kovářová, CSc.

.....……...

research articles Journal of proteome research

Cancer Drug-Resistance and a Look at Specific Proteins: Rho GDP-Dissociation Inhibitor 2, Y-Box Binding Protein 1, and HSP70/90 Organizing Protein in Proteomics Clinical Application

Helena Skalnikova,[†,#] Jirina Martinkova,[†,#] Rita Hrabakova,[†] Petr Halada,[‡] Marta Dziechciarkova,[§] Marian Hajduch,[§] Suresh Jivan Gadher,[∥] Andreas Hammar,[⊥] Daniel Enetoft,[⊥] Andreas Ekefjard,[⊥] Ola Forsstrom-Olsson,[⊥] and Hana Kovarova*[,†]

Institute of Animal Physiology and Genetics AS CR, v.v.i., Rumburska 89, 277 21 Libechov, Czech Republic, Institute of Microbiology AS CR, v.v.i., Videnska 1083, 142 20 Prague, Czech Republic, Laboratory of Experimental Medicine, Institute of Translational and Molecular Medicine, Faculty of Medicine and Dentistry, Palacky University and University Hospital, Puskinova 6, 775 20 Olomouc, Czech Republic, Millipore Bioscience, 15 Research Park Drive, St. Charles, Missouri 63304, United States, and Ludesi, Engelbrektsgatan 15, SE-211 33 Malmö, Sweden

Received May 14, 2010

Resistance to anti-cancer drugs is a well recognized problem and very often it is responsible for failure of the cancer treatment. In this study, the proteome alterations associated with the development of acquired resistance to cyclin-depedent kinases inhibitor bohemine, a promising anti-cancer drug, were analyzed with the primary aim of identifying potential targets of resistance within the cell that could pave a way to selective elimination of specific resistant cell types. A model of parental susceptible CEM T-lymphoblastic leukemia cells and its resistant counterpart CEM-BOH was used and advanced 2-D liquid chromatography was applied to fractionate cellular proteins. Differentially expressed identified proteins were further verified using immunoblotting and immunohistochemistry. Our study has revealed that Rho GDP-dissociation inhibitor 2, Y-box binding protein 1, and the HSP70/90 organizing protein have a critical role to play in resistance to cyclin-depedent kinases inhibitor. The results indicated not only that quantitative protein changes play an important role in drug-resistance, but also that there are various other parameters such as truncation, post-translational modification(s), and subcellular localization of selected proteins. Furthermore, these proteins were validated for their roles in drug resistance using different cell lines resistant to diverse representatives of anti-cancer drugs such as vincristine and daunorubicin.

Keywords: cancer • anti-cancer drugs • drug resistance • CEM T-lymphoblastic leukemia • CDK inhibitor • proteomics • Rho GDP-dissociation inhibitor 2 • Y-box binding protein 1 • Hsp70/90 organizing protein • biomarker

Introduction

Cancers represent group of unprecedentedly heterogeneous diseases that affect humans with high frequency and contribute significantly to overall morbidity and mortality. Development of resistance to cancer chemotherapeutic treatments is a major problem for successful therapy, especially in late stages of the disease.

Cancer cells can acquire drug resistance by several distinct mechanisms. One such group of mechanisms of extreme importance is represented by pharmacological and physiological parameters. Included within this group is the family of P450 enzymes in liver which controls the metabolism of drugs. Increased levels of these enzymes are observed in a variety of solid tumors and may contribute to drug resistance. The membrane proteins including channels, solute carriers, and ABC transporters are known to play a role in increased drug efflux from cancer cells. Inadequate metabolic activation of anti-cancer drug analogues of DNA precursors represents a synergistic enhancement to the drug resistance by cancer cells. Furthermore, the resistance to the drugs that directly affect structural integrity of DNA may result from the activation of DNA-repair systems which may nullify the effect of the drug. The second mechanism grouping of the factors contributing to the anti-cancer drug resistance includes altered survival pathways such as evasion of apoptosis, necrosis, mitotic catastrophe, or senescence.[1,2] Consideration has to be given to a third group represented by cancer stem cells. These cells are likely to share many of the properties of normal stem cells,

* To whom correspondence should be addressed. E-mail, kovarova@iapg.cas.cz; tel, +420 315 639 582; fax, +420 315 639 510.
[#] Both authors contributed equally to this work.
[†] Institute of Animal Physiology and Genetics AS CR, v.v.i.
[‡] Institute of Microbiology AS CR, v.v.i.
[§] Palacky University and University Hospital.
[∥] Millipore Bioscience.
[⊥] Ludesi.

Published on Web 11/10/2010
10.1021/pr100468w
© 2011 American Chemical Society

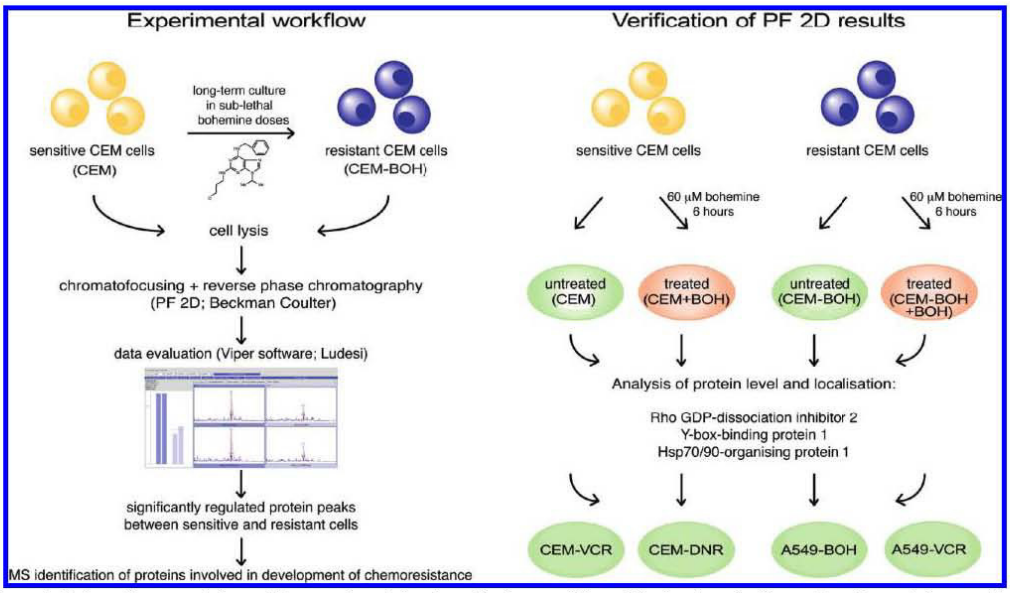


Figure 1. Schematic presentation of the experimental and verification workflows. The lysates of cell samples of parental susceptible CEM cell line and CEM-BOH cells resistant to cyclin-dependent kinases inhibitor bohemine were fractionated using 2-D liquid chromatography. The proteome maps were evaluated for differentially expressed protein peaks and identity of the proteins was determined by mass spectrometry. Selected protein changes were verified using immunoblotting and immunohistochemistry. The proteins were further validated for their roles in drug resistance using CEM and A549 cell lines resistant to vincristine or daunorubicin.

thus, mediating self-renewal and long life span including resistance to drugs and toxins through the expression of several ABC transporters, an active DNA-repair capacity, and a resistance to apoptosis.[3] Most of the above-described mechanisms were revealed using cell culture experiments and their correlation to clinical outcomes need further studies.

Recently, proteomic approaches have been applied to further our knowledge of the mechanisms underlying chemoresistance in context of overall protein expression and disease states. Such studies have been performed to date on selected cancer cell lines to address resistance to drugs including DNA damaging agents (doxorubicin, cisplatin, carboplatin, etoposide, daunorubicin, mitoxantrone) and drugs targeting microtubule dynamics (vincristine, vinblastine). Although the conventional 2-DE was utilized in most of these studies resulting predominantly in identification of abundant proteins, many particular mechanisms of resistance were identified for individually selected drugs and cancer cell lines with a commonality of several other features. Among them, the up-regulated expressions of HSP27, 14-3-3σ, and peroxiredoxins were evident and were further validated (reviewed in Zhang and Liu).[2] However, most of the proteins identified in the proteomic analyses of drug resistant cancer cells have not been verified for their expression changes using other approaches such as Western blot or for their prominent role in drug resistance using functional assays such as MTT cytotoxicity and colony formation.

Previously, we described the effects of bohemine, an inhibitor of cyclin-dependent kinases (CDKI) from the family of trisubstituted purines, on primarily sensitive T-lymphoblastic leukemia CEM cells as well as resistant lung adenoma cell line A549.[4,5] The cyclin-dependent kinases together with cyclins belong to the key molecules regulating cell cycle progression and numerous compounds that can suppress cyclin/cyclin-dependent kinases activities have been described as cytostatic drugs.[6] On the basis of the evaluation of the protein maps and possible pathways relevant to response to CDKI, the glycolytic enzymes, annexin IV, histones, and the Crkl adaptor protein implicated in many signal transduction events appeared to be the important targets. The level and phosphorylation of Crkl protein, which is the major tyrosine-phosphorylated protein in chronic myeloid leukemia, was down-regulated in CDKI treated CEM T-lymphoblastic leukemia cells. These changes were validated using immunoblot experiments and in our pilot experiments using K562 myeloid leukemia cells transplanted into SCID mice and treated/untreated with CDKI under *in vivo* conditions.[4]

In this study, the proteome alterations associated with the development of acquired resistance to CDKI bohemine were analyzed on a model of parental susceptible CEM cell line and its resistant counterpart CEM-BOH. 2-D liquid chromatography was used for protein fractionation of cell lysates. The proteome maps were evaluated for differentially expressed proteins and selected changes were further verified using immunoblotting and immunohistochemistry. Furthermore, the proteins were validated for their roles in drug resistance using different cell lines resistant to diverse representatives of anti-cancer drugs such as vincristine and daunorubicin (Figure 1).

Materials and Methods

Chemicals. Urea, Tris-base, thiourea, sodium dodecyl sulfate (SDS), *n*-octyl glucoside, Tris (2-carboxyethyl) phosphine hydrochloride, and iminodiacetic acid were obtained from Sigma-

Aldrich (St. Louis, MO). Nonidet P40, 3-3(cholamidolpropyl)-dimethylammonio-1-propane sulfonate and dithiothreitol were from USB Corporation (Cleveland, OH). Glycerol and β-glycerolphosphate were purchased from Penta (Prague, Czech Republic). Protease inhibitors cocktail was obtained from Roche (Mannheim, Germany). All other chemicals for protein fractionations were of HPLC or analytical grade and buffers were prepared using Mili-Q water system (Millipore Bedford, MA). Unless otherwise specified, all chemicals used for mass spectrometry were from Sigma (Steinheim, Germany).

Cell Cultures and Sample Preparation. The CEM (CEM-CCRF, human T-lymphoblastic leukemia cells) and A549 (human lung adenocarcinoma) cell lines were obtained from American Tissue Culture Collection (ATCC, Manassas, VA). The CEM and A549 cells were cultured in RPMI 1640 and DMEM, respectively, with 5 g/L glucose, 2 mM glutamine, 100 U/mL penicillin, 100 μg/mL streptomycin, and 10% fetal calf serum as described previously.[5] The CEM-BOH bulk cell line resistant to CDKI bohemine was derived from parental sensitive CEM cells by selective pressure of CDKI bohemine as described in previous study.[7] The process of selection started with the drug concentration equal to 10% tumor cells survival of parental CEM line and the concentration of the drug was subsequently increased to 10-fold of 50% tumor cells survival. The CEM cells resistant to vincristine (CEM-VCR) or daunorubicin (CEM-DNR) as well as A549 cells resistant to CDKI bohemine (A549-BOH) or vincristine (A549-VCR) were established using the same protocol and drug resistant lines were designated as the bulk culture and grown in the media mentioned above.[7]

For 2-D liquid chromatography fractionation on ProteomeLab PF 2D (PF 2D; Beckman Coulter, Fullerton, CA), parental sensitive CEM cells and resistant counterparts CEM-BOH were grown to approximately 80×10^6 cells, harvested, and washed three times with PBS. A total of 400 μL of cell suspensions was lysed in 1.6 mL of PF 2D lysis buffer containing 7.5 M urea, 2.5 M thiourea, 62.5 mM Tris, 2.5% octyl glucoside, 6.25 mM TCEP, 12.5% glycerol, and 1.25 mM protease inhibitor. The lysates were centrifuged at 20 000g at 4 °C for 1 h. The supernatants were stored at −80 °C for future use. Two biological replicates of each sample of CEM cells as well as CEM-BOH cells were analyzed. For SDS-PAGE followed by Western blot, parental sensitive CEM cells and their resistant counterparts CEM-BOH, CEM-VCR, and CEM-DNR as well as parental A549 cells and derived resistant cells A549-BOH or A549-VCR were grown in media as mentioned above. The cells were washed in ice-cold PBS, lysed in SDS sample buffer, and boiled and total cell protein extracts of 10^5 cells corresponding to approximately 10 μg of proteins were loaded on the gel. Additionally, CEM cells treated with 60 μM CDKI bohemine for 6 h were prepared in the same manner.

Two-Dimensional HPLC ProteomeLab PF 2D Chromatography and Image Analysis. Samples of CEM and CEM-BOH cell lines in denaturating buffer were loaded on PD10 column equilibrated with 25 mL of the start buffer (provided in PF 2D kit, Beckman Coulter, Fullerton, CA) to exchange denaturating lysis buffer to the start buffer. The protein concentration in the sample collected from PD10 column was determined by direct measurement of absorbance at 280 nm (DU 7400 spectrophotometer, Beckman Coulter, Fullerton, CA). For the first-dimension high-performance chromatofocusing fractionation (HPCF), two buffers, a start buffer pH 8.5 and an elution buffer pH 4.0, both provided in PF 2D kit were used to generate an internal linear pH gradient on the column. The HPCF column was equilibrated with 30 column volumes of start buffer and cell lysate of 3.6 mg of total protein was applied on HPCF column using 5 mL injection loop. The separation was performed at a flow rate of 0.2 mL/min. Once the pH in the column achieved a stable value of 8.5 (30 min), the linear gradient of elution buffer to pH of 4 was switched. The proteins remaining on the column at pH 4 were washed out by 1 M NaCl in 30% n-propanol solution. UV detection was performed at 280 nm and the pH of the effluent was monitored using a flow-through online pH probe. Fraction collection started when gradient reached pH 8.3 and individual fractions were collected in 0.3 pH intervals. In every run, pH was monitored for 150 min and UV was monitored for 220 min. In total, 15 fractions collected in the pH range 8.30−4.10 and one fraction collected in the pH > 8.30 (proteins that did not bind to the HPCF column) were collected during HPCF separation. The pH fractions were further separated on high-performance reversed phase column (HPRP) packed with C18 nonporous silica beads. Solvent A was 0.1% trifluoroacetic acid (TFA) in water and solvent B was 0.08% TFA in acetonitrile (MeCN). The separation was done at 50 °C at a flow rate 0.75 mL/min. The gradient was run from 0% to 100% B in 35 min, followed by 100% B for 4 min and 100% A for 10 min. UV absorptions were monitored at 214 nm. The fractions were collected in 0.13 min time intervals into 96-deep well plates using the fraction collector Gilson FC204 (Immunotech a.s., Prague, Czech Republic) and stored at −80 °C until further use.

2-D protein expression maps of sensitive CEM and resistant CEM-BOH cells displaying protein isoelectric point versus protein hydrophobicity were generated by ProteoVue software running on PF 2D system. ProteoVue software converts the UV peak intensity in the chromatograms from the second dimension HPRP column of each pH fraction to a band and line format and provides the mean to view and quantify protein levels. The novel Viper software version 2.3.0.0. was further used to evaluate protein maps. The above software was developed in collaboration with Ludesi (Malmö, Sweden), Beckman Coulter (Fullerton, CA), Johns Hopkins University (Baltimore, MD), and Academy of Sciences of the Czech Republic (Prague, Czech Republic). It is an analysis software for aligning, quantifying, normalizing, and comparing data in a multisample 2-D LC-experiment as described. At first, the baseline in chromatograms was detected and one sample was selected as a Master. Then, the UV profiles of fractions with corresponding pH were aligned to correct eventual pH shifts during the first-dimension separation. The second-dimension chromatograms of each consecutive pH fraction in the Master were then aligned to detect protein peaks eluting in the same retention time. The maximum span of the single protein peak in sequential pH fractions was set to 3 fractions. The second-dimension chromatograms of individual pH fractions of the samples were then aligned with the Master. Protein peaks were detected in the area of retention times from 10 to 26 min and the peak intensities were quantified and normalized to the sum of areas under the chromatograms in this retention time range for the whole sample (in all pH fractions). Additionally, for individual peak areas detected in each of the pH fractions, the Viper software allows calculation of total area for every protein peak with the same retention time that is present in several sequential pH fractions. The peaks with p-values in ANOVA test below 0.05 and/or peaks with fold change ≥1.6 were

Table 1. Differentially Expressed Proteins Identified in 2-D LC Experiment[a]

peak no.	protein name	UniProt no.	biological function	change	fold change	*p*-value
088	Tubulin-specific chaperone A	TBCA_HUMAN	protein folding	↓	2	0.056
115	Rho GDP-dissociation inhibitor 1	GDIR_HUMAN	Rho protein signal transduction	↑	2.02	0.22
	Tumor protein D54	TPD54_HUMAN	regulation of cell proliferation			
	Tropomyosin alpha-3 chain	TPM3_HUMAN	cellular component movement			
	Histone H2B type 1-B	H2B1B_HUMAN	nucleosome assembly			
163	Histone H2A type 1-H*	H2A1H_HUMAN	nucleosome assembly	↓	1.92	0.039
	Elongation factor 1-alpha 1	EF1A1_HUMAN	translational elongation			
200	Stress-induced-phosphoprotein 1	STIP1_HUMAN	response to stress	↑	8.18	0.008
	Macrophage-capping protein	CAPG_HUMAN	protein complex assembly			
362	Rho GDP-dissociation inhibitor 2	GDIR2_HUMAN	actin cytoskeleton organization Rho protein signal transduction	↑	2.36	0.591
365	Tropomyosin alpha-4 chain	TPM4_HUMAN	cellular component movement	↑	1.72	0.046
	Histone H4*	H4_HUMAN	nucleosome assembly			
648	60S ribosomal protein L6*	RL6_HUMAN	translation	↓	2.06	0.18
	60S ribosomal protein L4	RL4_HUMAN	translation			
	Histone H2B type 1-D	H2B1D_HUMAN	nucleosome assembly			
	Histone H4*	H4_HUMAN	nucleosome assembly			
649	Histone H2B type 1-J	H2B1J_HUMAN	nucleosome assembly	↓	2.4	0.006
	Histone H4	H4_HUMAN	nucleosome assembly			
701	Nuclease sensitive element-binding protein 1	YBOX1_HUMAN	regulation of transcription mRNA processing	↓	8.72	0.31
770	60S ribosomal protein L15	RL15_HUMAN	translation	↓	2.56	0.59
	40S ribosomal protein S8	RS8_HUMAN	translation			
780	40S ribosomal protein S24	RS24_HUMAN	translation	↓	1.82	0.107
800	40S ribosomal protein S25	RS25_HUMAN	translation	↑	1.62	0.006
	40S ribosomal protein S4, X isoform	RS4X_HUMAN	translation			
	Small nuclear ribonucleoprotein Sm D3	SMD3_HUMAN	mRNA processing, RNA splicing			
847	Nuclease sensitive element-binding protein 1	YBOX1_HUMAN	regulation of transcription mRNA processing	↓	2.68	0.13
	60S ribosomal protein L26	RL26_HUMAN	translation			
889	Histone H2A type 1-H*	H2A1H_HUMAN	nucleosome assembly	↑	1.67	0.025
1145	60S ribosomal protein L6*	RL6_HUMAN	translation	↓	2.04	0.15
	40S ribosomal protein S13	RS13_HUMAN	translation			
	60S ribosomal protein L7a	RL7A_HUMAN	translation			

[a] The arrows indicate change in the protein level in the resistant cells compared to sensitive cells. Detailed data from MS identification are supplied in the Supplemental Table 1. Asterisks (*) indicate proteins found in nonsequential fractions.

considered as significant differences and the corresponding fractions were processed by mass spectrometry (Table 1).

Protein Identification by MALDI-TOF Mass Spectrometry. The fractions from the second dimension of PF2D separation were completely dried using a SpeedVac and redissolved in 50 μL of a cleavage buffer containing 0.01% 2-mercaptoethanol, 50 mM 4-ethylmorpholine acetate, 5% MeCN, and 5 ng of sequencing grade trypsin (Promega, Madison, WI). After overnight digestion, the resulting peptides were acidified by the addition of 5 μL of 5% TFA in MeCN. A solution of α-cyano-4-hydroxycinnamic acid in aqueous 50% MeCN/0.2% TFA (5 mg/mL) was used as a MALDI matrix. A 0.5 μL of a sample was deposited on the MALDI target and allowed to air-dry at room temperature. After complete evaporation, 0.5 μL of the matrix solution was added. MALDI mass spectra were measured on an Ultraflex III instrument (Bruker Daltonics, Bremen, Germany) equipped with a Smartbeam solid state laser and LIFT technology for MS/MS analysis. The spectra were acquired in the mass range of 700−4000 Da and calibrated internally using the monoisotopic $[M + H]^+$ ions of trypsin autoproteolytic fragments (842.5 and 2211.1 Da).

Peak lists in XML data format were created using flexAnalysis 3.0 program with SNAP peak detection algorithm. No smoothing was applied and maximal number of assigned peaks was set to 50. After peak labeling, all known contaminant signals were manually removed. The peak lists were searched using MASCOT search engine against Swiss-Prot 57.6 database subset of human proteins with the following search settings: peptide tolerance of 20 ppm, missed cleavage site value set to two, variable oxidation of methionine and N-acetylation of protein N-terminus. No restriction on protein molecular weight and p*I* value was applied. Proteins with MOWSE score over the threshold 56 calculated for the used settings were considered as identified. If the score was only slightly higher than the threshold value or the sequence coverage too low, the identity of protein candidate was confirmed by MS/MS analysis. In addition to the above-mentioned MASCOT settings, fragment mass tolerance of 0.6 Da and Ultraflex III instrument (Bruker Daltonics, Bremen, Germany) equipped with a Smartbeam solid state laser and LIFT technology for MS/MS analysis was applied for MS/MS spectra searching.

The Protein Expression Analysis Using Immunoblot. The whole-cell lysates prepared as described above were used for SDS-PAGE. For electrophoretic separation of PF 2D fractions, 10% of the total volume of the first-dimension pH fractions was precipitated by trichloroacetic acid, dissolved in 15 μL of SDS sample buffer, and loaded on SDS-PAGE.

Following SDS-PAGE using 10, 12, or 15% polyacrylamide gels, separated proteins were transferred onto Immobilon P (Millipore, Bedford, MA) membranes using a semidry blotting system (Biometra, Göttingen, Germany) and transfer buffer containing 48 mM Tris, 39 mM glycine, and 20% methanol.[8] The membranes were blocked in 5% nonfat dry milk or in 5% BSA in Tris-buffered saline with 0.05% Tween 20 (TBST) pH 7.4 for 1 h and incubated overnight with the respective primary antibodies: anti-Rho-GDI2 (Rho GDP-dissociation inhibitor 2; Abcam ab13925; 1:500 in 5% BSA/TBST), anti-YB1 (Y-box binding protein 1; Abcam ab12148; 1:10 000 in 5% nonfat dry milk/TBST), anti-Hop (HSP 70/90 organizing protein; Abcam ab37752; 1:10 000 in 5% nonfat dry milk/TBST), or anti-β-tubulin (Sigma T4026; 1:1000 in 5% nonfat dry milk/TBST). Peroxidase-conjugated secondary anti-mouse and anti-rabbit IgG antibodies (Jackson Immunoresearch, Suffolk, U.K.) were diluted 1:10 000, and anti-chicken IgY (Abcam ab6753) was diluted 1:100 000 in 5% nonfat dry milk/TBST and applied as appropriate. The ECL+ chemiluminescence (GE Healthcare, Uppsala, Sweden) detection system was used to detect specific proteins. The exposed CL-XPosure films (Thermo Scientific, Rockford, IL) were scanned by a calibrated densitometer GS-800 (Bio-Rad, Hercules, CA).

Protein Expression Profiles Characterized by Immunohistochemistry. Paraffin-embedded samples of CEM cells, CEM cells treated with 60 μM CDKI bohemine for 6 h, CEM-BOH cells resistant to CDKI bohemine, and CEM-BOH cells resistant to CDKI bohemine treated with 60 μM CDKI bohemine for 6 h were cut in the sections, mounted on silane-coated slides, deparaffinized, rehydrated, and pretreated in a microwave at 650 W for 30 min in citrate buffer pH 6.0. Nonspecific binding was blocked with 5% rabbit serum in phosphate buffer solution. Sections were incubated in the primary anti-Hop antibody (Abcam ab37752; 1:500). As a secondary antibody, anti-chicken IgY (Abcam ab6753) was applied for 60 min (working dilution 1:400) followed by biotin–streptavidin–peroxidase complex (Dako, Copenhagen, Denmark). Diaminobenzidine substrate was used as a chromogen, according to the manufacturer's instructions (DAKO, Copenhagen, Denmark). Sections were counterstained with hematoxylin.

Computer Modeling of Protein Interaction Network. Interologous Interaction Database (I2D; an online database of known and predicted mammalian and eukaryotic protein–protein interactions) was used to search for possible protein–protein interaction partners for proteins identified as regulated during the development of acquired resistance to cyclin-dependent kinases inhibitor. Version 1.8 of I2D, including 254 588 source interactions and 238 553 predicted interactions (http://ophid.utoronto.ca/ophidv2.201/ppi.jsp) was used for interaction search with human selected as target organism. Protein–protein interaction network was visualized using NAViGaTOR (Network Analysis, Visualization & Graphing TORonto) software (http://ophid.utoronto.ca/navigator). In protein–protein interaction networks, nodes represent proteins and edges between nodes represent physical interactions between the proteins. NAViGaTOR allows nodes to be color-coded according to Gene Ontology (GO, a controlled vocabulary describing properties of genes) terms.

Results

Proteomic Changes Observed in CEM-BOH Cells Resistant to CDKI Bohemine Compared to Sensitive CEM Cells Using 2-D LC. The primary aim of our study was to identify differences in protein expression between CEM-BOH cells resistant to CDKI bohemine and bohemine-sensitive parental CEM cells. The lysates of cell samples were fractionated using 2-D liquid chromatography, resulting proteome maps were evaluated for differentially expressed protein peaks, and identity of the proteins was determined by mass spectrometry. Selected protein changes were verified using immunoblotting and immunohistochemistry. The proteins were further validated for their roles in drug resistance using CEM and A549 cell lines resistant to vincristine or daunorubicin (Figure 1).

The purpose of 2-D LC protein separation performed on PF 2D was to use an advanced gel-independent fractionation technique. This method has the distinct advantage over the 2-DE based approach in that it overcomes many of its drawbacks and, importantly, the fractions of intact proteins can be directly utilized for mass spectrometric analysis. The PF 2D involves 2-D separation and mapping of the total protein expression. Proteins are fractionated by isoelectric points in pH gradient using the chromatofocusing at 0.3 pH intervals in the first dimension. Each of these pH protein fractions is further separated by hydrophobicity using reversed phase in the second dimension.[9] The global information about protein expression obtained by means of PF 2D separation has been depicted using ProteoVue software that enables the construction of 2-D protein map showing pH fractions versus protein hydrophobicity. Reproducibility of the 2-D LC fractionation can be expressed by coefficient of variation which may be calculated using the values of retention time of all peaks, peak heights, or peak areas from several runs as exemplified in the study of Linke et al.[10] While the values of % of coefficient of variation (% CV) are usually low (in average 0.40) for peak retention time, they are obviously higher (around 20) for peak height or peak area. In our study, median % CV based on the values of normalized peak areas was 31. Coefficient of determination R^2 calculated for variations in peak areas between biological replicates was equal to 94% and 96% for protein patterns corresponding to CEM and CEM-BOH cells, respectively, indicating good reproducibility of separation and quantification methods.

In total, 15 fractions collected in the pH range of 8.30–4.10 and one fraction collected in the pH > 8.30 (proteins that did not bind to the HPCF column) were then separated on HPRP column (Figure 2). The 2-D protein maps of all runs performed in this study are shown in Supplemental Figure 1. The samples of CEM and CEM-BOH cells were separated in average into 1229 protein peaks and the evaluation of qualitative and quantitative differences by UV measurement between 2-D protein maps using Viper software identified 6 differentially expressed protein peaks with p-value ≤ 0.05 (Peak Nos: 163, 200, 365, 649, 800, 889) and 12 protein peaks with fold change ≥ 1.6 (Peak Nos: 88, 115, 163, 200, 362, 648, 649, 701, 770, 780, 847 and 1145) between sensitive CEM and resistant CEM-BOH cells. Nine of the differentially expressed protein peaks revealed by PF 2D approach were present at decreased level in resistant CEM-BOH cells. On the contrary, six protein bands were found in higher level in resistant CEM-BOH cells (Table 1). Relative differences in expression ranged from 1.6-fold to as much as 8.7-fold. Figure 3 demonstrates an example of differences found in fraction of pH 7.7–8.0 and other differences mentioned

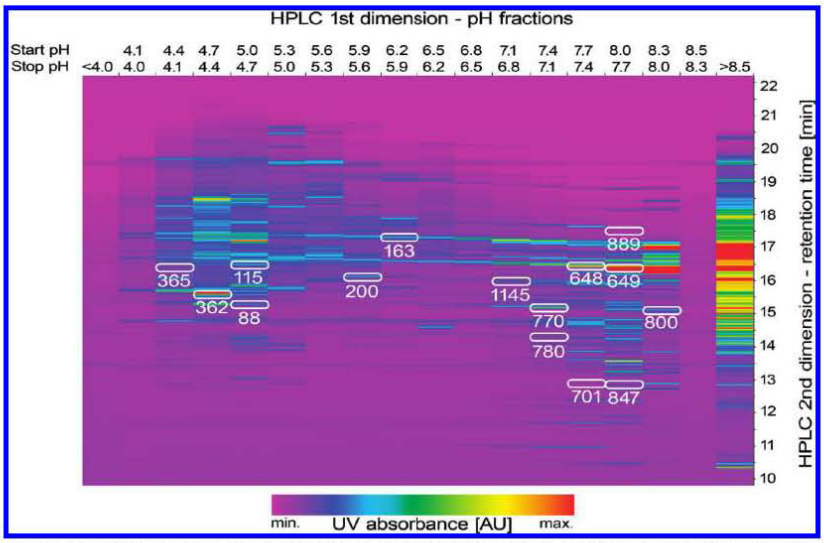


Figure 2. Two-dimensional liquid chromatography protein map of CEM cell line and set of protein peaks significantly different in resistant CEM-BOH cells compared to CEM cells. Lysates of cell samples were subjected to 2-D liquid chromatography and protein fractionation was monitored using UV detection. 2-D protein expression maps were generated by ProteoVue software and their images were evaluated using Viper software. Figure shows representative protein map from parental sensitive CEM cells and a set of protein bands significantly different in resistant CEM-BOH cells. The colors of the protein bands correspond to UV intensity and provide information about protein quantification. Regulated protein peaks are indicated by their numbers assigned by Viper software.

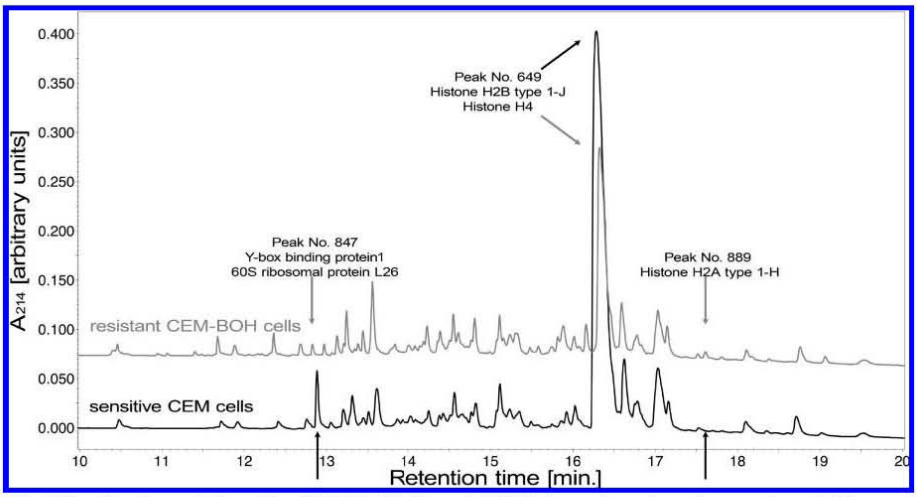


Figure 3. The UV profile of second dimension of 2-D HPLC ProteomeLabPF 2D chromatography and comparison of differences between analyzed samples. The UV chromatogram of pH fraction 7.7−8.0 separated in the second dimension on reversed phase column packed with C18 nonporous silica beads. The UV absorptions were monitored at 214 nm. Three protein peaks were found differentially expressed between sensitive CEM cells and CEM-BOH cells resistant to CDKI bohemine.

above are provided in Supplemental Figure 2). All these discriminate protein peaks were chosen for further mass spectrometry and the proteins in all of them were satisfactorily identified (Table 1). Supplementary Table 1 provides comprehensive information about the proteins (fraction numbers, protein names, database accession numbers, protein MW and p*I*, and all MS identification data including Mascot scores, sequence coverage, matched peaks, unmatched peaks, and MS/MS confirmation). Among the proteins identified in differentially regulated protein peaks in resistant CEM-BOH cells were several ribosomal proteins including the proteins of large 60S ribosomal subunit (proteins L4, L6, L7a, L15 and L26) as well as the proteins of the small 40S ribosomal subunit (S4_X isoform, S8, S13, S24, S25). Furthermore, we have detected

several histone variants, namely, histone H2A type 1-H, histone H2B type 1-B, histone H2B type 1-D, histone H2B type 1-J, and histone H4, to be differently expressed between susceptible and resistant cells. On the basis of our MS data (Supplemental Table 1), we have unambiguously distinguished ribosomal proteins according to the unique peptides that were observed for each identified protein. The only ambiguity in protein identification could be related to specific histone variants within a single core histone, namely, histone H2A and H2B where the top position with the highest score in the protein candidate list given by MASCOT was accepted without any other sequential confirmation. Nevertheless, the core histones H2A, H2B, and H4 were satisfactorily distinguished, and in our opinion, sufficient for the purpose of this study.

It was evident that many of the protein peaks collected after the second dimension contained more than one protein and this was reconfirmed by mass spectrometric analysis. However, there were also protein peaks fulfilling the criteria of one protein/one peak in a fraction: the protein peaks nos. 088 and 701 showing decrease in resistant CEM-BOH cells which corresponded to tubulin-specific chaperone A and Y-box binding protein 1; the protein peaks nos. 362 and 889 showing increase in resistant CEM-BOH cells corresponded to Rho GDP-dissociation inhibitor 2 and histone H2A type 1-H (Table 1, Figure 2).

In the subsequent work, we focused on detailed verification of the proteins (a) with highly elevated/significant increase in resistant CEM-BOH cells: Rho-GDP-dissociation inhibitor 2 (Rho GDI2) with 2.36-fold change and Hsp70/90 organizing protein (Hop; stress-induced phosphoprotein 1- STIP 1) reaching 8.18-fold change; (b) Y-box binding protein 1 (YB-1; nuclease sensitive element-binding protein 1) decreased to almost 9-fold in resistant cells.

Immunoblotting Verification of Protein Changes Typical for Resistant CEM-BOH Cells. To validate the results of the proteomic analysis, immunoblot experiments were performed to confirm the identity of the proteins Rho GDI2 and YB-1 which were increased and decreased, respectively, in resistant CEM-BOH cells compared to sensitive CEM cells on PF 2D chromatography. Furthermore, Hop protein identified as one of two unambiguously identified proteins in peak no. 200 from PF 2D with observed higher UV absorbance level in CEM-BOH cells was selected to demonstrate verification and contribution of a particular protein to UV absorbance level corresponding to protein amount.

First, monitoring of protein changes at the level of whole cell lysates was performed. The samples of untreated sensitive CEM and resistant CEM-BOH cells were completed by the cells treated with 60 μM CDKI bohemine for 6 h to monitor early response of sensitive as well as resistant cells to the drug that precedes onset of apoptosis. The results shown in Figure 4A confirmed significantly higher level of Rho GDI2 in resistant cells. The treatment by CDKI bohemine resulted in almost undetectable Rho GDI2 level in sensitive cells while in resistant cells showed high Rho GDI2 level. The level of YB-1 protein observed at 50 kDa corresponding to intact protein[11] did not reveal significant difference between the sensitive and resistant cells. In spite of this, similarly to Rho GDI2, treatment by CDKI bohemine resulted in decreased level of YB-1 in sensitive cells but not in resistant cells. The faint protein band observed at 32 kDa represented truncated form of the YB-1 protein[12] which appeared to be more evident in resistant CEM-BOH cells.

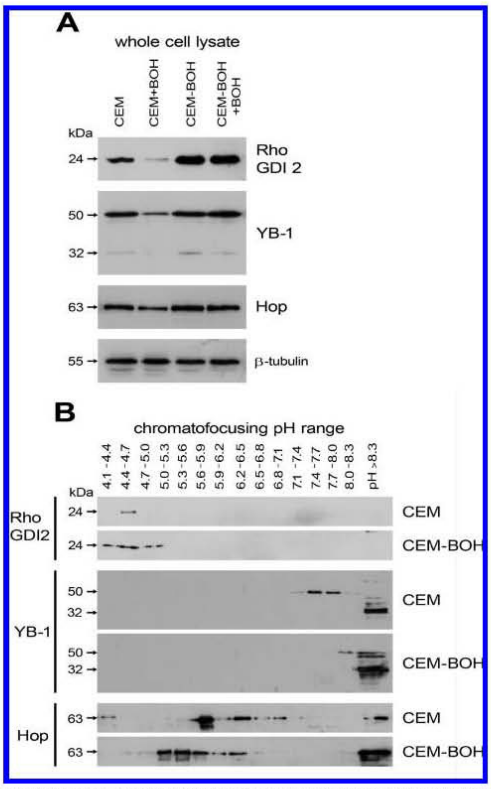


Figure 4. Immunoblot analysis of Rho GDP-dissociation inhibitor 2, Hsp70/90 organizing protein, and Y-box binding protein 1 in susceptible CEM cell line and CEM-BOH cells resistant to cyclin-dependent kinases inhibitor bohemine. (A) The whole-cell lysates were prepared from untreated sensitive CEM cell line and CEM-BOH cells resistant to cyclin-dependent kinases inhibitor bohemine (BOH). The samples of untreated cells were completed by the cells exposed by 60 μM CDKI bohemine: CEM+BOH and CEM-BOH +BOH. The lysates were examined on immunoblots using specific antibodies recognizing Rho GDP-dissociation inhibitor 2 (Rho GDI2), Hsp70/90 organizing protein (Hop), and Y-box binding protein 1 (YB-1). The β-tubulin was used as a loading control. (B) The pH fractions of the first dimension of 2-D fractionation were analyzed using Western blot to detect changes in specific isoforms of these three selected proteins. The shift in pH of YB-1 and Hop proteins between sensitive CEM cells and resistant CEM-BOH cells was detected.

Additionally, the total level of Hop did not reveal significant difference between the sensitive and resistant cells.

Second, protein changes were verified directly in pH fractions from PF 2D in order to look whether different protein forms/variants contribute to the observed alterations (Figure 4B). In case of Rho GDI2, immunoblot of PF 2D pH fractions confirmed massive elevation of the level in resistant cells with spread over several fractions that were symmetrically distributed around protein pH observed in sensitive cells. On the contrary, immunoblot of pH fractions confirmed the presence of acidic 50 kDa YB-1 protein forms (pH 7.1−8.0) in sensitive cells which were not observed in resistant cells. In resistant

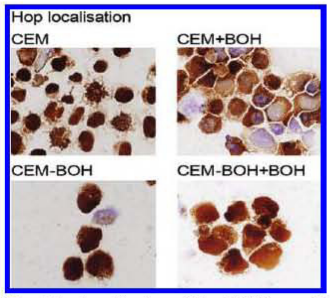


Figure 5. Subcellular localization of Hsp70/90 organizing protein in susceptible CEM cell line and CEM-BOH cells resistant to cyclin-dependent kinases inhibitor bohemine. Untreated sensitive CEM cell line, CEM-BOH cells resistant to cyclin-dependent kinases inhibitor bohemine (BOH), and both cell lines exposed by 60 μM CDKI bohemine: CEM+BOH and CEM-BOH+BOH were analyzed using immunohistochemistry (magnification 800×). Translocation of Hop from nuclei to cytoplasm was observed in sensitive CEM cells after treatment with bohemine. In resistant cells, the Hop protein was localized both in nuclei and cytoplasm and the treatment had no effect on protein level/localization.

cells, both protein forms at 50 and 32 kDa were found only in basic fraction with pH higher than 8.3. We could also observe the shift of Hop protein which was distributed in more acidic pH at 5.0−5.6 in resistant cells compared to its predominance at around pH 6.0 in susceptible counterparts. It is likely that the more acidic forms of Hop in CEM-BOH cells represent phosphorylated protein.[13]

Different Subcellular Distribution of the Hop Protein in Resistant CEM-BOH Cells. With respect to the published observations that phosphorylation of Hop protein has impact on its cellular functions as well as localization,[14,15] we used immunohistochemistry to study distribution of Hop protein in sensitive CEM and resistant CEM-BOH cells. As in the in above-mentioned immunoblot experiments, the samples of untreated sensitive CEM and resistant CEM-BOH cells were completed by the cells treated with 60 μM CDKI bohemine for 6 h.

The staining of the Hop protein was high in the nuclei of sensitive CEM cells and appeared to be closely associated to chromosomes. In comparison to this picture, the protein in resistant CEM-BOH cells was localized in both nuclei and cytoplasm. Treatment by CDKI bohemine resulted in decreased staining of Hop protein in nuclei and partial translocation to the cytoplasm in sensitive cells but did not evidently influence the expression pattern in resistant cells (Figure 5).

The Level of Rho GDI2, YB-1, and Hop Proteins in CEM and A549 Cell Lines Resistant to Bohemine, Vincristine, or Daunorubicin. To study the Rho GDI2, YB-1, and Hop proteins for their role in drug resistance, we further examined CEM cell lines resistant to vincristine (CEM-VCR) or daunorubicin (CEM-DNR) as well as representatives of solid tumor, lung adenocarcinoma cell lines A549 resistant to CDKI bohemine (A549-BOH) or vincristine (A549-VCR). Among conventional chemotherapeutic drugs, vincristine belongs to microtubule dynamics affecting drug and daunorubicin is DNA damaging agent. The resistant cell lines were derived and characterized previously.[7]

The immunoblot of whole-cell lysates confirmed increase in the level of Rho GDI2 in all resistant cell lines, including CEM-VCR and CEM-DNR cells compared to parental CEM cells and

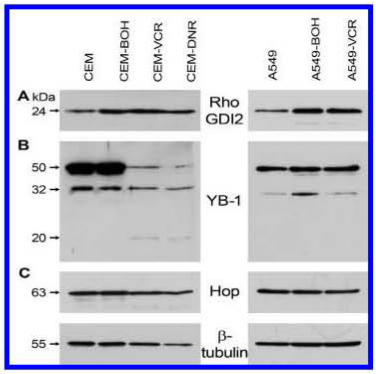


Figure 6. The level of Rho-GDP-dissociation inhibitor 2, Hsp70/90 organizing protein, and Y-box binding protein 1 in cell lines resistant to vincristine or daunorubicin. The samples of CEM cell lines resistant to vincristine (CEM-VCR) or daunorubicin (CEM-DNR) as well as A549 cell lines resistant to CDKI bohemine (A549-BOH) or vincristine (A549-VCR) were examined on immunoblots using specific antibodies recognizing Rho-GDP-dissociation inhibitor 2 (A), Y-box binding protein 1 (B), and Hsp70/90 organizing protein (C). The β-tubulin was used as a loading control.

A549-VCR or A549-DNR cells compared to parental A549 cells (Figure 6A). The expression of YB-1 protein observed in both CEM and CEM-BOH cells at the 50 and 32 kDa bands was without any evident changes between sensitive and resistant cells. On the contrary, the full-length YB-1 protein band at 50 kDa was almost diminished in CEM-VCR and CEM-DNR cells and, in addition to observed 32 kDa truncated form, the appearance of 20 kDa cleaved isoform was evident. Furthermore, the presence of a 32 kDa band of truncated YB-1 protein was also typical for A549-BOH resistant cell line (Figure 6B). The total level of Hop was not different among sensitive cells and cells resistant to bohemine, vincristine, or daunorubicin (Figure 6C); however, it does not exclude the role of specific protein form or its post-translational modification in resistant cells as evidenced by 2-D fractionation mentioned above.

Computer Modeling and Simulation of Possible Interaction Network Connecting Potential Candidate Proteins Regulated during the Development of Acquired Resistance to CDKI. Identified proteins differentially regulated during the development of acquired resistance to cyclin-dependent kinases inhibitor (Protein/Swiss-Prot accession numbers provided in Table 1) were introduced into I2D database in order to identify possible interaction partners and to construct a protein−protein interaction network that enables to graphically visualize possible functional relationships among identified molecules (Figure 7). The network exposed many additional interaction proteins with a role in the development of acquired resistance to anti-cancer drugs. In total, 2060 interactions were recognized for the 26 proteins identified in this study (Supplemental Table 2). Computer modeling highlighted a high number of direct as well as mediated interactions among ribosomal proteins, histones, and elongation factor 1-alpha 1, thus, networking transcriptional and translational pathways. Furthermore, it was of interest to observe interconnection of the YB-1 and Hop proteins with this network, namely, direct interaction of Hop protein with elongation factor 1-alpha 1 and link between YB-1 and Hop proteins mediated by three interacting proteins:

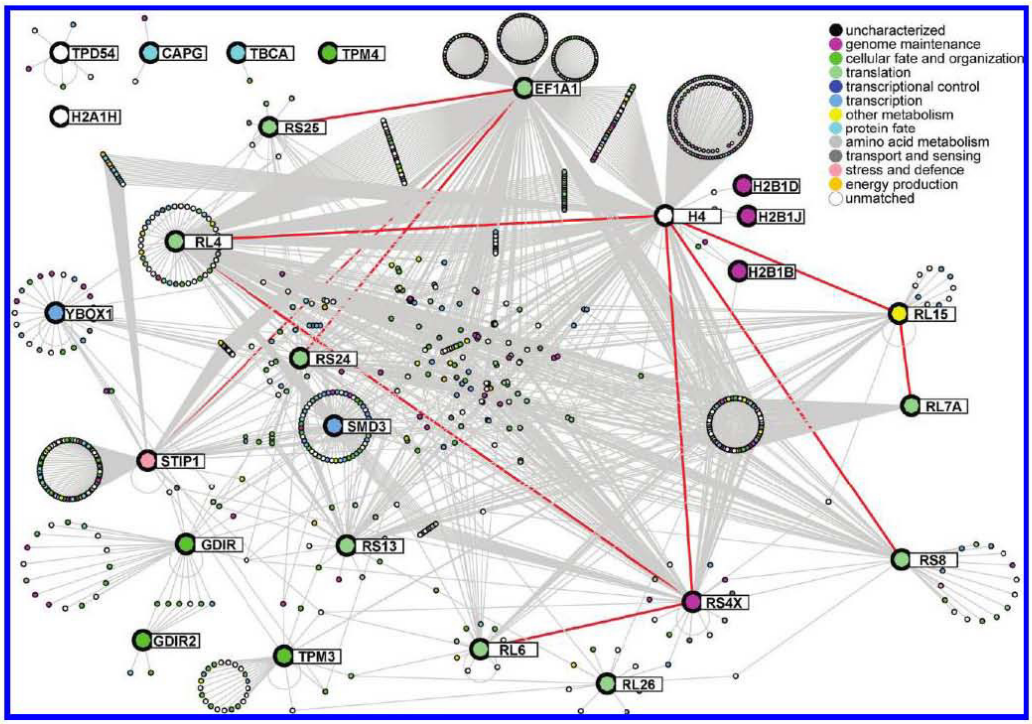


Figure 7. Computer modeling and simulation of possible interaction network connecting potential candidate proteins regulated during the development of acquired anti-cancer drug resistance. Network of possible protein−protein interactions, generated by querying I2D database and NAViGaTOR software for 26 identified proteins which were found to be regulated during the development of acquired anti-cancer drug resistance. Some interacting proteins, with direct interconnection are highlighted by red link. Color of nodes and edges represents Gene Ontology function.

Cullin-1 (CUL1; UniProt Q13616), Glycogen synthase kinase-3 beta (GSK3B; UniProt ID P49841), and S-phase kinase-associated protein 1 (SKP1A; UniProt P63208). Contrary to the above, the Rho GDI2 remains to be segregated from this interaction network.

Discussion

Resistance to anti-cancer drugs is a well-recognized problem and very often it is responsible for failure of the cancer treatment. Unfortunately, drug resistance has been observed not only to conventional chemotherapy but also to molecularly targeted anti-cancer drugs.[2] In our studies we considered selective cyclin-dependent kinases inhibitor as a promising anti-cancer drug. To date, some derivatives of this group of anti-cancer agents have been subjected to pilot clinical trials. Despite this, there are expectations of high probability of resistance development toward this type of selective drugs which may significantly contribute to failure of therapy.

Proteomic analyses of model cancer cell lines have been focused on molecular mechanisms of resistance to many different conventional anti-cancer chemotherapeutic drugs with the primary aim of identifying potential targets of resistance within the cell that would help in selective elimination of specific resistant cell types in actual disease state. The data published to date demonstrated a variety of protein alterations in drug-resistant cells that could contribute to resistance development.[2,16] The protein fractionation using 2-DE was most frequently applied in those experiments. Hence, many of the proteins on the list were relatively highly abundant proteins. Typically, it is exemplified by observed up-regulated expressions of HSP27, 14-3-3σ, and peroxiredoxins which are on the published list of the top 15 most often identified differentially expressed proteins/protein families in proteomics, regardless of the type of experiments, tissue, and even species.[17] The interpretation of such proteomic data has to be very carefully evaluated as regards specificity of these protein changes and before they are considered as relevant in a particular biological model. Hence, selection of the potential candidate proteins that may have crucial roles in molecular mechanisms of drug-resistance and verification using other independent techniques is critical and necessary. The advantage of the above-mentioned list of the top 15 proteins as suggested by Petrak et al.[17] is the possibility of short-listing of differentially expressed candidate proteins to access the more relevant potential drug targets.

To track down more specific proteins contributing to the development of resistance to CDKI, we used advanced gel-independent liquid-phase 2-D HPLC protein fractionation system that enabled in-depth study for selection of the key potential drug targets. We have used CEM T-lymphoblastic

leukemia cells, which are chemosensitive to a majority of anti-cancer drugs except for the glucocorticoids, and are frequently used for preparation and functional studies of drug resistant sublines.[7] Interestingly, although CEM cells have heterozygous mutations at codons 175/248 (175His/248His) of the p53 gene, the mutated protein forms complexes with DNA leading to transactivation and thus keeping pathway p53 functional.[18] In total, we have identified 26 protein species in 15 differentially expressed protein peaks between sensitive and resistant cells. A majority of the protein changes, in contrast to the previously published 2-DE-based studies, were found to belong to the ribosomal proteins and histones indicating deregulation of translational and transcriptional pathways, respectively, as well as possible epigenetic regulation. The results from our previous study showed down-regulation of three histone variants with different p*I* and hydrophobicity in response to CDKI bohemine, demonstrating that anti-mitotic and anti-cancer activities of this compound may be associated with epigenetic regulation at the level of chromatin structure.[9] In the study presented here, these activities involved in primary response to CDKI bohemine also contribute significantly to acquired resistance to anti-cancer drug.

Taking into consideration values of fold change and/or significance of the observed differences, it appeared evident that the best potential drug targets could be found among the proteins Rho GDI2, Hop and YB-1. As measured at the total protein levels, only the Rho GDI2 confirmed observed proteome data indicating increased level in resistant CEM-BOH cells. Despite this observation, sensitive CEM cells responded to CDKI bohemine treatment by decrease in the levels of all three candidate proteins, Rho GDI2, YB-1, and Hop, while their protein levels did not change after the treatment in CEM-BOH resistant cells. More detailed immunoblot verification after 2-D separation of cellular proteins clearly demonstrated that, in case of Hop and YB-1 proteins, the observed changes corresponded more to the presence of different protein forms or variants or modifications between susceptible and resistant cells. These findings have subsequently led us to hypothesize that up-regulation of Rho GDI2 level together with the presence of more basic YB-1 protein forms and more acidic Hop variants can make CEM cells less vulnerable to anti-cancer inhibitors of CDKs.

The Rho GDI2 belongs to a family of the GDP dissociation inhibitors, which are pivotal regulators of small GTPases, including Ras1, Cdc42, and RhoA. It was shown to be preferentially expressed in hematopoietic tissues and in B- and T-cell lines and its expression in bladder,[19−21] ovarian,[22] and breast cancer cells[23,24] has been demonstrated by various researchers. Some such published studies have attempted to relate the expression of this particular protein to the invasiveness or metastatic potential within different types of tumors with resultant controversy, indicating that RhoGDI2 may act differently in progression of different tumors.[19,21,24−26] More acceptable and clearly evident seems to be the link between increased RhoGDI2 expression and anti-cancer drug resistance in several cancer cell types.[27] In relation to these findings on Rho GDI2 and its overexpression in ovarian cancer resistant to paclitaxel or in fibrosarcoma cell line resistant to mitoxantrone,[27,28] our study shows that Rho GDI2 protein level is induced in leukemia CEM cells and lung adenocarcinoma A549 cells resistant to CDKI bohemine, vincristine, and daunorubicin. The mechanism by which overexpressed Rho GDI2 could most likely contribute to drug resistance would be due to an anti-apoptotic effect. This is supported by the fact that Rho GDIs form complexes with Rho, Ras or Cdc42, Rho GDI2 thereby blocking the apoptotic signal pathway mediated by Ras and c-Jun kinases.[27] Rho GDI2 thus represents a very promising potential marker of resistance to several different cytostatic drugs by various cancers. Such a multidrug resistance marker could be crucial in the determination of drug regimens for patients undergoing cytostatic chemotherapy and may have a significant bearing on the final outcome.

The YB-1 protein, which is the member of the cold shock domain protein family, has several pleiotropic functions in the regulation of gene transcription and translation, DNA repair, and cellular responses to environmental stimuli.[29] YB-1 activity and subcellular distribution may be regulated by its phosphorylation[11] and its proteolysis mediated by proteasome cleavage.[12] Sutherland et al.[30] showed that phosporylation by Akt kinase may induce nuclear translocation of YB-1. Furthermore, the YB-1 protein is transcriptionally activated via newly discovered transcriptional factor Twist, which also directly transactivates Akt2 gene in T-cell leukemias.[31] Akt2 kinase survival pathway is associated with chemoresistance against multiple cytotoxic and targeted therapies. The studies of truncated YB-1 forms revealed that its localization in nuclei of human cancers including breast, ovarian, prostate, colon, osteosarcoma, and synovial sarcoma could be a marker for poor patient outcome and multiple drug resistance.[12,29,32−34] We detected truncated form of YB-1 in leukemia CEM cells resistant to CDKI bohemine, vincristine, and daunorubicin and in lung adenocarcinoma A549 cells resistant to CDKI bohemine. This profile is in agreement with involvement of proteolytic clevage of YB-1 form in multidrug resistance. Furthermore, our study showed that the presence of more basic YB-1 form(s) is typical for CEM cell resistant to CDKI. The modifications causing this pH shift may include changes in protein phosphorylations but truncations or deletions cannot be excluded.[35]

Human Hop is a co-chaperone mediating the association of the molecular chaperones Hsp70 and Hsp90.[36] The best characterized function of Hop protein is its participation in steroid receptor signaling including glucocorticoid response (reviewed in Daniel et al.).[37] More recent findings suggest that Hop can not only associate with Hsp70 and 90 and modulate their activities, but also interact with several other proteins as mentioned above as well as the prion proteins.[15,37] There is evidence that murine homologue mSTI and human Hop may be phosphorylated and this modification affects protein localization.[14,38] In our study, the Hop in resistant CEM-BOH cells was more acidic than in parental CEM cells sensitive to CDKI bohemine but resistant to glucocorticoid dexamethasone suggesting that in CEM-BOH resistant cells Hop may undergo enhanced phosphorylation. Further findings from immunohistochemistry revealed that Hop is localized in nucleus as well as cytoplasm in CEM-BOH resistant cells in contrast to its prevailing accumulation in nucleus in CEM cells. Hence, the shift to more acidic forms appears to be associated with protein translocation to cytoplasm and development of resistance of CEM cells to anti-cancer CDKI bohemine. Interestingly, Longshaw et al.[14] showed that inhibition of cdc2 kinase triggered by CDKI olomoucine, belonging to the same group of anti-cancer compounds as bohemine, resulted in the nuclear accumulation of mSTI in mouse fibroblasts. On the basis of our findings, it is possible to hypothesize that Hop shuttling induced by CDKI bohemine and associated with development of resistance to this drug in CEM cells which are also resistant

to glucocorticoids may influence steroid receptor signaling via modulation of expression and/or post-translational modification of Hop co-chaperone.

Cancer, the world's second largest killer, has the highest need for new innovative treatments to increase the numbers of patients cured, and to decrease chemoresistant failures resulting in mortality. Drug resistance to synthetic CDK inhibitors is a poorly understood phenomenon and our results demonstrate that, unlike with other anti-cancer drugs, trisubstituted purine analogues represented by bohemine and roscovitine do not induce expression of multidrug resistance proteins. Moreover, roscovitine showed higher efficacy in P-glycoprotein overexpressing cells[39] highlighting these small molecules for therapy of multidrug resistant cancers. Collectively, our study has revealed that Y-box binding protein 1 and the HSP70/90 organizing protein have a critical role to play and interact with the protein nodes of transcriptional and translational networks that are also regulated by CDKI bohemine during the development of acquired resistance to this anti-cancer drug. To add to this, another important role may also be assigned to the Rho-GDP-dissociation inhibitor 2 due to an anti-apoptotic effect and potential effect in multidrug resistance.

Conclusion

While there is plenty of evidence for pre-eminence in basic research on chemoresistance for different cancers, there seems to be a profound lack of translational research (converting basic discoveries into innovative cures) for the benefit of cancer patients. Additionally, cancer related research and treatment costs are spiralling unless action is taken to improve research outcome on chemoresistance which in turn may impact survival rates as well as push down mortality rates. In particular, uptake of novel technologies and lack of specific biomarkers of the disease are proving to be key barriers to improvement. We have endeavored to work with several proteomic technologies and for a quest for proteins as specific biomarkers that may facilitate better and early diagnosis or as a handle for rapidly assessing chemoresistance to single or multidrug treatment.

The results presented in this study indicate that not only qualitative/quantitative protein changes play an important role in drug-resistance, but that there are various other parameters that too, may have a significant influence on the outcome. More importantly, truncation and/or post-translational modification(s) of selected proteins may alter their subcellular localization as well as their key role in controlling response of cancer cells to anti-cancer treatment. Additionally, simulation of possible interaction network could be used to extrapolate both the functional interpretation as well as the validity of such proteomic findings.

Further studies on these identified proteins are needed and may help to resolve many of the discrepancies between drug treatment for various cancers and poor outcome due to chemoresistance to the drugs in cancer medicine.

Abbreviations: A549-BOH, human A549 cells resistant to bohemine; A549-VCR, human A549 cells resistant to vincristine; CDKI, inhibitor of cyclin-dependent kinases; CEM-DNR, human CEM cells resistant to daunorubicin; CEM-VCR, human CEM cells resistant to vincristine; Hop, Hsp70/90 organizing protein (stress-induced phosphoprotein 1); HPCF, high-performance chromatofocusing fractionation; HPRP, high-performance reverse phase fractionation; MeCN, acetonitrile; SDS, sodium dodecyl sulfate; Rho GDI2, Rho GDP-dissociation inhibitor 2; TBST, Tris-buffered saline with 0.05% Tween 20; TFA, trifluoroacetic acid; YB-1, Y-box binding protein 1 (nuclease sensitive element-binding protein 1).

Acknowledgment. This study was supported by the Czech Ministry of School and Education (grant number LC07017) and Institutional Research Concepts AV0Z50450515 (IAPG AS CR,v.v.i.) and AV0Z50200510 (IMIC AS CR, v.v.i.), Grant Agency of the Czech Republic GACR 301/08/1649. Infrastructural part of this project (Institute of Molecular and Translational Medicine) was supported from the Operational Program Research and Development for Innovations (project CZ.1.05/2.1.00/01.0030).

Supporting Information Available: Supplemental Figure 1, 2-D liquid chromatography protein maps of sensitive CEM and resistant CEM-BOH cells; Supplemental Figure 2, the UV profiles of the second dimension HPRP fractionations of pH fractions with significant UV differences in protein peaks found between sensitive CEM cells and resistant CEM-BOH counterparts; Supplemental Table 1, table of differentially expressed proteins identified in 2-D HPLC experiment including mass spectrometry data; Supplemental Table 2, I2D protein−protein Interaction search results. This material is available free of charge via the Internet at http://pubs.acs.org.

References

(1) Raguz, S.; Yague, E. Resistance to chemotherapy: new treatments and novel insights into an old problem. *Br. J. Cancer* **2008**, *99* (3), 387–91.
(2) Zhang, J. T.; Liu, Y. Use of comparative proteomics to identify potential resistance mechanisms in cancer treatment. *Cancer Treat. Rev.* **2007**, *33* (8), 741–56.
(3) Dean, M.; Fojo, T.; Bates, S. Tumour stem cells and drug resistance. *Nat. Rev. Cancer* **2005**, *5* (4), 275–84.
(4) Hajduch, M., Skalnikova, H., Halada, P., Vydra, D., Dzubak, P., Dziechciarkova, M., Strnad, M., Radioch, D., Kovarova, H., Cyclin-dependent kinase inhibitors and cancer: usefulness of proteomic approaches in assessment of the molecular mechanisms and efficacy of novel therapeutics. In *Clinical Proteomics: From Diagnosis to Therapy*; Van Eyk, J. E., Dunn, M. J., Eds.; Wiley-VCH: Weinheim, 2007; pp 177−202.
(5) Kovarova, H.; Hajduch, M.; Korinkova, G.; Halada, P.; Krupickova, S.; Gouldsworthy, A.; Zhelev, N.; Strnad, M. Proteomics approach in classifying the biochemical basis of the anticancer activity of the new olomoucine-derived synthetic cyclin-dependent kinase inhibitor, bohemine. *Electrophoresis* **2000**, *21* (17), 3757–64.
(6) Dobashi, Y.; Takehana, T.; Ooi, A. Perspectives on cancer therapy: cell cycle blockers and perturbators. *Curr. Med. Chem.* **2003**, *10* (23), 2549–58.
(7) Noskova, V.; Dzubak, P.; Kuzmina, G.; Ludkova, A.; Stehlik, D.; Trojanec, R.; Janostakova, A.; Korinkova, G.; Mihal, V.; Hajduch, M. In vitro chemoresistance profile and expression/function of MDR associated proteins in resistant cell lines derived from CCRF-CEM, K562, A549 and MDA MB 231 parental cells. *Neoplasma* **2002**, *49* (6), 418–25.
(8) Towbin, H.; Staehelin, T.; Gordon, J. Electrophoretic transfer of proteins from polyacrylamide gels to nitrocellulose sheets: procedure and some applications. *Proc. Natl. Acad. Sci. U.S.A.* **1979**, *76* (9), 4350–4.
(9) Skalnikova, H.; Halada, P.; Dzubak, P.; Hajduch, M.; Kovarova, H. Protein fingerprints of anti-cancer effects of cyclin-dependent kinase inhibition: identification of candidate biomarkers using 2-D liquid phase separation coupled to mass spectrometry. *Technol. Cancer Res. Treat.* **2005**, *4* (4), 447–54.
(10) Linke, T.; Ross, A. C.; Harrison, E. H. Proteomic analysis of rat plasma by two-dimensional liquid chromatography and matrix-assisted laser desorption ionization time-of-flight mass spectrometry. *J. Chromatogr., A* **2006**, *1123* (2), 160–9.
(11) Bader, A. G. YB-1 activities in oncogenesis: transcription and translation. *Curr. Cancer Ther. Rev.* **2006**, *2* (1), 31–9.
(12) Sorokin, A. V.; Selyutina, A. A.; Skabkin, M. A.; Guryanov, S. G.; Nazimov, I. V.; Richard, C.; Th'ng, J.; Yau, J.; Sorensen, P. H.; Ovchinnikov, L. P.; Evdokimova, V. Proteasome-mediated cleavage

of the Y-box-binding protein 1 is linked to DNA-damage stress response. *EMBO J.* **2005**, *24* (20), 3602–12.
(13) Honore, B.; Leffers, H.; Madsen, P.; Rasmussen, H. H.; Vandekerckhove, J.; Celis, J. E. Molecular cloning and expression of a transformation-sensitive human protein containing the TPR motif and sharing identity to the stress-inducible yeast protein STI1. *J. Biol. Chem.* **1992**, *267* (12), 8485–91.
(14) Longshaw, V. M.; Chapple, J. P.; Balda, M. S.; Cheetham, M. E.; Blatch, G. L. Nuclear translocation of the Hsp70/Hsp90 organizing protein mSTI1 is regulated by cell cycle kinases. *J. Cell Sci.* **2004**, *117* (Pt. 5), 701–10.
(15) Odunuga, O. O.; Longshaw, V. M.; Blatch, G. L. Hop: more than an Hsp70/Hsp90 adaptor protein. *BioEssays* **2004**, *26* (10), 1058–68.
(16) Petrak, J.; Toman, O.; Simonova, T.; Halada, P.; Cmejla, R.; Klener, P.; Zivny, J. Identification of molecular targets for selective elimination of TRAIL-resistant leukemia cells. From spots to in vitro assays using TOP15 charts. *Proteomics* **2009**, *9* (22), 5006–15.
(17) Petrak, J.; Ivanek, R.; Toman, O.; Cmejla, R.; Cmejlova, J.; Vyoral, D.; Zivny, J.; Vulpe, C. D. Deja vu in proteomics. A hit parade of repeatedly identified differentially expressed proteins. *Proteomics* **2008**, *8* (9), 1744–9.
(18) Park, D. J.; Nakamura, H.; Chumakov, A. M.; Said, J. W.; Miller, C. W.; Chen, D. L.; Koeffler, H. P. Transactivational and DNA binding abilities of endogenous p53 in p53 mutant cell lines. *Oncogene* **1994**, *9* (7), 1899–906.
(19) Gildea, J. J.; Seraj, M. J.; Oxford, G.; Harding, M. A.; Hampton, G. M.; Moskaluk, C. A.; Frierson, H. F.; Conaway, M. R.; Theodorescu, D. RhoGDI2 is an invasion and metastasis suppressor gene in human cancer. *Cancer Res.* **2002**, *62* (22), 6418–23.
(20) Seraj, M. J.; Harding, M. A.; Gildea, J. J.; Welch, D. R.; Theodorescu, D. The relationship of BRMS1 and RhoGDI2 gene expression to metastatic potential in lineage related human bladder cancer cell lines. *Clin. Exp. Metastasis* **2000**, *18* (6), 519–25.
(21) Theodorescu, D.; Sapinoso, L. M.; Conaway, M. R.; Oxford, G.; Hampton, G. M.; Frierson, H. F., Jr. Reduced expression of metastasis suppressor RhoGDI2 is associated with decreased survival for patients with bladder cancer. *Clin. Cancer Res.* **2004**, *10* (11), 3800–6.
(22) Tapper, J.; Kettunen, E.; El-Rifai, W.; Seppala, M.; Andersson, L. C.; Knuutila, S. Changes in gene expression during progression of ovarian carcinoma. *Cancer Genet. Cytogenet.* **2001**, *128* (1), 1–6.
(23) Jiang, W. G.; Watkins, G.; Lane, J.; Cunnick, G. H.; Douglas-Jones, A.; Mokbel, K.; Mansel, R. E. Prognostic value of rho GTPases and rho guanine nucleotide dissociation inhibitors in human breast cancers. *Clin. Cancer Res.* **2003**, *9* (17), 6432–40.
(24) Schunke, D.; Span, P.; Ronneburg, H.; Dittmer, A.; Vetter, M.; Holzhausen, H. J.; Kantelhardt, E.; Krenkel, S.; Muller, V.; Sweep, F. C.; Thomssen, C.; Dittmer, J. Cyclooxygenase-2 is a target gene of rho GDP dissociation inhibitor beta in breast cancer cells. *Cancer Res.* **2007**, *67* (22), 10694–702.
(25) Cho, H. J.; Baek, K. E.; Park, S. M.; Kim, I. K.; Choi, Y. L.; Nam, I. K.; Hwang, E. M.; Park, J. Y.; Han, J. Y.; Kang, S. S.; Kim, D. C.; Lee, W. S.; Lee, M. N.; Oh, G. T.; Kim, J. W.; Lee, C. W.; Yoo, J. RhoGDI2 expression is associated with tumor growth and malignant progression of gastric cancer. *Clin. Cancer Res.* **2009**, *15* (8), 2612–9.
(26) Zhao, J.; Chang, A. C.; Li, C.; Shedden, K. A.; Thomas, D. G.; Misek, D. E.; Manoharan, A. P.; Giordano, T. J.; Beer, D. G.; Lubman, D. M. Comparative proteomics analysis of Barrett metaplasia and esophageal adenocarcinoma using two-dimensional liquid mass mapping. *Mol. Cell. Proteomics* **2007**, *6* (6), 987–99.
(27) Goto, T.; Takano, M.; Sakamoto, M.; Kondo, A.; Hirata, J.; Kita, T.; Tsuda, H.; Tenjin, Y.; Kikuchi, Y. Gene expression profiles with cDNA microarray reveal RhoGDI as a predictive marker for paclitaxel resistance in ovarian cancers. *Oncol. Rep.* **2006**, *15* (5), 1265–71.
(28) Sinha, P.; Hutter, G.; Kottgen, E.; Dietel, M.; Schadendorf, D.; Lage, H. Search for novel proteins involved in the development of chemoresistance in colorectal cancer and fibrosarcoma cells in vitro using two-dimensional electrophoresis, mass spectrometry and microsequencing. *Electrophoresis* **1999**, *20* (14), 2961–9.
(29) Kuwano, M.; Oda, Y.; Izumi, H.; Yang, S. J.; Uchiumi, T.; Iwamoto, Y.; Toi, M.; Fujii, T.; Yamana, H.; Kinoshita, H.; Kamura, T.; Tsuneyoshi, M.; Yasumoto, K.; Kohno, K. The role of nuclear Y-box binding protein 1 as a global marker in drug resistance. *Mol. Cancer Ther.* **2004**, *3* (11), 1485–92.
(30) Sutherland, B. W.; Kucab, J.; Wu, J.; Lee, C.; Cheang, M. C.; Yorida, E.; Turbin, D.; Dedhar, S.; Nelson, C.; Pollak, M.; Leighton Grimes, H.; Miller, K.; Badve, S.; Huntsman, D.; Blake-Gilks, C.; Chen, M.; Pallen, C. J.; Dunn, S. E. Akt phosphorylates the Y-box binding protein 1 at Ser102 located in the cold shock domain and affects the anchorage-independent growth of breast cancer cells. *Oncogene* **2005**, *24* (26), 4281–92.
(31) Tanji, H.; Ishikawa, C.; Sawada, S.; Nakachi, S.; Takamatsu, R.; Matsuda, T.; Okudaira, T.; Uchihara, J. N.; Ohshiro, K.; Tanaka, Y.; Senba, M.; Uezato, H.; Ohshima, K.; Duc Dodon, M.; Wu, K. J.; Mori, N. Aberrant expression of the transcription factor Twist in adult T-cell leukemia. *Blood* **2010**, *116* (8), 1386.
(32) Bargou, R. C.; Jurchott, K.; Wagener, C.; Bergmann, S.; Metzner, S.; Bommert, K.; Mapara, M. Y.; Winzer, K. J.; Dietel, M.; Dorken, B.; Royer, H. D. Nuclear localization and increased levels of transcription factor YB-1 in primary human breast cancers are associated with intrinsic MDR1 gene expression. *Nat. Med.* **1997**, *3* (4), 447–50.
(33) Fujita, T.; Ito, K.; Izumi, H.; Kimura, M.; Sano, M.; Nakagomi, H.; Maeno, K.; Hama, Y.; Shingu, K.; Tsuchiya, S.; Kohno, K.; Fujimori, M. Increased nuclear localization of transcription factor Y-box binding protein 1 accompanied by up-regulation of P-glycoprotein in breast cancer pretreated with paclitaxel. *Clin. Cancer Res.* **2005**, *11* (24 Pt. 1), 8837–44.
(34) Oda, Y.; Ohishi, Y.; Saito, T.; Hinoshita, E.; Uchiumi, T.; Kinukawa, N.; Iwamoto, Y.; Kohno, K.; Kuwano, M.; Tsuneyoshi, M. Nuclear expression of Y-box-binding protein-1 correlates with P-glycoprotein and topoisomerase II alpha expression, and with poor prognosis in synovial sarcoma. *J. Pathol.* **2003**, *199* (2), 251–8.
(35) Zhu, K.; Zhao, J.; Lubman, D. M.; Miller, F. R.; Barder, T. J. Protein pI shifts due to posttranslational modifications in the separation and characterization of proteins. *Anal. Chem.* **2005**, *77* (9), 2745–55.
(36) Lassle, M.; Blatch, G. L.; Kundra, V.; Takatori, T.; Zetter, B. R. Stress-inducible, murine protein mSTI1. Characterization of binding domains for heat shock proteins and in vitro phosphorylation by different kinases. *J. Biol. Chem.* **1997**, *272* (3), 1876–84.
(37) Daniel, S., Soti, C., Csermely, P., Bradley, G., Blatch, G. L. Hop: An Hsp70/Hsp90 co-chaperone that functions within and beyond Hsp70/Hsp90 protein folding pathways. In *Networking of Chaperones by Co-Chaperones*; Blatch, G. L., Ed.; Springer: New York, 2007; pp 26–37.
(38) Daniel, S.; Bradley, G.; Longshaw, V. M.; Soti, C.; Csermely, P.; Blatch, G. L. Nuclear translocation of the phosphoprotein Hop (Hsp70/Hsp90 organizing protein) occurs under heat shock, and its proposed nuclear localization signal is involved in Hsp90 binding. *Biochim. Biophys. Acta* **2008**, *1783* (6), 1003–14.
(39) Cappellini, A.; Chiarini, F.; Ognibene, A.; McCubrey, J. A.; Martelli, A. M. The cyclin-dependent kinase inhibitor roscovitine and the nucleoside analog sangivamycin induce apoptosis in caspase-3 deficient breast cancer cells independent of caspase mediated P-glycoprotein cleavage: implications for therapy of drug resistant breast cancers. *Cell Cycle* **2009**, *8* (9), 1421–5.

PR100468W

4.3. Charakterizace mechanismů působení antracyklinů na nádorové buňky

v publikaci

Cancer Cell Response to Anthracyclines Effects:
Mysteries of the Hidden Proteins Associated with these Drugs

Tylečková J, **Hrabáková R**, Mairychová K, Halada P, Radová L, Džubák P, Hajdúch M, Gadher SJ, Kovářová H.

Int J Mol Sci. 2012; 13(12): 15536-15564 (doi:10.3390/ijms131215536)
IF (2012): 2.60; 5-year IF (2012): 2.62

Prohlášení spoluautorů

„Prohlašuji, že Rita Hrabáková se patřičně podílela (30 %) na plánování proteomických experimentů, jejich provedení, interpretaci výsledků a sepisování této práce."

V Liběchově, dne..... RNDr. Hana Kovářová, CSc.

.....……...

Int. J. Mol. Sci. **2012**, *13*, 15536-15564; doi:10.3390/ijms131215536

OPEN ACCESS
International Journal of
Molecular Sciences
ISSN 1422-0067
www.mdpi.com/journal/ijms

Article

Cancer Cell Response to Anthracyclines Effects: Mysteries of the Hidden Proteins Associated with These Drugs

Jirina Tyleckova [1], Rita Hrabakova [1], Katerina Mairychova [1], Petr Halada [2], Lenka Radova [3], Petr Dzubak [3], Marian Hajduch [3], Suresh J. Gadher [4] and Hana Kovarova [1,*]

[1] Institute of Animal Physiology and Genetics AS CR, v.v.i., 277 21 Libechov, Czech Republic; E-Mails: tyleckova@iapg.cas.cz (J.T.); hrabakova@iapg.cas.cz (R.H.); mairychova@iapg.cas.cz (K.M.)

[2] Institute of Microbiology AS CR, v.v.i., 142 20 Prague, Czech Republic; E-Mail: halada@biomed.cas.cz

[3] Laboratory of Experimental Medicine, Institute of Translational and Molecular Medicine, Faculty of Medicine and Dentistry, Palacky University and University Hospital, 775 15 Olomouc, Czech Republic; E-Mails: avodar@gmail.com (L.R.); dzubakp@gmail.com (P.D.); marian.hajduch@upol.cz (M.H.)

[4] Life Technologies, Frederick, MD 21704, USA; E-Mail:gadhersuresh@hotmail.com

* Author to whom correspondence should be addressed; E-Mail: kovarova@iapg.cas.cz; Tel.: +420-315-639-582; Fax: +420-315-639-510.

Received: 31 August 2012; in revised form: 26 October 2012 / Accepted: 7 November 2012 / Published: 22 November 2012

Abstract: A comprehensive proteome map of T-lymphoblastic leukemia cells and its alterations after daunorubicin, doxorubicin and mitoxantrone treatments was monitored and evaluated either by paired comparison with relevant untreated control and using multivariate classification of treated and untreated samples. With the main focus on early time intervals when the influence of apoptosis is minimized, we found significantly different levels of proteins, which corresponded to 1%–2% of the total amount of protein spots detected. According to Gene Ontology classification of biological processes, the highest representation of identified proteins for all three drugs belong to metabolic processes of proteins and nucleic acids and cellular processes, mainly cytoskeleton organisation and ubiquitin-proteasome pathway. Importantly, we observed significant proportion of changes in proteins involved in the generation of precursor metabolites and energy typical for daunorubicin, transport proteins participating in response to doxorubicin and a group of proteins of immune system characterising response to mitoxantrone. Both a paired comparison and the multivariate evaluation of quantitative data revealed

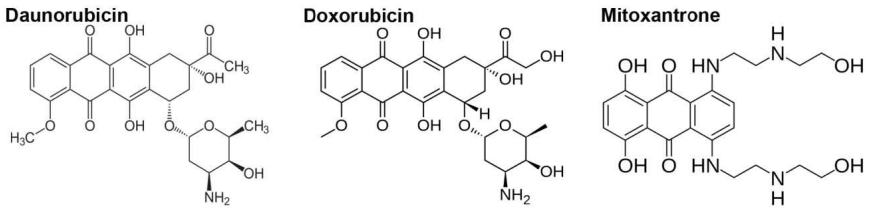
daunorubicin as a distinct member of the group of anthracycline/anthracenedione drugs. A combination of identified drug specific protein changes, which may help to explain anti-cancer activity, together with the benefit of blocking activation of adaptive cancer pathways, presents important approaches to improving treatment outcomes in cancer.

Keywords: anthracycline/anthracenedione; T-lymphoblastic leukemia; proteomics; early anti-cancer response; adaptive cancer mechanisms; protein biosynthesis; ubiquitin-proteasome system; energy metabolism; transport proteins; tumor immunity

1. Introduction

The anthracycline antibiotics doxorubicin (DOXO) and daunorubicin (DNR) belong to the most effective anti-cancer drugs. They have been widely used in clinics for the treatment of both solid tumors and hematological malignancies since the early 1960s, when these products of *Streptomyces peucetius* were first isolated [1]. Structurally, there is only a subtle difference between DNR and DOXO in the side chain of the molecules [2] and mitoxantrone (MTX), an anthracenedione, has also very similar structure to that of anthracyclines [3] (Figure 1).

Figure 1. Chemical structures of daunorubicin, doxorubicin and mitoxantrone.



The mechanism of action of these drugs is attributed mainly to the inhibition of topoisomerase II activity. Topoisomerase II binds to DNA and allows its cleavage but this covalent complex is trapped in the presence of anthracycline drug and DNA cannot re-ligate, thus subsequently blocking transcription and replication [4,5]. Other proposed mechanisms of action are DNA intercalation and the production of reactive oxygen species [6], which appears to be responsible for the serious toxic side effects of these chemotherapeutic drugs, namely cardiotoxicity [7,8]. Despite the similarity in the structure of anthracyclines and anthracenediones, they differ widely in clinical use. DOXO has the widest spectrum of activity amongst anthracyclines and is used for the treatment of both solid tumors and hematological malignancies. It is administered as a single agent or in combination chemotherapy regimens. On the contrary, DNR shows activity mainly in acute leukemia's [9]. MTX is active both in solid tumors and leukemia with slightly lower activity than DOXO but also with lower toxicity [3]. Even though these drugs are frequently used in clinics, the exact molecular mechanisms of their effects on tumor cells, as well as toxicity, are not completely understood. Importantly, such deeper knowledge might contribute to the clarification of different therapeutic efficiency of structurally very close groups of anthracyclines and anthracenediones.

Proteomic approaches involving gel-based techniques, gel-free chromatography and advanced mass spectrometry for protein fractionation, identification and quantification, allow us to study the effects of drug treatments on cells at protein level in a comprehensive way. The main advantage of 2-D gel based fractionation is the high resolution including assessment of multiple forms of individual protein (s) on the basis of differences in isoelectric point and molecular mass. Using a suitable protein stain, this popular and reliable technique may facilitate comprehensive quantification [10]. Several proteomic studies have been recently performed for monitoring the effect of DOXO on hepatocellular carcinoma [11], breast cancer [12], non-Hodgkin lymphoma [13], acute lymphoblastic leukemia cells [14] or the effect of DNR on pancreatic carcinoma [15] *in vitro*. In addition, proteomic techniques have been used for studying drug resistance mechanisms to DOXO or MTX in lung cancer cells [16,17].

In this study, we performed proteomic comparison of very early effects of DNR, DOXO and MTX treatments on T-lymphoblastic leukemia cells as representative of hematological malignancies. The main goals have been to characterise and identify typical markers of cell response to individual drugs, to define biological processes responsible for their anti-tumor activity and to compare the effects of these structurally linked drugs in order to explain their different therapeutic effectiveness in clinics.

2. Results

2.1. Determination of IC_{50}, TA_{50}

Our intention was to investigate the early effects of the anthracycline/anthracenedione anti-cancer drugs that precede the onset of apoptosis in CEM cells and loss of cell viability. The IC_{50} of drugs were determined using the MTT test as mentioned above. The induction of apoptosis in cells began at different time intervals for different drugs. It was therefore necessary to measure time to onset of apoptosis (TA) at first and then to adjust the time of the treatments for each individual drug to the half time of TA (TA_{50}). Hence, for all proteomic experiments the cells were treated with 10× IC_{50} doses of the drugs for time interval corresponding to TA_{50} (Table 1). This combination of dose and time of the treatment led to measurable changes in protein composition before onset of apoptosis in treated cells.

Table 1. The list of studied anti-cancer drugs with their abbreviations, 10 times of inhibitory concentrations corresponding to 50% of cell growth (10× IC_{50}) and half times to apoptosis induction (TA_{50}) for 10× IC_{50} doses of individual drugs.

Anti-cancer drug	Abbreviation	Mechanism of action	10× IC_{50} (μg/mL)	TA_{50} (min)
Daunorubicin	DNR	intercalation, topo II inhibitor	0.03	120
Doxorubicin	DOXO	intercalation, topo II inhibitor	0.05	250
Mitoxantrone	MTX	intercalation, topo II inhibitor	1.88×10^{-3}	150
Cisplatin	CisPt	alkylating-like	7.57	150
Paclitaxel	TAX	mitotic inhibitor	9.00×10^{-5}	120

2.2. Proteome 2-D Maps—Number of Spots per Gel and Number of Differentially Abundant Spots per Anti-Cancer Drug

In order to cover the most significant part of the cancer cell proteome, two different pH ranges, pH 4–7 and pH 6–11, were used. The 2D gel images were analyzed using Redfin Solo SW protocol. In

this approach, spot detection and image segmentation takes place in a composite image and the same spot positions and borders are then assigned to all images, after compensation for geometric distortions. On average, 2180 and 570 protein spots were detected in pH 4–7 and pH 6–11, respectively (Figure 2). In total for all five anticancer drugs in this study, 133 protein spots showed significantly increased intensity pattern after drug treatment, while 86 protein spots were decreased according to criteria of fold-change >1.2 for p-value <0.01 and fold-change >1.5 for p-value <0.05. Amongst these, 47 protein spots occurred at different levels in DOXO treatment, 40 protein spots in DNR treatment and 54 protein spots in MTX treatment. Differentially expressed protein spots were selected for mass spectrometry identification and 153 proteins were identified in 174 protein spots which were excised out of all 219 significantly different spots (Table 2). Amongst the identified proteins, there were seven proteins present in two spots and six proteins present in three spots. Contrary to this, two proteins in one spot were identified for seven spots (Table S1). More detailed data regarding mass spectrometry protein identifications including spot number, protein name, UniProt database number, number of peptides matched to the identified protein, number of unassigned peaks, sequence coverage, Mascot score of the identified protein, Mascot score for the highest ranked hit to a non-homologous protein, peptide sequences confirmed by MS/MS (Mascot score given in parenthesis), MW and pI are reported in Table S1.

Figure 2. Representative 2-D protein map of treated CEM T-lymphoblastic leukemia cells.

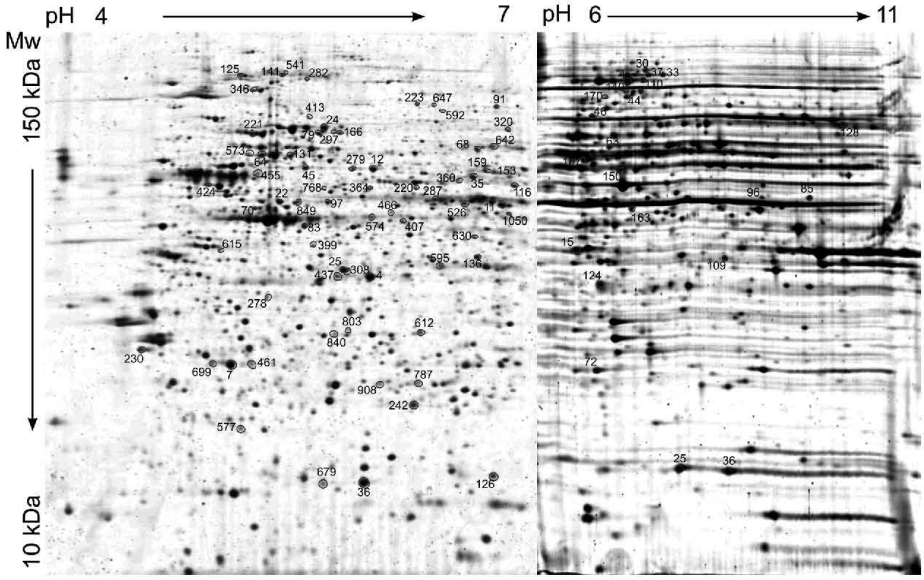


Table 2. The list of studied anti-cancer drugs with the numbers of significant protein spot changes, direction of their changes and the number of identified proteins. DNR, daunorubicin; DOXO, doxorubicin; MTX, mitoxantrone; CisPt, cisplatin; TAX, paclitaxel.

Anti-cancer drug	No. Different Spot	4–7		No. ID proteins	No. Different Spot	6–11		No. ID proteins	No. Different Spot	Total		No. ID proteins
		Up	Down			Up	Down			Up	Down	
DNR	32	8	24	24	8	1	7	5	40	9	31	29
DOXO	29	15	14	21	18	13	5	10	47	28	19	31
MTX	40	24	16	30	14	9	5	10	54	33	21	40
CisPt	24	21	3	18	23	16	7	13	47	37	10	31
TAX	29	25	4	21	2	1	1	1	31	26	5	22
Total	154	93	61	114	65	40	25	39	219	133	86	153

On average, 2180 protein spots could be detected on pH 4–7 gels and 570 protein spots could be detected on pH 6–11 gels. The spot numbers indicate significantly altered protein spots after daunorubicin, doxorubicin or mitoxantrone treatments (fold change >1.2 and p-value <0.01 and fold change >1.5 and p-value <0.05). Gels were stained using Sypro Ruby and Redfin SW was used for 2-D gel image analysis.

2.3. The Proteins Significantly Changing Their Abundance after Treatment by Individual Anthracycline/Anthracenedione Drugs and Their Distribution by Biological Processes

The proteins significantly changing their abundance and identified as single protein per protein spot for DNR, DOXO and MTX treatments and their classification into biological processes are in Table 3 and depicted in Figure 3. With regard to relatively short time intervals of individual drug treatments, observed increase or decrease in protein levels may be due to impact of drug on turn-over of these proteins.

Light blue squares represent anti-cancer drugs. The nodes show identified proteins marked according to their gene names, the color code represents Gene Ontology biological process based on PANTHER classification. The node shape shows trend of change in protein level, proteins with increased levels are depicted as triangles, proteins with decreased levels as arrowheads and proteins with opposite changes between different drugs as diamonds. Detailed information about the proteins is shown in Table 3.

Table 3. The list of identified changed proteins.

3A	DNR								
Drug	**Spot No.**	**Protein name**	**Gene Name**	**UniProt No.**	**Biological process**	**pH**	**Change**	**Fold change**	***p*-value**
DNR	4	L-lactate dehydrogenase B chain	*LDHB*	P07195	3	4–7	↑	1.34	0.0048
DNR	7	Rho GDP-dissociation inhibitor 2	*ARHGDIB*	P52566	1	4–7	↑	1.69	0.008
DNR	36	Stathmin	*STMN1*	P16949	1	4–7	↑	1.75	0.0022
DNR	64	60 kD a heat shock protein, mitochondrial	*HSPD1*	P10809	5	4–7	↓	1.52	0.0023
DNR	72b	Proteasome subunit beta type-2	*PSMB2*	P49721	5	6–11	↓	1.70	0033
DNR	96b	Obg-like ATPase 1	*OLA1*	Q9NTK5	8	6–11	↑	1.34	0.0022
DNR	97	Cytochrome b-c1 complex subunit 1, mitochondrial	*UQCRC1*	P31930	3	4–7	↓	1.36	0.0041
DNR	107b	Glucose-6-phosphate 1-dehydrogenase	*G6PD*	P11413	5	6–11	↓	2.95	0.0013
DNR	124b	*S*-formylglutathione hydrolase	*ESD*	P10768	8	6–11	↓	2.22	0.009
DNR	125	Heat shock 70 kDa protein 4	*HSPA4*	P34932	4	4–7	↓	2.25	0.0076
DNR	126	Cofilin-1	*CFL1*	P23528	1	4–7	↑	2.01	0.0045
DNR	159	Succinyl-CoA: 3-ketoacid-coenzyme A transferase 1, mitochondrial	*OXCT1*	P55809	5	4–7	↓	1.67	0.0059
DNR	166	Dihydrolipoyllysine-residue acetyltransferase component of pyruvate dehydrogenase complex, mitochondrial	*DLAT*	P10515	5	4–7	↓	2.34	0.0004
DNR	220	Heterogeneous nuclear ribonucleoprotein H	*HNRNPH1*	P31943	5	4–7	↓	1.56	0.0017
DNR	221	Plastin-2	*LCP1*	P13796	1	4–7	↓	1.63	0.0093
DNR	287	DnaJ homolog subfamily A member 2	*DNAJA2*	O60884	4	4–7	↓	1.63	0.0021
DNR	346	Transitional endoplasmic reticulum ATPase	*VCP*	P55072	7	4–7	↓	2.55	0.0098
DNR	360	Mitochondrial-processing peptidase subunit alpha	*PMPCA*	Q10713	3	4–7	↓	1.66	0.0029
DNR	399	Anamorsin	*CIAPIN1*	Q6FI81	8	4–7	↓	1.47	0.0049
DNR	407	Protein phosphatase methylesterase 1	*PPME1*	Q9Y570	5	4–7	↑	1.44	0.0083
DNR	424	ATP synthase subunit beta, mitochondrial	*ATP5B*	P06576	3	4–7	↓	2.21	0.0009
DNR	573	60 kDa heat shock protein, mitochondrial	*HSPD1*	P10809	5	4–7	↓	1.72	0.0009
DNR	574	TAR DNA-binding protein 43	*TARDBP*	Q13148	5	4–7	↑	1.33	0.0065
DNR	768	Glutathione synthetase	*GSS*	P48637	5	4–7	↓	2.00	0.0019
DNR	849	Heterogeneous nuclear ribonucleoprotein F	*HNRNPF*	P52597	5	4–7	↓	1.71	0.009

Table 3. *Cont.*

3B	DOXO								
Drug	**Spot No.**	**Protein name**	**Gene Name**	**UniProt No.**	**Biological process**	**pH**	**Change**	**Fold change**	***p*-value**
DOXO	29	Heat shock 70 kDa protein 1A/1B	*HSPA1A/ HSPA1B*	P08107	4	4–7	↑	1.43	0.0073
DOXO	44b	Far upstream element-binding protein 2	*KHSRP*	Q92945	5	6–11	↑	1.53	0.0079
DOXO	61b	KH domain-containing, RNA-binding, signal transduction-associated protein 1	*KHDRBS1*	Q07666	5	6–11	↓	1.78	0.0004
DOXO	63b	EH domain-containing protein 1	*EHD1*	Q9H4M9	7	6–11	↑	1.79	0.049
DOXO	91	DNA replication licensing factor MCM7	*MCM7*	P33993	1	4–7	↑	1.56	0.0081
DOXO	115b	Elongation factor 2	*EEF2*	P13639	5	6–11	↑	1.54	0.0023
DOXO	141	Caprin-1	*CAPRIN1*	Q14444	7	4–7	↑	1.54	0.0008
DOXO	163b	Medium-chain specific acyl-CoA dehydrogenase, mitochondrial	*ACADM*	P11310	3	6–11	↓	1.45	0.0025
DOXO	170b	Far upstream element-binding protein 2	*KHSRP*	Q92945	5	6–11	↑	1.89	0.0013
DOXO	278	Spermidine synthase	*SRM*	P19623	5	4–7	↑	1.64	0.0049
DOXO	282	Ubiquitin-like modifier-activating enzyme 1	*UBA1*	P22314	1	4–7	↑	1.97	0.0062
DOXO	308	F-actin-capping protein subunit alpha-2	*CAPZA2*	P47755	1	4–7	↑	1.45	0.0098
DOXO	364	4-trimethylaminobutyraldehyde dehydrogenase	*ALDH9A1*	P49189	5	4–7	↑	1.51	0.0033
DOXO	592	Ezrin	*EZR*	P15311	1	4–7	↑	2.59	0.0071
DOXO	595	L-aminoadipate-semialdehyde dehydrogenase-phosphopantetheinyl transferase	*AASDHPPT*	Q9NRN7	8	4–7	↓	1.54	0.0009
DOXO	630	Ubiquitin-like domain-containing CTD phosphatase 1	*UBLCP1*	Q8WVY7	8	4–7	↓	1.36	0.0025
DOXO	699	Rho GDP-dissociation inhibitor 2	*ARHGDIB*	P52566	1	4–7	↓	2.00	0.0015
DOXO	787	Glutathione *S*-transferase P	*GSTP1*	P09211	4	4–7	↓	1.54	0.0089
DOXO	908	GTP-binding protein SAR1b	*SAR1B*	Q9Y6B6	7	4–7	↓	1.33	0.0073

Table 3. *Cont.*

3C	MTX								
Drug	**Spot No.**	**Protein name**	**Gene Name**	**UniProt No.**	**Biological process**	**pH**	**Change**	**Fold change**	***p*-value**
MTX	11	Elongation factor 1-gamma	*EEF1G*	P26641	5	4–7	↑	1.32	0.0056
MTX	12	Protein disulfide-isomerase A3	*PDIA3*	P30101	5	4–7	↑	1.48	0.0056
MTX	22	Heterogeneous nuclear ribonucleoprotein F	*HNRNPF*	P52597	5	4–7	↑	1.37	0.0011
MTX	24	Stress-70 protein, mitochondrial	*HSPA9*	P38646	4	4–7	↑	1.47	0.007
MTX	25	60 S acidic ribosomal protein P0	*RPLP0*	P05388	5	4–7	↑	1.3	0.0012
MTX	30b	Staphylococcal nuclease domain-containing protein 1	*SND1*	Q7KZF4	5	6–11	↑	1.53	0.024
MTX	35	T-complex protein 1 subunit beta	*CCT2*	P78371	5	4–7	↑	1.47	0.0017
MTX	36b	Peptidyl-prolyl cis-*trans* isomerase	*PPIA*	P62937	4	6–11	↓	1.75	0.0072
MTX	68	T-complex protein 1 subunit gamma	*CCT3*	P49368	5	4–7	↑	1.56	0.00014
MTX	83	Activator of 90 kDa heat shock protein ATPase homolog 1	*AHSA1*	O95433	4	4–7	↑	1.47	0.00035
MTX	109b	Heterogeneous nuclear ribonucleoproteins A2/B1	*HNRNPA2B1*	P22626	5	6–11	↓	1.87	0.0071
MTX	110b	ATP-dependent RNA helicase DDX1	*DDX1*	Q92499	5	6–11	↑	1.51	0.008
MTX	116	RuvB-like 1	*RUVBL1*	Q9Y265	5	4–7	↑	1.66	0.00004
MTX	128b	Eukaryotic translation initiation factor 2 subunit 3	*EIF2S3L*	Q2VIR3	5	6–11	↓	1.73	0.02
MTX	131	60 kDa heat shock protein, mitochondrial	*HSPD1*	P10809	5	4–7	↑	1.52	0.001
MTX	136	Transaldolase	*TALDO1*	P37837	5	4–7	↑	1.33	0.0042
MTX	223	Mitochondrial inner membrane protein	*IMMT*	Q16891	8	4–7	↑	1.58	0.0028
MTX	230	Proteasome subunit alpha type-5	*PSMA5*	P28066	5	4–7	↑	2.51	0,004
MTX	297	Heat shock 70 kDa protein 1A/1B	*HSPA1A/HSPA1B*	P08107	4	4–7	↑	1.36	0.0066
MTX	455	G-rich sequence factor 1	*GRSF1*	Q12849	5	4–7	↑	1.66	0.0016
MTX	461	Rho GDP-dissociation inhibitor 2	*ARHGDIB*	P52566	1	4–7	↓	1.46	0.0033
MTX	466	Eukaryotic translation initiation factor 3 subunit G	*EIF3G*	O75821	5	4–7	↓	1.46	0.002
MTX	615	Transformer-2 protein homolog beta	*TRA2B*	P62995	5	4–7	↓	1.93	0.0025
MTX	647	Mitochondrial inner membrane protein	*IMMT*	Q16891	8	4–7	↑	1.34	0.0006
MTX	679	Stathmin	*STMN1*	P16949	1	4–7	↓	2.26	0.0028
MTX	1050	Adenylosuccinate synthetase isozyme 2	*ADSS*	P30520	5	4–7	↑	1.52	0.00005

Table 3. *Cont.*

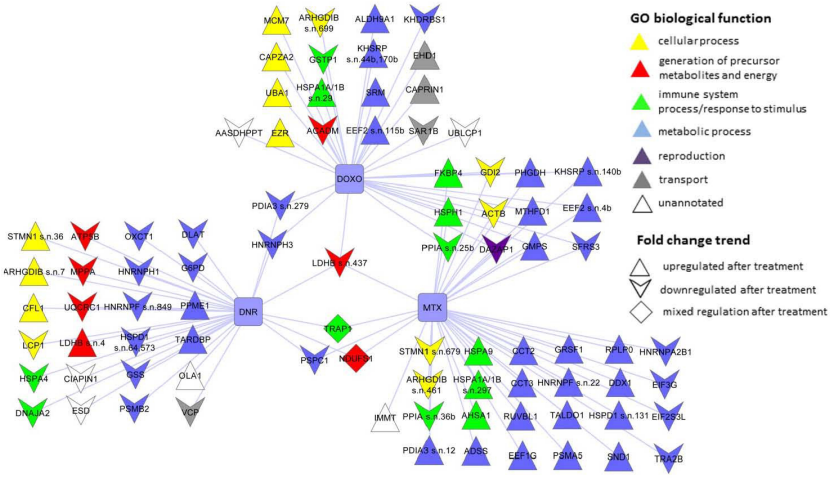
3D	DNR + DOXO								
Drug	**Spot No.**	**Protein name**	**Gene Name**	**UniProt No.**	**Biological process**	**pH**	**Change**	**Fold change**	***p*-value**
DNR	15b	Heterogeneous nuclear ribonucleoprotein H3	*HNRNPH3*	P31942	5	6–11	↓	1.88	0.04
DOXO	15b	Heterogeneous nuclear ribonucleoprotein H3	*HNRNPH3*	P31942	5	6–11	↓	2.25	0.025
DNR	279	Protein disulfide-isomerase A3	*PDIA3*	P30101	5	4–7	↓	1.50	0.0056
DOXO	279	Protein disulfide-isomerase A3	*PDIA3*	P30101	5	4–7	↓	1.59	0.004
3E	**DNR + MTX**								
Drug	**Spot No.**	**Protein name**	**Gene Name**	**UniProt No.**	**Biological process**	**pH**	**Change**	**Fold change**	***p*-value**
DNR	320	Heat shock protein 75 kDa, mitochondrial	*TRAP1*	Q12931	4	4–7	↓	1.66	0.001
MTX	320	Heat shock protein 75 kDa, mitochondrial	*TRAP1*	Q12931	4	4–7	↑	1.33	0.0045
DNR	413	NADH-ubiquinone oxidoreductase 75 kDa subunit, mitochondrial	*NDUFS1*	P28331	3	4–7	↓	1.37	0.0015
MTX	413	NADH-ubiquinone oxidoreductase 75 kDa subunit, mitochondrial	*NDUFS1*	P28331	3	4–7	↑	1.6	0.0073
DNR	642	Paraspeckle component 1	*PSPC1*	Q8WXF1	5	4–7	↓	4.11	0.0028
MTX	642	Paraspeckle component 1	*PSPC1*	Q8WXF1	5	4–7	↓	2.44	0.0077
3F	**DOXO + MTX**								
Drug	**Spot No.**	**Protein name**	**Gene Name**	**UniProt No.**	**Biological process**	**pH**	**Change**	**Fold change**	***p*-value**
DOXO	4b	Elongation factor 2	*EEF2*	P13639	5	6–11	↑	1.47	0.00038
MTX	4b	Elongation factor 2	*EEF2*	P13639	5	6–11	↑	1.47	0.00035
DOXO	25b	Peptidyl-prolyl cis-*trans* isomerase	*PPIA*	P62937	4	6–11	↓	1.85	0.0023
MTX	25b	Peptidyl-prolyl cis-*trans* isomerase	*PPIA*	P62937	4	6–11	↓	1.7	0.0025
DOXO	33b	*C*-1-tetrahydrofolate synthase, cytoplasmic	*MTHFD1*	P11586	5	6–11	↑	1.77	0.013
MTX	33b	*C*-1-tetrahydrofolate synthase, cytoplasmic	*MTHFD1*	P11586	5	6–11	↑	1.67	0.011
DOXO	37b	*C*-1-tetrahydrofolate synthase, cytoplasmic	*MTHFD1*	P11586	5	6–11	↑	1.69	0.0074
MTX	37b	*C*-1-tetrahydrofolate synthase, cytoplasmic	*MTHFD1*	P11586	5	6–11	↑	1.62	0.0122
DOXO	45	Peptidyl-prolyl cis-*trans* isomerase FKBP4	*FKBP4*	Q02790	4	4–7	↑	1.38	0.0066
MTX	45	Peptidyl-prolyl cis-*trans* isomerase FKBP4	*FKBP4*	Q02790	4	4–7	↑	1.53	0.0052

Table 3. *Cont.*

3F	**DOXO + MTX**								
Drug	**Spot No.**	**Protein name**	**Gene Name**	**UniProt No.**	**Biological process**	**pH**	**Change**	**Fold change**	***p*-value**
DOXO	46b	GMP synthase [glutamine-hydrolyzing]	*GMPS*	P49915	5	6–11	↑	1.6	0.014
MTX	46b	GMP synthase [glutamine-hydrolyzing]	*GMPS*	P49915	5	6–11	↑	1.65	0.0038
DOXO	70	Actin, cytoplasmic 1	*ACTB*	P60709	1	4–7	↓	1.38	0.0017
MTX	70	Actin, cytoplasmic 1	*ACTB*	P60709	1	4–7	↓	1.47	0.0009
DOXO	85b	DAZ-associated protein 1	*DAZAP1*	Q96EP5	6	6–11	↓	1.71	0.0011
MTX	85b	DAZ-associated protein 1	*DAZAP1*	Q96EP5	6	6–11	↓	2.22	0.0059
DOXO	140b	Far upstream element-binding protein 2	*KHSRP*	Q92945	5	6–11	↑	1.68	0.035
MTX	140b	Far upstream element-binding protein 2	*KHSRP*	Q92945	5	6–11	↑	1.61	0.0131
DOXO	153	D-3-phosphoglycerate dehydrogenase	*PHGDH*	O43175	5	4–7	↑	1.68	0.0068
MTX	153	D-3-phosphoglycerate dehydrogenase	*PHGDH*	O43175	5	4–7	↑	1.9	0.0097
DOXO	242	Splicing factor, arginine/serine-rich 3	*SFRS3*	P84103	5	4–7	↓	1.31	0.0064
MTX	242	Splicing factor, arginine/serine-rich 3	*SFRS3*	P84103	5	4–7	↓	1.58	0.0034
DOXO	526	Rab GDP dissociation inhibitor beta	*GDI2*	P50395	1	4–7	↓	2.08	0.0009
MTX	526	Rab GDP dissociation inhibitor beta	*GDI2*	P50395	1	4–7	↓	1.51	0.0052
DOXO	541	Heat shock protein 105 kDa	*HSPH1*	Q92598	4	4–7	↑	1.47	0.0028
MTX	541	Heat shock protein 105 kDa	*HSPH1*	Q92598	4	4–7	↑	1.75	0.0015
3G	**DNR + DOXO + MTX**								
Drug	**Spot No.**	**Protein name**	**Gene Name**	**UniProt No.**	**Biological process**	**pH**	**Change**	**Fold change**	***p*-value**
DOXO	437	L-lactate dehydrogenase B chain	*LDHB*	P07195	3	4–7	↓	1.83	0.0064
MTX	437	L-lactate dehydrogenase B chain	*LDHB*	P07195	3	4–7	↓	1.86	0.0048
DNR	437	L-lactate dehydrogenase B chain	*LDHB*	P07195	3	4–7	↓	2.50	0.0032

Identified proteins typical for individual treatment with 3A: daunorubicin (DNR); 3B: doxorubicin (DOXO); 3C: mitoxantrone (MTX). Proteins with overlap between DNR and DOXO are listed in 3D; between DNR and MTX in 3E; between DOXO and MTX in 3F. Proteins with overlap between all three drugs are in 3G. Proteins from basic pH 6–11 are annotated as "b" beside spot number. The Gene Ontology biological process classification using PANTHER software is indicated by numbers 1 for cellular process, 2 for developmental process, 3 for generation of precursor metabolites and energy, 4 for immune system process/response to stimulus, 5 for metabolic process, 6 for reproduction, 7 for transport and 8 for un-annotated proteins.

Figure 3. Graphical representation of identified differentially abundant proteins after doxorubicin (DOXO), daunorubicin (DNR) and mitoxantrone (MTX) treatment of CEM T-lymphoblastic leukemia cells.

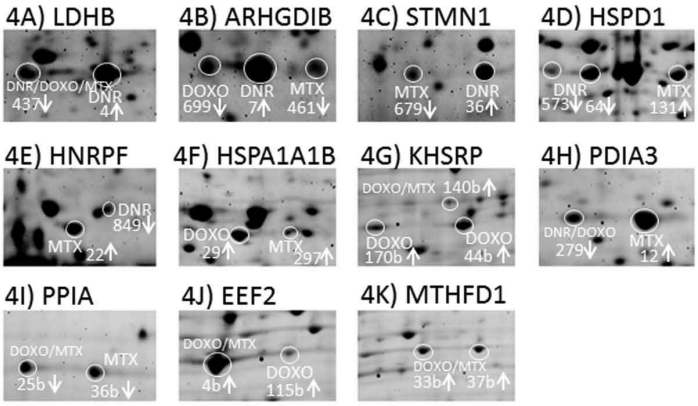


2.3.1. DNR Induced Protein Changes

Based on the evaluation criteria applied in this study we have identified 24 proteins at different levels after DNR treatment in CEM cells (Table 3A, Figure 3). Among them, five proteins (L-lactate dehydrogenase B chain, LDHB, spot no. 4; Rho GDP-dissociation inhibitor 2, ARHGDIB, spot No. 7; stathmin, STMN1, spot No. 36; 60 kDa heat shock protein, HSPD1, spots No. 64 and 573; heterogeneous nuclear ribonucleoprotein F, HNRNPF, spot No. 849) represented protein variants specifically affected by DNR whilst another protein forms of these individual proteins observed as distinct protein spots on 2DE were also regulated by DOXO or MTX (Figure 4A–E). Only for HSPD1 there were two protein forms separated by 2DE significantly changed after DNR treatment (Figure 4D). The annotations of the identified proteins in terms of their integration into biological processes according to Gene Ontology implemented in PANTHER software tool were used to classify DNR associated changes in treated cells. The proteins involved in metabolic processes represented 42% of total changes followed by 17% of proteins participating in cellular processes as well as 17% of proteins regulating generation of precursor metabolites and energy (Figure 5A). Interestingly, majority of proteins of metabolic processes were seen to decrease after DNR treatment which is opposite to what we observed for DOXO and MTX (Figure 3). The most expressed DNR induced changes in metabolic processes include decreased levels of glucose-6 phosphate 1-dehydrogenase (G6PD, spot no. 107 b), dihydrolipoyllysine-residue acetyltransferase component of pyruvate dehydrogenase complex (DLAT, spot No. 166), the important part of glycolysis, and glutathione synthetase (GSS, spot No. 768). Additionally, decrease of two heterogeneous nuclear ribonucleoproteins (HNRNPH1, spot No. 220 and a variant of HNRNPF, spot No. 849) involved in mRNA processing was observed. There were only two proteins belonging to the group of metabolic processes with increased levels after DNR treatment, protein phosphatase metylesterase 1 (PPME1, spot No. 407) and TAR DNA-binding protein 43

(TARDBP, spot No. 574). Cellular processes involved in DNR effect were represented by one decreased level of protein, plastin-2 (LCP1, spot No. 221), and three increased levels of proteins including cofilin-1 (CFL1, spot No. 126), STMN1 and ARHGDIB. Common targets of these proteins are actin cytoskeleton and microtubule filaments and their organization. The proteins of group of generation of precursor metabolites and energy appeared to be typical for DNR (Figure 5A) with their only negligible proportion observed after MTX and DOXO treatments (Figure 5B,C). This group consisted of three decreased mitochondrial proteins such as ATP synthase subunit beta (ATP5B, spot No. 424), mitochondrial-processing peptidase subunit alpha (PMPCA, spot No. 360) and cytochrome b-c1 complex subunit 1 (UQCRC1, spot No. 97) as well as increased isoform of LDHB (spot No. 4).

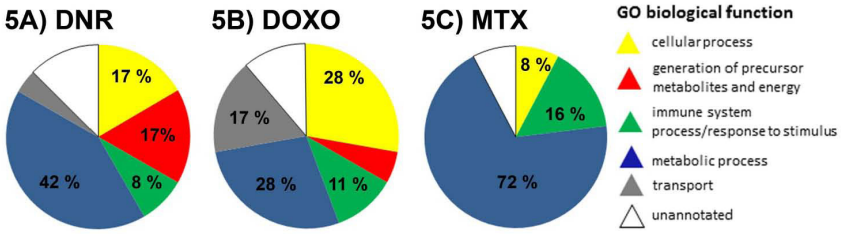
Figure 4. Distinct protein variants of several individual proteins after treatment of CEM T-lymphoblastic leukemia cells with doxorubicin (DOXO), daunorubicin (DNR) and mitoxantrone (MTX).



Protein variants were represented by different protein spots of the same protein and are marked with 2DE spot numbers. Arrows indicated trend of protein level changes after drug treatment. 4(A): L-lactate dehydrogenase B chain, LDHB, spot no. 4 was increased by DNR treatment and spot no. 437 was decreased by all three DNR, DOXO and MTX treatments; 4(B): Rho GDP-dissociation inhibitor 2, ARHGDIB, spot No. 7 was increased by DNR, spot No. 699 was decreased by DOXO and spot No. 461 was decreased by MTX; 4(C): stathmin, STMN1, spot No. 36 was increased by DNR and spot No. 679 was decreased by MTX; 4(D): 60 kDa heat shock protein, HSPD1, spots No. 64 and 573 were decreased by DNR and spot No. 131 was increased by MTX; 4(E): heterogeneous nuclear ribonucleoprotein F, HNRNPF, spot No. 849 was decreased by DNR and spot No. 22 was increased by MTX; 4(F): heat shock 70 kDa protein 1A/1B, HSPA1A1B, spot No. 29 was increased by DOXO and spot No. 297 was increased by MTX; 4(G): Far upstream element-binding protein 2, KHSRP spots No. 44b and 170b were increased by DOXO and spot No. 140b was increased by both DOXO and MTX treatment; 4(H): protein disulfide isomerase A3, PDIA3, spot No. 12 was increased by MTX and spot No. 279 was decreased by DNR and DOXO treatment; 4(I): peptidyl-prolyl cis-*trans* isomerase A, PPIA, spot No. 36b was decreased by MTX and spot No. 25b was decreased by both DOXO and MTX; 4(J): elongation factor 2, EEF2, spot No. 4b was increased by MTX and DOXO and spot No. 115b was

increased solely by DOXO treatment; 4(K): *C*-1-tetrafydrofolate synthase, MTHFD1, spots No. 33b and 37b were increased by DOXO and MTX treatments.

Figure 5. Distribution of anthracycline/anthracenedione regulated proteins by biological processes.



Pie charts of Gene Ontology classification of biological processes based on the contribution of proteins differentially abundant after treatment of CEM cells by: 5(A) daunorubicin (DNR); 5(B) doxorubicin (DOXO); 5(C) mitoxantrone (MTX).

2.3.2. DOXO Induced Protein Changes

In total, we found 18 proteins significantly changed after treatment of CEM cells by DOXO (Table 3B, Figure 3). Four of these proteins (Heat shock 70 kDa protein 1A/1B, HSPA1A1B, spot No. 29; Far upstream element-binding protein 2, KHSRP spots No. 44b and 170b; ARHGDIB, spot No.699 and elongation factor 2, EEF2 spot No. 115 b) were identified from the protein spots specifically influenced by DOXO although another variants of these proteins were also identified from distinct protein spots which were regulated by DNR or MTX treatment (Figure 4B,F,G,J). KHSRP was found in two evidently separated 2DE spots thus representing multiple forms of this protein (Figure 4G). As regards Gene Ontology classification of identified proteins and their incorporation into biological processes, the proteins involved in metabolic processes represented 28% of total changes and the same percentage was observed for cellular processes, followed by 17% of transport proteins and 11% of proteins from the group of immune system process and response to stimuli (Figure 5B). Metabolic processes were represented by decrease in KH domain-containing, RNA binding, signal transduction-associated protein 1 (KHDRBS1, spot No. 61b) which is an important adapter protein in signal transduction as well as regulator of RNA stability. Furthermore, we found three proteins with increased levels after DOXO treatment including KHSRP, spermidine synthase (SRM, spot No. 278), and EEF2. Among the proteins of cellular processes, there was significant decrease in ARHGDIB and increased expression of three proteins, namely ezrin (EZR, spot No. 592, ubiquitin-like modifier-activating enzyme 1 (UBA1, spot No. 282), and DNA replication licensing factor MCM7 (MCM7, spot No. 91). Transport proteins were observed as selective group of proteins responding to DOXO treatment. They were represented by lowered GTP-binding protein SAR1b (SAR1B, spot No. 908), and higher levels of EH domain-containing protein 1 (EHD1, spot No. 63b) and caprin 1 (CAPRIN1, spot No.141), stress granule associated protein.

2.3.3. MTX Induced Protein Changes

We have identified 25 proteins differentially abundant in CEM T-lymphoblastic leukemia cells followed by MTX treatment (Table 3, Figure 3). Among them there were seven proteins (protein disulfide isomerase A3, PDIA3, spot No. 12; HNRNPF, spot No. 22; peptidyl-prolyl cis-*trans* isomerase A, PPIA, spot No. 36b; HSPD1, spot No. 131; HSPA1A1B, spot No. 297; ARHGDIB, spot No. 461; *STMN1*, spot No. 679) presented as MTX specific protein variants despite distinct forms recognized after DNR or DOXO treatment (Figure 4B–F,H,I). For MTX treatment the proportion of the proteins involved in metabolic processes was the highest observed among DNR, DOXO and MTX drugs and covered 72% of total changes followed by 16% of proteins of immune system process and response to stimuli. Only 8% of proteins involved in cellular processes represented the lowest contribution of this category among DNR, DOXO and MTX drugs (Figure 5C). Amongst the proteins of metabolic processes only a few decreased proteins were observed including transformer-2 protein homolog beta (TRA2B, spot No. 615) and heterogeneous nuclear ribonucleoprotein A2/B1 (HNRNPA2B1, spot No. 109b) driving mRNA splicing and mRNA processing, as well as eukaryotic translation initiation factor 2 subunit 3 (EIF2S3L, spot No. 128b) (Figure 3). The changes of the majority of increased proteins from the metabolic group were mostly moderate with a fold change around 1.4. The most pronounced change observed was the increase in proteosome subunit alpha type (PSMA5, spot No. 230) with a fold change of 2.51, and RuvB-like 1 protein (RUVBL1, spot No. 116) as well as G-rich sequence factor (GRSF1, spot No. 455) (Table 3). Beside metabolic proteins, emerging MTX selective group of proteins of immune system process and response to stimuli was evident (Figure 5C). Majority of these proteins were increased including activator of 90 kDa heat shock protein ATPase homolog 1 (AHSA1, spot no. 83), stress-70 protein (HSPA9, spot No. 24), and HSPA1A1B. Small proportions of proteins of cellular processes were characterized by evident decrease of STMN1 and also lower level of ARHGDIB (Figure 3).

2.4. The Protein Changes Linking the Effects of Anthracycline/Anthracenedione Drugs DNR, DOXO, and MTX

In order to evaluate similarities among studied anthracycline/anthracenedione anti-cancer drugs, we looked for the overlap of the proteins changed after treatments. The highest number of such shared proteins was revealed for DOXO and MTX (Table 3, Figure 3). Three proteins, including EEF2 (spot No. 4b), PPIA (spot No. 25b) and KHSRP (spot No. 140b) were also present in another distinct spots affected exclusively either by DOXO or MTX treatment (Figure 4G,I,J. The enzyme *C*-1-tetrahydrofolate synthase (MTHFD1, spots No. 33b and 37b) was present in two spots for both DOXO as well as MTX treatments (Figure 4K). Among these twelve proteins common for DOXO and MTX (Figure 4), the fold changes of increased proteins from the category of metabolic processes ranged between 1.47 and 1.9 including EEF2, MTHFD1, GMP synthase (GMPS, spot No. 46b), D-3-phosphoglycerate dehydrogenase (PHGDH, spot No.153) and KHSRP. Only one protein from this category, splicing factor, arginine/serine-rich3 (SFRS3, spot No. 242) was decreased (Table 3). The group of proteins of immune system process and response to stimuli consisted of two functionally different proteins with isomerase activity PPIA and peptidyl-prolyl cis-*trans* isomerase FKBP4 (FKBP4, spot No. 45) with

opposite direction of protein change. Additionally, increased heat shock protein 105 kDa (HSPH1, spot No. 541) was seen to be a part of this group too (Figure 3). Small proportion of cellular processes was directed to regulation of cytoskeleton organization mediated by decreased actin (ACTB, spot No. 70) and small GTP signaling protein Rab GDP dissociation inhibitor beta (GDI2, spot No. 526). Interestingly, a decrease in one protein was observed in this study which was DAZ- associated protein 1 (DAZAP1, spot No. 85b) which belongs to the category of reproduction (Figure 3).

Compared to the overlapping of twelve different proteins for DOXO and MTX treatments, the numbers of common protein overlaps for DNR/MTX and DNR/DOXO were three and two, respectively, with only one protein common for the effect of all three drugs (Table 3 and Figure 3). The proteins common for DNR and MTX included paraspeckle component 1 (PSPC1, spot No. 642), which decreased with evidently high values of fold change for both drugs. On the contrary, two other proteins, heat shock protein 75 kDa (TRAP1, spot No. 320) and NADH-ubiquinone oxidoreductase 75 kDa subunit (NDUFS1, spot No. 413) exhibited opposite trend in protein level showing a decrease after DNR treatment and an increase induced by MTX (Table 3, Figure 3). Different abundance of two proteins of metabolic processes shared between DNR and DOXO regarded heterogeneous nuclear ribonucleoprotein H3 (HNRNPH3, spot. No. 15b) and protein disulfide-isomerase A3 (PDIA3, spot No. 279) (Table 3, Figure 3). The enzyme from the group of generation of metabolic precursors and energy, LDHB (spot No. 437) was significantly decreased after treatment with anthracyclines DNR and DOXO as well as anthracenedione MTX. Interestingly as mentioned above, this enzyme was also identified from protein spot No. 4 increased in response to DNR (Table 3, Figure 3, Figure 4A).

2.5. The Proteins Commonly Affected by Five Anti-Cancer Drugs: Anthracycline/Anthracenedione DNR, DOXO, MTX and Distinct Chemotherapeutics CisPt and TAX

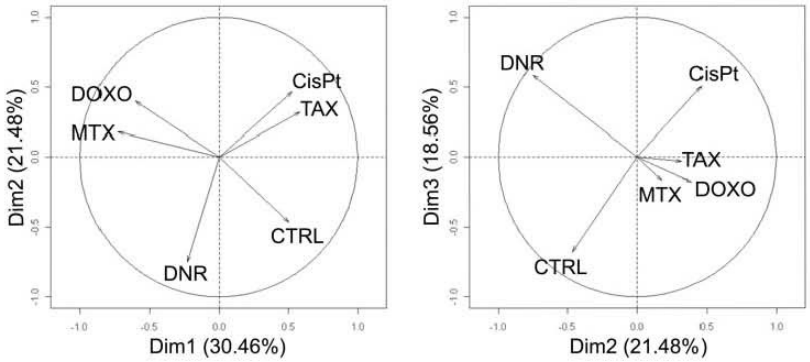
Comparison of all five anti-cancer treatments is depicted in Figure S1. The response to cisplatin (CisPt) is presented by 19 unique proteins (Table S2) whilst effect of paclitaxel (TAX) is characterized by 13 proteins (Table S2). Nevertheless, the main purpose of this part of our study was selection of proteins overlapping between CisPt, TAX and anthracycline/anthracenedione drugs (Table S2) to underline common protein features of anti-cancer response. Four proteins (EHD1, spot no. 63b; Medium-chain specific acyl-CoA dehydrogenase, mitochondrial, ACADM, spot No. 163b; KHSRP, spot No. 170b; EZR, spot. No. 592) overlapped for CisPt and DOXO treatments and two proteins (4-trimethylaminobutyraldehyde dehydrogenase, ALDH9A1, spot No. 364; ARHGDIB, spot. No. 699) were shared between TAX and DOXO treatments. Another eight proteins (PPIA, spot No. 25b; CFL1, spot No. 126;, HNRNPA2B1, spot No. 109b; NDUFS1, spot No. 413; PHGDH, spot No. 153, G6PD, spot No. 107b; PPME1, spot No. 407; and TRA2B, spot No. 615) were common for one of the anthracycline/anthracenedione drugs and CisPt or TAX.

2.6. Principal Component Analysis of Quantitative Data

Besides pair comparison of protein alterations induced by each treatment, unsupervised multivariate classification (PCA) was performed to provide an overview of the variance in the whole data set including all studied drugs. PCA reduces the huge amount of data into several components named principal components (PCs) on the basis of similarities in the data set. When visualized in two

dimensional graphs, the objects/samples with similar behavior tend to "sit together" whilst distance in the position indicates dissimilarity. The first PC accounted for approximately 30% of the total variance in the data, whilst the second PC accounted for approximately 21% of total variance and finally the third PC for nearly 19% of variance (Figure 6). In the first dimension, DNR, DOXO and MTX were separated from CTRL, CisPt and TAX. In the second dimension, DNR separated mainly from DOXO and MTX. Finally, in the third dimension, DNR was more sequestered from CTRL untreated cells.

Figure 6. Multivariate principal component analysis of quantitative 2DE data to classify anti-cancer treatments.

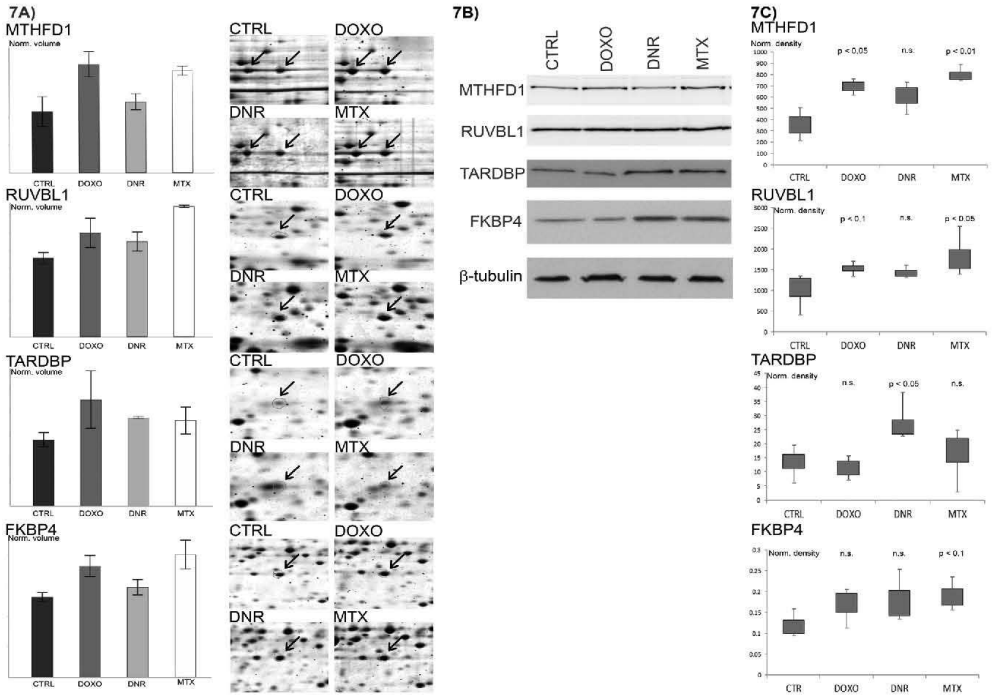


Principal component analysis was performed to obtain an overview of the variance in the data set and classify treatments according to their similarities or dissimilarities. Quantitative 2DE data of control untreated cells (CTRL), anthracyclines daunoribicin (DNR) and doxorubicine (DOXO), anthracenedione mitoxantrone (MTX), and distinct chemotherapeutics cisplatin (CisPt) and paclitaxel (TAX) were used for evaluation. In the first dimension, untreated controls, CisPt and TAX were separated from DOXO, DNR and MTX treatments, the second and third dimensions evidently distinguished DNR from DOXO and MTX as well as CisPt and TAX.

2.7. Verification of Selected Protein Changes Using Immunoblot

Several of the differentially abundant proteins were selected for verification of 2DE observations using Western blot analysis (Figure 7). Among them, significant increase of MTHFD1 after both DOXO and MTX treatments was confirmed. Further, FKBP4, another increased protein on 2DE after both DOXO and MTX treatment, was also tracked using specific antibody and significant increase reflecting a probability of 90% was confirmed for MTX whilst DOXO showed a slight increase. Using 2-DE, RUVBL1, one of the proteins typical for MTX response, was significantly increased not only after MTX treatment but a non-significant increase observed after DOXO was shown as a significant change by immunoblot. Amongst the proteins typical for DNR response the transcription factor TARDBP was verified as significantly increased after DNR treatment.

Figure 7. Western blot analysis of selected proteins.



Immunoblot analysis of *C*-1-tetrahydrofolate synthase (MTHFD1), RuvB-like 1 protein (RUVBL1), TAR DNA-binding protein 43 (TARDBP) and peptidyl-prolyl cis-*trans* isomerase FKBP4 (FKBP4) in untreated CEM cells and CEM cells treated with anthracycline drugs doxorubicin (DOXO), daunorubicin (DNR) and mitoxantrone (MTX) was performed. (7A) Bar plots of normalized volume intensities of selected differentially abundant protein spots calculated and graphically represented from 2D gels by Redfin software and corresponding protein features on 2D gels of control cells and drug treatments. Significantly regulated protein spots between control cells and individual treatments are in graphs indicated by an asterisk. The arrows indicate the location of each protein feature. (7B) The whole cell lysates were examined on immunoblot using specific antibodies directed against selected proteins. β-tubulin was used as a loading control. (7C) The protein bands from immunoblot were quantified using Quantity one software for at least three replicates analyzed per protein and the density of individual band was normalized for total density in given protein line. The results were illustrated as boxplots. Significance of differences between controls and each treatment was calculated using Student's *t*-test for $p < 0.05$ and $p < 0.01$ (n.s., not significant).

3. Discussion

To gain insight into molecular mechanisms and biological processes underlying the treatments with representative anti-cancer anthracycline/anthracenedione drugs DNR, DOXO and MTX, we have used CEM T-lymphoblastic leukemia cells and investigated protein fingerprints of the drug effects

employing combination of zoomed 2DE with fluorescent protein stain and MALDI-TOF/TOF mass spectrometry. The CEM T-lymphoblastic leukemia cells have been considered as suitable model of hematological malignancies as well as tumor cells sensitive to various anti-cancer drugs [18]. Several previous studies focused on the effects of DOXO or DNR with mostly applied 24 h or 48 h treatments and low micromolar concentrations of drugs, which may correspond to relevant clinical doses [11–15]. In our study, we designed proteomic experiments focused on earlier time intervals in order to reliably monitor protein alterations that precede induction of apoptosis and minimize its impact on observed protein changes. Using individual half time to onset of apoptosis (TA_{50}), corresponding 10 times IC_{50} doses of the drugs instead of the same time interval for all treatments allowed us to optimize comparable stage of all used anti-cancer treatments. Whilst for four out of five drugs TA_{50} ranged from 120 min to 150 min, the longest 250 min interval was confirmed for DOXO and even this was still at least 6 times shorter than what was used in previously published studies [11–15].

To date, the effect of DOXO treatment on different cancer cell lines has mainly been studied by proteomic techniques [11,13,14]. To extend current observations and with the view to help translation of molecular findings toward improvements in clinical use, we focused on the effects of several clinically relevant representatives of the group of anthracycline/anthracenedione drugs. Hence, comprehensive proteome map of model T-lymphoblastic leukemia cells and its alterations after DNR, DOXO and MTX drug treatments were monitored and evaluated either by pair comparison to relevant untreated control or multivariate classification of drug treated and untreated samples.

In order to emphasise proteins specific for response toward anthracycline/anthracenedione drugs among all identified differentially abundant proteins, we performed in the same design, analysis of the effects of two additional anti-cancer drugs, CisPt and TAX, taken from distinct groups of chemotherapeutics, and compared protein alterations to those found after DNR, DOXO and MTX. As expected, using this step we marked the proteins affected and shared in anti-cancer response of such drug treatments. These proteins belong to the enzymes critical for cellular metabolism such as G6PD, the enzyme producing pentose sugars essential for nucleic acid synthesis; PHGDH, the enzyme involved in syntheses of purines and amino acids; NDUFS1, core subunit of the mitochondrial membrane respiratory chain NADH dehydrogenase (Complex I). More interestingly and corroborating our findings are the observations that many of these "promiscuous" general anti-cancer response proteins are the ones already known to play a vital role in various human cancers. For example PPME1 that demethylates protein phosphatase 2A was recently described as tumor suppressor [19]. TRA2B or HNRNPA2B1 regulating repair of double strand breaks have elevated levels in various cancers [20] and changed in levels by anti-cancer treatments as shown here. HNRNPA2B1 has been even assigned as proto-oncogene [21]. Further evidence is presented by KHSRP regulating transcription and mRNA processing which was shown to support migration in liver cancer cells [22]. Additionally, involvement of multifunctional protein PPIA in cancer progression has been described [23]. Interestingly, several cytoskeleton regulating proteins including CFL1 [24] and EZR [25] were associated with invasion and metastasis and ARHGDIB was linked to the development of chemoresistance [26]. These proteins, although non-specific as regards used drugs and functioning in various biological processes, most probably present important targets underlying anti-cancer mechanisms and possibly play role of anchor molecules which may connect different pathways in a very complex regulation of cancer cell processes. Despite their importance, the major aim of this study has been to identify specific proteins

typical for the response to anthracycline/anthracenedione drugs DNR, DOXO and MTX and to characterize similarities in the effects of these structurally very close drugs.

In total, we found several tens of proteins with significantly changed levels at early time intervals after DNR, DOXO and MTX treatments which corresponded only to 1%–2% of the total number of spots detected. According to Gene Ontology classification of biological processes the highest representation of identified proteins for all three drugs belongs to metabolic processes of nucleic acids or proteins and cellular processes involved mainly in cytoskeleton organisation. It corresponds to well-known observations that metabolic alterations on glucose consumption and biosynthetic activity of nucleotides, amino acids and lipids are the changes for sustaining cell proliferation in cancer cells. Typical evidence of this fact is the Warburg effect, the conditions when the cancer cells switch from oxidative phosphorylation to glycolysis to produce ATP and set of enzymes such as lactate dehydrogenase and pyruvate dehydrogenase play crucial role [27]. Evidently and surprisingly, we observed in our study such changes in CEM T-lymphoblastic leukemia cells at very early time intervals after anti-cancer DNR treatment. The most probable explanation of this behaviour is adaptive effort of tumor cells to make even stronger the essential mechanisms supporting cancer growth. Regulation of metabolic enzymes offers new directions for anti-cancer treatments and lactate dehydrogenase which catalyses the final step in the glycolytic cascade constitutes a relatively new anti-cancer target [28]. Nevertheless, design of the combination of the enzymes or even their isoforms and development of specific inhibitors that would eliminate robustness of cancer cells is not a simple task.

In addition to changes in energy metabolism, DNR treatment of CEM cells leads to the decrease of two heterogeneous nuclear ribonucleoproteins which are involved in RNA processing but we also observed increase of TARDBP which is homologous to the heterogeneous nuclear ribonucleoproteins. The higher level of this protein was further confirmed using Western blot. The TARDBP has been identified as a cause of neuropathology in a wide spectrum of neurodegenerative diseases, including amyotrophic lateral sclerosis. Using Drosophila model for proteinopathy associated with TARDBP, it was shown that increasing human wild-type TARDBP expression is sufficient to cause neurotoxicity *in vivo* [29]. The protein may also be involved in microRNA biogenesis, apoptosis and cell division [30]. The finding of increased level of TARDBP in CEM leukemic cells after anti-cancer DNR treatment let us hypothesise that it might significantly contribute to the toxicity toward the tumor cell and positively influence outcome of anti-cancer response. Higher levels of this protein may also result from its decreased clearance, which was shown as mediated by lower activity of ubiqutin-proteasome system and autophagosome in synergy [31]. Hence, the link between the level of TARDBP and activity of ubiqutin-proteasome system and autophagosome is another good example underlying importance of these cellular mechanisms in regulation of carcinogenesis or response of cancer cell to anti-cancer treatment.

Doxorubicin, the other member of anthracyclines, also affected metabolic and cellular biological processes in CEM leukemic cells and majority of targeted proteins were exclusively specific for this drug and increased in cells after drug treatment. Among them, the role of spermidine synthase is aimed to redox regulation of tumor cell followed by anti-cancer treatment. Overproduction of spermidine increases resistance to oxidative stress with spermidine serving as a free-radical scavenger *in vitro* as well as *in vivo* [32]. Hence, increase of spermidine synthase in DOXO treated cancer cell may present regulatory response which may increase resistance of cancer cell.

EEF2 translates growth and stress impulses to the regulation of protein synthesis by catalyzing ribosomal translocation step during translation elongation. However, phosphorylation of EEF2 by EEF2 kinase inactivates this factor which indicates that EEF2 kinase could be promising anti-cancer target. Interestingly, using pharmacological inhibition of EEF2 kinase demonstrated that anti-cancer activity of widely accepted inhibitor and anti-proliferation agent against different cancer cells was more correlated with induction of EEF2 phosphorylation than inhibition of EEF2 kinase activity. In addition, stronger induction of EEF2 phosphorylation mediated by AMPK activators and mTOR inhibitor was linked to more effective cancer cell growth inhibition. Accordingly, EEF2 phosphorylation appears to be mediated through multiple pathways thus alarming the need of combinatory inhibition of EEF2 kinase in anti-cancer therapy [33]. In our study, we identified EEF2 in two protein spots from 2DE (Figure 4J). The more basic and less abundant spot was increased after DOXO treatment and may represent non-phosphorylated form, whilst the more acidic and more abundant protein spot may be representative of phosphorylated form increased by DOXO and MTX. The presence of more abundant/phosphorylated form might contribute to anti-cancer effect of DOXO and MTX, whilst the less abundant basic/non-phosphorylated form would have a role in regulation of protein synthesis and sustaining cancer cell growth.

One of a few examples of proteins decreased in level after DOXO treatment was found to be metabolic protein KHDRBS1. In case of human breast tumors it was shown that phosphorylation of this protein regulated its intracellular localization and anti-proliferative properties were blocked by phosphorylation [34]. Therefore, in addition to quantitative changes observed in this study, it would be necessary to investigate its post-translationally modified forms and localization as regards contribution to anti-cancer effect of DOXO.

Among the proteins of cellular processes affected by DOXO, we observed increase of UBA1 controlling ubiquitin conjugation pathway, and MCM7 having a role in DNA strand elongation involved in DNA replication. MCM7 is a known component of minichromosome maintenance complex which is the putative replicative helicase in eukaryotic cells and demonstrated to be efficient and sensitive marker to assess disease progression in the uterine cervix [35], prognosis of patients with non-small cell lung cancer [36], or Hodgkin lymphoma [37]. Comprehensive comparative analysis of pre-replication complex proteins in transformed and normal cells indicated that cellular transformation was associated with an overexpression and increased chromatin association of the pre-replication complex proteins including MCM7 [38]. From this point of view, increased level of MCM7 at early time interval after anti-cancer DOXO treatment may reflect other adaptive mechanisms of cancer cell contributing to the transformation of cell.

Transport proteins appeared to be an important group of proteins responding to DOXO treatment. They included SAR1B involved in protein transport from endoplasmic reticulum to Golgi, and cytoplasmic activation/proliferation-associated protein-1, CAPRIN1, stress granule associated protein. These findings may suggest possible role of induction of endoplasmic reticulum stress associated with proteotoxic stress. Subsequently, such stress stimulates either apoptosis of cancer cell which is involved in anti-cancer effects or autophagy as a cytoprotective, stress-induced adaptive pathway following disruption of protein homeostasis [39]. CAPRIN1 may also regulate the transport and translation of mRNAs of proteins with impact on cell proliferation and negative regulation of translation. The protein is putative target of miR-16 thus linking miRNA to the regulation of cell

proliferation [40]. Overexpression of CAPRIN1 induced phosphorylation of eukaryotic translation initiation factor 2 alpha resulted in global inhibition of protein synthesis [41]. This may be synergistic with above mentioned role of phosphorylated EEF2 in suppression of protein synthesis as a part of anti-cancer effect of DOXO.

The majority of MTX induced protein alterations were moderate metabolic changes. Interesting, EIF2S3L which functions in the early steps of protein synthesis, PSMA5 and RUVBL1 with the roles in transcriptional regulation, DNA replication and probably DNA repair, were observed. Evidently, decrease of protein level mediated by decrease of EIF2S3L may play an important role in MTX anti-cancer effect. Furthermore, protein homeostasis which is controlled by ubiquitin–proteasome system as mentioned above seemed to be critical mechanisms for cancer cell. Pharmacologic inhibitors of the proteasome promote tumor cytotoxicity and clinical studies have showed improvement in patient survival. Despite success of the proteasome inhibitor bortezomib in the treatment of the hematologic malignancy such as multiple myeloma, treatment of the more complex solid tumors has been less successful [42]. Our results document that MTX similarly to DOXO exploit proteins of ubiquitin-proteasome system to trigger or modulate cancer cell stress response to anti-cancer treatment in order to induce either apoptosis or autophagy.

RUVBL1 is a highly conserved AAA(+) ATPase whose expression as well as expression of its homolog RUVBL2 was high in different cancers. In case of human hepatocellular carcinoma silencing of RUVBL2 reduced cell growth and increased apoptosis whilst overexpression enhances tumorigenicity [43]. The level of RUVBL1 was significantly increased in CEM cells treated with MTX, and Western blot analysis confirmed a significantly increased level not only after MTX but also DOXO drug treatment. The question remains whether RUVBL1 at an increased level is involved in promotion of tumorigenicity in CEM T-lymphoblastic cells similarly as described in the study on human hepatocellular carcinoma.

It was possible to see that very selective group of MTX treatment are the proteins of immune system process and response to stimuli, namely chaperones thus indicating significant contribution of protein folding and stress response in tumorigenesis and anti-cancer treatment [44]. Furthermore, these chaperone proteins may be involved in presentation of tumor antigens for direct recognition of tumor by T cells [45,46] or as autoantigens which can give raise to the production of autoantibodies [47]. As regards anthracyclines, Fucikova *et al.* [48] investigated the effectiveness of anthracyclines to induce immunogenic cell death in human tumor cell lines and primary tumor cells. The data demonstrated induction of immunogenic cell death in sensitive human tumor cells including human prostate cancer, ovarian cancer, and acute lymphoblastic leukemia cells treated by anthracyclines as anti-cancer drugs. Our findings of increased chaperone proteins after MTX treatment corroborate such published data and support the role of chaperons in tumor immunity.

This study has shown that each of the studied anti-cancer anthracycline/anthracenedione drugs possess typical proteins or protein variants which are specifically changed in level by individual drugs despite of their very close structural similarity which is currently used for their grouping within chemotherapeutic drugs. However, the design of our study allowed us to evaluate and classify proteome maps of all tested anti-cancer drugs to characterize the similarities that would link drug responses. Importantly, the observation of significant decrease of LDHB after treatment of anthracyclines DNR and DOXO as well as anthracenedione MTX thus underlies common anti-cancer

effect of this group of drugs directed to the energy metabolism of cancer cell. Nevertheless, it has been important to be aware of the fact, as shown in several examples mentioned above, that the given drug may affect preferentially certain isoform/species of an individual protein hence, in many cases the specific role of such protein isoform/species may play decisive role compared to the quantitative change at the total level of a given protein.

Furthermore, we found several proteins common in DOXO and MTX, among them mainly those directed to the regulation protein synthesis as well as purine and amino acid biosynthesis including MTHFD1 whose increase after treatment by DOXO and MTX was confirmed by Western blot. Regulation of SFRS3 appeared to be a new emerging role because it was recently described as a proto-oncogene critical for cell proliferation and tumor induction and maintenance. It was highly expressed in various cancers and its reduction, mediated by RNAi, resulted in G2/M arrest, growth retardation, and apoptosis [49]. Accordingly, decreased level of SFRS3after DOXO and MTX treatments offers a new mechanism contributing to anti-cancer activities common to anthracycline/anthracenedione drugs.

Compared to a group of proteins linking the effect of DOXO and MTX, there were only a few proteins shared between DNR and DOXO or MTX thus indicating the distinct position of DNR among the anthracycline/antracenedione drugs. This finding was further corroborated by principal component analysis showing DNR sequestered from DOXO and MTX as well as other treatments such as CisPt and TAX in the first three components covering in total 71% of variances of the whole experimental set. Interestingly, there were two proteins, PSPC1 and HNRNPH3 which were shared between DNR/MTX and DNR/DOXO treatments, respectively, with surprisingly high fold changes observed. PSPC1 is required for the formation of nuclear paraspeckles, subnuclear bodies that alter gene expression via the nuclear retention of RNAs [50]. It belongs to the family of proteins of the Drosophila behavior/human splicing (DBHS) which are predominately nuclear and influence various biological processes, including carcinogenesis. The significant increase of PSPC1 after DNR and MTX treatments points to possible important role of nuclear paraspeckles in anti-cancer activities of anthracycline/anthracenedione drugs.

4. Materials and Methods

4.1. Cell Cultures and Sample Preparation—Determination of IC_{50} and TA_{50}

Human T-lymphoblastic leukemia CEM cells (American Tissue Culture Collection, Manassas, VA, USA) were cultured at a density of 1×10^6 cells/mL in RPMI-1640 medium supplemented with 2 mM glutamine, 100 U/mL penicillin, 100 μg/mL streptomycin, and 10% of heat inactivated fetal bovine serum with or without addition of anti-cancer drug in a humidified incubator with 5% CO_2 at 37 °C. Drugs were dissolved directly in RPMI-1640 medium.

The cytotoxicity of DNR, DOXO, MTX, cisplatin (CisPt) and paclitaxel (TAX) was determined by the three-day MTT test as described previously and the inhibitory concentration corresponding to 50% of cell growth (IC_{50}) was calculated [51]. Early time interval studies, when the influence of apoptosis is minimal, facilitate reliable observation of protein changes and hence time to apoptosis induction (TA) was measured for five times IC_{50} and 10 times IC_{50} doses of the drugs using caspase 3 and/or 7 activation Magic Red™ caspase detection kit [52]. For these relatively high drug doses used, no significant

differences in TA for individual drugs were found. Hence, for proteomic analysis, the cells were treated with ten times IC_{50} doses of the drugs and harvested at half time to apoptosis induction (TA_{50}) (Table 1). Cells were washed three times in ice-cold PBS and 6×10^6 cells were lysed in 200 µL of lysis buffer containing 7 M urea, 2 M thiourea, 3% *w/v* CHAPS, 2% *v/v* Nonidet-P40, 5 mM TCEP in presence of inhibitors of proteases and phosphatases (Roche, Basel, Switzerland) according to manufacturers' directions. After centrifugation at 4 °C, 20,000× *g*, 10 min, the supernatant was collected and protein concentration was determined by the Pierce 660 nm protein assay. Samples were frozen to −80 °C for future use. At least three biological replicates were analyzed for each drug treatment.

4.2. Two-Dimensional Gel Electrophoresis (2DE)

Aliquots of samples corresponding to 100 µg of proteins and 0.5% IPG buffer 4–7 were loaded on pH 4–7 Immobiline Drystrips using active in gel rehydration (IPG strip 18 cm, pH 4–7) in buffer containing 7 M urea, 2 M thiourea, 4% CHAPS, 200 mM DeStreak, inhibitors of proteases, phosphatases (Roche, Basel, Switzerland), 0.5% IPG buffer 4–7 and a trace of bromophenol blue. Isoelectric focusing separation (IEF) was performed on IEF Cell (Bio-Rad, Hercules, CA, USA) system using the following program: 1 h to 200 V, 10 h 200 V, 30 min to 500 V, 30 min to 1000 V, 1.5 h to 5000 V, and 5000 V until total of 55 kVh was reached. After IEF separation, the gel strips were equilibrated in 50 mM Tris, pH 6.8, 6 M urea, 30% glycerol, 4% SDS, 100 mM DeStreak, and a trace of bromophenol blue for 25 min [53].

Aliquots of samples corresponding to 70 µg of proteins and 0.5% IPG buffer 6–11 were cup-loaded on pH 6–11 Immobiline DryStrips (IPG strip 18 cm, pH 6–11) passively rehydrated in buffer containing 7 M urea, 2 M thiourea, 4% CHAPS, 30 mM DTT, inhibitors of proteases, phosphatases (Roche, Basel, Switzerland), 0.5% IPG buffer 6–11 and a trace of bromophenol blue overnight. IEF was performed on IEF Cell system using the following program: 1 h to 150 V, 12 h 150 V, 1 h to 1000 V, 3 h to 8000 V, and 8000 V for 12 kVh. After IEF separation, the strips were equilibrated in 50 mM Tris, pH 6.8, 6 M urea, 30% glycerol, 8% SDS, and 1% DTT for 15 min, followed by equilibration in 50 mM Tris, pH 6.8, 6 M urea, 30% glycerol, 8% SDS, 4% IAA and a trace of bromophenol blue for 15 min.

After equilibration, both 4–7 and 6–11 IPG strips were rinsed and applied to vertical 12% SDS-PAGE (18 mm × 18 mm × 1 mm gel). SDS-PAGE was carried out at a constant current of 40 mA per gel using in series connected Protean II xi Cells (Bio-Rad, Hercules, CA, USA) allowing simultaneous run of six gels. Gels were then stained with Sypro Ruby according to manufacturers' directions. Stained gels were scanned and digitized at 50 µm resolution at Pharos FX fluorescent scanner (Bio-Rad, Hercules, CA, USA) with excitation length 488 nm and emission length 605 nm.

The images were evaluated using Redfin 3.3.2 Solo software (Ludesi, Malmo, Sweden, 2010). Pair comparison between untreated controls and each single treatment was performed for all 5 drugs. At least three biological replicates were used for each treatment or control samples. Protein spots that were statistically significant according to Student's *t*-tests with $p < 0.01$ and fold-change >1.2 as well as $p < 0.05$ and fold-change >1.5 and accepted by visual inspection were selected for identification by mass spectrometry.

4.3. Protein Identification by Mass Spectrometry

Preparative 2D gels were prepared for spot excision and in gel digestion of selected protein spots according to the protocol above with the following modifications. Protein load was 500 μg of total protein amount per pH 4–7 gels and 150 μg of total protein amount per pH 6–11 gels. Gels were stained with reverse zinc staining [54]. Protein spots were excised from gels, cut into small pieces and destained using chelating agent. After complete destaining, the gel was washed with water, shrunk by dehydration in ACN and re-swollen again in water. The supernatant was removed and the gel was partly dried in a SpeedVac concentrator. The gel pieces were then rehydrated in a cleavage buffer containing 25 mM 4-ethylmorpholine acetate, 5% ACN and trypsin (5 ng/μL), and incubated overnight at 37 °C. The digestion was stopped by addition of 5% TFA in ACN and the aliquot of the resulting peptide mixture was desalted using a GELoader microcolumn (Eppendorf, Hamburg, Germany) packed with a Poros Oligo R3™ material [55]. The purified and concentrated peptides were eluted from the microcolumn in several droplets directly onto MALDI plate using 1 μL of *R*-cyano-4-hydroxycinnamic acid (CCA) matrix solution (5 mg/mL in 50% ACN/ 0.1% TFA).

Mass spectra were measured on an Ultraflex III MALDI-TOF/TOF instrument (Bruker Daltonics, Bremen, Germany) as described before [56]. Briefly, peptide mass fingerprint spectra were acquired in the mass range 700–3500 Da and peak list in XML format created using FlexAnalysis 3.0 searched using MASCOT search engine against Swiss-Prot 2011_09 database subset of human proteins with the following search settings; peptide tolerance of 50 ppm, missed cleavage site value set to one, variable carbamidomethylation of cysteine, oxidation of methionine and protein *N*-terminal acetylation. Proteins with Mascot score over the threshold 56 calculated for the used settings were considered as identified. If the score was lower or only slightly higher than the threshold value, the identity of protein candidate was confirmed by MS/MS analysis.

4.4. Western Blot Analysis

Protein lysates prepared as described above were diluted in 2× SDS buffer (4% SDS, 50% glycerol, 140 mM mercaptoethanol, 125 mM Tris pH 6.8 and a trace of bromophenol blue) and separated by 10%, 12% or 15% SDS-PAGE. Separated proteins were transferred onto Immobilone-P membrane (Millipore, Bedford, MA, USA) using a semidry blotting system (Biometra, Gottingen, Germany). The membranes were blocked in 5% non-fat dry milk or in 5% BSA in Tris-buffered saline with 0.05% Tween 20 (TBST) pH 7.4 for 1 h and incubated overnight with the respective primary antibodies: anti-MTHFD1 (Sigma-Aldrich, St. Louis, MO, USA) (HPA000704, 1:20000 in 5% BSA); anti-RUVBL1 (Sigma-Aldrich, St. Louis, MO, USA) (HPA019947, 1:200,00 in 5% BSA); anti-TARDBP (Sigma-Aldrich, St. Louis, MO, USA) (HPA017284, 1:1000 in 5% milk); anti-FKBP4 (Sigma-Aldrich, St. Louis, MO, USA) (HPA006148, 1:200,00 in 5% BSA) and anti-β-tubulin (Sigma-Aldrich, T4026, 1:5000 in 5% milk). Peroxidase-conjugated secondary anti-mouse or anti-rabbit antibodies (Jackson Immunoresearch, Suffolk, UK) were diluted 1:100,00 in 5% non-fat dry milk in TBST and incubated for 1 h at RT. The ECL+ chemiluminescence (GE Healthcare, Uppsala, Sweden) detection system was used to detect the proteins. The exposed CL-XPosure films (Thermo Scientific, Rockford, IL, USA) were scanned by a calibrated densitometer GS-800 (Bio-Rad, Hercules, CA, USA). QuantityOne 4.6.5. (Bio-Rad, Hercules, CA, USA, 2008) software was used for analysis and quantification of Western blot results.

4.5. Data Analysis Applying Principal Component Analysis (PCA)

Statistical analyses were performed using freeware R 2.14.1. (www.r-project.org) (R Foundation, Vienna, Austria, 2011). PCA was used to determine grouping of the drugs on the basis of similarities/differences in protein patterns. For each drug, arithmetical means of ratios measured intensity/volume of the spot were taken as input data [57].

4.6. Protein Classification According to Gene Ontology

The PANTHER (Protein ANalysis THrough Evolutionary Relationships) classification software was used to assign identified proteins according to Gene Ontology to biological processes (PANTHER version 7) [58].

5. Conclusions

To help translation of molecular findings toward improvements in clinical use we focused on the effects of several clinically relevant representatives of the group of anthracycline/anthracenedione drugs on the tumor cell.

It was evident that each of the drugs of anthracycline/anthracenedione group of chemotherapeutics was capable of inducing exclusively specific protein changes in tumor cells, many of which represent possible new molecular mechanisms contributing to anti-cancer activity. On the other hand, we observed several protein changes that corresponded to the adaptive effort of cancer cells to sustain growth. The findings of drug specific protein changes induced by structurally related drugs might help in explaining their different clinical use. Additionally, protein changes common in the drugs may be exploited for further enhancement of anti-cancer activities.

In summary, together with induction of anti-cancer activities, there may be significant benefits in blocking the activation of adaptive pathways in order to improve the outcomes of a specific treatment in cancer patients undergoing therapy.

Acknowledgments

This work was supported in part by grants from the Ministry of Education, Youth and Sports LC07017 and by Institutional Research Concepts RVO 67985904 (IAPG, AS CR, v.v.i.) and RVO 61388971 (IMIC, AS CR, v.v.i.). Infrastructural part of this project was supported from the Operational Program Research and Development for Innovations (CZ.1.05/2.1.00/01.0030).

Conflict of Interest

The authors declare no conflict of interest.

References

1. Carvalho, C.; Santos, R.X.; Cardoso, S.; Correia, S.; Oliveira, P.J.; Santos, M.S.; Moreira, P.I. Doxorubicin: The good, the bad and the ugly effect. *Curr. Med. Chem.* **2009**, *16*, 3267–3285.

2. Minotti, G.; Menna, P.; Salvatorelli, E.; Cairo, G.; Gianni, L. Anthracyclines: Molecular advances and pharmacologic developments in antitumor activity and cardiotoxicity. *Pharmacol. Rev.* **2004**, *56*, 185–229.
3. Hande, K.R. Clinical applications of anticancer drugs targeted to topoisomerase II. *Biochim. Biophys. Acta* **1998**, *1400*, 173–184.
4. Nitiss, J.L. Targeting DNA topoisomerase II in cancer chemotherapy. *Nat. Rev. Cancer* **2009**, *9*, 338–350.
5. Pommier, Y.; Leo, E.; Zhang, H.; Marchand, C. DNA topoisomerases and their poisoning by anticancer and antibacterial drugs. *Chem. Biol.* **2010**, *17*, 421–433.
6. Gewirtz, D.A. A critical evaluation of the mechanisms of action proposed for the antitumor effects of the anthracycline antibiotics adriamycin and daunorubicin. *Biochem. Pharmacol.* **1999**, *57*, 727–741.
7. Kremer, L.C.; van Dalen, E.C.; Offringa, M.; Ottenkamp, J.; Voute, P.A. Anthracycline-induced clinical heart failure in a cohort of 607 children: Long-term follow-up study. *J. Clin. Oncol.* **2001**, *19*, 191–196.
8. Simunek, T.; Sterba, M.; Popelova, O.; Adamcova, M.; Hrdina, R.; Gersl, V. Anthracycline-induced cardiotoxicity: Overview of studies examining the roles of oxidative stress and free cellular iron. *Pharmacol. Rep.* **2009**, *61*, 154–171.
9. Cortes-Funes, H.; Coronado, C. Role of anthracyclines in the era of targeted therapy. *Cardiovasc. Toxicol.* **2007**, *7*, 56–60.
10. Hanash, S.; Taguchi, A. The grand challenge to decipher the cancer proteome. *Nat. Rev. Cancer* **2010**, *10*, 652–660.
11. Hammer, E.; Bien, S.; Salazar, M.G.; Steil, L.; Scharf, C.; Hildebrandt, P.; Schroeder, H.W.; Kroemer, H.K.; Volker, U.; Ritter, C.A. Proteomic analysis of doxorubicin-induced changes in the proteome of HepG2cells combining 2-D DIGE and LC-MS/MS approaches. *Proteomics* **2010**, *10*, 99–114.
12. Chen, S.T.; Pan, T.L.; Tsai, Y.C.; Huang, C.M. Proteomics reveals protein profile changes in doxorubicin-treated MCF-7 human breast cancer cells. *Cancer Lett.* **2002**, *181*, 95–107.
13. Jiang, Y.J.; Sun, Q.; Fang, X.S.; Wang, X. Comparative mitochondrial proteomic analysis of Rji cells exposed to adriamycin. *Mol. Med.* **2009**, *15*, 173–182.
14. Dong, X.; Xiong, L.; Jiang, X.; Wang, Y. Quantitative proteomic analysis reveals the perturbation of multiple cellular pathways in jurkat-T cells induced by doxorubicin. *J. Proteome Res.* **2010**, *9*, 5943–5951.
15. Moller, A.; Malerczyk, C.; Volker, U.; Stoppler, H.; Maser, E. Monitoring daunorubicin-induced alterations in protein expression in pancreas carcinoma cells by two-dimensional gel electrophoresis. *Proteomics* **2002**, *2*, 697–705.
16. Keenan, J.; Murphy, L.; Henry, M.; Meleady, P.; Clynes, M. Proteomic analysis of multidrug-resistance mechanisms in adriamycin-resistant variants of DLKP, a squamous lung cancer cell line. *Proteomics* **2009**, *9*, 1556–1566.
17. Murphy, L.; Clynes, M.; Keenan, J. Proteomic analysis to dissect mitoxantrone resistance-associated proteins in a squamous lung carcinoma. *Anticancer Res.* **2007**, *27*, 1277–1284.

18. Skalnikova, H.; Halada, P.; Dzubak, P.; Hajduch, M.; Kovarova, H. Protein fingerprints of anti-cancer effects of cyclin-dependent kinase inhibition: identification of candidate biomarkers using 2D liquid phase separation coupled to mass spectrometry. *Tech. Cancer Res. Treat* **2005**, *4*, 447–454.
19. Puustinen, P.; Junttila, M.R.; Vanhatupa, S.; Sablina, A.A.; Hector, M.E.; Teittinen, K.; Raheem, O.; Ketola, K.; Lin, S.; Kast, J.; *et al.* PME-1 protects extracellular signal-regulated kinase pathway activity from protein phosphatase 2A-mediated inactivation in human malignant glioma. *Cancer Res.* **2009**, *69*, 2870–2877.
20. Haley, B.; Paunesku, T.; Protic, M.; Woloschak, G.E. Response of heterogeneous ribonuclear proteins (hnRNP) to ionising radiation and their involvement in DNA damage repair. *Int. J. Radiat. Biol.* **2009**, *85*, 643–655.
21. He, Y.; Rothnagel, J.A.; Epis, M.R.; Leedman, P.J.; Smith, R. Downstream targets of heterogeneous nuclear ribonucleoprotein A2 mediate cell proliferation. *Mol. Carcinog.* **2009**, *48*, 167–179.
22. Malz, M.; Weber, A.; Singer, S.; Riehmer, V.; Bissinger, M.; Riener, M.O.; Longerich, T.; Soll, C.; Vogel, A.; Angel, P.; *et al.* Overexpression of far upstream element binding proteins: A mechanism regulating proliferation and migration in liver cancer cells. *Hepatology* **2009**, *50*, 1130–1139.
23. Obchoei, S.; Wongkhan, S.; Wongkham, C.; Li, M.; Yao, Q.; Chen, C. Cyclophilin A: Potential functions and therapeutic target for human cancer. *Med. Sci. Monit.* **2009**, *15*, RA221–32.
24. Wang, W.; Eddy, R.; Condeelis, J. The cofilin pathway in breast cancer invasion and metastasis. *Nat. Rev. Cancer* **2007**, *7*, 429–440.
25. Ren, L.; Hong, S.H.; Cassavaugh, J.; Osborne, T.; Chou, A.J.; Kim, S.Y.; Gorlick, R.; Hewitt, S.M.; Khanna, C. The actin-cytoskeleton linker protein ezrin is regulated during osteosarcoma metastasis by PKC. *Oncogene* **2009**, *28*, 792–802.
26. Skalnikova, H.; Martinkova, J.; Hrabakova, R.; Halada, P.; Dziechciarkova, M.; Hajduch, M.; Gadher, S.J.; Hammar, A.; Enetoft, D.; Ekefjard, A.; *et al.* Cancer drug-resistance and a look at specific proteins: Rho GDP-dissociation inhibitor 2, Y-box binding protein 1, and HSP70/90 organizing protein in proteomics clinical application. *J. Proteome Res.* **2010**, *10*, 404–415.
27. Resendis-Antonio, O.; Checa, A.; Encarnacion, S. Modeling core metabolism in cancer cells: Surveying the topology underlying the Warburg effect. *PLoS One* **2010**, *5*, e12383.
28. Granchi, C.; Roy, S.; De Simone, A.; Salvetti, I.; Tuccinardi, T.; Martinelli, A.; Macchia, M.; Lanza, M.; Betti, L.; Giannaccini, G.; *et al.* *N*-Hydroxyindole-based inhibitors of lactate dehydrogenase against cancer cell proliferation. *Eur. J. Med. Chem.* **2011**, *46*, 5398–5407.
29. Li, Y.; Ray, P.; Rao, E.J.; Shi, C.; Guo, W.; Chen, X.; Woodruff, E.A., III; Fushimi, K.; Wu, J.Y. A Drosophila model for TDP-43 proteinopathy. *Proc. Natl. Acad. Sci. USA* **2010**, *107*, 3169–3174.
30. Kawahara, Y.; Mieda-Sato, A. TDP-43 promotes microRNA biogenesis as a component of the Drosha and Dicer complexes. *Proc. Natl. Acad. Sci. USA* **2012**, *109*, 3347–3352.
31. Urushitani, M.; Sato, T.; Bamba, H.; Hisa, Y.; Tooyama, I. Synergistic effect between proteasome and autophagosome in the clearance of polyubiquitinated TDP-43. *J. Neurosci. Res.* **2010**, *88*, 784–797.
32. Nilsson, J.; Gritli-Linde, A.; Heby, O. Skin fibroblasts from spermine synthase-deficient hemizygous gyro male (Gy/Y) mice overproduce spermidine and exhibit increased resistance to oxidative stress but decreased resistance to UV irradiation. *Biochem. J.* **2000**, *352*, 381–387.

33. Chen, Z.; Gopalakrishnan, S.M.; Bui, M.H.; Soni, N.B.; Warrior, U.; Johnson, E.F.; Donnelly, J.B.; Glaser, K.B. 1-Benzyl-3-cetyl-2-methylimidazolium iodide (NH125) induces phosphorylation of eukaryotic elongation factor-2 (eEF2): A cautionary note on the anticancer mechanism of an eEF2 kinase inhibitor. *J. Biol. Chem.* **2011**, *286*, 43951–43958.
34. Lukong, K.E.; Larocque, D.; Tyner, A.L.; Richard, S. Tyrosine phosphorylation of sam68 by breast tumor kinase regulates intranuclear localization and cell cycle progression. *J. Biol. Chem.* **2005**, *280*, 38639–38647.
35. Lobato, S.; Tafuri, A.; Fernandes, P.A.; Caliari, M.V.; Silva, M.X.; Xavier, M.A.; Vago, A.R. Minichromosome maintenance 7 protein is a reliable biological marker for human cervical progressive disease. *J. Gynecol. Oncol.* **2012**, *23*, 11–15.
36. Liu, Y.Z.; Jiang, Y.Y.; Hao, J.J.; Lu, S.S.; Zhang, T.T.; Shang, L.; Cao, J.; Song, X.; Wang, B.S.; Cai, Y.; *et al.* Prognostic significance of MCM7 expression in the bronchial brushings of patients with non-small cell lung cancer (NSCLC). *Lung Cancer* **2012**, *77*, 176–182.
37. Marnerides, A.; Vassilakopoulos, T.P.; Boltetsou, E.; Levidou, G.; Angelopoulou, M.K.; Thymara, I.; Kyrtsonis, M.C.; Pappi, V.; Tsopra, O.; Panayiotidis, P.; *et al.* Immunohistochemical expression and prognostic significance of CCND3, MCM2 and MCM7 in Hodgkin lymhoma. *Anticancer Res.* **2011**, *31*, 3585–3594.
38. Di Paola, D.; Zannis-Hadjopoulos, M. Comparative analysis of pre-replication complex proteins in transformed and normal cells. *J. Cell. Biochem.* **2012**, *113*, 1333–1347.
39. Kumano, M.; Furukawa, J.; Shiota, M.; Zardan, A.; Zhang, F.; Beraldi, E.; Wiedmann, R.M.; Fazli, L.; Zoubeidi, A.; Gleave, M.E. Cotargeting Stress-Activated Hsp27 and Autophagy as a Combinatorial Strategy to Amplify Endoplasmic Reticular Stress in Prostate. Cancer *Mol. Cancer Therapeut.* **2012**, doi:10.1158/1535-7163.MCT-12-0072.
40. Kaddar, T.; Rouault, J.P.; Chien, W.W.; Chebel, A.; Gadoux, M.; Salles, G.; Ffrench, M.; Magaud, J.P. Two new miR-16 targets: Caprin-1 and HMGA1, proteins implicated in cell proliferation. *Biol. Cell* **2009**, *101*, 511–524.
41. Solomon, S.; Xu, Y.; Wang, B.; David, M.D.; Schubert, P.; Kennedy, D.; Schrader, J.W. Distinct structural features of caprin-1 mediate its interaction with G3BP-1 and its induction of phosphorylation of eukaryotic translation initiation factor 2alpha, entry to cytoplasmic stress granules, and selective interaction with a subset of mRNAs. *Mol. Cell Biol.* **2007**, *27*, 2324–2342.
42. Driscoll, J.J.; Woodle, E.S. Targeting the ubiquitin+proteasome system in solid tumors. *Semin. Hematol.* **2012**, *49*, 277–283.
43. Rousseau, B.; Menard, L.; Haurie, V.; Taras, D.; Blanc, J.F.; Moreau-Gaudry, F.; Metzler, P.; Hugues, M.; Boyault, S.; Lemiere, S.; *et al.* Overexpression and role of the ATPase and putative DNA helicase RuvB-like 2 in human hepatocellular carcinoma. *Hepatology* **2007**, *46*, 1108–1118.
44. Luo, B.; Lee, A.S. The critical roles of endoplasmic reticulum chaperones and unfolded protein response in tumorigenesis and anticancer therapies. *Oncogene* **2012**, doi:10.1038/onc.2012.130.
45. Calderwood, S.K.; Murshid, A.; Gong, J. Heat shock proteins: Conditional mediators of inflammation in tumor immunity. *Front. Immunol.* **2012**, *3*, 75.
46. Tsuji, T.; Matsuzaki, J.; Caballero, O.L.; Jungbluth, A.A.; Ritter, G.; Odunsi, K.; Old, L.J.; Gnjatic, S. Heat shock protein 90-mediated peptide-selective presentation of cytosolic tumor antigen for direct recognition of tumors by CD4(+) T cells. *J. Immunol.* **2012**, *188*, 3851–3858.

47. Kiyamova, R.; Garifulin, O.; Gryshkova, V.; Kostianets, O.; Shyian, M.; Gout, I.; Filonenko, V. Preliminary study of thyroid and colon cancers-associated antigens and their cognate autoantibodies as potential cancer biomarkers. *Biomarkers* **2012**, *17*, 362–371.
48. Fucikova, J.; Kralikova, P.; Fialova, A.; Brtnicky, T.; Rob, L.; Bartunkova, J.; Spisek, R. Human tumor cells killed by anthracyclines induce a tumor-specific immune response. *Cancer Res.* **2011**, *71*, 4821–4833.
49. Jia, R.; Li, C.; McCoy, J.P.; Deng, C.X.; Zheng, Z.M. SRp20 is a proto-oncogene critical for cell proliferation and tumor induction and maintenance. *Int. J. Biol. Sci.* **2010**, *6*, 806–826.
50. Passon, D.M.; Lee, M.; Rackham, O.; Stanley, W.A.; Sadowska, A.; Filipovska, A.; Fox, A.H.; Bond, C.S. Structure of the heterodimer of human NONO and paraspeckle protein component 1 and analysis of its role in subnuclear body formation. *Proc. Natl. Acad. Sci. USA* **2012**, *109*, 4846–4850.
51. Mihal, V.; Hajduch, M.; Noskova, V.; Janostakova, A.; Safarova, M.; Orel, M.; Kouzmina, G.; Stary, J.; Blazek, B.; Pospisilova, D. The analysis of correlations between drug resistance and clinical/laboratory measures found in a group of children with all treated by ALL-BFM 90 protocol. *Bull. Cancer* **2004**, *91*, 10080–10089.
52. Lee, B.W.; Johnson, G.L.; Hed, S.A.; Darzynkiewicz, Z.; Talhouk, J.W.; Mehrotra, S. DEVDase detection in intact apoptotic cells using the cell permeant fluorogenic substrate, (z-DEVD)2-cresyl violet. *Biotechniques* **2003**, *35*, 1080–1085.
53. Luche, S.; Diemer, H.; Tastet, C.; Chevallet, M.; van Dorsselaer, A.; Leize-Wagner, E.; Rabilloud, T. About thiol derivatization and resolution of basic proteins in two-dimensional electrophoresis. *Proteomics* **2004**, *4*, 551–561.
54. Hardy, E.; Castellanos-Serra, L.R. "Reverse-staining" of biomolecules in electrophoresis gels: Analytical and micropreparative applications. *Anal. Biochem.* **2004**, *328*, 1–13.
55. Gobom, J.; Nordhoff, E.; Mirgorodskaya, E.; Ekman, R.; Roepstorff, P. Sample purification and preparation technique based on nano-scale reversed-phase columns for the sensitive analysis of complex peptide mixtures by matrix-assisted laser desorption/ionization mass spectrometry. *J. Mass Spectrom.* **1999**, *34*, 105–116.
56. Jarkovska, K.; Martinkova, J.; Liskova, L.; Halada, P.; Moos, J.; Rezabek, K.; Gadher, S.J.; Kovarova, H. Proteome mining of human follicular fluid reveals a crucial role of complement cascade and key biological pathways in women undergoing *in vitro* fertilization. *J. Proteome Res.* **2010**, *9*, 1289–1301.
57. Team, RDevelopment Core. *R: A Language and Environment for Statistical Computing*; R Foundation for Statistical Computing: Vienna, Austria, 2011.
58. Thomas, P.D.; Campbell, M.J.; Kejariwal, A.; Mi, H.; Karlak, B.; Daverman, R.; Diemer, K.; Muruganujan, A.; Narechania, A. PANTHER: A library of protein families and subfamilies indexed by function. *Genome Res.* **2003**, *13*, 2129–2141.

© 2012 by the authors; licensee MDPI, Basel, Switzerland. This article is an open access article distributed under the terms and conditions of the Creative Commons Attribution license (http://creativecommons.org/licenses/by/3.0/).

4.4. Analýza reálných biologických vzorků v rámci hledání kandidátních proteinů pro včasnou diagnostiku ovariálního hyperstimulačního syndromu.

v publikaci

Development of Ovarian Hyperstimulation Syndrome:
Interrogation of Key Proteins and Biological Processes in Human Follicular Fluid of Women Undergoing In Vitro Fertilization

Jarkovská K, Kupcová Skalníková H, Halada P, **Hrabáková R**, Moss J, Řežábek K, Gadher SJ, Kovářová H.

Mol hum Reprod. 2011 Nov; 17(11): 679-92. Epub 2011 Jun 22.
IF (2011): 3.85; 5-year IF (2011): 3.53

Prohlášení spoluautorů

„Prohlašuji, že Rita Hrabáková se patřičně podílela (30 %) na plánování proteomických experimentů, jejich provedení, interpretaci výsledků a sepisování této práce."

V Liběchově, dne..... RNDr. Hana Kovářová, CSc.

.....……...

Molecular Human Reproduction, Vol.17, No.11 pp. 679–692, 2011
Advanced Access publication on June 22, 2011 doi:10.1093/molehr/gar047

MHR Basic science of reproductive medicine **ORIGINAL RESEARCH**

Development of ovarian hyperstimulation syndrome: interrogation of key proteins and biological processes in human follicular fluid of women undergoing *in vitro* fertilization

Karla Jarkovska[1], Helena Kupcova Skalnikova[1], Petr Halada[2], Rita Hrabakova[1], Jiri Moos[3,4], Karel Rezabek[4], Suresh Jivan Gadher[1,5], and Hana Kovarova[1,*]

[1]Department of Reproductive and Developmental Biology, Institute of Animal Physiology and Genetics AS CR, v.v.i., 277 21 Libechov, Czech Republic [2]Laboratory of Molecular Structure Characterisation, Institute of Microbiology AS CR, v.v.i., 142 00 Prague, Czech Republic [3]Sigma-Aldrich spol. s.r.o., 186 00 Prague, Czech Republic [4]Centre of Assisted Reproduction, Department of Obstetrics and Gynaecology, General Teaching Hospital, 128 51 Prague, Czech Republic [5]Merck Millipore, 15 Research Park Drive, St. Charles, MO 63304, USA

*Correspondence address. Tel: +420-315-639-582; Fax: +420-315-639-510; E-mail: kovarova@iapg.cas.cz

Submitted on March 10, 2011; resubmitted on June 7, 2011; accepted on June 14, 2011

ABSTRACT: Ovarian hyperstimulation syndrome (OHSS) is an iatrogenic complication and potentially life-threatening condition resulting from excessive ovarian stimulation during assisted reproductive technologies. Our aim was to identify candidate proteins in follicular fluid (FF) using various proteomic approaches which may help to identify patients at risk of OHSS. We analysed the proteome alterations in FF from patients suffering from severe forms of OHSS (OHSS+) compared with a control group of women without or with only mild signs of OHSS (OHSS−). The 12 abundant proteins of FF were removed using an immunoaffinity system. Pools of remaining depleted proteins were applied to the two-dimensional (2D) electrophoresis and 2D liquid chromatography and proteins in differentially expressed protein spots/fractions were identified by mass spectrometry. Among a total of 19 candidate proteins differentially expressed ($P < 0.05$) between OHSS+ and OHSS− FF samples, three proteins, namely ceruloplasmin, complement C3 and kininogen-1, were found using both 2D techniques. Computer modelling highlighted the important role of kininogen-1 as an anchor for mediated interactions with other identified proteins including ferritin light chain and ceruloplasmin, hepatocyte growth factor-like protein, as well as complement C3 and gelsolin, thus linking various biological processes including inflammation and angiogenesis, iron transport and storage, blood coagulation, innate immunity, cell adhesion and actin filament polymerization. The delineation of such processes may allow the development of informed corrective therapeutic intervention in patients at risk of OHSS and a set of key proteins of the FF may be helpful as potential biomarkers for monitoring IVF therapy.

Key words: biomarkers / computer modelling / human follicular fluid / ovarian hyperstimulation syndrome / proteomics

Introduction

There are millions of couples around the world battling infertility and experts are reporting a steady increase in the number of people who are affected by this problem. International estimates of infertility prevalence and demand for infertility medical care highlight a depressing picture showing a 9% prevalence of infertility (of 12 months) with 56% of couples seeking medical care (Boivin *et al.*, 2007). Such couples, having difficulties conceiving, resort to assisted reproductive technology (ART) such as IVF followed by embryo transfer into the woman's uterus. Results of treatments using ARTs indicated that for IVF, the values of the clinical pregnancy rates per follicle/oocyte aspiration and per embryo transfer in 2006 in Europe were 29.0 and 32.4%, respectively (de Mouzon *et al.*, 2010). Although there was a significant increase in

© The Author 2011. Published by Oxford University Press on behalf of the European Society of Human Reproduction and Embryology. All rights reserved.
For Permissions, please email: journals.permissions@oup.com

the reported number of ART cycles and fewer embryos were transferred per treatment in Europe, there was only marginal increase in pregnancy rates as well as only minor reduction in multiple deliveries as observed in 2005 and 2006 (Andersen et al., 2009; de Mouzon et al., 2010).

Controlled ovarian hyperstimulation is a key factor in the success of IVF. Since human chorionic gonadotrophin (hCG)—a common substitute for natural LH in IVF cycles —is widely used, many studies have been carried out to assess its implication (Lei et al., 1992; Rao et al., 1993; Albert et al., 2002). The resultant evidence suggested that hCG played a significant role in the development of ovarian hyperstimulation syndrome (OHSS; Wulff et al., 2000). The onset of this iatrogenic complication usually occurs during luteal phase in ovulation stimulation or during early pregnancy with prevalence between 0.5 and 1.5% of all IVF cycles (Andersen et al., 2009; de Mouzon et al., 2010). OHSS presents itself in various forms from mild stage (33%) to moderate (3–6%) to severe disease state (0.1–3%); the latter can be highly complicated, may be fatal and definitely requires intensive care management (Nastri et al., 2010).

The main symptom of OHSS is cystic enlargement of ovaries and fluid leakage from the intravascular space due to increased permeability and ovarian neoangiogenesis (Gerris et al., 2006). Subsequently, such an increase in the capillary permeability of the ovaries and mesothelial surfaces can lead to massive ascites, pleural effusion and occasionally even pericardial effusion. Severe forms of OHSS are also accompanied by electrolyte and hemodynamic disturbances (Chen et al., 2008) resulting in thrombosis (Chipwete et al., 2009) or renal failure (Merrilees et al., 2008). Unfortunately, prediction and diagnosis mostly involves measurement of blood estradiol levels and number of growing follicles which is certainly not sufficient and treatment strategies remain symptomatic without any specific treatment for OHSS. Hence, an accurate and reliable investigative approach is needed for early prognosis/diagnosis and prompt prevention. Possibility of utilizing a protein or a set of proteins present in the follicular fluid (FF) of patients which constitutes the *in vivo* environment of the oocyte as potential biomarker(s) was highlighted by Gadher et al. (2009). FF representing the intrafollicular milieu is easily accessible as a resultant by-product during aspiration of oocytes from mature ovarian follicle (Fortune, 1994) and certain proteins observed here may be contributory to development of OHSS.

Previously, we used a proteomic approach and showed involvement of innate immune function of complement cascade in FF of women undergoing controlled ovarian hyperstimulation for IVF. Low complement activity and the presence of C-terminal fragment of perlecan suggested possible links to angiogenesis, which is a vital process in physiological folliculogenesis and placental development. Differences in proteins associated with blood coagulation were also found in the follicular milieu (Jarkovska et al., 2010). In this study, the proteome alterations in FF which might be associated with the development of OHSS were analysed utilizing samples of FF from patients suffering from severe form of OHSS (patient group; OHSS+) compared with control group of women without or with only mild signs of OHSS (control group; OHSS−). We used a combination of several proteomic techniques to obtain two-dimensional (2D) protein profiles of FF samples as well as to access important middle and low abundant proteins. First, 12 abundant proteins of FF were removed using the IgY-12 immunoaffinity system. Pools of remaining depleted proteins were then applied to the 2D electrophoresis (2-DE) and 2D liquid chromatography (2D LC). The resulting 2D protein maps were evaluated using software tools and protein spots/fractions with significant increase or decrease in FF from OHSS+ group compared with OHSS− group of women were subjected to protein identification by mass spectrometry (MS). Selected protein changes were further verified by independent immunoblotting (Fig. 1) and computer modelling was used to reveal protein interaction network integrating severe OHSS related proteins to help judge the severity of the onset.

Materials and Methods

Chemicals

IgY-12 High Capacity LC 10 Proteome Partitioning kit and ProteomeLab™ PF 2D kit (includes chromatofocusing column, high-resolution reverse-phase column, start buffer, eluent buffer and PD-10 columns) were purchased from Beckman Coulter (Fullerton, CA, USA). Amicon Ultra-15 Centrifugal Filter Device was from Millipore (Bedford, MA, USA). Acrylamide, bis-acrylamide, urea, Tris-base, thiourea, sodium dodecyl sulphate (SDS), bromophenol blue, amonium persulfate (APS), tetramethylethylenediamine (TEMED), n-octyl glucoside, Tris(2-carboxyethyl)phosphine hydrochloride (TCEP), iminodiacetic acid and trifluoroacetic acid (TFA) were obtained from Sigma (St. Louis, MO, USA). Nonidet-40, 3-[(3-cholamidopropyl)dimethylammonio]-1-propanesulfonate (CHAPS) and dithiothreitol (DTT) were from USB Corporation (Cleveland, OH, USA). Glycerol and β-glycerolphosphate were purchased from Serva Electrophoresis GmbH (Heidelberg, Germany). Protease inhibitors cocktail was obtained from Roche (Basel, Switzerland). Immobiline DryStrip (18 cm, 4–7) and ampholytes pH 4–7 were purchased from GE Healthcare (Uppsala, Sweden). Sypro Ruby Protein Gel Stain was from Bio-Rad Laboratories (Hercules, CA, USA). All other chemicals for protein fractionations and silver staining were of HPLC or analytical grade and buffers were prepared using Milli-Q water system (Millipore Bedford, MA, USA). Unless otherwise specified, all chemicals used for MS were from Sigma (Steinheim, Germany).

Female patients and collection of FF

Women undergoing controlled ovarian hyperstimulation for IVF were recruited for the study at the Centre of Assisted Reproduction, Department of Obstetrics and Gynecology, General Teaching Hospital in Prague. All female patients gave their informed consent prior to sample collection.

To achieve stimulation, standard treatment protocol was applied including controlled ovarian FSH hyperstimulation using GnRH short antagonists or GnRH long agonists with hCG administration to induce oocyte maturation. Oocyte transvaginal retrieval was performed 36 h after hCG administration according to the strict procedure approved by the Centre of Assisted Reproduction. Each FF sample was obtained from puncture of dominant ovarian follicles (in diameter from 14 to 22 mm). Only macroscopically clear fluids, indicating lack of contamination, were considered in the study. After oocyte isolation, FF was centrifuged to remove cellular components and debris and then transferred to sterile polypropylene tubes and frozen at −70°C until further analysis (Moos et al., 2009).

Samples were obtained from a total number of 31 women (average BMI 23.25 ± 4.19; average age 30.07 ± 3.19; average number of follicles 28.16 ± 9.37) and were separated into two groups: (i) OHSS+ patient group including 13 women (average BMI 22.94 ± 4.37; average age 29.46 ± 3.60; average number of follicles 29.84 ± 6.30) suffering from severe form of OHSS characterized by massive ascites,

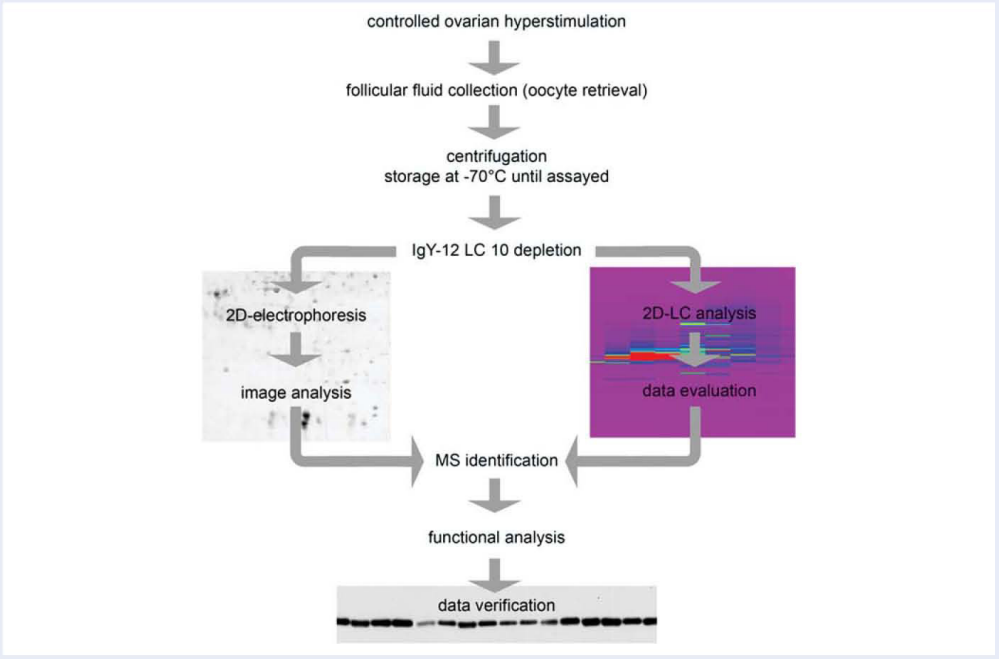


Figure 1 Schematic presentation of the IgY-12, 2-DE and 2D LC workflows. Samples of FF were retrieved from women undergoing controlled ovarian stimulation and were depleted of the 12 most abundant plasma/human FF matched proteins and processed for 2-DE and 2D HPLC analyses as indicated in the workflows. Subsequently, proteomic data were verified by immunoblotting and computer modelling was used to reveal protein interaction network integrating OHSS discriminating proteins.

haemoconcentration (hematocrit > 45%, WBC > 15 000/ml), oliguria, creatinine > 130 m mol/l, creatinine clearance < 50 ml/min and enlarged ovaries (>5 cm); (ii) OHSS− control group consisting of 18 women (average BMI 23.47 ± 4.17; average age 30.53 ± 2.87; average number of follicles 26.94 ± 11.10) either without any symptoms of OHSS or with only mild form presented by bloating, nausea, abdominal distention and sonography-determined size of ovaries <5 cm (Navot *et al.*, 1992). Both groups were matched as to BMI, age and number of growing follicles. Additionally, around 39% of all IVF cycles resulted in successful pregnancy without any significant difference between OHSS+ and OHSS− groups of women.

The distribution of the samples with reference to applied proteomic technologies is graphically illustrated in Fig. 2: 9 samples of FF (4 OHSS+ patients and 5 OHSS− controls) were applied to 2-DE, whilst 12 FF samples (6 OHSS+ patients and 6 OHSS− controls) were analysed using 2D LC. Of all the samples, 6 were shared and analysed using both proteomic techniques. For independent verification of proteomic findings, a set of 23 samples were used (11 OHSS+ patients and 12 OHSS− controls) of which 7 were included in 2D LC fractionation. Four of all samples were processed using all approaches applied in this study.

Depletion of major abundance proteins

Depletion of the 12 abundant plasma matched proteins (albumin, IgG, transferrin, fibrinogen, IgA, α2-macroglobulin, IgM, α1-antitrypsin,

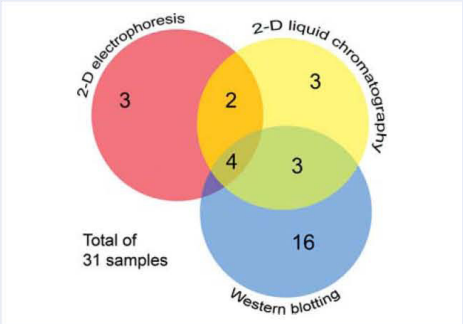


Figure 2 The distribution of the samples among applied proteomic technologies. Nine samples of FF (4 OHSS+ patients and 5 OHSS− controls) were applied to 2-DE, whilst 12 FF samples (6 OHSS+ patients and 6 OHSS− controls) were analysed using 2D LC. For western blot, a set of 23 samples were used (11 OHSS+ patients and 12 OHSS− controls).

haptoglobin, α1-acidic glycoprotein and apolipoproteins A-I and A-II) present in FF (Shalgi et al., 1973; Huang et al., 2005) was carried out using multiple immunoaffinity ProteomeLab IgY-12 LC10 column (binding capacity equal to 250 μl of blood plasma; Beckman Coulter, Fullerton, CA, USA) as described previously (Jarkovska et al., 2010). Protein concentration of samples was measured at first using a BCA protein assay kit (Thermo Scientific, Rockford, IL, USA). Aliquot of FF sample containing 20 mg of proteins was diluted to final volume of 750 μl using dilution buffer containing 10 mM Tris–HCl, 0.15 M NaCl, pH 7.4. The diluted sample was filtered through a 0.45 μm membrane using spin filters provided in IgY-12 LC 10 kit, loaded on IgY-12 LC 10 column and standard LC protocol provided by manufacturer was carried out. Flow-through fractions from six cycles of the each individual FF sample were then pooled, concentrated on Amicon Ultra—15 centrifugal filter devices to approximate volume 0.5 ml and diluted in denaturation buffer (7.5 M urea, 2.5 M thiourea, 12.5% glycerol, 62.5 mM Tris–HCl, 2.5% *n*-octylglucoside, 1.25 mM EDTA) for 2D LC and 2-DE.

Two-dimensional electrophoresis and image analysis

Sample aliquots corresponding to 250 and 500 μg of FF depleted proteins were precipitated by addition of 0.15% sodium deoxycholate for 10 min and 72% trichloroacetic acid for 30 min (both in 1/10 of total volume) with 80% yield in average thus providing 200 and 400 μg of proteins to be loaded on 2-DE. After washing with ice-cold acetone, pellets were resolubilized in 150 μl of the sample buffer containing 9 M urea, 3% (w/v) CHAPS, 2% (v/v) Nonidet 40, 70 mM DTT, pH 4–7 ampholytes (0.5% w/v), 10 mM β-glycerol phosphate, 5 mM sodium fluoride, 0.1 mM sodium orthovanadate and protease inhibitors. After 30 min of resolubilization at room temperature, samples were loaded on the first dimension isoelectric focusing (IEF) separation using active in gel rehydration at 50 V of Immobiline DryStrips (IPG strip 18 cm 4–7) in rehydration buffer containing 7 M urea, 2 M thiourea, 4% CHAPS, pH 4–7 ampholytes (2% w/v), 1 mM β-glycerol phosphate, 5 mM sodium fluoride, 1 mM sodium orthovanadate, 1× protease inhibitors cocktail (Roche) and 0.003% bromophenol blue. 2-DE was performed as described previously (Jarkovska et al., 2010). Briefly, IEF was performed on IEF Cell (Bio-Rad, Hercules, CA, USA) system. After IEF separation the gel strips were equilibrated in 50 mM Tris–HCl, pH 6.8, 6 M urea, 30% glycerol, 4% SDS, 1.2% (v/v) DeStreak reagent and bromophenol blue for 20 min and applied to vertical 12% SDS–PAGE (180 × 180 × 1 mm gel). Gels were then stained with MS compatible fluorescent dye Sypro Ruby. Stained gels were scanned and digitized at 800 dpi resolution using a Pharos FX scanner (Bio-Rad, Hercules, CA, USA). The images were evaluated using Imagemaster 2D Platinum version 6.0 software (GE Healthcare, Uppsala, Sweden). The evaluation was done separately for protein images corresponding to the lower load of 200 μg depleted FF proteins with 4 OHSS+ patient and 4 OHSS− control samples, and higher load of 400 μg of depleted FF proteins including 3 OHSS+ patient and 3 OHSS− control samples. After automatic spot detection and matching, manual editing was performed and the results were in good agreement with those from visual inspection. Data were normalized, i.e. expressed as relative intensity of all valid spots, analysed using Student *t*-test available within the Imagemaster 2D Platinum software, and the protein spots with statistically different expression (*P*-value of ≤ 0.05) in the two types of samples were selected for identification by MS. The gels were re-stained using silver staining according to the protocol published by Shevchenko et al. (1996) and were stored at 4°C in 10% MeOH.

Two-dimensional ProteomeLab PF 2D chromatography and image analysis

Samples of depleted FFs in denaturating buffer were loaded on a PD10 column equilibrated with 25 ml of the PF 2D start buffer to exchange denaturating lysis buffer with start buffer. The total protein concentration in the sample collected from PD 10 column was determined by direct measurement of absorbance at 280 nm (DU 7400 spectrophotometer, Beckman, Fullerton, CA, USA). Fractionation of the proteins on 2D LC was performed as described previously (Jarkovska et al., 2010). For the first dimension, chromatofocusing fractionation (HPCF) using two buffers, a start buffer pH 8.55 and an elution buffer pH 4.0, to generate an internal linear pH gradient on the column, was utilized. The proteins remaining on the HPCF column at pH 4.0 were washed out by 1 M NaCl in 30% *n*-propanol solution. UV detection was performed at 280 nm and the pH of the effluent was monitored using a flow-through online pH probe. Fraction collection (pI fractions) started at the beginning of the analysis and individual fractions were collected in 0.3 pH intervals (during the linear pH gradient, started when pH reached 8.3) or with maximum time 8.5 min when the pH did not change. The percentage of protein recovery from the column with pH gradient 8.3–4 was about 45%, while the remaining part of the loaded proteins was collected in either basic (flow-through) or acidic (wash out) fractions. The pI fractions containing any proteins detected at 280 nm were further separated on reversed phase column packed with non-porous silica beads (HPRP). Solvent A was 0.1% trifluoracetic acid (TFA) in water and solvent B 0.08% TFA in acetonitrile (MeCN). The separation was performed at 50°C at a flow rate 0.75 ml/min. The gradient was run from 0 to 100% B in 30 min, followed by 100% B for 4 min and 100% A for 10 min for re-equilibration of the column. UV absorption was monitored at 214 nm. The fractions were collected in 0.13 min time intervals into 96-deep well plates using the fraction collector Gilson FC204 (Immunotech, a.s. Prague, Czech Republic) and stored at −80°C until further use.

2D protein expression maps of FF samples displaying pH corresponding to protein isoelectric point (pI) versus protein hydrophobicity were generated by ProteoVue software running on PF 2D system. The Viper software version 2.3.0.0 (Ludesi, Malmö, Sweden) was used for PF 2D data evaluation of protein maps of 6 OHSS+ patient samples and 6 OHSS− controls. The profiles of the second dimension were matched, normalized and quantitative data were analysed using analysis of variance implemented in Viper software. Only statistically significant (*P*-value of ≤ 0.05) and reproducible protein peaks were selected for follow-up protein identification using MS.

Enzymatic digestion, MALDI MS and protein identification

Tryptic digestion and MALDI mass spectrometric identification of proteins from 2-DE gels were done as described previously (Jarkovska et al., 2010) using SwissProt 2011_01 database. The fractions from 2D-HPLC were dried completely using the SpeedVac concentrator, dissolved in 50 μl of the cleavage buffer containing 25 mM 4-ethylmorpholine acetate, 5% MeCN, and trypsin (5 ng/μl; Promega, Madison, WI, USA), and incubated overnight at 37°C. The digestion was stopped by addition of 7 μl of 5% TFA in MeCN. The aliquot (0.5 μl) of the resulting peptide mixture was deposited on the MALDI target and allowed to air-dry at room temperature. After complete evaporation, 0.5 μl of MALDI matrix solution (α-cyano-4-hydroxycinnamic acid in 50% MeCN/0.1% TFA; 5 mg/ml) was added. Mass spectra were measured on the APEX-Qe FTMS instrument equipped with a 9.4 T superconducting magnet and a Combi ESI/MALDI ion source (Bruker Daltonics, Billerica, MA, USA). The spectra were acquired in the mass range of 650–3500 kDa and calibrated

internally using the monoisotopic $[M+H]^+$ ions of trypsin autoproteolytic fragments. The peak lists in mgf data format were created using DataAnalysis 4.0 program (Bruker Daltonics) with SNAP peak detection algorithm. The peak lists were searched using ProFound search engine (http://prowl.rockefeller.edu/prowl-cgi/profound.exe) against IPI human database (2010/02/01) with the following search settings: peptide tolerance of 3 ppm, missed cleavage site value set to one, variable oxidation of methionine and protein N-term acetylation.

Immunoblot and quantitative analysis

Aliquots of the total protein extracts of non-depleted FF corresponding 5 μg were separated in 10% SDS–PAGE gels (except for ceruloplasmin where 6% gels were used) using Mini PROTEAN® 3 system (Bio-Rad, Hercules, CA, USA). Proteins were then transferred to Immobilon P (Millipore, Bedford, MA, USA) membranes using a semidry blotting system (Biometra, Göttingen, Germany) and transfer buffer containing 48 mM Tris, 39 mM glycine and 20% methanol (except for ceruloplasmin, where 10% MeOH was used). The membranes were blocked for 1 h with 5% skimmed milk (except for ceruloplasmin, where 3% milk was used) in Tris-buffered saline with 0.05% Tween 20 (TBST, pH 7.4) and incubated overnight with primary antibodies specific for apolipoprotein A-IV (Sigma Aldrich, St. Louis, MO, USA; HPA001352; 1:10 000), kininogen-1 (Sigma Aldrich, St. Louis, MO, USA; HPA001616; 1:5000), ceruloplasmin (Abcam, Cambridge, MA, USA; ab51083; 1:10 000) and α-2-HS-glycoprotein (fetuin-A, Santa Cruz Biot., CA, USA; sc-28924; 1:20 000). Peroxidase-conjugated secondary anti-rabbit or anti-mouse IgG antibodies (Jackson Immunoresearch, Suffolk, UK) were diluted 1:10 000 (except for fetuin-A, where 1:100 000 dilution was used) in 5% skimmed milk in TBST, and the ECL+ chemiluminiscence (GE Healthcare, Uppsala, Sweden) detection system was used to detect specific proteins. The exposed CL-XPosure films (Thermo Scientific, Rockford, IL, USA) were scanned by a calibrated densitometer GS-800 (Bio-Rad, Hercules, CA, USA). The proteins bands of each sample were quantified as Trace Quantity (the quantity of a band as measured by the area under its intensity profile curve, units are intensity × mm) using Quantity One software (Bio-Rad, Hercules, CA, USA). The total protein load was checked visually using silver staining of the membranes after immunodetection.

Computer modelling of protein network

To analyse functional aspects including possible protein interactions among identified proteins discriminating OHSS and to reveal further as yet unspecified interacting partners, we used an Interologous Interaction Database (I2D; version 1.8). This database version of both known and predicted protein–protein interactions contained 102 740 source interactions, 59 373 predicted interactions for human and is available online on http://ophid.utoronto.ca/ophidv2.201/. For modelling of the protein interaction network, we entered a list of our identified proteins, except three known highly abundant proteins (alpha-1-antitrypsin, apolipoprotein A-I and serum albumin) in which, despite attempts to deplete completely, trace amounts detectable by MS remained in the samples. In addition, we included in the modelling vascular endothelial growth factor (VEGF), growth factor with recognized importance in human fertility and ovarian function but also implicated in pathogenesis of OHSS when dysregulated (Chen *et al.*, 2010; Rodewald *et al.*, 2009). Search criteria for observing interactions were set to select humans as target organism and graph viewer was set to output format. The final illustration was exported and visualized using NAViGaTOR (Network Analysis, Visualization & Graphing TORonto) software (http://ophid.utoronto.ca/navigator) version 2.1.13. In protein–protein interaction networks, nodes represent proteins and edges between nodes represent physical interactions between the proteins. NAViGaTOR allows nodes to be colour-coded according to Gene Ontology (GO—a controlled vocabulary describing properties of genes; http://www.geneontology.org/) terms.

Results

Depletion of the most abundant proteins of FF for follow-up proteomic analyses

In order to overcome limitations of commonly used proteomic techniques related to high dynamic range of protein concentration in biological fluids and access middle or low abundant proteins (μg/ml–pg/ml), FF samples were depleted of 12 abundant proteins (mg/ml). The immunoaffinity column IgY-12 LC 10 was utilized for this purpose and removal of abundant proteins was monitored using 2-DE fractionation of flow-through and bound fractions (Jarkovska *et al.*, 2010). One cycle provided on average 610 μg of flow-through depleted proteins, which corresponded to removal of 97% of original protein amount (20 mg). In total, six depletion cycles for each sample were necessary to obtain 2 mg of depleted proteins of each individual sample for one run of 2D LC PF 2D analysis and as well as for 2-DE analysis.

Proteomic changes observed in depleted FF of OHSS patients compared with asymptomatic/mild control group using two different approaches: 2D LC and 2-DE

The depleted proteins for 2-DE analysis were precipitated as described above. We decided to analyse two protein loads: (i) the lower dose equal to 200 μg to allow monitoring of middle abundant proteins among depleted FF proteins, most of which are present in the upper part of gel; (ii) the higher dose of 400 μg protein to reveal lower abundant protein spots mainly in the gel region with Mw under 60 kDa. The separation was carried out on gels of the pH 4–7 and Mw 10–200 kDa range and resulted in 674 ± 96 and 1064 ± 191 distinct protein spots for 200 and 400 μg protein loads, respectively (Fig. 3A–D). The statistical comparison between the OHSS+ patients compared with the control OHSS− group revealed 23 and 28 differentially expressed protein spots (*P*-value of ≤0.05) for 200 and 400 μg protein loads, respectively. After considering spot reproducibility and intensity, 19 of these protein spots were chosen for further MS identification and proteins in 16 of them were satisfactorily identified (Supplementary data, Table SI; Fig. 3A–D). Among the 16 quantitatively altered protein spots, nine were decreased in FF of OHSS+ samples (Fig. 3E Nos. 336, 898, 1612, 1843 and F Nos. 2244, 2634, 2896, 2897, 3230) and seven spots were significantly increased (Fig. 3E Nos. 1390, 1438, 1439 and F Nos. 1968, 2102, 2573 and 2666). An abbreviated list of identified differentially expressed proteins and their biological functions is presented in Table I. Supplementary data, Table SI provides comprehensive information about the identified proteins (spot numbers, protein names, database accession numbers, regulations, fold changes, theoretical values of MW and pI, and all MS identification data including Mascot scores, sequence coverage, matched peaks, unmatched peaks and MS/MS confirmation).

The purpose of 2D LC PF 2D experiments was to use an advanced gel-independent fractionation technique which overcomes many of

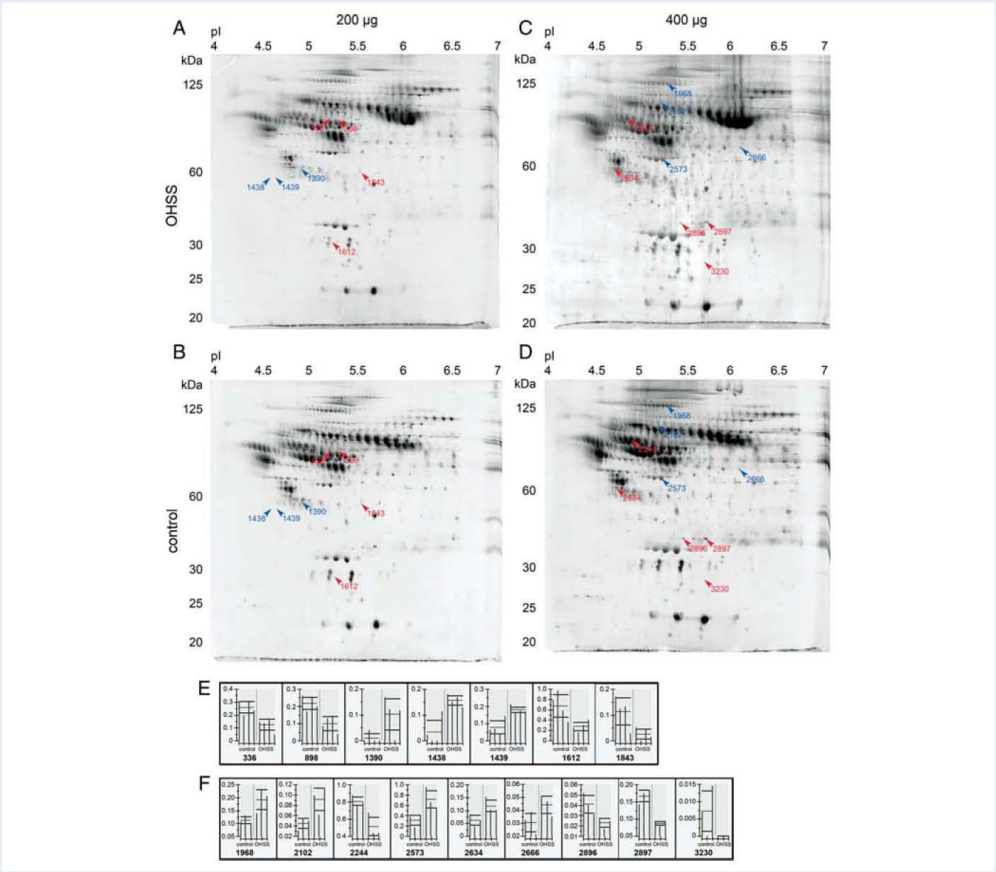


Figure 3 2D electrophoretic protein maps of human FF depleted of the 12 most abundant plasma matched proteins and set of protein spots. Protein lysates of samples of depleted FF were subjected to 2-DE, followed by fluorescent Sypro Ruby staining and image analysis using Imagemaster 2D Platinum version 6.0 software. (**A**–**D**) Representative gels from depleted FF of 200 and 400 µg loads, respectively, and protein spots that were differentially expressed (*P*-value of ≤ 0.05). Regulated proteins are indicated by their spot numbers assigned by the software. Blue numbers indicate higher protein level in FF of OHSS+ samples and red numbers denote lower level in OHSS+ FF compared with control OHSS− samples. (**E** and **F**) Relative volume intensities of identified regulated protein spots calculated and graphically presented by Imagemaster 2D Platinum version 6.0 software. Left columns correspond to control OHSS− FF samples (control) and right columns to OHSS+ FF samples (OHSS).

2-DE drawbacks and allows the fractions of intact proteins to be directly utilized for MS analysis. A typical 2D-LC analysis resulted in separation on average into 1026 protein peaks, which are depicted in the 2D protein map generated using ProteoVue software (Fig. 4). The evaluation of qualitative and quantitative differences between 2D protein maps using Viper software identified 33 differentially expressed protein bands with *P*-value of ≤ 0.05 between the samples representing OHSS+ patients and OHSS− control group. Five of protein peaks with area under curve higher than 1×10^{-5} at 214 nm (which corresponds to the protein amount enough for reliable MS protein identification) and reproducible peak profile were chosen for MS (Fig. 4) and the proteins were satisfactorily identified. All of these protein peaks collected after the second dimension, contained more than one protein and this was re-confirmed by MS analysis. A summary of 2D LC differentially expressed proteins and their functions are presented in Table II. Supplementary data, Table SII provides comprehensive information about the identified proteins (fraction numbers, protein names, database accession numbers, regulations, fold changes, theoretical values of MW and pI, and MS identification data including ProFound Expectation values, sequence coverage and

Table 1 The list of significantly different proteins identified (*P*-value of ≤0.05) between FF of OHSS+ and OHSS− selected using 2-DE.

Spot No	Protein name	SwissProt No.	MW, kDa	pI	Up-regulation, fold change	Functionality
	200 μ load protein					
336	Gelsolin precursor Ig alpha-1 chain C region	GELS_HUMAN IGHA1_HUMAN	85 38	5.9 6.1	OHSS−, 2.0	Actin filament polymerization Immune response
0898	Gelsolin precursor	GELS_HUMAN	86	5.9	OHSS−, 2.2	Actin filament polymerization
1390	Complement factor I precursor	CFAI_HUMAN	66	7.7	OHSS+, 8.3	Complement activation, classical pathway Innate immune response
1438, 1439	Complement C3 precursor[a]	CO3_HUMAN	187	6.0	OHSS+, 4.7/2.4	Complement activation, alternative pathway Complement activation, classical pathway Positive regulation VEGF production
1612	Retinol-binding protein 4	RET4_HUMAN	23	5.8	OHSS−, 2.2	Glucose homeostasis Positive regulation of immunoglobulin secretion Response to retinoic acid Retinol metabolic process
1843	Inter-alpha-trypsin inhibitor heavy chain H4 precursor[a]	ITIH4_HUMAN	103	6.5	OHSS−, 5.0	Acute-phase response Hyaluronan metabolic process
	400 μ load protein					
1968	Ceruloplasmin precursor	CERU_HUMAN	125	5.4	OHSS+, 2.3	Cellular iron ion homeostasis Copper ion transport Oxidation reduction
2102	Inter-alpha-trypsin inhibitor heavy chain H4 precursor[b]	ITIH4_HUMAN	103	6.5	OHSS+, 2.8	Acute-phase response Hyaluronan metabolic process
2244	Kininogen-1 precursor	KNG1_HUMAN	72	6.3	OHSS−, 3.8	Blood coagulation Inflammatory response Negative regulation of blood Coagulation Negative regulation of cell adhesion Vasodilation
2573	Apolipoprotein A-IV precursor	APOA4_HUMAN	47	5.3	OHSS+, 2.2	Cholesterol homeostasis Chylomicron assembly Innate immune response in mucosa Leucocyte cell−cell adhesion Lipoprotein metabolic process
2634	Complement C3 precursor[a]	CO3_HUMAN	187	6.0	OHSS+, 1.9	Complement activation, alternative pathway Complement activation, classical pathway Positive regulation VEGF production
2666	Pigment epithelium-derived factor precursor	PEDF_HUMAN	46	6.0	OHSS+, 1.35	Cell proliferation Negative regulation of angiogenesis
2896, 2897	Serum amyloid P-component precursor	SAMP_HUMAN	25	6.1	OHSS−, 2.4/3.0	Acute-phase response
3230	Ferritin light chain	FRIL_HUMAN	20	5.5	OHSS−, 7.9	Cellular iron ion homeostasis Iron ion transport Oxidation reduction

The table shows spot number, protein name, SwissProt No., predicted MW and pI, regulation/fold of the change and functionality based on search in UniProt/Gene Ontology/Biological Process.
[a]C-terminal fragment.
[b]N-terminal fragment.

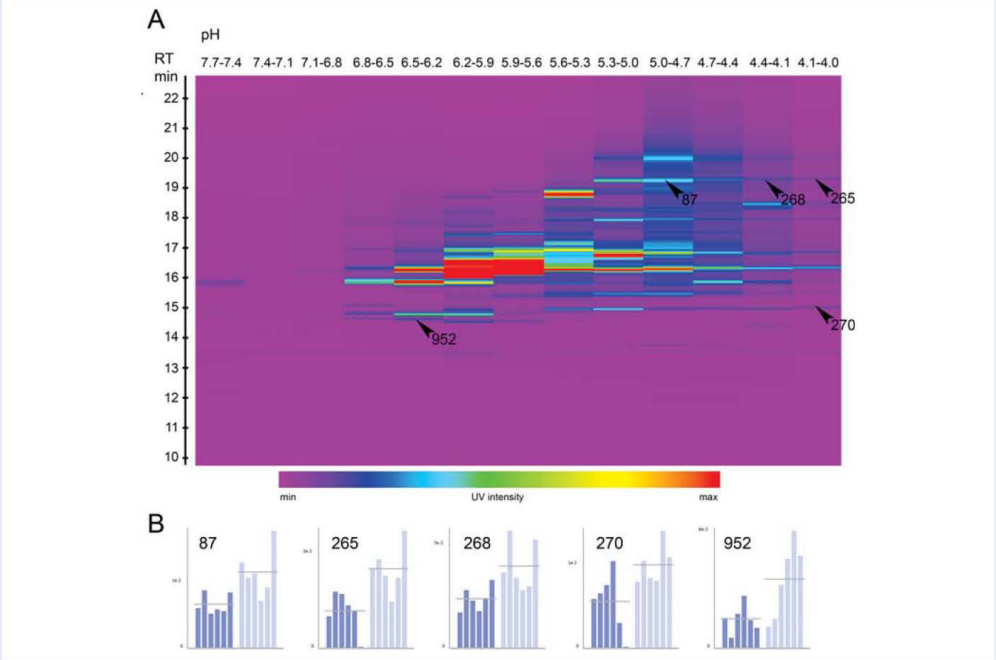


Figure 4 2D liquid chromatography protein map of human FF depleted of the 12 most abundant plasma matched proteins and set of protein bands significantly different significantly different in patients suffering from severe OHSS. Protein lysates of paired samples of depleted FF were subjected to 2D liquid chromatography and protein fractionation/level was monitored using UV detection. 2D protein expression maps were generated by ProteoVue software and their images were evaluated using Viper software. (**A**) Representative protein map from depleted FF and protein bands that were present in significantly different levels (P-value of ≤ 0.05) in OHSS+ FF compared with OHSS− FF and were selected for follow-up identification using MS. The colours of the protein bands correspond to UV intensity and provide information about protein quantification. Regulated proteins are indicated by their numbers assigned by Viper software. (**B**) Relative volume intensities of regulated protein bands calculated and graphically presented by Viper software. The left columns correspond to biological replicates of OHSS+ FF and right columns to OHSS− FF.

number of the matched peaks). All of the differentially expressed protein peaks revealed by PF 2D approach and identified were present at a significantly increased level in FF of OHSS+ patient samples (Table II, Fig. 4). Relative differences in expression ranged from 1.67-fold to as much as 2.38-fold. These protein peaks contained non-target proteins such as ceruloplasmin, complement C3, alpha-2-HS-glycoprotein, haemopexin and alpha-1B-glycoprotein and it was demonstrated (Liu *et al.*, 2006) that these proteins may partly bind to IgY-12 affinity column and it occurs in a highly reproducible manner. On the other hand, we found proteins like kininogen-1, complement factor H-related protein 1 and hepatocyte growth factor-like protein, which were typical non-target not bound proteins (Huang *et al.*, 2005; Liu *et al.*, 2006). The presence of alpha-1-antitrypsin, apolipoprotein A-I and albumin is due to incomplete removal of these proteins in the course of depletion of major abundant proteins as the manufacturer guarantees the removal of 95% (for Apo-AI and α-1-antitrypsin) or 99% (for human albumin) of protein amount. The robustness, reproducibility and specificity of the ProteomeLab IgY-12 high abundance protein depletion system were evaluated using human plasma proteome characterization in combination with high resolution LC-MS/MS (Liu *et al.*, 2006). Because the patterns and distribution of the proteins of human FF, similarly to plasma, between bound and flow-through fractions are highly reproducible for the biological replicates of the same sample, such processes most likely do not significantly affect the quantification of the proteins. This was confirmed using human plasma samples spiked with non-human protein standards in different concentrations.

Amongst all proteins identified in differentially regulated protein spots and peaks from OHSS+ FF samples after 2-DE and 2D LC fractionation were the proteins of the complement cascade and its regulatory proteins, several proteins involved in transport functions, as well as proteins regulating blood coagulation or participating in acute phase, inflammatory and immune responses. Several proteins participating in actin filament polymerization, regulation of angiogenesis and mineral balance were also identified. Three proteins, e.g. ceruloplasmin, kininogen-1 and complement C3 were shared between both

Table II The list of significantly different proteins identified (*P*-value of ≤0.05) between FF of OHSS+ and OHSS− selected using 2D LC.

Fraction No	Protein name	SwissProt No.	MW, kDa	pI	Up-regulation, fold change	Functionality
87	Alpha-1-antitrypsin	A1AT_HUMAN	47	5.4	OHSS+, 1.74	Acute-phase response
	Ceruloplasmin	CERU_HUMAN	122	5.4		Cellular iron ion homeostasis Copper ion transport Oxidation reduction
	Apolipoprotein A-I	APOA1_HUMAN	31	5.6		Cholesterol homeostasis
	Complement C3 precursor	CO3_HUMAN	187	6.0		Complement activation, alternative pathway Complement activation, classical pathway Positive regulation VEGF production
	Alpha-2-HS-glycoprotein	FETUA_HUMAN	39	5.4		Acute-phase response Regulation of inflammatory response
	Kininogen-1 precursor	KNG1_HUMAN	47	6.3		Blood coagulation Inflammatory response Negative regulation of blood coagulation Negative regulation of cell adhesion Vasodilation
265	Alpha-1-antitrypsin	A1AT_HUMAN	47	5.4	OHSS+, 1.79	Acute-phase response
	Ceruloplasmin	CERU_HUMAN	N	5.4		Cellular iron ion homeostasis Copper ion transport Oxidation reduction
268	Alpha-1-antitrypsin	A1AT_HUMAN	47	5.4	OHSS+, 1.67	Acute-phase response
	Ceruloplasmin	CERU_HUMAN	122	5.4		Cellular iron ion homeostasis Copper ion transport Oxidation reduction
	Alpha-2-HS-glycoprotein	FETUA_HUMAN	39	5.4		Acute-phase response Regulation of inflammatory response
270	Hemopexin	HEMO_HUMAN	52	6.6	OHSS+, 2.14	Cellular iron ion homeostasis Interspecies interaction between organisms
	Alpha-1B-glycoprotein precursor	A1BG_HUMAN	54	5.6		
	Serum albumin	ALBU_HUMAN	69	5.9		Cellular response to starvation Maintenance of mitochondrion location Negative regulation of apoptosis
952	Complement factor H-related protein 1	FHR1_HUMAN	38	7.8	OHSS+, 2.38	Complement activation
	Hepatocyte growth factor-like protein	HGFL_HUMAN	80	9.0		Blood coagulation Proteolysis

The table indicates band number, protein name, SwissProt No., predicted MW and pI, regulation/fold of the change and functionality based on search in UniProt/Gene Ontology/Biological Process.

proteomic approaches utilized in this study (Tables I and II) thus corroborating the validity of the findings.

Validation of proteomic data using western blotting

To confirm the results of 2D proteomic analyses, western blot experiments were performed for the following proteins: (i) highly elevated/significantly increased proteins in FF from OHSS+ patients: apolipoprotein A-IV with 2.2-fold change, ceruloplasmin reaching 2.3-fold change and alpha-2-HS-glycoprotein (fetuin-A) with 1.67 and 1.74-fold change; (ii) down-regulated kininogen-1 in OHSS+ patients by 2-DE (Table I), but present in protein peak up-regulated in OHSS+ FF samples according to 2D LC (Table II). In this protein peak kininogen-1 was identified as one of several unambiguously identified proteins from 2D LC with observed higher UV absorbance/protein level in OHSS+ FF. Such observations demonstrate a need for verification of such individual proteins from the overall pool of proteins identified.

In total, we used 23 FF samples (11 OHSS+ and 12 OHSS−) including 16 independent samples not previously used in proteomic

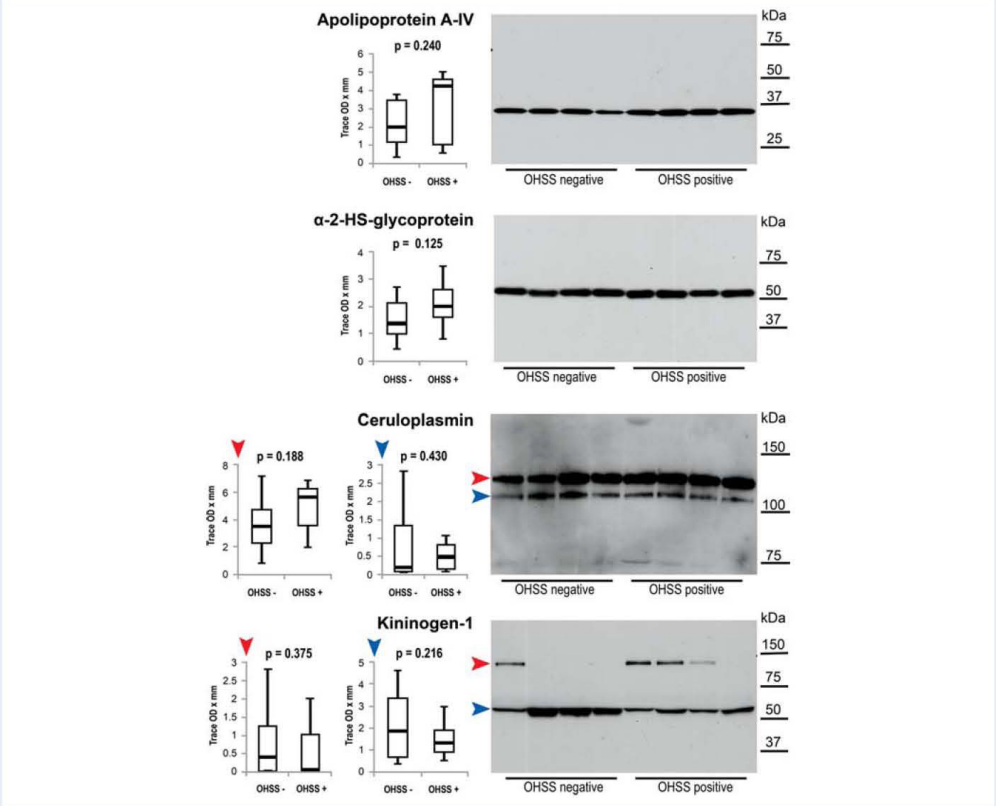


Figure 5 Immunoblot analysis of apolipoprotein A-IV, ceruloplasmin, alpha-2-HS-glycoprotein and kininogen-1 in samples of non-depleted FF of women undergoing IVF. Protein lysates prepared from samples of FF OFSS+ and OHSS− were examined on immunoblots using specific antibodies recognizing apolipoprotein A-IV, ceruloplasmin, alpha-2-HS-glycoprotein and kininogen-1. The protein bands were quantified using Quantity One software and distribution of the values was illustrated using box-plot. Significance of differences was calculated by Student *t*-test (*P*-value).

analyses. The non-depleted samples were separated using 1D SDS–PAGE followed by protein transfer and specific immunodetection. The representative results of 4 OHSS+ and 4 OHSS− samples of FF are shown in Fig. 5. The box-plots on the left side were created using optical density values for all 23 samples utilized in this study. The results demonstrated increase in the level of apolipoprotein A-IV, ceruloplasmin and apha-2-HS-glycoprotein in OHSS+ versus OHSS− FF samples whilst the level of kininogen-1 was lower in FF OHSS+ samples. Although the statistical evaluation did not find any significant differences at the level of *P*-value of ≤ 0.05, there was evident confirmation of the trends of protein changes observed by proteomic approaches with the probability varying from 57 to 88%. Many proteins present in fractionated spots or fractions may represent various forms (post-translationally modified, splicing variants, fragments etc.) of an individual protein. Hence, their possible quantitative differences found between samples may remain hidden or non-significant when detecting the total level of the same protein in the samples.

Computer modelling and simulation of possible interaction network connecting potential candidate proteins discriminating OHSS

Computer modelling techniques are very useful in examining the cellular pathways involved in maintaining the functions and cascades where many of the defined proteins may have a vital role to play. Identified proteins differentially regulated in FF from women undergoing IVF and suffering from severe form of OHSS (Protein/UniProt accession numbers provided in Table I) were introduced into a I2D

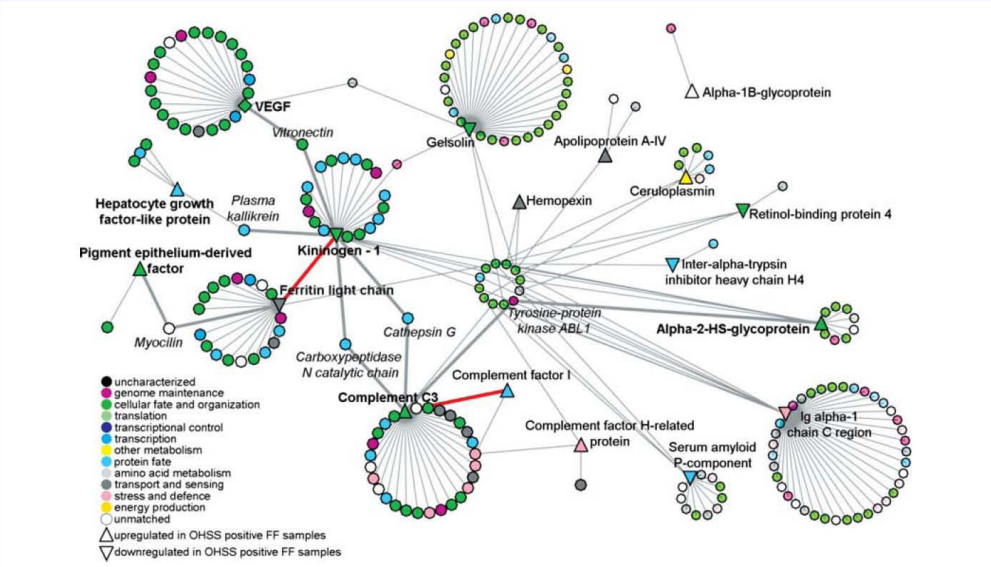


Figure 6 Computer modelling and simulation of possible interaction network connecting potential candidate proteins regulated during the development of severe OHSS. Network of possible protein–protein interactions, generated by querying I2D database and NAViGaTOR software for 16 identified proteins which were found to be regulated during the development of severe OHSS and VEGF. Some interacting proteins, with mediated interconnection are highlighted. Colour of nodes and edges represents Gene Ontology function.

database in order to identify possible interacting proteins and to construct protein–protein interaction networks enabling graphical visualization and possibly functional relationships amongst identified molecules (Fig. 6). The resulting interaction map contained in total 223 protein nodes and 240 interactions for the 16 proteins identified in this study and VEGF. Computer modelling highlighted the important role of kininogen-1 as an anchor for mediated interactions with other identified proteins such as complement C3 and Ig alpha-1 chain, VEGF, ferritin light chain and ceruloplasmin, hepatocyte growth factor-like protein as well as gelsolin, thus networking biological processes including inflammation and innate immunity, angiogenesis, iron transport and storage, blood coagulation and actin filament polymerization. The network revealed many other additional interacting proteins with possible role in OHSS, namely vitronectin (VTNC_HUMAN; P04004), cathepsin G (CATG_HUMAN; P08311) and carboxypeptidase N catalytic chain (CBPN_HUMAN; P15169), plasminogen (PLMN_HUMAN; P00747) and kallikrein (KLKB1_HUMAN, P03952). Contrary to the above, the apolipoprotoein A-IV (APOA4_HUMAN, P06727) and alpha-2-HS glycoprotein (FETUA_HUMAN, P02765; fetuin-A) remain segregated from this interaction network.

Discussion

A successful outcome from IVF depends on a preliminary phase of controlled ovarian hyperstimulation using exogenous gonadotrophins. The aim is to produce multiple follicles/oocytes without incurring the risk of OHSS. Currently, there is a lack of ability to predict success of the IVF treatment and better understanding of molecular processes might help increase IVF birth rate and at the same time avoid this life-threatening scenario which is associated with presence of inflammatory cytokines, neutrophil activation and increased capillary permeability (Orvieto, 2004; Orvieto *et al.*, 2006).

The milieu of FF is rich in hormones, growth factors, cytokines, anti-apoptotic factors, polysaccharides and various proteins which can give us a clue to the triggering of OHSS. Advances in -omics technologies, namely metabolomics and proteomics have helped immensely towards monitoring complex regulatory networks involved in ovarian physiology and responses to exogenous stimulation. Proteomic analyses of human FF identified a variety of proteins present in the FF and most of them were matched to plasma proteins (Spitzer *et al.*, 1996; Anahory *et al.*, 2002; Lee *et al.*, 2005; Angelucci *et al.*, 2006; Kim *et al.*, 2006; Schweigert *et al.*, 2006; Liu *et al.*, 2007; Hanrieder *et al.*, 2008; Estes *et al.*, 2009; Jarkovska *et al.*, 2010).

To our knowledge, this is the first study to date comparing the protein patterns of FF obtained from women suffering from severe form of OHSS and women with negligeble or mild symptoms of the disease. Our aim was to identify potential candidate proteins differentially represented in the two sample types used in our study and which may harbour parameters useful as 'handle' for identifying women at the risk of developing severe OHSS. Additionally, the interaction of

proteins might also help to increase our understanding of the molecular mechanisms involved in the progression of the disease. Firstly, we utilized an immunoaffinity system capable of removing 12 abundant blood plasma proteins and FF samples were processed using this system to remove plasma-matched follicular proteins. The proteins of flow-through fractions of FF were fractionated using a combination of two proteomic approaches and significant reproducible differences in protein composition of FF OFSS+ versus OHSS− were further analysed and identified by MS.

In summary, we identified a total of 19 candidate proteins differentially expressed between OHSS+ and OHSS− FF samples. Three proteins, namely ceruloplasmin, complement C3 and kininogen-1 were found using both 2D techniques. Several proteins including gelsolin, complement C3, serum amyloid P-component, ceruloplasmin and alpha-2-HS-glycoprotein were present in several protein spots or peaks with different pH indicating possible protein isoforms and/or post-translation modifications. In order to extrapolate both the functional interpretation as well as the validity of our proteomic findings, we utilized computer modelling to demonstrate that kininogen-1 may function as a key anchoring protein for other proteins participating in OHSS development and interacting with processes such as inflammation, angiogenesis, blood coagulation, iron transport and storage as well as innate immunity, cell adhesion and actin filament polymerization.

Kininogen-1 also known as high molecular weight kininogen (theoretical MW 72 kDa) is a multi-domain, multi-functional protein with middle concentration of around 80 μg/ml in plasma. It is known to play an important role in blood coagulation (Lalmanach *et al.*, 2010). Kininogen-1 is also a protein component of kallikrein–kinin system producing various mediators including mediators of inflammation and increased vascular permeability. The role of the kallikrein–kinin system in the pathophysiology of OHSS was suggested by Kobayashi *et al.* (1998) on the bases of the observation that OHSS ascites fluid caused microvascular hyperpermeability by a mechanism depending on kinin release. The association of the kinin–kallikrein system with the development of OHSS was also studied by Ujioka *et al.* (1998) on the rat model. Kallikrein cleaves kininogen-1 to pro-inflammatory kinins–bradykinin and cleaved kininogen. Bradykinin, in turn, is known to stimulate the release of mediators of pain and vascular dilation, whilst cleaved kininogen is involved in the release of elastase and superoxide. Importantly, cleaved kininogen induces release of pro-inflammatory cytokines TNF-α, IL-1β and IL-6 as well as chemokines IL-8 and MCP-1 from monocytes (Sainz *et al.*, 2007). Furthermore, computer simulation indicated that kallikrein may interact directly with hepatocyte growth factor-like protein, other protein differentially expressed in OHSS+ FF and also known as a macrophage stimulatory protein involved in macrophage activation (Suzuki *et al.*, 2008). Pro-inflammatory activities of bradykinin and cleaved kininogen are known to impact angiogenic activities and it is of interest that anti-angiogenic activity of cleaved kininogen can be blocked by binding ferritin (Coffman *et al.*, 2009; De Domenico *et al.*, 2009), thus allowing prevalence of pro-angiogenic activities of bradykinin and other molecules, which may subsequently lead to vessel formation (Coffman *et al.*, 2009). Ferritin, a direct binding partner of kininogen-1, similarly to cleaved kininogen, is recognized as an acute phase reactant and marker of both acute and chronic inflammation and known to increase in concentration 10–100-fold during inflammation (Coffman *et al.*, 2009). Another protein identified in our study was pigment epithelium-derived factor (PEDF), involved in inhibition of proliferation and cell migration of endothelial cells in ovaries (Cheung *et al.*, 2006). Recently, *in vivo* studies demonstrated anti-angiogenic properties of PEDF to inhibit VEGF mediated retina endothelial cell permeability through modulation of the Src kinase pathway (Sheikpranbabu *et al.*, 2010). Therefore, the tight regulation and direct or mediated interactions between the three proteins identified in this study, namely kininogen-1, ferritin and PEDF have strong implications in providing the balance between inflammatory process and angiogenesis, the two key processes that appear to be vital in the control of OHSS development. Taking into consideration the crucial role of VEGF in the increased endothelial/vessel permeability and development of OHSS, it was interesting to find an interconnecting link between VEGF and kininogen-1 mediated by vitronectin, a cell adhesion and spreading factor, thus confirming the role of cell adhesion proteins in the control of the angiogenesis in this study. Recent advances due to *in vitro* human cell co-culture model have successfully managed to show the paracrine effect of hCG on increase endothelial permeability by up-regulating VEGF in luteinized granulosa cells. This causes reduction of membrane-bound adhesion protein claudin 5 and impacts endothelial permeability (Rodewald *et al.*, 2009). In addition to the processes mentioned above that appear to play a central role in the development of severe OHSS, we also observed a relationship between kininogen-1 and complement component C3 mediated by cathepsin G and carboxypeptidase N catalytic chain. This provided a clear indication that the role of kininogen-1 and its associated processes can be extended to the control of innate immunity mediated by complement cascade. Whilst inhibition of complement activity in FF of women undergoing controlled ovarian hyperstimulation for IVF is critical in physiological folliculogenesis (Jarkovska *et al.*, 2010), it also appears to be implicated in the development of severe OHSS.

Additionally, we identified two other proteins in our study that were sequestered out of the above described network: apolipoprotein A-IV and alpha-2-HS-glycoprotein (fetuin-A). Apoa-IV is a major component of high density lipoprotein and chylomicron involved in lipid transportation. The regulation of this protein associated with the development of severe OHSS observed in this study indicated that lipid metabolism may be closely related to reproductive processes. Alpha-2-HS-glycoprotein (fetuin-A), a low abundant protein with normal levels in serum reaching around 300–600 pg/ml, is known to decrease during inflammation. Interestingly, inflammation itself stimulates the release of anti-inflammatory mediators, such as IL-10, steroids and spermine which in turn leads to activation of the acute phase response and decrease in fetuin-A level (Ombrellino *et al.*, 2001). Based on our finding of decreased level of kininogen-1, ferritin, and increased level of fetuin-A in severe OHSS+ women, we postulate that such changes are part of a counter-balancing response to the inflammatory process, which if not controlled, can have a detrimental effect on the patient and the therapy outcome.

Looking at the molecular processes underlying the pathogenesis of OHSS, the central role of inflammation and its tight link to angiogenesis was very evident. Furthermore, the contributions from innate immunity, transport mechanisms and cell adhesion played a significant part too. Biological variability is a common challenge in any study using limited number of patient samples in such discovery-related proteomic analyses because patient variability can simply lower or mask

many important qualitative and quantitative differences. Additionally, it is important to consider that not only do quantitative protein changes play an important role, but also that there may be various other parameters such as truncation and post-translational modification(s) of selected proteins impacting the overall picture. Hence, a combined group of several biomarkers would be more beneficial and reliable than a single protein as marker or indicator of the disease process and its onset. In this study, we propose a set of key proteins as potential biomarker candidates useful in the prognosis/diagnosis of the development of severe OHSS and for monitoring IVF therapy.

Larger, preferably multicentric joint collaborative studies on patient groups are necessary to confirm our findings. Hopefully, any positive outcome of such studies should advance our understanding of the processes involved in the onset of OHSS, as well as provide a direction for novel therapeutic interventions.

Supplementary data

Supplementary data are available at http://molehr.oxfordjournals.org/.

Authors' roles

H.K., J.M. and S.J.G. were responsible for the conception and design of this study. K.R. performed the sample collection and clinical data acquisition. K.J., H.K.S. and R.H. carried out the electrophoretic and liquid chromatography experiments whilst P.H. identified the differentially expressed proteins. The proteomic data were analysed and interpreted by K.J., R.H. and H.K.; K.J., P.H., R.H., J.M., K.R. contributed to drafting of the article and H.K.S., S.J.G. and H.K. critically revised the manuscript. All of the authors contributed to the final approval of the manuscript for publication.

Acknowledgements

Special thanks to A. Ekefjärd and D. Enetoft from Ludesi for providing Viper software.

Conflict of interest

With the recent acquisition of Millipore by Merck GmbH, and the usage of several biologicals for this study from previously Millipore (now Merck Millipore Bioscience) as well as Sigma Aldrich, all authors see no conflict of Interest. None of these companies had any other participating interests in this study. All participating authors declare that they have no competing interests.

Funding

This research was supported by Ministry of Health of the Czech Republic (NS9781-32009), and Institutional Research Concepts AV0Z50450515 (IAPG), AV0Z50200510 (IMIC).

References

Albert C, Garrido N, Mercader A, Rao CV, Remohi J, Simon C, Pellicer A. The role of endothelial cells in the pathogenesis of ovarian hyperstimulation syndrome. *Mol Hum Reprod* 2002;**8**:409–418.

Anahory T, Dechaud H, Bennes R, Marin P, Lamb NJ, Laoudj D. Identification of new proteins in follicular fluid of mature human follicles. *Electrophoresis* 2002;**23**:1197–1202.

Andersen AN, Goossens V, Bhattacharya S, Ferraretti AP, Kupka MS, de Mouzon J, Nygren KG. Assisted reproductive technology and intrauterine inseminations in Europe, 2005: results generated from European registers by ESHRE: ESHRE. The European IVF Monitoring Programme (EIM), for the European Society of Human Reproduction and Embryology (ESHRE). *Hum Reprod* 2009;**24**:1267–1287.

Angelucci S, Ciavardelli D, Di Giuseppe F, Eleuterio E, Sulpizio M, Tiboni GM, Giampietro F, Palumbo P, Di Ilio C. Proteome analysis of human follicular fluid. *Biochim Biophys Acta (BBA) - Proteins Proteomics* 2006;**1764**:1775–1785.

Boivin J, Bunting L, Collins JA, Nygren KG. International estimates of infertility prevalence and treatment-seeking: potential need and demand for infertility medical care. *Hum Reprod* 2007;**22**:1506–1512.

Chen SU, Chen CD, Yang YS. Ovarian hyperstimulation syndrome (OHSS): new strategies of prevention and treatment. *J Formos Med Assoc* 2008;**107**:509–512.

Chen SU, Chou CH, Lin CW, Lee H, Wu JC, Lu HF, Chen CD, Yang YS. Signal mechanisms of vascular endothelial growth factor and interleukin-8 in ovarian hyperstimulation syndrome: dopamine targets their common pathways. *Hum Reprod* 2010;**25**:757–767.

Cheung LW, Au SC, Cheung AN, Ngan HY, Tombran-Tink J, Auersperg N, Wong AS. Pigment epithelium-derived factor is estrogen sensitive and inhibits the growth of human ovarian cancer and ovarian surface epithelial cells. *Endocrinology* 2006;**147**:4179–4191.

Chipwete SE, Bugren S, Raffa N. Thrombosis post ovarian hyperstimulation. *Fertil Steril* 2009;**91**:1956.e13–1956.e14.

Coffman LG, Parsonage D, D'Agostino R Jr, Torti FM, Torti SV. Regulatory effects of ferritin on angiogenesis. *Proc Natl Acad Sci USA* 2009;**106**:570–575.

De Domenico I, Ward DM, Kaplan J. Serum ferritin regulates blood vessel formation: a role beyond iron storage. *Proc Natl Acad Sci USA* 2009;**106**:1683–1684.

de Mouzon J, Goossens V, Bhattacharya S, Castilla JA, Ferraretti AP, Korsak V, Kupka M, Nygren KG, Nyboe Andersen A; The European Ivf-monitoring Consortium ftESoHR. Assisted reproductive technology in Europe, 2006: results generated from European registers by ESHRE. *Hum Reprod* 2010;**25**:1851–1862.

Estes SJ, Ye B, Qiu W, Cramer D, Hornstein MD, Missmer SA. A proteomic analysis of IVF follicular fluid in women ≤32 years old. *Fertil Steril* 2009;**92**:1569–1578.

Fortune JE. Ovarian follicular growth and development in mammals. *Biol Reprod* 1994;**50**:225–232.

Gadher SJ, Jarkovska K, Kovarova H. Reproductive therapies and a need for potential biomarkers for prognostic and diagnostic screening of women desperate to conceive. *Expert Rev Proteomics* 2009;**6**:591–593.

Gerris J, Delvinge A, Olivennes F. *Ovarian Hyperstimulation Syndrome*. London, UK: Informa Healthcare, 2006.

Hanrieder J, Nyakas A, Naessen T, Bergquist J. Proteomic analysis of human follicular fluid using an alternative bottom-up approach. *J Proteome Res* 2008;**7**:443–449.

Huang L, Harvie G, Feitelson JS, Gramatikoff K, Herold DA, Allen DL, Amunngama R, Hagler RA, Pisano MR, Zhang WW *et al.* Immunoaffinity separation of plasma proteins by IgY microbeads: meeting the needs of proteomic sample preparation and analysis. *Proteomics* 2005;**5**:3314–3328.

Jarkovska K, Martinkova J, Liskova L, Halada P, Moos J, Rezabek K, Gadher SJ, Kovarova H. Proteome mining of human follicular fluid

reveals a crucial role of complement cascade and key biological pathways in women undergoing in vitro fertilization. *J Proteome Res* 2010;**9**:1289–1301.

Kim YS, Kim MS, Lee SH, Choi BC, Lim JM, Cha KY, Baek KH. Proteomic analysis of recurrent spontaneous abortion: identification of an inadequately expressed set of proteins in human follicular fluid. *Proteomics* 2006;**6**:3445–3454.

Kobayashi H, Okada Y, Asahina T, Gotoh J, Terao T. The kallikrein-kinin system, but not vascular endothelial growth factor, plays a role in the increased vascular permeability associated with ovarian hyperstimulation syndrome. *J Mol Endocrinol* 1998;**20**:363–374.

Lalmanach G, Naudin C, Lecaille F, Fritz H. Kininogens: More than cysteine protease inhibitors and kinin precursors. *Biochimie* 2010;**92**:1568–1579.

Lee HC, Lee SW, Lee KW, Cha KY, Kim KH, Lee S. Identification of new proteins in follicular fluid from mature human follicles by direct sample rehydration method of two-dimensional polyacrylamide gel electrophoresis. *J Korean Med Sci* 2005;**20**:456–460.

Lei ZM, Reshef E, Rao V. The expression of human chorionic gonadotropin/luteinizing hormone receptors in human endometrial and myometrial blood vessels. *J Clin Endocrinol Metab* 1992;**75**:651–659.

Liu T, Qian WJ, Mottaz HM, Gritsenko MA, Norbeck AD, Moore RJ, Purvine SO, Camp DG 2nd, Smith RD. Evaluation of multiprotein immunoaffinity subtraction for plasma proteomics and candidate biomarker discovery using mass spectrometry. *Mol Cell Proteomics* 2006;**5**:2167–2174.

Liu AX, Zhu YM, Luo Q, Wu YT, Gao HJ, Zhu XM, Xu CM, Huang HF. Specific peptide patterns of follicular fluids at different growth stages analyzed by matrix-assisted laser desorption/ionization time-of-flight mass spectrometry. *Biochim Biophys Acta* 2007;**1770**:29–38.

Merrilees DA, Kennedy-Smith A, Robinson RG. Obstructive uropathy as the etiology of renal failure in ovarian hyperstimulation syndrome. *Fertil Steril* 2008;**89**:992e991–992.

Moos J, Filova V, Pavelkova J, Moosova M, Peknicova J, Rezabek K. Follicular fluid and serum levels of inhibin A and pregnancy-associated plasma protein A in patients undergoing IVF. *Fertil Steril* 2009;**91**:1739–1744.

Nastri CO, Ferriani RA, Rocha IA, Martins WP. Ovarian hyperstimulation syndrome: pathophysiology and prevention. *J Assist Reprod Genet* 2010;**27**:121–128.

Navot D, Bergh PA, Laufer N. Ovarian hyperstimulation syndrome in novel reproductive technologies: prevention and treatment. *Fertil Steril* 1992;**58**:249–261.

Ombrellino M, Wang H, Yang H, Zhang M, Vishnubhakat J, Frazier A, Scher LA, Friedman SG, Tracey KJ. Fetuin, a negative acute phase protein, attenuates TNF synthesis and the innate inflammatory response to carrageenan. *Shock* 2001;**15**:181–185.

Orvieto R. Controlled ovarian hyperstimulation—an inflammatory state. *J Soc Gynecol Investig* 2004;**11**:424–426.

Orvieto R, Zagatsky I, Yulzari-Roll V, La Marca A, Fisch B. Substituting human chorionic gonadotropin by gonadotropin-releasing hormone agonist to trigger final follicular maturation, during controlled ovarian hyperstimulation, results in less systemic inflammation. *Gynecol Endocrinol* 2006;**22**:437–440.

Rao CV, Li X, Toth P, Lei ZM, Cook VD. Novel expression of functional human chorionic gonadotropin/luteinizing hormone receptor gene in human umbilical cords. *J Clin Endocrinol Metab* 1993;**77**:1706–1714.

Rodewald M, Herr D, Duncan WC, Fraser HM, Hack G, Konrad R, Gagsteiger F, Kreienberg R, Wulff C. Molecular mechanisms of ovarian hyperstimulation syndrome: paracrine reduction of endothelial claudin 5 by hCG in vitro is associated with increased endothelial permeability. *Hum Reprod* 2009;**24**:1191–1199.

Sainz IM, Pixley RA, Colman RW. Fifty years of research on the plasma kallikrein-kinin system: from protein structure and function to cell biology and in-vivo pathophysiology. *Thromb Haemost* 2007;**98**:77–83.

Schweigert FJ, Gericke B, Wolfram W, Kaisers U, Dudenhausen JW. Peptide and protein profiles in serum and follicular fluid of women undergoing IVF. *Hum Reprod* 2006;**21**:2960–2968.

Shalgi R, Kraicer P, Rimon A, Pinto M, Soferman N. Proteins of human follicular fluid: the blood-follicle barrier. *Fertil Steril* 1973;**24**:429–434.

Sheikpranbabu S, Ravinarayanan H, Elayappan B, Jongsun P, Gurunathan S. Pigment epithelium-derived factor inhibits vascular endothelial growth factor-and interleukin-1beta-induced vascular permeability and angiogenesis in retinal endothelial cells. *Vascul Pharmacol* 2010;**52**:84–94.

Shevchenko A, Wilm M, Vorm O, Mann M. Mass spectrometric sequencing of proteins silver-stained polyacrylamide gels. *Anal Chem* 1996;**68**:850–858.

Spitzer D, Murach KF, Lottspeich F, Staudach A, Illmensee K. Different protein patterns derived from follicular fluid of mature and immature human follicles. *Hum Reprod* 1996;**11**:798–807.

Suzuki Y, Funakoshi H, Machide M, Matsumoto K, Nakamura T. Regulation of cell migration and cytokine production by HGF-like protein (HLP)/macrophage stimulating protein (MSP) in primary microglia. *Biomed Res* 2008;**29**:77–84.

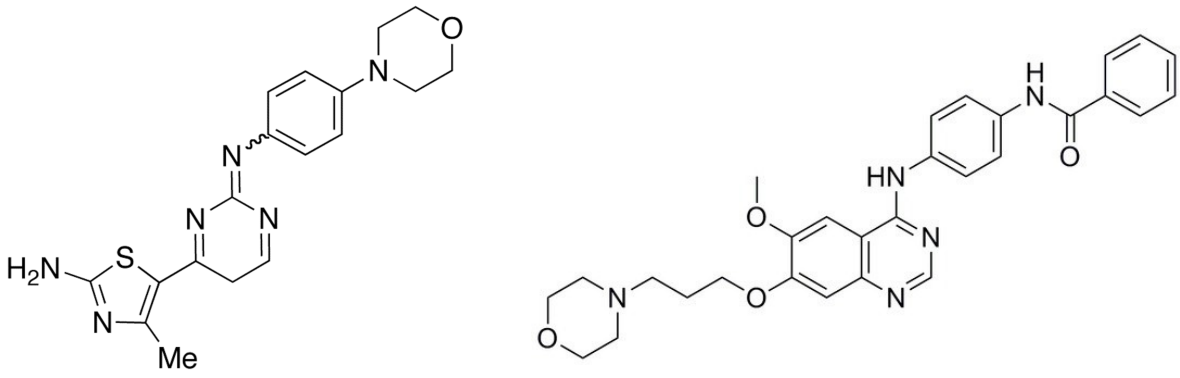
Ujioka T, Matsuura K, Tanaka N, Okamura H. Involvement of ovarian kinin-kallikrein system in the pathophysiology of ovarian hyperstimulation syndrome: studies in a rat model. *Hum Reprod* 1998;**13**:3009–3015.

Wulff C, Wilson H, Largue P, Duncan WC, Armstrong DG, Fraser HM. Angiogenesis in the human corpus luteum: localization and changes in angiopoietins, tie-2, and vascular endothelial growth factor messenger ribonucleic acid. *J Clin Endocrinol Metab* 2000;**85**:4302–4309.

5. Diskuze

5.1. Charakterizace mechanismů nádorové rezistence k působení inhibitorů Aurora kináz

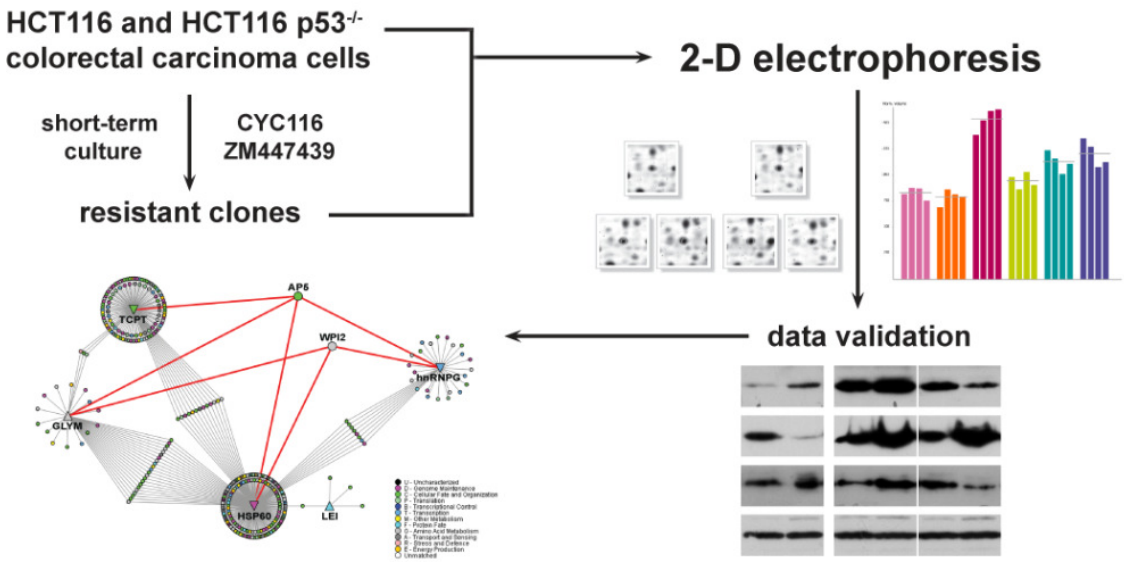
Současný trend staví do popředí nová biologická léčiva, která v kombinační terapii se zavedenými protinádorovými preparáty významně zvyšují úspěšnost léčby nádorových onemocnění a dávají tak naději onkologickým pacientům na potlačení progrese onemocnění, zlepšení kvality života nebo dokonce úplné vyléčení. Biologická léčba je namířená proti specifickým molekulám jako jsou např. proteinkinázy, enzymy důležité pro karcinogenezi a růst nádorů. V onkologické praxi se používají pro inhibici proteinkináz nízkomolekulární organické látky nebo monoklonální protilátky, které se vážou s vysokou afinitou na příslušné molekuly přítomné v učitých tkáních. Aurora kinázy jsou významné onkoproteiny jejichž součinnost je klíčová pro kontrolu mitózy (Kollareddy et al. 2008). Odchylky v expresi AURK se nachází u různých typů nádorů a do klinických zkoušek proto byla zařazena léčiva inhibující jejich funkci. V této práci byl testován nízkomolekulární inhibitor **CYC116** (obr. 7), jehož protinádorový účinek vychází z inhibice AURK-A, B, C, a také receptoru pro VEGF-2 (Kollareddy et al. 2012; Wang et al. 2010). Dále jsme použili inhibitor **ZM447439** (obr. 7), který se již mnoho let používá pro studium funkce AURK a spolehlivě inhibuje AURK-A a AURK-B (Ditchfield et al. 2003). Zatímco biologicky dostupný inhibitor CYC116 postoupil do klinického testování, ZM447439 neuspěl v preklinických zkouškách a zůstává tak modelovým inhibitorem AURK.



Obrázek 7. Strukturní vzorec inhibitorů AURK (CYC116, ZM447439).

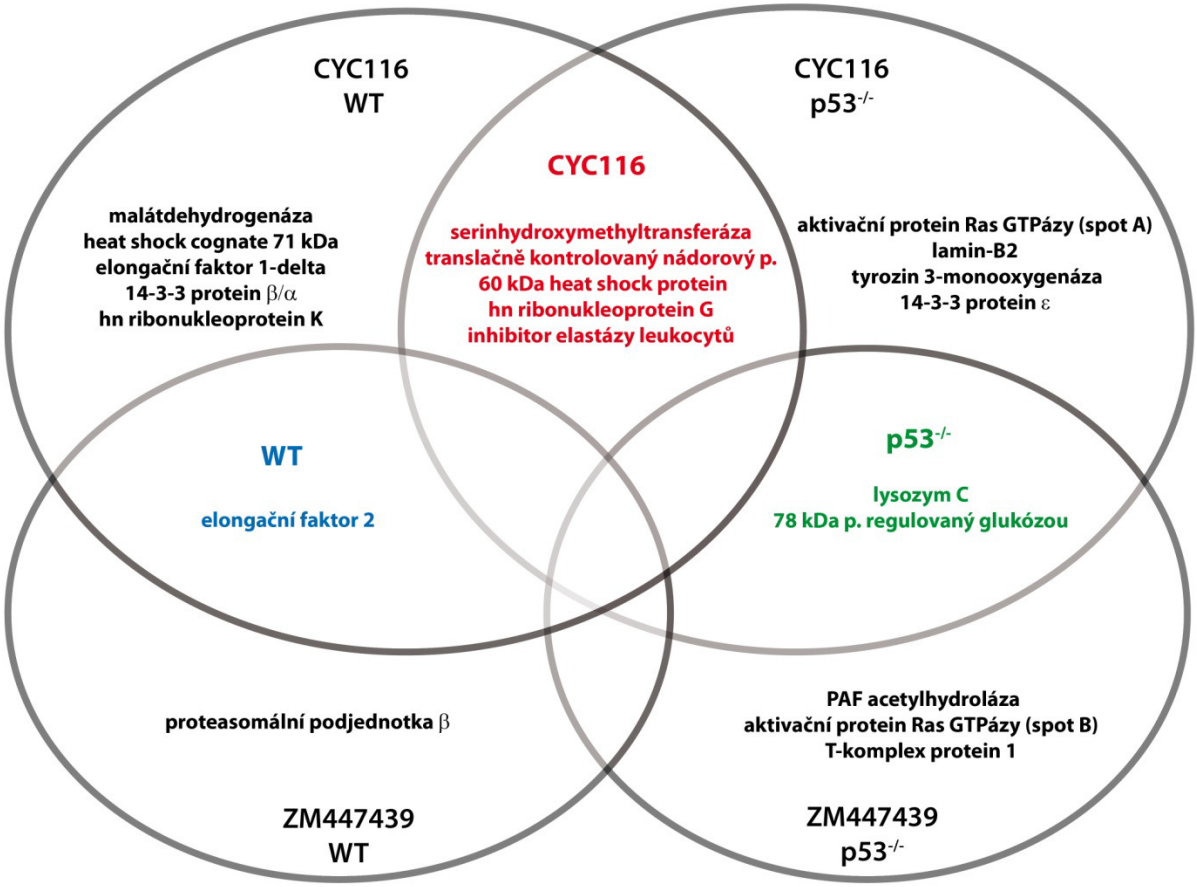
Účinnost protinádorové léčby závísí na molekulární výbavě nádorových buněk, které mohou rozvíjet rezistenci. Ta představuje hlavní problém protinádorové léčby a může značně komplikovat probíhající léčbu i aplikaci dalších léků. Bylo prokázáno, že mutace proteinu p53, který kontroluje buněčné dělení a apotózu, vedou ke karcinogenezi a zvyšují rezistenci na protinádorovou léčbu (Gasco and Crook 2003). Popsané byly také interakce AURK s p53 a jejich velmi křehká funkční rovnováha. Protein p53 potlačuje onkogenní aktivitu AURK (S. S. Chen et al. 2002). AURK-A je zároveň klíčový protein regulace p53 a její zvýšená hladina způsobuje degradaci p53 a přispívá tak ke karcinogenezi (Katayama et al. 2004). Inhibitory AURK by mohly najít uplatnění v léčbě nádorových onemocnění s mutací p53, protože apoptóza způsobená touto inhibicí na p53 nezávisí (den Hollander et al. 2010). Další studie ale ukázaly, že buňky bez funkčního p53 získávají určitou výhodu při inhibici AURK-A a buňky s wild-type p53 dokonce omezují jeho aktivitu (Mao et al. 2007). Otázkou však zůstává vliv p53 na rozvoj rezistence k působení inhibitorů AURK.

Pro charakterizaci nádorové rezistence jsme použili buňky kolorektálního karcinomu HCT116 rezistentní k působení inhibitorů CYC116 a ZM447439 a tyto buňky buď měly (**HCT116 wild-type**) či neměly exprimovaný protein p53 (**HCT116 p53$^{-/-}$**). Rezistentní buňky byly ustaveny krátkodobou kultivací ve vysoké dávce léčiva a od každého fenotypu byly analyzovány 2 rezistentní klony. Celkem jsme tedy porovnávali 8 rezistentních klonů (2x CYC116 wild-type, 2x CYC116 p53$^{-/-}$, 2x ZM447439 wild-type, 2x ZM447439 p53$^{-/-}$) a 2 senzitivní linie (wild-type, p53$^{-/-}$). Buňky jsme lyzovali a extrahované proteiny separovali pomocí **2DE v pH gradientu 4–7 a 6–11**. Diferenční proteiny jsme identifikovali pomocí hmotnostního spektrometru **MALDI-TOF/TOF** a vybrané změny proteinů jsme ověřili pomocí specifických protilátek a **WB** (obr. 8). Do validačních experimentů jsme zařadili také leukemické buňky **CCRF-CEM** a buňky adenokarcinomu plic **A549** rezistentní k působení protinádorových léčiv s různou strukturou a mechanismem účinku. Zatímco buňky A549 protein p53 exprimují (L. Zhang et al. 2009), u buněk CCRF-CEM byly popsány mutace tohoto proteinu (Cheng and Haas 1990).



Obrázek 8. Schéma experimentu (grafické znázornění) v publikaci *Cancer Cell Resistance to Aurora Kinase Inhibitors: Identification of Novel Targets for Cancer Therapy.*

Zjistili jsme, že při rozvoji rezistence na inhibitory AURK dochází k regulaci buněčného metabolismu, což bylo popsáno již dříve ve spoustě prací studujících nádorovou rezistenci (J. T. Zhang and Liu 2007). My jsme se zaměřili na kvantitativní změny související více s regulací proliferace a apoptózy a méně s obecnou odpovědí nádorových buněk na cytotoxické podmínky, k čemuž významně přispěl plán studie a použití více klonů. Mohli jsme tak z výsledků "odfiltrovat" individuální odpověď jednotlivých klonů a dostat se k jádru věci. Pozorováním překryvu mezi různými fenotypy se podařilo zredukovat skupinu 144 diferenčních proteinů na 21 relevantních změn v expresi proteinů (obr. 9). Identifikovali jsme pět proteinů typických pro rezistenci k působení CYC116 bez patrného vlivu exprese p53, jediný protein charakteristický pro všechny rezistentní buňky s p53 wild-type fenotypem a dva proteiny související s rozvojem rezistence u všech buněk s mutovaným p53. Kupodivu jsme nenašli žádný protein typických pouze pro p53-nezávislou rezistenci k působení ZM447439. Dále jsme identifikovali celkem 13 proteinů, jejichž změny byly závislé na p53 a vyskytovaly se pouze u CYC116 nebo ZM447439.



Obrázek 9. Překryv kvantitativních změn u buněk HCT116 rezistentních k působení AURK. Podle tabulky 1, 2 a 3 v publikaci *Cancer Cell Resistance to Aurora Kinase Inhibitors: Identification of Novel Targets for Cancer Therapy.*

V tomto úzkém výběru signifikantních změn byly proteiny měnící svou hladinu několikanásobně, ale také proteiny s menšími rozdíly v expresi, ale za to velkým biologickým významem. Kvantitativní změny byly mnohem výraznější u buněk rezistentních k působení CYC116, který je účinný v řádově nižších koncentracích oproti ZM447439 (Kollareddy et al. 2012), a některé proteiny byly u CYC116 specificky regulované navzdory rozdílnému stavu p53. Usuzujeme tedy, že buňky odpovídají na různé inhibitory odlišným způsobem a rezistenci rozvíjí odlišnými mechanismy. Na základě recentních publikací jsme diskutovali nalezené změny a navrhli molekulární mechanismy rozvoje rezistence na inhibitory AURK. Pro získání komplexnějšího pohledu na rezistenci k působení CYC116 jsme proteiny analyzovali pomocí softwaru NAVIGaTOR. Zjistili jsme, že proteiny mezi sebou udržují vysoký stupeň komunikace, která může být přímo zprostředkována autofagickými proteiny AP5 a WPI2 (obr. 8). Autofagie, lysozomální degradace cytoplazmických organel a proteinů,

je často aktivovaná v nádorových buňkách (Mizushima and Klionsky 2007) a podle našich výsledků přispívá k rozvoji specifické rezistence k působení CYC116.

V rámci verifikačních experimentů jsme jednoznačně potvrdili, že enzym serinhydroxymethyltransferáza, který svou katalýzou poskytuje hydroxymethylovou skupinu tetrahydrofolátu pro syntézu purinů, je s nejvyšší pravděpodobností stimulován nádorovými buňkami a zajišťuje tak navzdory ošetření inhibitorem CYC116 dostatek purinů pro replikaci DNA, důležitý krok buněčného dělení. Hladina tohoto enzymu byla zvýšená také u buněk CCRF-CEM a A549 rezistentních k působení protinádorových léčiv s odlišným mechanismem účinku. U rezistentních buněk HCT116, CCRF-CEM a A549 jsme našli také zvýšenou hladinu serpinu B5, který byl overexprimovaný u většiny klonů rezistentních k působení inhibitorů AURK. Serpin B5 pravděpodobně nepodporuje proliferaci nádorových buněk, ale brání jejich apoptóze, jak již bylo pozorováno u kolorektálního karcinomu (Payne et al. 2011). Serpin B5 a serinhydroxymethyltransferáza byly výrazně overexprimované u nádorových buněk různého histogenetického původu a rezistentních na různá protinádorová léčiva. Nazávisle na přítomnosti p53 tyto proteiny společně podporují progresi nádoru a představují proto potenciální cíle pro vývoj nových léčiv.

V naší studii jsme identifikovali i další proteiny regulující apoptózu a podařilo se nám ověřit zvýšenou hladinu calretininu a voltage-dependent anion-selective channel protein 2. Calretinin a voltage-dependent anion-selective channel protein 2 ovlivňují osud buněk a podporují jejich přežívání na úrovni regulace hladiny vápníku a prostupnosti mitochondriální membrány, což jsou klíčové procesy apoptózy. Calretinin a voltage-dependent anion-selective channel protein 2 byly detekovatelné pouze v buňkách odvozených ze solidních nádorů (HCT116, A549) a představují proto potenciální cíle pro léčiva, která by mohla ovlivnit aktivitu těchto proteinů v solidních nádorech.

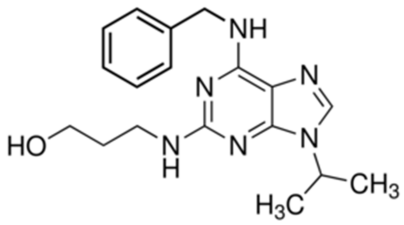
Jediný protein regulovaný ve všech buňkách s p53 je elongační faktor 2. Pokles hladiny tohoto proteinu jsme pozorovali u buněk rezistentních k působení jak ZM447439 tak CYC116. Elongační faktor 2 určuje translaci různých proteinů a jeho exprese i aktivita závisí na cytoplazmatické asociaci s p53 (Yin et al. 2003). Při rozvoji rezistence v nádorových buňkách je pravděpodobně narušena interakce p53 a elongačního faktoru 2 a buňky tak brání vzniku proteinů potřebných pro apoptózu indukovanou AURK inhibitory. Buňky s mutovaným p53 reagují při rozvoji rezistence zvýšenou expresí lysozymu C, který chrání buňky před poškozením oxidačním stresem (Liu et al. 2006) a pomáhá tak odolávat účinku inhibitorů CYC116 a ZM447439. Specificky regulovaná byla u mutovaných buněk také hladina 78 kDa proteinu regulovaného glukózou. Ten byl už u rezistentních nádorových

buněk popsán a kromě vlivu na oxidační stres má také anti-apoptotické účinky (Chang et al. 2012).

Protinádorová léčba vychází ze statistického hodnocení různých léčebných režimů. Pro stratifikaci onkologických pacientů a personalizaci léčby je třeba najít prediktivní markery a markery pro monitorování léčby. Serpin B5 a calretinin patřily v naší studii k proteinům s nejvyšším nárůstem exprese ve většině rezistentních buněk. Serpin B5 je navíc protein sekretovaný buňkami do extracelulárního prostoru a je proto velká šance na jeho detekci v tekutině obklopující nádorové buňky nebo dokonce v plazmě pacientů. Na tyto proteiny by měla být zaměřena pozornost při terapii.

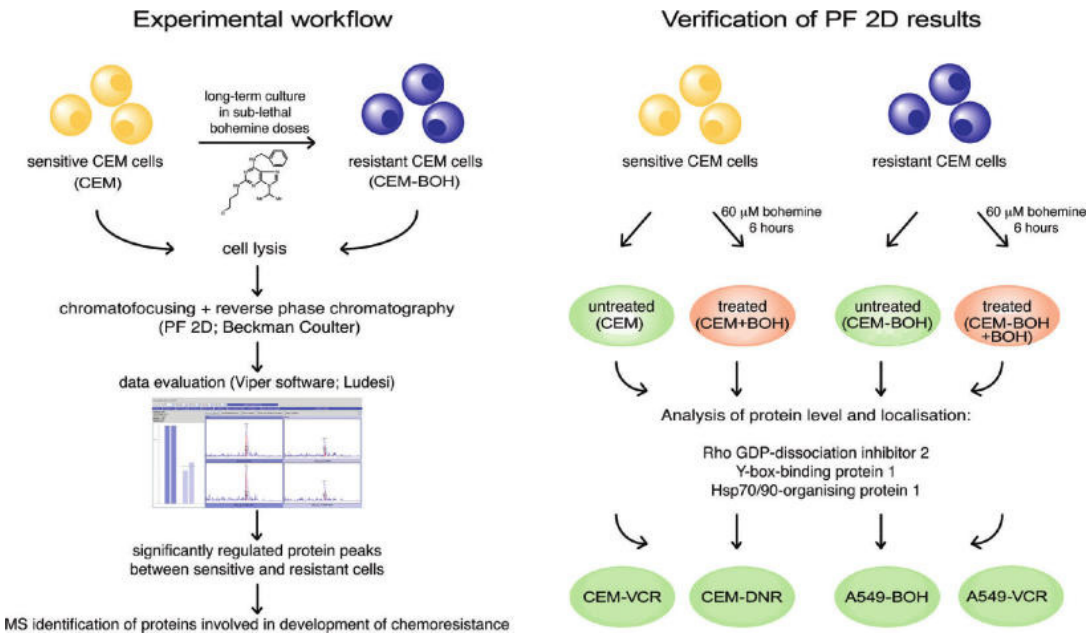
5.2. Charakterizace mechanismů nádorové rezistence k působení inhibitorů cyklin-dependentních kináz

Snížení aktivity CDK pomocí syntetických inhibitorů představuje slibnou strategii v léčbě nádorových onemocnění (Rizzolio et al. 2010). V další studii byl proto testován nízkomolekulární **bohemin** odvozený ze struktury olomoucinu (obr. 10), jehož účinek vychází z inhibice CDK a má za následek narušení metabolismu buněk, epigenetickou regulaci a útlum proliferační aktivity nádorových buněk (Kovarova et al. 2000; Kovarova et al. 2002; Skalnikova et al. 2005).



Obrázek 10. Strukturní vzorec boheminu.

Rezistence byla ustavena pomocí protokolu dlouhodobé kultivace v subletální dávce léčiva. T-lymfoblastické leukemické buňky **CCRF-CEM rezistentní** k působení boheminu jsme analyzovali pomocí **2D-LC** a do experimentu jsme zařadili také **senzitivní buňky ošetřené boheminem a rezistentní buňky ošetřené boheminem.** Diferenční proteiny jsme identifikovali pomocí hmotnostního spektrometru **MALDI-TOF/TOF** a vybrané změny proteinů jsme ověřili pomocí **WB** a **imunohistochemie** (obr. 11). Do validačních experimentů jsme zařadili také další buňky **CCRF-CEM** a buňky adenokarcinomu plic **A549** rezistentní k působení protinádorových léčiv s různou strukturou a mechanismem účinku.

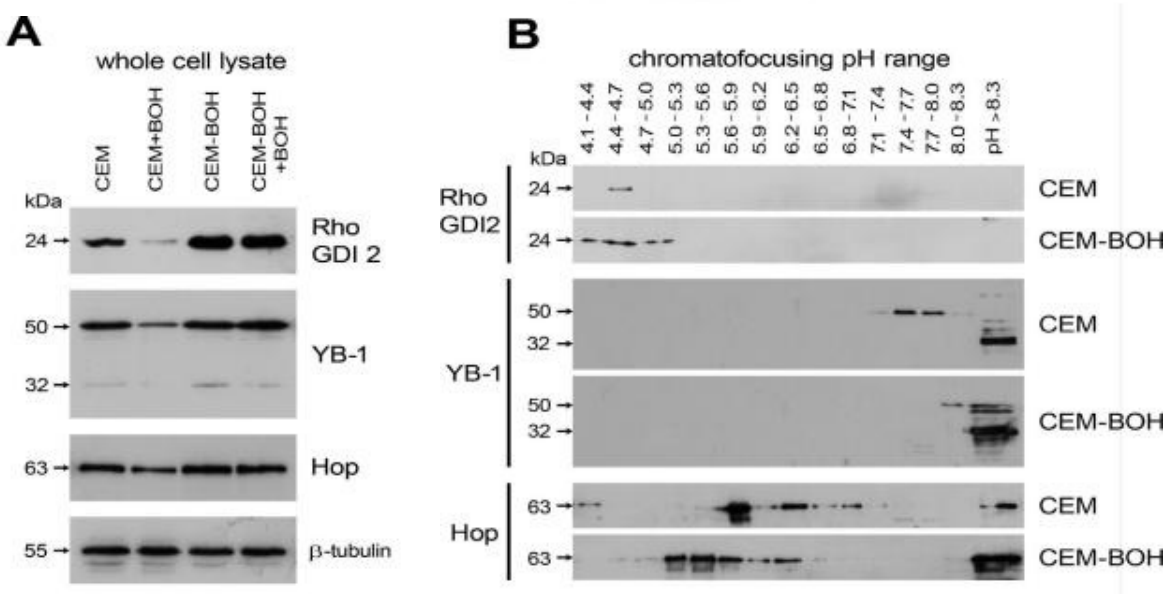


Obrázek 11. Schéma experimentu (obr. 1) v publikaci *Cancer Drug-Resistance and a Look at Specific Proteins: Rho GDP-Dissociation Inhibitor 2, Y-Box Binding Protein 1 and HSP70/90 Organizing Protein in Proteomics Clinical Application.*

Identifikovali jsme 26 diferenčních proteinů, nejčastěji se jednalo o ribosomální proteiny a histony. Pro verifikace nalezených změn jsme vybrali proteiny, jejichž funkce by mohly objasnit mechanismy rozvoje rezistence. Zajímavé bylo, že hladina všech verifikovaných proteinů klesala po ošetření boheminem a po ustavení rezistence už zůstala konstantní (obr. 12A). Na úrovni celobuněčného lyzátu se však v rezistentních buňkách podařilo potvrdit pouze zvýšenou expresi Rho GDP-disociačního inhibitoru 2 (z angl. *Rho GDP-Dissociation Inhibitor 2*, Rho GDI2) (obr. 12A). Tento protein patří do rodiny proteinů regulujících GTPázy. Studie na jedné straně ukazují, že exprese Rho GDI2 je úzce spjata s invazivitou a metastatickým potenciálem celé řady nádorových onemocnění (Fujita et al. 2012; Gildea et al. 2002; Cho et al. 2009), zatímco jiné práce demonstrují pozitivní protinádorové účinky Rho GDI2 (Schunke et al. 2007; Theodorescu et al. 2004). Úloha Rho GDI2 v rozvoji rezistence pravděpodobně spočívá v jeho anti-apoptotickém účinku prostřednictvím inhibice Ras a c-Jun (Goto et al. 2006).

Zvýšenou expresi Y-Box vázajícího proteinu 1 (z angl. *Y-Box-Binding Protein 1,* YB-1) a proteinu organizujícího Hsc70/Hsp90 (z angl. *Hsc70/Hsp90-Organizing Protein,* Hop) jsme na celobuněčné úrovni nepotvrdili (obr. 12A) a rozhodli jsme se proto podívat na jejich hladinu v jednotlivých pH frakcích 2D-LC (obr. 12B). Tento přístup odhalil zajímavé rozdíly v hladině YB-1 a Hop závislé na pI těchto proteinů. Post-translační modifikace významně ovlivňují izoelektrické vlastnosti proteinů a naše výsledky proto naznačují, že

rozvoj rezistence k působení boheminu určují specifické formy YB-1 a Hop. Fosforylace patří mezi nejčastější PTM, která prostřednictvím konformačních změn proteinů reguluje důležité buněčné procesy. Každá taková PTM nahrazuje neutrální hydroxylovou skupinu za negativně nabitou fosfátovou skupinu. V rozsahu pH 5,5–7,5 uděluje fosforylace 1–2 negativní náboje a způsobuje tak snížení pI proteinu (Halligan 2009). Teoretické pI proteinu Hop je 6,40 a jsou u něj známa 4 fosforylační místa. U senzitivních i rezistentních buněk jsme detekovali Hop ve frakci 6,2–6,5 a s rozvojem rezistence docházelo k posunu do kyselejší části gradientu (do pH okolo 5,0–5,6), tedy k potenciální fosforylaci (obr. 12B). Studie ukázaly, že fosforylace proteinu Hop ovlivňuje buněčnou lokalizaci a inhibice cdc2 pomocí olomoucinu, který je svou strukturou velmi podobný boheminu, způsobuje akumulaci Hop v jádře (Daniel et al. 2008; Longshaw et al. 2004). Pomocí imunohistochemie jsme zjistili, že ošetření senzitivních buněk CCRF-CEM boheminem opravdu způsobuje translokaci proteinu Hop do jádra a tento mechanismus rezistentní buňky postrádají. Úloha proteinu Hop v rezistenci k působení boheminu nemusí spočívat v pouhé organizaci Hsc70/Hsp90, ale také v interakci s dalšími proteiny (Arruda-Carvalho et al. 2007; Odunuga et al. 2004).



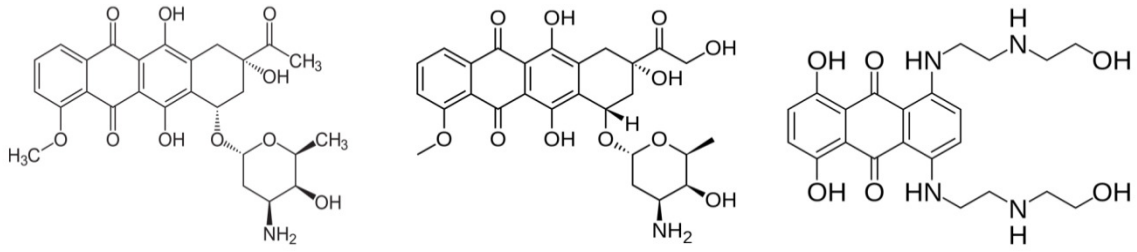
Obrázek 12. Verifikace výsledků pomocí WB (obr. 4) v publikaci *Cancer Drug-Resistance and a Look at Specific Proteins: Rho GDP-Dissociation Inhibitor 2, Y-Box Binding Protein 1 and HSP70/90 Organizing Protein in Proteomics Clinical Application.*

Protein YB-1 má 8 známých fosyforylačních míst a v našem modelu docházelo s rozvojem rezistence k přesunu do bazické části (z pH přibližně 7,5 do pH okolo 8,1;

obr. 12B), což by mohlo poukazovat na defosforylaci YB-1. Existuje však celá řada PTM, které sice nejsou tak běžné, ale mohou také způsobit změnu pI (Barrabes et al. 2010; Gauci et al. 2008; Nagai et al. 2012). Další otázka vyvstává s faktem, že teoretické pI proteinu YB-1 je 9,9 a jeho MW je přibližně 36 kDa. Jak je vidět na obrázku 12B, nejvyšší hladina YB-1 byla opravdu ve frakci pH > 8.3 s MW okolo 36 kDa. Fosforylace však nemůže způsobit dvojnásobný nárůst MW, protože by v případě YB-1 znamela navázání přibližně 450 fosfátových skupin, což převyšuje celkový počet aminokyselin tohoto proteinu. Spíše než jiná modifikace by zde mohlo hrát roli navázání dalšího proteinu např. APEX1, který v komplexu s YB-1 přispívá k rozvoji MDR (Chattopadhyay et al. 2008). Aktivitu a subcelulární lokalizaci YB-1 reguluje nejen fosforylace ale také štěpení pomocí proteasomu (Bader and Vogt 2008; Sorokin et al. 2005). Zkrácenou formu YB-1 o MW přibližně 20 kDa jsme pozorovali u CCRF-CEM buněk rezistentních k působení boheminu, daunorubicinu a vinkristinu, ale také u buněk A549 rezistentních na bohemin. Přítomnost zkrácené formy YB-1 v nádorových buňkách pravděpodobně ukazuje špatnou prognózu a již zmíněný rozvoj MDR (Bargou et al. 1997; Oda et al. 2003).

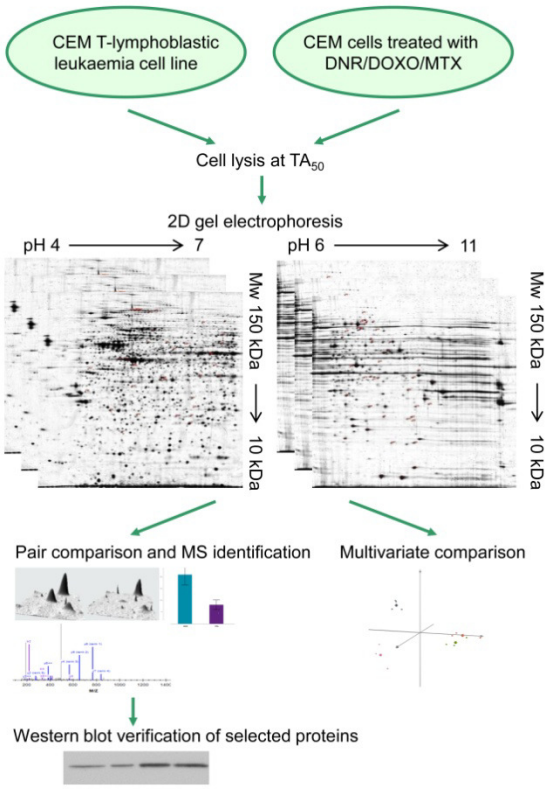
5.3. Charakterizace mechanismů působení antracyklinů na nádorové buňky

Antracyklinová antibiotika se používají k účinné léčbě celé řady onkologických onemocnění. V této práci jsme se zabývali účinkem antracyklinů, **daunorubicinu** a **doxorubicinu**, a také antracyklinového analogu, **mitoxantronu**. Tato léčiva mají velmi podobnou strukturu (obr. 13) ale odlišné aplikace v onkologické léčbě. Jejich mechanismus účinku tedy pravděpodobně nevychází z pouhé interkalace DNA, inhibice topoisomerázy II a tvorby kyslíkových radikálů.



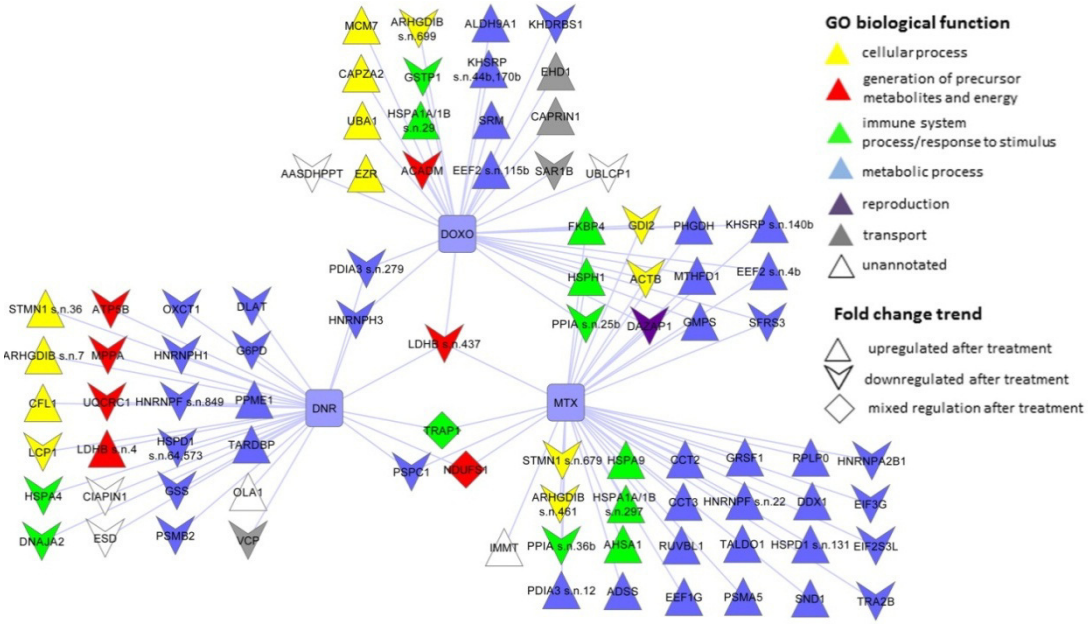
Obrázek 13. Strukturní vzorec daunorubicinu, doxorubicinu a mitoxantronu.

Design studie spočíval v kvantitativním porovnání proteomu buněk **CCRF-CEM** po **ošetření antracykliny**. Abychom zachytili časnou odpověď nádorových buněk, vystavili jsme je krátkodobě (**poloviční čas do spuštění apoptózy**) působení vysoké dávky léčiv (10 × IC50) a následovala analýza pomocí **2DE v pH gradientu 4–7 a 6–11** (obr. 14). Diferenční proteiny jsme identifikovali pomocí hmotnostního spektrometru **MALDI-TOF/TOF** a vybrané změny proteinů jsme ověřili pomocí **WB**. Důležitým nástrojem pro objektivní klasifikaci účinků byla multivariační analýza kvantitativních změn proteinů. Pro identifikaci mechanismů specifických pro antracykliny jsme do analýzy zařadili také cisplatinu a paklitaxel s odlišnými mechanismy účinku. Tento přístup nám pomohl "odfiltrovat" změny v expresi doprovázející obecnou protinádorovou odpověď.



Obrázek 14. Schéma experimentu (grafické znázornění) v publikaci *Cancer Cell Response to Anthracyclines effects: Mysteries of the Hidden Proteins Associated with these Drugs.*

Podle očekávání nebyly nalezené kvantitativní změny velké a týkaly se pouze 1–2 % všech detekovaných proteinů. Jejich ověření pomocí WB často vyžadovalo pro přesnější kvantifikaci místo klasické chemiluminiscence fluorescenční detekci. Výsledky párového vyhodnocení ukázaly významný překryv kvantitativních změn mezi doxorubicinem a mitoxantronem a velmi malý překryv s daunorubicinem (obr. 15). Tento jev potvrdila i multivariační analýza PCA, která oddělila daunorubicin nejen od ostatních antracyklinů, ale také od cisplatiny a paklitaxelu.



Obrázek 15. Překryv kvantitativních změn u buněk CCRF-CEM po ošetření antracykliny (obr. 3) v publikaci *Cancer Cell Response to Anthracyclines effects: Mysteries of the Hidden Proteins Associated with these Drugs.*

Klasifikace podle Gene Ontology pomocí softwaru PANTHER ukázala, že nejvíce regulovaných proteinů se účastní metabolických procesů. Tyto změny demonstrují jak protinádorový efekt, tak snahu nádorových buněk překonat účinky léčby a pokračovat v proliferaci. Po ošetření daunorubicinem jsme pozorovali specificky regulovanou hladinu TAR DNA-vázajícího proteinu 43, který se účastní biogeneze miRNA, apoptózy a dělení buněk (Kawahara and Mieda-Sato 2012). Tento protein byl dříve popsán pouze v kontextu neurodegenerativního poškození (Warraich et al. 2010) a naše výsledky ukazují, že jeho vyšší hladina může doprovázet také poškození nádorových buněk během terapie daunorubicinem. Po ošetření daunorubicinem byl narušený také energetický metabolismu buněk.

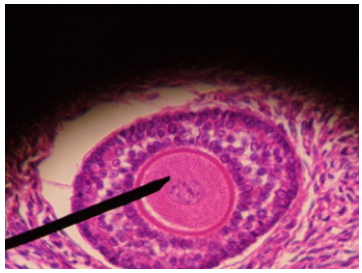
Důležitou roli po ošetření doxorubicinem sehrál enzym spermidinsyntáza, jehož zvýšená hladina ukazuje snahu buněk rozvinout rezistenci prostřednictvím spermidinu, který vychytává volné radikály a brání tak oxidačnímu poškození (Johnson et al. 2012; Nilsson et al. 2000). U buněk ošetřených doxorubicinem nebo mitoxanronem jsme pozorovali signifikantně zvýšenou hladinu regulačních proteinů C-1-tetrahydrofolátsyntázy a proteinu RuvB-like 1. Zatímco, tetrahydrofolátsyntáza je klíčová pro regulaci syntézy purinů, aminokyselin a proteinů, protein RuvB-like 1 reguluje transkripci, replikaci a opravu DNA. Metabolické změny byly po ošetření mitoxantronem nejvýznamnější a specificky regulovaná byla také hladina peptidyl-prolyl cis-trans izomerázy FKBP4. Ta byla nedávno označena jako prediktivní marker nádorové rezistence (Yang et al. 2012).

Velmi důležitou úlohu sehrály opět formy proteinů, např. elongačního faktoru 2 a laktátdehydrogenázy B. Výsledky této práce velmi dobře dokládají, jak nádorové buňky po ošetření léčivem využívají specifické varianty proteinů. I přes značnou strukturální podobnost odpovídaly buňky na působení doxorubicinu zvýšenou hladinou bazické i kyselejší formy elongačního faktoru 2, zatímco po působení mitoxantronu vykazovaly buňky pouze vysokou hladinu kyselejší formy proteinu. Elongační faktor 2 reguluje syntézu celé řady proteinů. Fosforylace vede k jeho inaktivaci a může být zprostředkována různými kinázami, jejichž cílená inhibice má protinádorové účinky (Z. Chen et al. 2011). Pokud je kyselejší forma elongačního faktoru 2 fosforylovaná, přispívá s nejvyšší pravděpodobností k protinádorovému účinku. Zvýšená hladina bazické formy pak ukazuje snahu nádorových buněk o zachování syntézy proteinů. Elongační faktor 2 byl regulovaný také u buněk HCT116 rezistentních k působení inhibitorů AURK a patří dokonce mezi nejčastěji regulované proteiny v proteomických experimentech (Petrak et al. 2008). Další změny specifických forem jsme pozorovali u laktátdehydrogenázy B. Jednalo se o jedinou kvantitativní změnu společnou pro všechna antracyklinová léčiva. V tomto případě docházelo k regulaci různými směry, kde nízká hladina kyselejší formy byla společná pro všechny druhy ošetření a vyšší hladina bazické formy byla typická pouze pro daunorubicin. Hladina laktátdehydrogenázy B by mohla být rozhodující pro výsledný protinádorový účinek.

5.4. Analýza reálných biologických vzorků v rámci hledání kandidátních proteinů pro včasnou diagnostiku ovariálního hyperstimulačního syndromu

V tomto projektu jsme mohli využít naše zkušenosti s kvantitativní proteomikou a získali jsme nové zkušenosti s deplecí majoritních proteinů. V rámci studia reálných biologických vzorků jsme analyzovali folikulární tekutinu pacientek centra pro asistovanou reprodukci. Ve folikulární tekutině jsme hledali kandidátní proteiny pro včasnou diagnostiku OHSS. Tento syndrom je doprovázen cystickým zvětšením vaječníků, zvýšenou prostupností kapilár a může způsobit vážné zdravotní problémy, např. ascites, poruchy hemodynamiky nebo dokonce selhání ledvin (De Neubourg and Gerris 2005). **Hormonální stimulace** byla provedena podle standardního protokolu. Po aplikaci agonistů GnRH (z angl. *Gonadotropin-Releasing Hormone*, krátký protokol) nebo antagonistů GnRH (dlouhý protokol) společně s hCG (z angl. *Human Chorionic Gonadotropin*) došlo k hyperstimulaci FSH (z angl. *Follicle-Stimulating Hormone*) a zrání folikulů.

S informovaným souhlasem byly pacientkám po 36 hodinách odebrány ovariální folikuly včetně tekutiny, která byla po izolaci oocytu zbavena zbytků buněk pomocí centrifugace a bezprostředně zamražena (-70 °C). Folikuly měly průměr 14–22 mm a pro analýzu jsme použili pouze **folikulární tekutinu** bez makroskopické kontaminace. Celkem jsme analyzovali 31 vzorků rozdělených do skupin: a) těžký OHSS (OHSS+, 13), b) asymptomatický průběh (OHSS- , 18).



Obrázek 16. Lidský ovariální folikul (převzato z http://en.wikipedia.org/).

Abychom snížili dynamický rozsah koncentrací a dostali se na detekční limit proteinů s nízkou hladinou, ze vzorku jsme odstranili majoritní proteiny. Zvolili jsme imunoafinitní purifikaci 12 proteinů nejvíce zastoupených v plazmě: **albumin, IgG, transferin, fibrinogen, IgA, α2-makroglobulin, IgM, α1-antitrypsin, haptoglobin, α1-kyselý glykoprotein, apolipoproteiny A-I** a **A-II**. Vzorky zbavené 97 % proteinů jsme pak mohli kvantitativně porovnávat pomocí 2DE a 2D-LC. S využitím **2DE** (pH 4–7) jsme porovnávali 4 OHSS+ vs. 5 OHSS- vzorků, pomocí **2D-LC** pak 6 OHSS+ vs. 6 OHSS- vzorků. Pomocí **MALDI-FT-ICR** jsme identifikovali 35 diferenčně exprimovaných proteinů a verifikace výsledků byla provedena pomocí **WB na původních vzorcích bez deplece.**

Ve vzorku jsme detekovali minimum majoritních proteinů a změny v hladině albuminu, α1-antitrypsinu, α1-glykoproteinu byly pravděpodobně způsobené neúplnou deplecí. Pomocí 2DE jsme identifikovali 16 diferenčních proteinů a pomocí 2D-LC pak 19 diferenčních proteinů. Zajímavé bylo, že 2D-LC v širším gradientu (CF, pH 4–8,5) neodhalila oproti 2DE (IEF, pH 4–7) mnoho diferenčních proteinů s pI nad 7,0 (pouze komplementový faktor 1) a rozmezí MW proteinů bylo velmi podobné (20–187 kDa pro 2D-LC, 31–187 kDa pro 2DE). Odlišné složení proteinů po frakcinonaci tedy určují spíše rozdíly v hydrofobních vlastnostech proteinů a kombinace těchto komplementárních technik pomáhá zachytit více biologicky relevantních změn.

Překryv kvantitativních rozdílů mezi **2DE** a **2D-LC** nebyl velký a jednalo se pouze o ceruloplasmin, kininogen-1 a tři proteiny komplementového systému. Ve folikulární tekutině zdravých žen dochází k inhibici komplementového systému (Jarkovska et al. 2010) a zvýšená hladina některých složek, kterou pozorujeme pouze u pacientek s těžkým OHSS, pravděpodobně ukazuje abnormální aktivaci imunitního systému s rozvojem OHSS.

Zatímco u 2D-LC jsme pozorovali menší nárůst hladiny proteinů (1,67× – 2,38×) pouze u pacientek s OHSS, pomocí 2DE jsme identifikovali také proteiny klesající u OHSS a změny byly až osminásobné. Při verifikačních pokusech jsme bohužel nebyli tak úspěšní a nepodařilo se nám potvrdit významný nárůst ani pokles hladiny proteinů, přestože trend změn byl evidentní. **Obtížná verifikace** může mít několik příčin a v první řadě vždy posuzujeme **experimentální vlivy**. Software při 2D-LC vyhodnocuje jednotlivé chromatogramy a hledá diferenční píky. Hmotnostní spektrometrie pak v jedné frakci často identifikuje několik proteinů nebo naopak jeden protein ve více frakcích a nelze přesně určit, který je diferenční. Pro verifikaci změn se vybírá protein podle biologického významu a ne vždy se podaří zvolit protein, který je za kvantitativní změnu opravdu zodpovědný.

V této studii jsme nacházeli v jedné frakci 2D-LC 2–6 proteinů a všechny vykazovaly vyšší hladinu u pacientek s OHSS. V nejobsáhlejší frakci se nacházel ceruloplasmin, α2-HS-glykoprotein a kininogen-1. Ceruloplasmin a α2-HS-glykoprotein byly přítomné i v dalších frakcích 2D-LC. Ceruloplasmin a kininogen-1 byly navíc diferenční v 2D-LC i 2DE. Hladina kininogenu-1 však byla u pacientek s OHSS podle 2D-LC zvýšená a podle 2DE snížená. Zapomínat nesmíme ani na předchozí krok analýzy, tj. depleci proteinů. I přes vysokou reprodukovatelnost deplece je možné, že rozdíly v hladině některých proteinů jsou způsobené nespecifickým navázáním na protilátky imunoafinitní kolony nebo také (ne)specifickým navázáním na depletované proteiny. Všechny tyto okolnosti mohou být společným důvodem pro malý úspěch verifikačních pokusů.

Protože ale pracujeme s reálnými vzorky, nesmíme zapomínat na **biologickou variabilitu**, která odráží individuální odpověď organismů. Ty reagují na řadu dalších stimulů prostřednictvím velmi komplexních dějů a může tak dojít k zakrytí méně výrazných změn v expresi proteinů. Pro překonání biologické variability je nezbytné analyzovat velký počet vzorků a tuto limitaci jsme bohužel z důvodu omezené dostupnosti vzorků překonat nemohli. Trend změny byl ale evidentní a většina pacientek s OHSS měla zvýšenou hladinu apolipoproteinu A-IV, α2-HS-glykoproteinu, ceruloplasminu a nižší hladinu kininogenu-1.

6. Závěr

Disertační práce byla zaměřena na charakterizaci molekulárních mechanismů působení protinádorových léčiv, zejména pak na rozvoj nádorové rezistence k působení inhibitorů proteinkináz. Pro pochopení těchto mechanismů jsme využili modely lidských buněčných linií, 2D separaci intaktních proteinů a hmotnostní spektrometrii. V rámci sledování buněčné odpovědi jsme hledali rozdíly v expresi proteinů včetně jejich modifikací. Buňky byly ošetřeny různými léčivy po různou dobu a rezistence byla ustavena podle protokolů, které simulují běžnou onkologickou terapii (postupné zvyšování subletální dávky) a odráží také její toxické účinky (jednorázová vysoká dávka). Pomocí kvantitativní proteomiky se nám podařilo identifikovat proteiny regulované po působení protinádorových léčiv a také proteiny přispívající k rozvoji nádorové rezistence.

Klíčovou úlohu v odpovědi na protinádorovou léčbu mají specifické formy proteinů, které za různých podmínek vykonávají specifické funkce. Pouze určité formy Y-box vázajícího proteinu 1 a proteinu organizujícího Hsc70/Hsp90 jsou zodpovědné za progresi nádorového onemocnění a rozvoj rezistence na protinádorovou léčbu. Naše výsledky ukazují velmi nízkou hladinu těchto proteinů stejně jako Rho GDP-disociačního inhibitoru 2 po ošetření léčivem. S rozvojem rezistence tento efekt v nádorových buňkách mizí a dochází k významným změnám izoelektrických vlastností proteinů, které jsou doprovázené změnou funkce a buněčné lokalizace.

Naše výsledky také ukazují, že nádorové buňky odpovídají na léčbu stejným typem léčiva odlišným způsobem a rezistenci rozvíjí odlišnými mechanismy. Specifická odpověď nádorových buněk závisí nejen na druhu léčiva ale také na způsobu ustavení rezistence. Po ošetření buněk protinádorovými léčivy dochází k bezprostřednímu ovlivnění buněčného metabolismu, který je u rezistentních buněk modulován trvale. K rozvoji nádorové rezistence významně přispívá vysoká hladina serinhydroxymethyltransferázy a serpinu B5. Tyto proteiny jsou výrazně zvýšené u nádorových buněk různého histogenetického původu rezistentních na různá protinádorová léčiva a představují proto potenciální cíle pro vývoj nových biologických léčiv. Calretinin a voltage-dependent anion-selective channel protein 2 představují na druhé straně potenciální cíle pro nová biologická léčiva, která by mohla cílit tyto molekuly v solidních nádorech.

Zatímco serinhydroxymethyltransferáza, serpin B5 a calretinin podporují progresi nádoru nezávisle na expresi p53, voltage-dependent anion-selective channel protein 2 přispívá k rozvoji rezistence pouze u nádorových buněk s funkčním p53. U těchto buněk je potřebná

také nízká exprese elongačního faktoru 2. Buňky s mutovaným p53 pak během rozvoje rezistence posilují antioxidační mechanismy a brání apoptóze jinými způsoby než prostřednictvím regulace p53. Serpin B5 a calretinin patří k proteinům s nejvyšším nárůstem exprese ve většině rezistentních buněk. Prostřednictvím patentové aplikace navrhujeme sledovat hladinu těchto proteinů u onkologických pacientů.

Zatímco buňky v kultuře odpovídají na různé stimuly pouze na základě vlastní výbavy, v organismu reagují na změnu podmínek také okolní tkáně a dochází k velmi komplexním procesům. V rámci přípravy na validační experimenty a získávání zkušeností pro práci s reálnými biologickými vzorky jsme se zapojili do projektu hledání biomarkerů v lidské folikulární tekutině, která se svým složením velmi podobá krevní plazmě. Zjistili jsme, že imunoafinitní chromatografie dokáže reprodukovatelně odstranit naprostou vetšinu majoritních proteinů bez velkého vlivu na následné kvantitativní porovnání proteinů. Měly jsme také možnost pozorovat, jak velkou roli hraje biologická variabilita v analýze reálných vzorků. To klade extremní požadavky na odběr reálných vzorků a jejich přípravu pro následnou analýzu či validace.

Výsledky této práce přispěly k lepšímu pochopení mechanismů účinku protinádorových léčiv i nádorové rezistence a ukázaly molekulární mechanismy, kterými buňky podporují progresi onemocnění a rozvoj rezistence na protinádorovou léčbu. Identifikovali jsme proteiny, jejichž inhibice by mohla vést k překonání nádorové rezistence a také proteiny, které by mohly najít využití při monitorování protinádorové léčby. Nejen kvalita a kvantita proteinového složení, ale hlavně modifikace proteinů a jejich buněčná lokalizace určují osud nádorových buněk. Pro vývoj nových účinných léků je však nezbytná podrobnější validace vybraných proteinů na velkém počtu vzorků onkologických pacientů.

7. Citovaná literatura

Acosta-Martin, A. E., et al. (2011), 'Quantitative mass spectrometry analysis using PAcIFIC for the identification of plasma diagnostic biomarkers for abdominal aortic aneurysm', *PLoS One*, 6 (12), e28698.

Aebersold, R. and Mann, M. (2003), 'Mass spectrometry-based proteomics', *Nature*, 422 (6928), 198–207.

Anderson, L. and Hunter, C. L. (2006), 'Quantitative mass spectrometric multiple reaction monitoring assays for major plasma proteins', *Mol Cell Proteomics*, 5 (4), 573–88.

Anderson, N. L. and Anderson, N. G. (1998), 'Proteome and proteomics: new technologies, new concepts, and new words', *Electrophoresis*, 19 (11), 1853–61.

Anderson, N. L. and Anderson, N. G. (2002), 'The human plasma proteome: history, character, and diagnostic prospects', *Mol Cell Proteomics*, 1 (11), 845–67.

Anderson, N. L., et al. (2004), 'Mass spectrometric quantitation of peptides and proteins using Stable Isotope Standards and Capture by Anti-Peptide Antibodies (SISCAPA)', *J Proteome Res*, 3 (2), 235–44.

Anonymous (2002), 'Bevacizumab. Anti-VEGF monoclonal antibody, avastin, rhumab-VEGF', *Drugs R D*, 3 (1), 28–30.

Antberg, L., et al. (2012), 'Critical comparison of multidimensional separation methods for increasing protein expression coverage', *J Proteome Res*, 11 (5), 2644–52.

Arruda-Carvalho, M., et al. (2007), 'Hop/STI1 modulates retinal proliferation and cell death independent of PrPC', *Biochem Biophys Res Commun*, 361 (2), 474–80.

Bader, A. G. and Vogt, P. K. (2008), 'Phosphorylation by Akt disables the anti-oncogenic activity of YB-1', *Oncogene*, 27 (8), 1179–82.

Balonova, L., et al. (2010), 'Multimethodological approach to identification of glycoproteins from the proteome of Francisella tularensis, an intracellular microorganism', *J Proteome Res*, 9 (4), 1995–2005.

Barderas, R., et al. (2012), 'An optimized predictor panel for colorectal cancer diagnosis based on the combination of tumor-associated antigens obtained from protein and phage microarrays', *J Proteomics*, 75 (15), 4647–55.

Bargou, R. C., et al. (1997), 'Nuclear localization and increased levels of transcription factor YB-1 in primary human breast cancers are associated with intrinsic MDR1 gene expression', Nat Med, 3 (4), 447–50.

Barrabes, S., et al. (2010), 'Effect of sialic acid content on glycoprotein pI analyzed by two-dimensional electrophoresis', *Electrophoresis*, 31 (17), 2903–12.

Baselga, J., et al. (1998), 'Recombinant humanized anti-HER2 antibody (Herceptin) enhances the antitumor activity of paclitaxel and doxorubicin against HER2/neu overexpressing human breast cancer xenografts', *Cancer Res*, 58 (13), 2825–31.

Bauer, K. M., Lambert, P. A., and Hummon, A. B. (2012), 'Comparative label-free LC-MS/MS analysis of colorectal adenocarcinoma and metastatic cells treated with 5-fluorouracil', *Proteomics*, 12 (12), 1928–37.

Beaufour, M., et al. (2012), 'Interaction Proteomics Suggests a New Role for the Tfs1 Protein in Yeast', *J Proteome Res*.

Bock, T., et al. (2012), 'Proteomic analysis reveals drug accessible cell surface N-glycoproteins of primary and established glioblastoma cell lines', *J Proteome Res*, 11 (10), 4885–93.

Boersema, P. J., et al. (2010), 'In-depth qualitative and quantitative profiling of tyrosine phosphorylation using a combination of phosphopeptide immunoaffinity purification and stable isotope dimethyl labeling', *Mol Cell Proteomics*, 9 (1), 84–99.

Brown, K. R. and Jurisica, I. (2007), 'Unequal evolutionary conservation of human protein interactions in interologous networks', *Genome Biol*, 8 (5), R95.

Buchdunger, E., et al. (1996), 'Inhibition of the Abl protein-tyrosine kinase in vitro and in vivo by a 2-phenylaminopyrimidine derivative', *Cancer Res*, 56 (1), 100–4.

Ciardiello, F. (2000), 'Epidermal growth factor receptor tyrosine kinase inhibitors as anticancer agents', *Drugs*, 60 Suppl 1, 25-32; discussion 41–2.

Contrepois, K., et al. (2010), 'Ultra-high performance liquid chromatography-mass spectrometry for the fast profiling of histone post-translational modifications', *J Proteome Res*, 9 (10), 5501–9.

Cortes-Funes, H. and Coronado, C. (2007), 'Role of anthracyclines in the era of targeted therapy', *Cardiovasc Toxicol*, 7 (2), 56–60.

Craig-Schapiro, R., et al. (2011), 'Multiplexed immunoassay panel identifies novel CSF biomarkers for Alzheimer's disease diagnosis and prognosis', *PLoS One*, 6 (4), e18850.

Cullen, K. J., et al. (2003), 'Glutathione S-transferase pi amplification is associated with cisplatin resistance in head and neck squamous cell carcinoma cell lines and primary tumors', *Cancer Res*, 63 (23), 8097–102.

Cummings, J., et al. (2002), 'Enhanced clearance of topoisomerase I inhibitors from human colon cancer cells by glucuronidation', *Biochem Pharmacol*, 63 (4), 607–13.

Daemen, A., et al. (2008), 'Integrating microarray and proteomics data to predict the response on cetuximab in patients with rectal cancer', *Pac Symp Biocomput*, 166–77.

Dai, L., et al. (2011), 'Dose-dependent proteomic analysis of glioblastoma cancer stem cells upon treatment with gamma-secretase inhibitor', *Proteomics*, 11 (23), 4529–40.

Daniel, S., et al. (2008), 'Nuclear translocation of the phosphoprotein Hop (Hsp70/Hsp90 organizing protein) occurs under heat shock, and its proposed nuclear localization signal is involved in Hsp90 binding', *Biochim Biophys Acta*, 1783 (6), 1003–14.

De Azevedo, W. F., et al. (1997), 'Inhibition of cyclin-dependent kinases by purine analogues: crystal structure of human cdk2 complexed with roscovitine', *Eur J Biochem*, 243 (1–2), 518–26.

De Las Rivas, J. and Fontanillo, C. (2010), 'Protein-protein interactions essentials: key concepts to building and analyzing interactome networks', *PLoS Comput Biol*, 6 (6), e1000807.

De Neubourg, D. and Gerris, J. (2005), 'Can we eliminate severe ovarian hyperstimulation syndrome? Comment 2', *Hum Reprod*, 20 (8), 2369; author reply 69–70.

Deford, J. H., et al. (2009), 'High-throughput liquid-liquid fractionation of multiple protein post-translational modifications', *J Proteome Res*, 8 (2), 907–16.

Dehay, C. and Kennedy, H. (2007), 'Cell-cycle control and cortical development', *Nat Rev Neurosci*, 8 (6), 438–50.

den Hollander, J., et al. (2010), 'Aurora kinases A and B are up-regulated by Myc and are essential for maintenance of the malignant state', *Blood*, 116 (9), 1498–505.

Deutsch, E. W., Lam, H., and Aebersold, R. (2008), 'PeptideAtlas: a resource for target selection for emerging targeted proteomics workflows', *EMBO Rep*, 9 (5), 429–34.

Di Michele, M., et al. (2010), 'Glycoproteomics of paclitaxel resistance in human epithelial ovarian cancer cell lines: towards the identification of putative biomarkers', *J Proteomics*, 73 (5), 879–98.

Ditchfield, C., et al. (2003), 'Aurora B couples chromosome alignment with anaphase by targeting BubR1, Mad2, and Cenp-E to kinetochores', *J Cell Biol*, 161 (2), 267–80.

Domon, B. and Aebersold, R. (2010), 'Options and considerations when selecting a quantitative proteomics strategy', *Nat Biotechnol*, 28 (7), 710–21.

Dzubak, P., et al. (2006), 'New derivatives of silybin and 2,3-dehydrosilybin and their cytotoxic and P-glycoprotein modulatory activity', *Bioorg Med Chem*, 14 (11), 3793–810.

Edelmann, M. J. (2011), 'Strong cation exchange chromatography in analysis of posttranslational modifications: innovations and perspectives', *J Biomed Biotechnol*, 2011, 936508.

Fang, L., et al. (2012), 'Mapping the protein interaction network of the human COP9 signalosome complex using a label-free QTAX strategy', *Mol Cell Proteomics*, 11 (5), 138–47.

Farlow, E. C., et al. (2010), 'Development of a multiplexed tumor-associated autoantibody-based blood test for the detection of non-small cell lung cancer', *Clin Cancer Res*, 16 (13), 3452–62.

Faulkner, S., et al. (2011), 'Immunodepletion of albumin and immunoglobulin G from bovine plasma', *Proteomics*, 11 (11), 2329–35.

Fenn, J. B., et al. (1989), 'Electrospray ionization for mass spectrometry of large biomolecules', *Science*, 246 (4926), 64–71.

Fortin, T., et al. (2009), 'Clinical quantitation of prostate-specific antigen biomarker in the low nanogram/milliliter range by conventional bore liquid chromatography-tandem mass spectrometry (multiple reaction monitoring) coupling and correlation with ELISA tests', *Mol Cell Proteomics*, 8 (5), 1006–15.

Fujita, A., et al. (2012), 'Clinical significance of Rho GDP dissociation inhibitor 2 in colorectal carcinoma', *Int J Clin Oncol*, 17 (2), 137–42.

Gahmberg, C. G. and Tolvanen, M. (1996), 'Why mammalian cell surface proteins are glycoproteins', *Trends Biochem Sci*, 21 (8), 308–11.

Gao, Q., et al. (2010), 'Coupling protein complex analysis to peptide based proteomics', *J Chromatogr A*, 1217 (49), 7661–8.

Gasco, M. and Crook, T. (2003), 'p53 family members and chemoresistance in cancer: what we know and what we need to know', *Drug Resist Updat*, 6 (6), 323–8.

Gauci, S., et al. (2008), 'A versatile peptide pI calculator for phosphorylated and N-terminal acetylated peptides experimentally tested using peptide isoelectric focusing', *Proteomics*, 8 (23-24), 4898–906.

Geiger, T., et al. (2012), 'Comparative proteomic analysis of eleven common cell lines reveals ubiquitous but varying expression of most proteins', *Mol Cell Proteomics*, 11 (3), M111 014050.

Gibson, D. S., et al. (2009), 'Stratification and monitoring of juvenile idiopathic arthritis patients by synovial proteome analysis', *J Proteome Res*, 8 (12), 5601–9.

Gildea, J. J., et al. (2002), 'RhoGDI2 is an invasion and metastasis suppressor gene in human cancer', *Cancer Res*, 62 (22), 6418–23.

Giron, P., et al. (2011), 'Quantitative analysis of human cerebrospinal fluid proteins using a combination of cysteine tagging and amine-reactive isobaric labeling', *J Proteome Res*, 10 (1), 249–58.

Gobom, J., et al. (1999), 'Sample purification and preparation technique based on nano-scale reversed-phase columns for the sensitive analysis of complex peptide mixtures by matrix-assisted laser desorption/ionization mass spectrometry', *J Mass Spectrom*, 34 (2), 105–16.

Goto, T., et al. (2006), 'Gene expression profiles with cDNA microarray reveal RhoGDI as a predictive marker for paclitaxel resistance in ovarian cancers', *Oncol Rep*, 15 (5), 1265–71.

Gottesman, M. M., Fojo, T., and Bates, S. E. (2002), 'Multidrug resistance in cancer: role of ATP-dependent transporters', *Nat Rev Cancer*, 2 (1), 48–58.

Gromov, P., et al. (2010), 'Up-regulated proteins in the fluid bathing the tumour cell microenvironment as potential serological markers for early detection of cancer of the breast', *Mol Oncol*, 4 (1), 65–89.

Gundry, R. L., et al. (2009), 'The mouse C2C12 myoblast cell surface N-linked glycoproteome: identification, glycosite occupancy, and membrane orientation', *Mol Cell Proteomics*, 8 (11), 2555–69.

Gunther, N. W. th, et al. (2012), 'pH fractionation and identification of proteins: comparing column chromatofocusing versus liquid isoelectric focusing techniques', *J Sep Sci*, 35 (12), 1399–405.

Guo, W., et al. (1999), 'Mechanisms of methotrexate resistance in osteosarcoma', *Clin Cancer Res*, 5 (3), 621–7.

Halligan, B. D. (2009), 'ProMoST: a tool for calculating the pI and molecular mass of phosphorylated and modified proteins on two-dimensional gels', *Methods Mol Biol*, 527, 283–98, ix.

Hande, K. R. (1998), 'Clinical applications of anticancer drugs targeted to topoisomerase II', *Biochim Biophys Acta*, 1400 (1-3), 173–84.

Hardy, E. and Castellanos-Serra, L. R. (2004), '"Reverse-staining" of biomolecules in electrophoresis gels: analytical and micropreparative applications', *Anal Biochem*, 328 (1), 1–13.

Hause, R. J., et al. (2011), 'Targeted protein-omic methods are bridging the gap between proteomic and hypothesis-driven protein analysis approaches', *Expert Rev Proteomics*, 8 (5), 565–75.

Held, J. M., et al. (2010), 'Targeted quantitation of site-specific cysteine oxidation in endogenous proteins using a differential alkylation and multiple reaction monitoring mass spectrometry approach', *Mol Cell Proteomics*, 9 (7), 1400–10.

Henry, M. and Meleady, P. (2011), 'Clinical proteomics: liquid chromatography-mass spectrometry purification systems', *Methods Mol Biol*, 681, 473–83.

Hodgkinson, V. C., et al. (2012), 'Proteomic identification of predictive biomarkers of resistance to neoadjuvant chemotherapy in luminal breast cancer: a possible role for 14-3-3 theta/tau and tBID?', *J Proteomics*, 75 (4), 1276–83.

Hochegger, H., Takeda, S., and Hunt, T. (2008), 'Cyclin-dependent kinases and cell-cycle transitions: does one fit all?', *Nat Rev Mol Cell Biol*, 9 (11), 910–6.

Hollstein, M., et al. (1991), 'p53 mutations in human cancers', Science, 253 (5015), 49–53.

Hu, Q., et al. (2005), 'The Orbitrap: a new mass spectrometer', *J Mass Spectrom*, 40 (4), 430–43.

Chaney, S. G. and Sancar, A. (1996), 'DNA repair: enzymatic mechanisms and relevance to drug response', *J Natl Cancer Inst*, 88 (19), 1346–60.

Chang, Y. J., et al. (2012), 'GRP78 knockdown enhances apoptosis via the down-regulation of oxidative stress and Akt pathway after epirubicin treatment in colon cancer DLD-1 cells', *PLoS One*, 7 (4), e35123.

Chattopadhyay, R., et al. (2008), 'Regulatory role of human AP-endonuclease (APE1/Ref-1) in YB-1-mediated activation of the multidrug resistance gene MDR1', *Mol Cell Biol*, 28 (23), 7066–80.

Chen, S. S., et al. (2002), 'Suppression of the STK15 oncogenic activity requires a transactivation-independent p53 function', *EMBO J*, 21 (17), 4491–9.

Chen, Z., et al. (2011), '1-Benzyl-3-cetyl-2-methylimidazolium iodide (NH125) induces phosphorylation of eukaryotic elongation factor-2 (eEF2): a cautionary note on the anticancer mechanism of an eEF2 kinase inhibitor', *J Biol Chem*, 286 (51), 43951–8.

Cheng, J. and Haas, M. (1990), 'Frequent mutations in the p53 tumor suppressor gene in human leukemia T-cell lines', *Mol Cell Biol*, 10 (10), 5502–9.

Chmela, Z., et al. (2001), 'In vivo metabolism of 2,6,9-trisubstituted purine-derived cyclin-dependent kinase inhibitor bohemine in mice: glucosidation as the principal metabolic route', *Drug Metab Dispos*, 29 (3), 326–34.

Cho, H. J., et al. (2009), 'RhoGDI2 expression is associated with tumor growth and malignant progression of gastric cancer', *Clin Cancer Res*, 15 (8), 2612–9.

Jacobs, J. M., et al. (2004), 'Multidimensional proteome analysis of human mammary epithelial cells', *J Proteome Res*, 3 (1), 68–75.

Jarkovska, K., et al. (2010), 'Proteome mining of human follicular fluid reveals a crucial role of complement cascade and key biological pathways in women undergoing in vitro fertilization', *J Proteome Res*, 9 (3), 1289–301.

Jemal, A., et al. (2011), 'Global cancer statistics', *CA Cancer J Clin*, 61 (2), 69–90.

Jensen, O. N. (2004), 'Modification-specific proteomics: characterization of post-translational modifications by mass spectrometry', *Curr Opin Chem Biol*, 8 (1), 33–41.

Johnson, L., et al. (2012), 'Surface-localized spermidine protects the Pseudomonas aeruginosa outer membrane from antibiotic treatment and oxidative stress', *J Bacteriol*, 194 (4), 813–26.

Karas, M. and Hillenkamp, F. (1988), 'Laser desorption ionization of proteins with molecular masses exceeding 10,000 daltons', *Anal Chem*, 60 (20), 2299–301.

Katayama, H., et al. (2004), 'Phosphorylation by aurora kinase A induces Mdm2-mediated destabilization and inhibition of p53', *Nat Genet*, 36 (1), 55–62.

Kawahara, Y. and Mieda-Sato, A. (2012), 'TDP-43 promotes microRNA biogenesis as a component of the Drosha and Dicer complexes', *Proc Natl Acad Sci U S A*, 109 (9), 3347–52.

Kim, B. K., et al. (2009), 'The multiplex bead array approach to identifying serum biomarkers associated with breast cancer', *Breast Cancer Res*, 11 (2), R22.

Kim, M. J., Frankel, A. H., and Tam, F. W. (2011), 'Urine proteomics and biomarkers in renal disease', *Nephron Exp Nephrol*, 119 (1), e1–7.

Kohli, B. M., et al. (2012), 'Interactome of the amyloid precursor protein APP in brain reveals a protein network involved in synaptic vesicle turnover and a close association with Synaptotagmin-1', *J Proteome Res*, 11 (8), 4075–90.

Kollareddy, M., et al. (2008), 'Aurora kinases: structure, functions and their association with cancer', *Biomed Pap Med Fac Univ Palacky Olomouc Czech Repub*, 152 (1), 27–33.

Kollareddy, M., et al. (2012), 'Aurora kinase inhibitors: Progress towards the clinic', *Invest New Drugs*, 30 (6), 2411–32.

Komlodi-Pasztor, E., et al. (2011), 'Mitosis is not a key target of microtubule agents in patient tumors', *Nat Rev Clin Oncol*, 8 (4), 244–50.

Kovarova, H., et al. (2002), 'Application of proteomics in the search for novel proteins associated with the anti-cancer effect of the synthetic cyclin-dependent kinases inhibitor, bohemine', *Technol Cancer Res Treat*, 1 (4), 247–56.

Kovarova, H., et al. (2000), 'Proteomics approach in classifying the biochemical basis of the anticancer activity of the new olomoucine-derived synthetic cyclin-dependent kinase inhibitor, bohemine', *Electrophoresis*, 21 (17), 3757–64.

Kuhn, E., et al. (2012), 'Interlaboratory evaluation of automated, multiplexed peptide immunoaffinity enrichment coupled to multiple reaction monitoring mass spectrometry for quantifying proteins in plasma', *Mol Cell Proteomics*, 11 (6), M111 013854.

Layton, M. J., et al. (2012), 'Solubilisation of the armadillo-repeat protein beta-catenin using a zwitterionic detergent allows resolution of phosphorylated forms by 2DE', *Electrophoresis*, 33 (12), 1804–13.

Levine, A. J. (1997), 'p53, the cellular gatekeeper for growth and division', *Cell*, 88 (3), 323–31.

Li, C., et al. (2012), 'Quantitative proteomics reveal up-regulated protein expression of the SET complex associated with hepatocellular carcinoma', *J Proteome Res*, 11 (2), 871–85.

Li, E. and Hristova, K. (2006), 'Role of receptor tyrosine kinase transmembrane domains in cell signaling and human pathologies', *Biochemistry*, 45 (20), 6241–51.

Liu, H., et al. (2006), 'Amelioration of oxidant stress by the defensin lysozyme', *Am J Physiol Endocrinol Metab*, 290 (5), E824–32.

Loch, C. M. and Strickler, J. E. (2012), 'A microarray of ubiquitylated proteins for profiling deubiquitylase activity reveals the critical roles of both chain and substrate', *Biochim Biophys Acta*, 1823 (11), 2069–78.

Longley, D. B. and Johnston, P. G. (2005), 'Molecular mechanisms of drug resistance', *J Pathol*, 205 (2), 275–92.

Longshaw, V. M., et al. (2004), 'Nuclear translocation of the Hsp70/Hsp90 organizing protein mSTI1 is regulated by cell cycle kinases', *J Cell Sci*, 117 (Pt 5), 701–10.

Makawita, S. and Diamandis, E. P. (2010), 'The bottleneck in the cancer biomarker pipeline and protein quantification through mass spectrometry-based approaches: current strategies for candidate verification', *Clin Chem*, 56 (2), 212–22.

Makawita, S., et al. (2011), 'Integrated proteomic profiling of cell line conditioned media and pancreatic juice for the identification of pancreatic cancer biomarkers', *Mol Cell Proteomics*, 10 (10), M111 008599.

Mao, J. H., et al. (2007), 'Crosstalk between Aurora-A and p53: frequent deletion or downregulation of Aurora-A in tumors from p53 null mice', *Cancer Cell*, 11 (2), 161–73.

Marshall, A. G., Hendrickson, C. L., and Jackson, G. S. (1998), 'Fourier transform ion cyclotron resonance mass spectrometry: a primer', *Mass Spectrom Rev*, 17 (1), 1–35.

Matlin, A. J., Clark, F., and Smith, C. W. (2005), 'Understanding alternative splicing: towards a cellular code', *Nat Rev Mol Cell Biol*, 6 (5), 386–98.

McDonald, T., et al. (2006), 'Expanding the subproteome of the inner mitochondria using protein separation technologies: one- and two-dimensional liquid chromatography and two-dimensional gel electrophoresis', *Mol Cell Proteomics*, 5 (12), 2392–411.

McQueen, P. and Krokhin, O. (2012), 'Optimal selection of 2D reversed-phase-reversed-phase HPLC separation techniques in bottom-up proteomics', *Expert Rev Proteomics*, 9 (2), 125–8.

Mizushima, N. and Klionsky, D. J. (2007), 'Protein turnover via autophagy: implications for metabolism', *Annu Rev Nutr*, 27, 19–40.

Moll, U. M., et al. (2005), 'Transcription-independent pro-apoptotic functions of p53', *Curr Opin Cell Biol*, 17 (6), 631–6.

Mosley, A. L., et al. (2011), 'Highly reproducible label free quantitative proteomic analysis of RNA polymerase complexes', *Mol Cell Proteomics*, 10 (2), M110 000687.

Mounicou, S., et al. (2010), 'Identification of metallothionein subisoforms in HPLC using accurate mass and online sequencing by electrospray hybrid linear ion trap-orbital ion trap mass spectrometry', *Anal Chem*, 82 (16), 6947–57.

Munoz, J. and Heck, A. J. (2011), 'Quantitative proteome and phosphoproteome analysis of human pluripotent stem cells', *Methods Mol Biol*, 767, 297–312.

Nagai, K., et al. (2012), 'Altered posttranslational modification on U1 small nuclear ribonucleoprotein 68k in systemic autoimmune diseases detected by 2D Western blot', *Electrophoresis*, 33 (13), 2028–35.

Narumi, R., et al. (2012), 'A Strategy for Large-Scale Phosphoproteomics and SRM-Based Validation of Human Breast Cancer Tissue Samples', *J Proteome Res*, 11 (11), 5311–22.

Nilsson, J., Gritli-Linde, A., and Heby, O. (2000), 'Skin fibroblasts from spermine synthase-deficient hemizygous gyro male (Gy/Y) mice overproduce spermidine and exhibit increased resistance to oxidative stress but decreased resistance to UV irradiation', *Biochem J*, 352 Pt 2, 381–7.

Noskova, V., et al. (2002), 'In vitro chemoresistance profile and expression/function of MDR associated proteins in resistant cell lines derived from CCRF-CEM, K562, A549 and MDA MB 231 parental cells', *Neoplasma*, 49 (6), 418–25.

Oda, Y., et al. (2003), 'Nuclear expression of Y-box-binding protein-1 correlates with P-glycoprotein and topoisomerase II alpha expression, and with poor prognosis in synovial sarcoma', *J Pathol*, 199 (2), 251–8.

Odunuga, O. O., Longshaw, V. M., and Blatch, G. L. (2004), 'Hop: more than an Hsp70/Hsp90 adaptor protein', *Bioessays*, 26 (10), 1058–68.

Olsen, J. V., et al. (2006), 'Global, in vivo, and site-specific phosphorylation dynamics in signaling networks', *Cell*, 127 (3), 635–48.

Olsson, I., et al. (2002), 'Organic disulfides as a means to generate streak-free two-dimensional maps with narrow range basic immobilized pH gradient strips as first dimension', *Proteomics*, 2 (11), 1630–2.

Pan, S., et al. (2012), 'Multiplex targeted proteomic assay for biomarker detection in plasma: a pancreatic cancer biomarker case study', *J Proteome Res*, 11 (3), 1937–48.

Pappin, D. J., Hojrup, P., and Bleasby, A. J. (1993), 'Rapid identification of proteins by peptide-mass fingerprinting', *Curr Biol*, 3 (6), 327–32.

Pawar, H., et al. (2011), 'Quantitative tissue proteomics of esophageal squamous cell carcinoma for novel biomarker discovery', *Cancer Biol Ther*, 12 (6), 510–22.

Payne, C. M., et al. (2011), 'Maspin is a deoxycholate-inducible, anti-apoptotic stress-response protein differentially expressed during colon carcinogenesis', *Clin Exp Gastroenterol*, 4, 239–53.

Petrak, J., et al. (2008), 'Deja vu in proteomics. A hit parade of repeatedly identified differentially expressed proteins', *Proteomics*, 8 (9), 1744–9.

Petrak, J., et al. (2011), 'Proteomic and transcriptomic analysis of heart failure due to volume overload in a rat aorto-caval fistula model provides support for new potential therapeutic targets - monoamine oxidase A and transglutaminase 2', *Proteome Sci*, 9 (1), 69.

Polanski, M. and Anderson, N. L. (2007), 'A list of candidate cancer biomarkers for targeted proteomics', *Biomark Insights*, 1, 1–48.

Pucci, B. and Giordano, A. (1999), 'Cell cycle and cancer', *Clin Ter*, 150 (2), 135–41.

Qian, W. J., et al. (2008), 'Enhanced detection of low abundance human plasma proteins using a tandem IgY12-SuperMix immunoaffinity separation strategy', *Mol Cell Proteomics*, 7 (10), 1963–73.

Raynaud, F. I., et al. (2005), 'In vitro and in vivo pharmacokinetic-pharmacodynamic relationships for the trisubstituted aminopurine cyclin-dependent kinase inhibitors olomoucine, bohemine and CYC202', *Clin Cancer Res*, 11 (13), 4875–87.

Rigbolt, K. T., et al. (2011), 'System-wide temporal characterization of the proteome and phosphoproteome of human embryonic stem cell differentiation', *Sci Signal*, 4 (164), rs3.

Righetti, P. G. and Drysdale, J. W. (1973), 'Small-scale fractionation of proteins and nucleic acids by isoelectric focusing in polyacrylamide gels', *Ann N Y Acad Sci*, 209, 163–86.

Rizzolio, F., et al. (2010), 'CDK inhibitors: from the bench to clinical trials', *Curr Drug Targets*, 11 (3), 279–90.

Rogers, S., et al. (2008), 'Investigating the correspondence between transcriptomic and proteomic expression profiles using coupled cluster models', *Bioinformatics,* 24 (24), 2894–900.

Ruperez, P., et al. (2012), 'Quantitative phosphoproteomic analysis reveals a role for serine and threonine kinases in the cytoskeletal reorganization in early T cell receptor activation in human primary T cells', *Mol Cell Proteomics*, 11 (5), 171–86.

Saha, S., et al. (2012), 'Computational framework for analysis of prey-prey associations in interaction proteomics identifies novel human protein-protein interactions and networks', *J Proteome Res*, 11 (9), 4476–87.

Samyn, B., Sergeant, K., and Van Beeumen, J. (2009), 'C-terminal sequence analysis of 2DE-separated proteins', *Methods Mol Biol*, 519, 469–82.

Sandstrom, A., et al. (2012), 'Serum proteome profiling of pancreatitis using recombinant antibody microarrays reveals disease-associated biomarker signatures', *Proteomics Clin Appl*, 6 (9-10), 486–96.

Santamaria, E., et al. (2012), 'A combination of affinity chromatography, 2D DIGE, and mass spectrometry to analyze the phosphoproteome of liver progenitor cells', *Methods Mol Biol*, 909, 165–80.

Sarkaria, J. N., et al. (2008), 'Mechanisms of chemoresistance to alkylating agents in malignant glioma', *Clin Cancer Res*, 14 (10), 2900–8.

Sauter, G., Simon, R., and Hillan, K. (2003), 'Tissue microarrays in drug discovery', *Nat Rev Drug Discov*, 2 (12), 962–72.

Seredina, T. A., et al. (2012), 'Association of cytochrome P450 genetic polymorphisms with neoadjuvant chemotherapy efficacy in breast cancer patients', *BMC Med Genet*, 13, 45.

Shapiro, A. L., Vinuela, E., and Maizel, J. V., Jr. (1967), 'Molecular weight estimation of polypeptide chains by electrophoresis in SDS-polyacrylamide gels', *Biochem Biophys Res Commun*, 28 (5), 815–20.

Sheng, S., et al. (2011), 'Intact protein separation by one- and two-dimensional liquid chromatography for the comparative proteomic separation of partitioned serum or plasma', *Methods Mol Biol*, 728, 29–46.

Shevchenko, A., et al. (1996), 'Linking genome and proteome by mass spectrometry: large-scale identification of yeast proteins from two dimensional gels', *Proc Natl Acad Sci U S A,* 93 (25), 14440–5.

Schunke, D., et al. (2007), 'Cyclooxygenase-2 is a target gene of rho GDP dissociation inhibitor beta in breast cancer cells', *Cancer Res*, 67 (22), 10694–702.

Simpson, R. J., et al. (2008), 'Proteomics-driven cancer biomarker discovery: looking to the future', *Curr Opin Chem Biol*, 12 (1), 72–7.

Skalnikova, H., et al. (2005), 'Protein fingerprints of anti-cancer effects of cyclin-dependent kinase inhibition: identification of candidate biomarkers using 2-D liquid phase separation coupled to mass spectrometry', *Technol Cancer Res Treat*, 4 (4), 447–54.

Smoot, M. E., et al. (2011), 'Cytoscape 2.8: new features for data integration and network visualization', *Bioinformatics*, 27 (3), 431–2.

Snel, B., et al. (2000), 'STRING: a web-server to retrieve and display the repeatedly occurring neighbourhood of a gene', *Nucleic Acids Res*, 28 (18), 3442–4.

Sorokin, A. V., et al. (2005), 'Proteasome-mediated cleavage of the Y-box-binding protein 1 is linked to DNA-damage stress response', *EMBO J*, 24 (20), 3602–12.

Stahl-Zeng, J., et al. (2007), 'High sensitivity detection of plasma proteins by multiple reaction monitoring of N-glycosites', *Mol Cell Proteomics*, 6 (10), 1809–17.

Suk, K. (2010), 'Combined analysis of the glia secretome and the CSF proteome: neuroinflammation and novel biomarkers', *Expert Rev Proteomics*, 7 (2), 263–74.

Surinova, S., et al. (2011), 'On the development of plasma protein biomarkers', *J Proteome Res*, 10 (1), 5–16.

Teicher, B. A., et al. (1999), 'The proteasome inhibitor PS-341 in cancer therapy', *Clin Cancer Res*, 5 (9), 2638–45.

Theodorescu, D., et al. (2004), 'Reduced expression of metastasis suppressor RhoGDI2 is associated with decreased survival for patients with bladder cancer', *Clin Cancer Res,* 10 (11), 3800–6.

Thomas, P. D., et al. (2003), 'PANTHER: a browsable database of gene products organized by biological function, using curated protein family and subfamily classification', *Nucleic Acids Res*, 31 (1), 334–41.

Tiberti, N., et al. (2010), 'Discovery and verification of osteopontin and Beta-2-microglobulin as promising markers for staging human African trypanosomiasis', *Mol Cell Proteomics,* 9 (12), 2783–95.

Uhlen, M. and Hober, S. (2009), 'Generation and validation of affinity reagents on a proteome-wide level', *J Mol Recognit*, 22 (2), 57–64.

Uhlen, M., et al. (2005), 'A human protein atlas for normal and cancer tissues based on antibody proteomics', *Mol Cell Proteomics*, 4 (12), 1920–32.

Unwin, R. D., Griffiths, J. R., and Whetton, A. D. (2009), 'A sensitive mass spectrometric method for hypothesis-driven detection of peptide post-translational modifications: multiple reaction monitoring-initiated detection and sequencing (MIDAS)', *Nat Protoc*, 4 (6), 870–7.

Van Leene, J., et al. (2010), 'Targeted interactomics reveals a complex core cell cycle machinery in Arabidopsis thaliana', *Mol Syst Biol*, 6, 397.

Vesely, J., et al. (1994), 'Inhibition of cyclin-dependent kinases by purine analogues', *Eur J Biochem*, 224 (2), 771–86.

Wang, S., et al. (2010), 'Discovery of N-phenyl-4-(thiazol-5-yl)pyrimidin-2-amine aurora kinase inhibitors', *J Med Chem*, 53 (11), 4367–78.

Ward, H. W. (1973), 'Anti-oestrogen therapy for breast cancer: a trial of tamoxifen at two dose levels', *Br Med J*, 1 (5844), 13–4.

Warraich, S. T., et al. (2010), 'TDP-43: a DNA and RNA binding protein with roles in neurodegenerative diseases', *Int J Biochem Cell Biol*, 42 (10), 1606–9.

Waxman, E. S. and Herbst, R. S. (2002), 'The role of the epidermal growth factor receptor in the treatment of colorectal carcinoma', *Semin Oncol Nurs*, 18 (2 Suppl 2), 20–9.

Wen, J. J., et al. (2012), 'Serum proteomic signature of human chagasic patients for the identification of novel potential protein biomarkers of disease', *Mol Cell Proteomics*, 11 (8), 435–52.

Wilson, T. R., Johnston, P. G., and Longley, D. B. (2009), 'Anti-apoptotic mechanisms of drug resistance in cancer', *Curr Cancer Drug Targets*, 9 (3), 307–19.

Wingren, C. and Borrebaeck, C. A. (2004), 'High-throughput proteomics using antibody microarrays', *Expert Rev Proteomics*, 1 (3), 355–64.

Wittig, I., Braun, H. P., and Schagger, H. (2006), 'Blue native PAGE', *Nat Protoc,* 1 (1), 418–28.

Wu, C. C., et al. (2010), 'Candidate serological biomarkers for cancer identified from the secretomes of 23 cancer cell lines and the human protein atlas', *Mol Cell Proteomics,* 9 (6), 1100–17.

Wu, H. Y., et al. (2009), 'Proteomics analysis of nasopharyngeal carcinoma cell secretome using a hollow fiber culture system and mass spectrometry', *J Proteome Res*, 8 (1), 380–9.

Wu, J., et al. (2012), 'Identification and quantification of osteopontin splice variants in the plasma of lung cancer patients using immunoaffinity capture and targeted mass spectrometry', *Biomarkers,* 17 (2), 125–33.

Yang, W. S., et al. (2012), 'Proteomic approach reveals FKBP4 and S100A9 as potential prediction markers of therapeutic response to neoadjuvant chemotherapy in patients with breast cancer', *J Proteome Res*, 11 (2), 1078–88.

Yin, X., et al. (2003), 'Cytoplasmic complex of p53 and eEF2', *J Cell Physiol*, 196 (3), 474–82.

Yip, T. T. and Hutchens, T. W. (1992), 'Mapping and sequence-specific identification of phosphopeptides in unfractionated protein digest mixtures by matrix-assisted laser desorption/ionization time-of-flight mass spectrometry', *FEBS Lett*, 308 (2), 149–53.

Ytterberg, A. J. and Jensen, O. N. (2010), 'Modification-specific proteomics in plant biology', *J Proteomics*, 73 (11), 2249–66.

Zhang, J. T. and Liu, Y. (2007), 'Use of comparative proteomics to identify potential resistance mechanisms in cancer treatment', *Cancer Treat Rev*, 33 (8), 741–6.

Zhang, L., et al. (2009), 'Efficient activation of p53 pathway in A549 cells exposed to L2, a novel compound targeting p53-MDM2 interaction', *Anticancer Drugs*, 20 (6), 416–24.

Zhang, Q., et al. (2011), 'Comprehensive identification of glycated peptides and their glycation motifs in plasma and erythrocytes of control and diabetic subjects', *J Proteome Res*, 10 (7), 3076–88.

Zoumaro-Djayoon, A. D., Heck, A. J., and Munoz, J. (2012), 'Targeted analysis of tyrosine phosphorylation by immuno-affinity enrichment of tyrosine phosphorylated peptides prior to mass spectrometric analysis', *Methods*, 56 (2), 268–74.

8. Použité zkratky

2DE	2D elektroforéza (z angl. *2D electrophoresis*)
ABC	z angl. *ATP-Binding Casette*
AC	afinitní chromatografie (z angl. *Affinity Chromatography*)
AURK	Aurora kináza
BN-PAGE	nativní elektroforéza (z angl. *Blue Native PolyAcrylamide Gel Electrophoresis*)
BCRP	z angl. *Breast Cancer Resistance Protein*
CDK	cyklin-dependentní kináza
CF	chromatofokusace (z angl. *ChromatoFocusing*)
CIP	z angl. *CDK Interacting Protein*
DTT	dithiothreitol
EGF	z angl. *Epidermal Growth Factor*
ELISA	enzymová imunoanalýza (z angl. *Enzyme-Linked ImmunoSorbent Assay*)
ESI	ionizace elektrosprejem (z angl. *Electrospray Ionization*)
FDA	Úřad pro kontrolu potravin a léčiv (z angl. *Food and Drug Administration*)
FSH	z angl. *Follicle-Stimulating Hormone*
FT-ICR	iontová cyklotronová rezonance s Fourierovou transformací (z angl. *Fourier Transform Ion Cyclotron Resonance*)
GnRH	z angl. *Gonadotropin-Releasing Hormone*
GO	z angl. *Gene Ontology*
hCG	z angl. *Human Chorionic Gonadotropin*
HER2	z angl. *Human Epidermal Growth Factor Receptor 2*
Hop	z angl. *Hsc70/Hsp90-Organizing Protein*
IAA	jodacetamid (z angl. *Iodoacetamide*)
IC	inhibiční koncentrace (z angl. *Inhibition Concentration*)
IEC	iontoměničová chromatografie (z angl. *Ion Exchange Chromatography*)
IEF	izoelektrická fokusace (z angl. *IsoElectric Focusing*)
INK	z angl. *Inhibitor of Kinase*
IT	iontová past (z angl. *Ion Trap*)
KIP	z angl. *Kinase Inhibitory Protein*
LC	kapalinová chromatografie (z angl. *Liquid Chromatography*)
LRP	z angl. *Lung Resistance-Associated Protein*
MALDI	ionizace laserem za účasti matrice (z angl. *Matrix-Assisted Laser Desorption/Ionization*)
MDR	mnohočetná léková rezistence (z angl. *Multi-Drug Resistance*)
MRM	z angl. *Multiple Reaction Monitoring*
MRP2	z angl. *Multidrug Resistance-Associated Protein 2*

MS	hmotnostní spektrometrie (z angl. *Mass Spectrometry*)
MTT	3-[4,5-dimethylthiazol-2-yl]-2,5-difenyl tetrazolium bromid
MW	molekulová hmotnost (z angl. *Molecular Weight*)
OHSS	ovariální hyperstimulační syndrom
PCA	z angl. *Principal Component Analysis*
P-gp	glykoprotein P
PMF	peptidové mapování (z angl. *Peptide Mass Fingerprinting*)
PTM	post-translační modifikace
PVDF	polyvinylidendifluorid
Q	kvadrupólový analyzátor (z angl. *Quadrupole*)
Rho GDI2	z angl. *Rho GDP-Dissociation Inhibitor 2*
RP	reverzní fáze (z angl. *Reversed Phase*)
SDS-PAGE	SDS polyakrylamidová gelová elektroforéza (z angl. *Sodium Dodecyl Sulfate PolyAcrylamide Gel Electrophoresis*)
SEC	gelová chromatografie (z angl. *Size Exclusion Chromatography*)
SRM	z angl. *Selected Reaction Monitoring*
TCS	z angl. *Tumor Cells Survival*
TMA	tkáňové profilování (z angl. *Tissue MicroArrays)*
TOF	průletový analyzátor (z angl. *Time-Of-Flight*)
VEGF	z angl. *Vascular Endothelial Growth Factor*
WB	imunoblot (z angl. *Western Blot*)
YB-1	z angl. *Y-Box-Binding Protein 1*

9. Přehled publikací

9.1. Publikace v časopise s IF

Skalnikova H, Martinkova J, **Hrabakova R**, Halada P, Dziechciarkova M, Hajduch M, Gadher SJ, Hammar A, Enetoft D, Ekefjard A, Forsstrom-Olsson O, Kovarova H. *Cancer drug-resistance and a look at specific proteins: Rho GDP-dissociation inhibitor 2, Y-box binding protein 1, and HSP70/90 organizing protein in proteomics clinical application*. J Proteome Res. 2011 Feb 4; 10(2): 404–15**.**

IF (2011): 5.46; 5-year IF (2011): 5.62; Cited by 3 articles.

Tyleckova J, **Hrabakova R**, Mairychova K, Halada P, Radova L, Dzubak P, Hajduch M, Gadher SJ, Kovarova H. *Cancer cell response to anthracyclines effects: mysteries of the hidden proteins associated with these drugs*. Int J Mol Sci. 2012; 13(12): 15536-15564 (doi:10.3390/ijms131215536).

IF (2012): 2.60; 5-year IF (2012): 2.62; Cited by 0 articles.

Jarkovska K, Kupcova Skalnikova H, Halada P, **Hrabakova R**, Moos J, Rezabek K, Gadher SJ, Kovarova H. *Development of ovarian hyperstimulation syndrome: interrogation of key proteins and biological processes in human follicular fluid of women undergoing in vitro fertilisation*. Mol Hum Reprod. 2011 Nov; 17(11): 679–92.

IF (2011): 3.85; 5-year IF (2011): 3.53; Cited by 0 articles.

9.2. Publikace přijaté k uveřejnění v časopise s IF

Hrabakova R, Kollareddy M, Tyleckova J, Halada P, Hajduch M, Gadher SJ, Kovarova H. *Cancer cell resistance to Aurora kinase inhibitors: identification of novel targets for cancer therapy*. J Proteome Res. (DOI: 10.1021/pr300819m).

IF (2012): 5.11; 5-year IF (2012): 5.41.

9.3. Patentové žádosti

Kollareddy M, Hajduch M, Dzubak P, Srovnal J, **Hrabakova R,** Kovarova H. *Method of Determination of Cancer Cell Drug Sensitivity towards Aurora Kinase Inhibitors and Overcoming their Resistance*. European Patent Office Application No. 11192330.6 – 2402.

9.4. Publikace v časopise bez IF

Gadher SJ, **Hrabakova R**, Drahos L, Vekey K, Allmaier G, Kovarova H. *Central and Eastern European Proteomics Conference 2009*. Meeting Report in goPROTEOMICS.

9.5. Publikace v knižních sbornících

Skalnikova H, Martinkova J, **Hrabakova R**, Novak P, Pompach P, Man P, Strohalm M, Havlicek V, Dzubak P, Hajduch M, Gadher SJ, Kovarova H. *Effect of anti-cancer drug cis-platin on leukemia cells – protein profiling using three independent analytical techniques.* In 3rd EuPA congress – Clinical Proteomics; Marko-Varga, G.; Laurell, T., Eds. 2009; pp 235–237. ISBN: 978-963-86156-4-0.

Jarkovska K, Martinkova J, Skalnikova H, **Hrabakova R**, Halada P, Kavan D, Gadher SJ, Kovarova H. *In-depth study of the human follicular fluid for a diagnostic / prognostic marker of ovarian hyperstimulation syndrome*. In 3rd EuPA congress – Clinical Proteomics; Marko-Varga, G.; Laurell, T., Eds. 2009; pp 243–245.
ISBN: 978-963-86156-4-0.

9.6. Prezentace výsledků

9.6.1. Přednášky

Hrabakova R, Kollareddy M, Tyleckova J, Halada P, Hajduch M, Gadher SJ, Kovarova H. *Cancer cell resistance to AURK-directed therapy*. From Physiology of Reproduction to Reproduction Failures in Minipig Model of Huntington Disease (2012), Libechov, CR.

Hrabakova R, Zizkova M, Tyleckova J, Mairychova K, Halada P, Motlik J, Kovarova H. *Zavedení techniky imunoprecipitace pro analýzu proteinových interakcí v proteomické laboratoři*. XII. dny ÚŽFG AV ČR, v.v.i. (2012), Liběchov, ČR.
Přednáška oceněná juniorskou cenou ÚŽFG.

Hrabakova R, Kollareddy M, Mairychova K, Halada P, Hajduch M, Kovarova H. *Cancer cell resistance to AURK-directed therapy: implications for anti-cancer strategies*. 5th Central and Eastern European Proteomic Conference (2011), Prague, CR.

9.6.2. Plakátová sdělení

Hrabakova R, Kollareddy M, Tyleckova J, Halada P, Hajduch M, Kovarova H. *Proteomic signature of drug resistance to Aurora kinase inhibitors*. HUPO 2011, Geneva, Switzerland.

Hrabakova R, Kollareddy M, Tyleckova J, Halada P, Hajduch M, Kovarova H. *Characterisation of novel biomarkers for cancer therapy monitoring*. 5th European Summer School Proteomic basics (2011), Brixen, Italy.

Hrabakova R, Martinkova J, Skalnikova H, Novak P, Radova L, Dzubak P, Kollareddy MR, Hajduch M, Gadher SJ, Kovarova H. *Anti-cancer drug treatment evaluation using multivariate statistical analysis*. 3rd European Summer School in Proteomic Basics (2009), Brixen, Italy.

Hrabakova R, Martinkova J, Skalnikova H, Halada P, Novak P, Dzubak P, Hajduch M, Gadher SJ, Kovarova H. *Proteomic approach to study cancer chemoresistance: focus on Rho GDP-dissociation inhibitor 2, stress-induced-phosphoprotein 1 and Y-box-binding protein 1*. Cancer Proteomics (2009), Dublin, Ireland.

9.6.3. Spoluautorství

Mairychova K, **Hrabakova R**, Vodicka P, Halada P, Motlik J, Kovarova H. *Proteomic signature of porcine induced pluripotent stem cells*. 6th Central and Eastern European Proteomic Conference (2012), Budapest, Hungary.

Zizkova M, **Hrabakova R**, Juhasova J, Juhas S, Halada P, Kovarova H, Motlik J. *β-catenin expression in minipigs transgenic for human mutated huntingtin*. J Neurol Neurosurg Psychiatry 2012 Sep; 83(Suppl 1): A15-A16 doi:10.1136/jnnp-2012-303524.49.

Rausova P, Solc P, **Hrabakova R**, Klima J, Juhasova J, Juhas S, Motlik J. *Genotoxic stress in fibroblasts and mesenchymal stem cells isolated form miniature pigs transgenic for N-terminal part of mutated human huntingtin*. J Neurol Neurosurg Psychiatry 2012 Sep; 83(Suppl 1): A7 doi:10.1136/jnnp-2012-303524.22.

Tyleckova J, **Hrabakova R**, Mairychova K, Halada P, Radova L, Dzubak P, Hajduch M, Kovarova H. *Proteomic study of cancer cells response to anthracycline anticancer treatment*. HUPO 2011, Geneva, Switzerland.

Tyleckova J, **Hrabakova R**, Mairychova K, Halada P, Radova L, Dzubak P, Hajduch M, Kovarova H. *Proteomic study of cancer cells response to anthracycline anticancer treatment*. Proteomic Forum 2011, Berlin, Germany.

Martinkova J, **Hrabakova R**, Halada P, Skalnikova H, Hajduch M, Kovarova H. *Proteomic profiling of cancer cells after anti-cancer treatment*. EMBO Young Scientist Forum 2010, Prague, CR.

Kovarova H, **Hrabakova R**, Halada P, Kollareddy M, Gadher SJ, Hajduch M. *Drug resistance to Aurora kinase inhibitors in cancer therapy.* 4th Central and Eastern European Proteomic Conference (2010), Vienna, Austria.

Martinkova J, **Hrabakova R**, Skalnikova H, Novak P, Radova L, Džubák P, Kollareddy MR, Hajduch M, Gadher SJ, Kovarova H. *Mapping of proteomic profiles of anti-cancer drugs and their evaluation using multivariate statistical analysis*. Cancer Proteomics (2009), Dublin, Ireland.

Kovarova H, Martinkova J, **Hrabakova R**, Skalnikova H, Novak P, Hajduch M, Gadher SJ. *Proteomics of anti-cancer drugs*. 34th Congress of the Federation of European Biochemical Societies (2009), Prague, CR.

Martinkova J, **Hrabakova R**, Skalnikova H, Novak P, Dzubak P, Hajduch M, Gadher SJ, Kovarova H. *Monitoring of anti-cancer therapies and chemoresistance.* 3rd International Conference of the Hellenic Proteomic Society (2009), Nafplio, Greece.

Martinková J, Skalníková H, Halada P, Novák P, **Hrabáková R**, Džubák P, Hajdúch M, Dziechciarková M, Kovářová H. *Proteomická studie mechanismů chemoresistence T-lymfoblastické leukémie k inhibitorům cyklin-dependentních kináz*. IV. dny diagnostické, prediktivní a experimentální onkologie (2008), Olomouc, ČR.

10. Curriculum Vitae

Mgr. RITA HRABÁKOVÁ
Datum narození: 15.8.1984
Národnost: česká
E-mail: hrabakova@iapg.cas.cz

Vzdělání:

od r. 2008	postgraduální studium obor Vývojová a buněčná biologie Přírodovědecká fakulta, Univerzita Karlova v Praze
2006 – 2008	magisterské studium obor Zdravotnická bioanalytika Farmaceutická fakulta v Hradci Králové, Univerzita Karlova v Praze
2003 – 2006	bakalářské studium obor Zdravotnická bioanalytika Farmaceutická fakulta v Hradci Králové, Univerzita Karlova v Praze

Vědecké společnosti:

od r. 2012	Proteomická sekce ČSBMB
od r. 2011	Human Proteome Organisation
od r. 2011	Česká společnost pro hmotnostní spektrometrii

Specializace:

- separační techniky, hmotnostní spektrometrie
- sledování účinku protinádorových léčiv a studium mechanismů nádorové rezistence
- analýza kmenových buněk a selekce buněk vhodných pro transplantační terapii
- vypracování biomedicínských modelů pro testování nových léčebných postupů